PHARMACOGENOMIC AND MECHANISTIC STUDIES ON DIETARY FACTORS IN CHEMOPREVENTION OF CANCER

by

SUJIT SUKUMAR NAIR

A Dissertation submitted to the

Graduate School-New Brunswick

Rutgers, The State University of New Jersey

in partial fulfillment of the requirements

for the degree of

Doctor of Philosophy

Graduate Program in Pharmaceutical Science

written under the direction of

Professor Ah-Ng Tony Kong, Ph.D.,

and approved by

_____

_____

_____

_____

New Brunswick, New Jersey

May, 2008

ABSTRACT OF THE DISSERTATION

Pharmacogenomic and Mechanistic studies on Dietary Factors in Chemoprevention of Cancer

by SUJIT SUKUMAR NAIR

Dissertation Director: Professor Ah-Ng Tony Kong

Pharmacogenomic profiling of cancer has recently seen much activity with the accessibility of the newest generation of high-throughput platforms and technologies. A myriad of mechanistic studies have been devoted to identifying dietary factors that can help prevent cancer, with evidence gleaned from epidemiologic studies revealing an inverse correlation between the intake of cruciferous vegetables and the risk of certain types of cancer. To develop a comprehensive understanding of cancer pathogenesis, and potential for chemopreventive intervention with dietary factors, an integrated approach that encompasses both pharmacogenomic and mechanistic aspects is desirable. Our transcriptomic profiling of butylated hydroxyanisole-induced Nuclear Factor-E2-related factor 2 (Nrf2)-dependent genes in Nrf2-deficient mice identified several germane molecular targets for prevention. Toxicogenomic analyses of endoplasmic reticulum stress inducer tunicamycin in Nrf2-deficient mice elucidated Nrf2-regulated unfolded protein response effects. Mechanistic studies on a combination of sulforaphane and (-)

epigallocatechin-3-gallate in HT-29 AP-1 (Activator Protein-1) cells revealed a synergy in colon cancer chemoprevention. Pharmacogenomic studies of this combination in PC-3 AP-1 cells provided a discursive framework for understanding putative crosstalk between Nrf2 and AP-1 in prostate cancer chemoprevention. Regulatory potential for concerted modulation of Nrf2 and Nuclear Factor-κB (Nfκb1) in inflammation and carcinogenesis was delineated by bioinformatic analyses. Metabolomic approaches identified potential prognostic biomarkers in human prostate cancer. Differential biological networks in prostate cancer were elicited in androgen-dependent 22Rv1 cells, androgen- and estrogen-dependent LNCaP cells and androgen-independent DU 145 and PC-3 cells. Taken together, our identification of Nrf2-regulated molecular targets by expression profiling using dietary factors, synergistic effects in combinatorial use of dietary factors in colon cancer, regulatory studies on crosstalk between Nrf2 and AP-1 in prostate cancer, bioinformatic analyses of concerted modulation of Nrf2 and Nfkb1 in inflammation and carcinogenesis, metabolomic identification of biomarkers, and delineation of target hubs in differential prostate cancer biological networks, greatly enhance our understanding of the transcriptional circuitry in cancer and important master regulatory nodes including Nrf2 that might potentially be exploited for chemopreventive intervention with dietary factors.

PREFACE

This dissertation is submitted for the Degree of Doctor of Philosophy in Pharmaceutical Science at Rutgers, The State University of New Jersey. It serves as documentation of my research work carried out between August 2002 and April 2008 under the supervision of Dr. Ah-Ng Tony Kong at the Department of Pharmaceutics, Ernest Mario School of Pharmacy, Rutgers, The State University of New Jersey. To the best of my knowledge, this work is original, except where suitable references are made to previous work.

The dissertation consists of eight chapters. Chapter 1 reviews anti-cancer chemopreventive compounds and provides pharmacogenomic and mechanistic insights into the etiopathogenesis of cancer and the potential for chemopreventive intervention. The following seven chapters consist of manuscripts that are already accepted by or are intended to be submitted to peer-reviewed journals. Chapter 2 investigates the pharmacogenomics and the spatial regulation of global gene expression profiles elicited by cancer chemopreventive agent butylated hydroxyanisole (BHA) in Nrf2-deficient mice. Chapter 3 elucidates the toxicogenomics and the spatial regulation of global gene expression profiles elicited by endoplasmic reticulum stress inducer tunicamycin in Nrf2-deficient mice. Chapter 4 investigates the synergistic effects of a combination of dietary factors sulforaphane and (-) epigallocatechin-3-gallate (EGCG) in HT-29 AP-1 human colon carcinoma cells. Chapter 5 delineates the regulation of gene expression by a combination of dietary factors sulforaphane and EGCG in PC-3 AP-1 human prostate adenocarcinoma cells and Nrf2-deficient murine prostate. Chapter 6 elucidates the

regulatory potential for concerted modulation of Nrf2- and Nfkb1-mediated gene expression in inflammation and carcinogenesis. Chapter 7 describes the pharmacogenomic investigation of potential prognostic biomarkers in human prostate cancer. Chapter 8 elucidates differential regulatory networks elicited in androgen-dependent, androgen- and estrogen-dependent, and androgen-independent human prostate cancer cell lines using a systems biology approach. Finally, the Appendix to the dissertation consists of Tables of results from all eight chapters that have been referred to when applicable in the main body of the text comprising these chapters. Together, these findings provide extensive pharmacogenomic and mechanistic evidence that underscore the important utility of dietary factors, alone or in combination, as rational and efficacious strategies in the chemoprevention of cancer.

Sujit Nair

April 2008

ACKNOWLEDGEMENT

I write these words with a profound sense of gratitude towards my beloved Guru and Mother - Śrī Mātā Amritānandamayi Dēvi – known universally as 'The Hugging Saint', or simply 'Ammā'. It was Her Love and Her Compassion that helped me persevere in this doctoral program. I know for sure that but for Her Grace, and Her constant guidance at every step of the way over these past six years, this dissertation would never have seen the light of day. Indeed, it would be imprudent for me to attempt to describe Her whom I do not comprehend myself. I can only dedicate this dissertation in all humility at Her Lotus Feet and pray for Her Grace.

I thank my Advisor Dr. Ah-Ng Tony Kong, for all that I have learnt from him in the past six years in the Department of Pharmaceutics at the Ernest Mario School of Pharmacy. Without him as my Advisor, many of the wonderful lessons that came my way would simply not have been, and I deeply thank him for playing his part as an instrument of Divine Will to impeccable perfection. I also acknowledge the members of my Committee - Dr. Tamara Minko and Dr. Guofeng You from the Department of Pharmaceutics, and Dr. Li Cai from the Biomedical Engineering program. My deepest thanks are due to Dr. Tamara Minko for her tremendous support and help at all times. I am extremely grateful to this wonderfully kind person who stood by me in hard times so that I could successfully graduate with my doctoral degree, and left no stone unturned in helping people whenever she could - I do wish we could have more faculty who would be more like her. I am also grateful to Dr. Li Cai for his patient training on the various

bioinformatic approaches during our highly-productive collaboration with four manuscripts (Chapters 5 through 8) standing as mute testimony to the fruits of our hard work.

Many thanks are due to Dean Barbara Bender, Ph.D., Associate Dean of the Graduate School-New Brunswick for all her support over the past three years, initially during the Head-TA (Teaching Assistant) program and later when I served as Project Facilitator for New International TAs at two consecutive Annual TA Orientations, and not least of all for her tremendous help and support in ensuring the successful completion of this doctoral program. I remain extremely grateful to this wonderfully exuberant and kind person for all her efforts to help me at all times. I also thank Jay Rimmer and Barbara Sirman from the Graduate School-New Brunswick for their willingness to help at all times.

I thank Dean John L. Colaizzi, Ph.D., R.Ph., for his terrific training while I was his TA in the Department of Pharmacy Practice and Administration for his courses in Introduction to Pharmaceutical Care, Pharmacy Convocations, and History of Pharmacy. He is an eloquent speaker who puts his heart into his lectures that he delivers in the most impeccable manner, and I am deeply inspired by his teaching style and his degree of perfection. I also thank Dean Christopher Molloy, Ph.D., R.Ph., for his help and kindness in ensuring the successful completion of this doctoral program. I am extremely grateful to Ms. Margaret Snyder (Margie) in the Dean's Office for her tremendous help and support to me in the past six years, even past her retirement from the Ernest Mario School of

Pharmacy. She was always there for me, whether for tuition remission cards, health insurance questions, TA/GA (Teaching Assistant/Graduate Assistant) funding issues, and right through my successful Defense of this dissertation. She is a wonderful person and I thank her wholeheartedly for her help at all times. I also thank Ms. Jenny Visaggio, Business Manager of the Ernest Mario School of Pharmacy, for continuing to make me feel welcome in the Dean's Office after Margie's retirement and for all her gracious support and help. Thanks are also due to Ms. Lisa Mulé and Ms. Rosemary Hayes in the Dean's Office for their help at all times. I also acknowledge the terrific help of Ms. Marianne Shen, Ms. Sharana Taylor and Ms. Amy Grabowski throughout my stay here.

I would like to acknowledge the various faculty members whom I worked with as Head-TA in the Department of Pharmaceutics, some of whom I have already made mention of earlier. These included Dr. Tamara Minko (Drug Delivery II), Dr. Guofeng You (Introduction to Pharmaceutics and Laboratory), Dr. Thomas Cook (Drug Delivery I and Laboratory) and Dr. Ah-Ng Tony Kong (Introduction to Biopharmaceutics and Pharmacokinetics). I also thank Dean Nancy-Cintron Budét for her kindness and help with arrangements for special-needs students first during my tenure as TA with Dean Colaizzi and later as Head-TA in the Department of Pharmaceutics.

This acknowledgement would be sorely incomplete without mentioning my beloved students of the Pharm.D. program at the Ernest Mario School of Pharmacy. I have a deep sense of gratitude as I thank the almost 1200 students of the Pharm. D. classes of 2006, 2008, 2009 and 2010, with an average class strength of approximately 300 students, for whom I served as TA and Head-TA during two years between Fall 2004 and Spring

2006. I especially thank the Pharm.D. class of 2008 since these fantastic students stayed with me for four consecutive semesters, and I was able to strike a personal chord with every one of these wonderful students on a first-name basis. I bow down before the intelligence, enthusiasm and joie de vivre of these terrific students from all these classes who were all so friendly to me, and I wish them all great success in their future pursuits.

It would be impossible to do research work without adequate funding for biological and chemical necessities, and I am grateful to the National Institutes of Health (NIH) for their grants NIH RO1CA094828 (Nrf2 grant), NIH RO1CA073674 (Colon cancer and isothiocyanates grant) and NIH RO1CA118947 (Prostate cancer grant) all awarded to Dr. Ah-Ng Tony Kong. I am also grateful to these grants for facilitating my funding as a Graduate Assistant (GA) for four years, and to the Department of Pharmaceutics for funding me as a Teaching Assistant (TA) for two years at the Ernest Mario School of Pharmacy.

It is with great pleasure that I acknowledge the unique fraternity of the members of my laboratory – Room 013 – at the Ernest Mario School of Pharmacy. Firstly, I would like to make special mention of Dr. Vidya Hebbar for all her help and friendship over the last six years, for training me on various aspects of laboratory techniques and for all the help in the initial years and later, even after she left this laboratory. I also thank Avanthika Gopalakrishnan-Barve, Wen Lin, Celine Liew, Young-Sam Keum, Jung-Hwan Kim, Rong Hu, Changjiang Xu, Wenge Li, Chi Chen, Guoxiang Shen, Bok-Ryang Kim, Woo-Sik Jeong, In-Wha Kim, Tin-Oo Khor, Siwang Yu, Xiaoling Yuan, Sherif Ibrahim, Yury

Gomez, Hang Guo, Usha Yerramilli, William Ka Lung Cheung, Jin-Liern Hong, Rachel Wu, Tien-Yuan Wu and Constance Lay-Lay Saw. Without this eclectic mix of talent and expertise, life would not have been so interesting at Rutgers, The State University of New Jersey, and I am very grateful for the wonderful sense of fraternity that we shared together. I am also very grateful to Mrs. Hui Pung for handling all our Purchase Order (PO) requests very promptly, for all her help and understanding over the past six years, and for bringing in her own unique flavor of maternal kindness to our wonderful group.

Indeed, graduate student life, embellished as it is with the rigors of academic requirements, financial considerations, and a certain degree of acquiescing compromise, could never be complete without a group of friends both at home and outside the workplace that make it so much easier to breathe. It is with gratitude that I thank the Sharma family, Volkan Demirbas, Srinivas Maloor, Siddharth Madan, Manjul Apratim, Vishal Jain, Aakash Jain and Vatsal Shah for all the help they have provided me.

I thank my parents, Indira and Sukumar, who kindled the lamp of my life and took great pains in furthering the cause of my academic pursuits. Sunita, my sister, as well as Jayaprakash, Aditya and Aiswarya also deserve thanks for their tremendous help and support. I also thank my uncle, Prabhakaran, who has been a great source of inspiration and support over all these years. Finally, I will gladly seize this opportunity to express my deepest thanks to some of my most wonderful brothers and sisters, all beloved children of Ammā, without whose help I could not have survived alone in the United States during all these trying and testing years. I also know that mere words would not

suffice to express the depth of emotion that binds us all together in Ammā's Pure Love. I am indebted to Pushpa Nayar for her terrific help at all times, whether it was providing me with food, or attending to the various needs of my dissertation, and offering words of supportive encouragement whenever adversity struck me. I am also indebted to Damu and Radhika Menon for the perspicacious words of advice and strong support at every hour of crisis that befell me. I am very grateful to Roopa, Shrirang and Ayush for their great support on so many various occasions. I also thank Seetha, Ramesh, Sashu and Shivesh for making me so welcome in their home at all times, and for all the terrific support in completing this doctoral program. Further, I thank Meera and Venkatesh for their tremendous encouragement and concern for me over the years. I also thank Shabarinath, Sai Achuthan, Deepak and Shimona Nambiar for their help and encouragement during the course of my program. I am extremely indebted to my dear friends Pavithra and Vipin for their inimitable support, encouragement and help at very crucial and grief-stricken hours of this doctoral program. I do also thank Dr. Geetha Kumar for her support, understanding and compassion in empathizing with me at all times. Besides, my most beloved friends – Sankaran, Kaushal and Kartik, Ajay, Arun and Raji, Ranjith, and Sahil – outshone themselves in their ability to empathize with me and provide me much-needed succour in hours of grief. I also thank Swāmi Rāmakrishnānanda Puri, Swāmi Amritātmananda Puri, Swāmi Pranavāmritānanda Puri, Swāmi Amritaswaroopānanda Puri, Swāmi Poornāmritānanda Puri, Swāmi Dayāmritā Chaitanyā and Swāmi Shubāmritā Chaitanyā for providing me inspiration, guidance and love in my difficult times. I simply bow down before all the above-mentioned children of Ammā who beautifully expressed Ammā's Love and Compassion in repeatedly bailing

me out of difficult situations. But for this wonderful social network created by Ammā's Divine Grace, this dissertation would not have been possible today. I also thank all my beloved brothers and sisters of the New York and New Jersey Satsangs who have extended a helping hand to me on so many occasions during the past six years.

In the last analysis, it is Ammā's Grace, Ammā's Love, Ammā's Compassion, and Ammā's Will that prevailed over all else. This dissertation is but a minuscule fragment in the plethora of divine events that stand wondrous testimony to Her Infinite Power and Grace. Yet, I am overjoyed and grateful that the Divine Mother granted me a once-in-a-lifetime opportunity to dedicate this dissertation, howsoever insignificant, at Her Lotus Feet. May our love for Ammā blossom like the scintillating radiance of the rising sun, and may Ammā's Divine Grace, Love and Light flood all our lives with eternal peace.

DEDICATION

To my beloved Guru and Mother,

Śrī Mātā Amritānandamayi Dēvi (Ammā)

TABLE OF CONTENTS

Abstract of the Dissertation …… ii

Preface …….. iv

Acknowledgement……. vi

Dedication ……. xiii

Table of Contents ……. xiv

List of Tables in Appendix……... xxii

List of Figures ……... xxvi

CHAPTER 1 **Natural Dietary Anti-cancer chemopreventive compounds: Redox-mediated Differential Signaling Mechanisms in Cytoprotection of Normal Cells Versus Cytotoxicity in Tumor Cells**

1.1. Abstract 1

1.2. Introduction 3

1.3. Natural dietary anti-cancer chemopreventive compounds 6

1.4. Redox-mediated signaling 9

1.4.1. Oxidative stress and redox circuitry **9**

1.4.2. Redox-sensitive transcription factors **11**

1.4.3. The Keap1-Nrf2 axis in redox signaling **13**

1.5. Gene expression and *in vivo* pharmacological effects **16**

1.5.1. The Nrf2 paradigm in gene expression **16**

1.5.2. Transcriptome profiling of putative Nrf2 coactivators and corepressors **17**

1.5.3. Coordinated regulation of Phase I, II and III drug metabolizing enzyme/transporter genes via Nrf2 **19**

1.5.4. Spatial and temporal control of Nrf2-mediated gene expression **20**

1.5.5. Pharmacotoxicogenomic relevance of redox-sensitive Nrf2 **21**

1.5.6. Redox regulation of cellular signaling molecules leading to cell death mechanisms **23**

1.5.7. Modulation of apoptosis and cell-cycle control genes via Nrf2 **26**

1.6. Integrated systems biology approach to cancer chemoprevention **26**

1.7. Concluding Remarks **27**

1.8. Acknowledgements **28**

CHAPTER 2 Pharmacogenomics of Phenolic Antioxidant Butylated hydroxyanisole (BHA) in the Small Intestine and Liver of Nrf2 Knockout and C57BL/6J Mice

2.1. Abstract **33**

2.2. Introduction **34**

2.3. Materials and Methods **37**

2.4. Results **42**

2.4.1. BHA-Modulated Gene Expression Patterns in Mouse Small Intestine and Liver **42**

2.4.2. Quantitative Real–Time PCR Validation of Microarray Data **42**

2.4.3. BHA-Induced Nrf2-Dependent Genes in Small Intestine and Liver **43**

2.4.4. BHA-Suppressed Nrf2-Dependent Genes in Small Intestine and Liver **46**

2.5. Discussion **47**

2.6. Acknowledgements **55**

CHAPTER 3 Toxicogenomics of Endoplasmic Reticulum stress inducer Tunicamycin in the Small Intestine and Liver of Nrf2 Knockout and C57BL/6J Mice

3.1. Abstract **60**

3.2. Introduction **61**

3.3. Materials and Methods **64**

3.4. Results **68**

3.4.1. TM-Modulated Gene Expression Patterns in Mouse Small Intestine and Liver **68**

3.4.2. Quantitative Real–Time PCR Validation of Microarray Data **69**

3.4.3. TM-Induced Nrf2-Dependent Genes in Small Intestine and Liver **69**

3.4.4. TM-Suppressed Nrf2-Dependent Genes in Small Intestine and Liver **71**

3.5. Discussion **72**

3.6. Acknowledgements **82**

CHAPTER 4 Synergistic effects of a combination of dietary factors sulforaphane and (-) epigallocatechin-3-gallate in HT-29 AP-1 human colon carcinoma cells

4.1. Abstract **88**

4.2. Introduction **90**

4.3. Materials and Methods **94**

4.4. Results **100**

4.4.1. Transactivation of AP-1 luciferase reporter by combinations of SFN and EGCG **100**

4.4.2. SOD attenuates the synergism elicited by combinations of SFN and EGCG **101**

4.4.3. Isobologram analyses and combination indices for the combinations of SFN and EGCG **102**

4.4.4. Viability of the HT-29 AP-1 cells with the combinations of SFN and EGCG **102**

4.4.5. Inhibition of EGCG-induced senescence by the combinations of SFN and EGCG **103**

4.4.6. Temporal gene expression profiles elicited by combinations of SFN and EGCG and attenuation by SOD **104**

4.4.7. Protein expression with the combinations of SFN and EGCG **106**

4.4.8. HDAC inhibitor Trichostatin A potentiates the synergism elicited by the low-dose combination of SFN and EGCG **106**

4.4.9. Cytoplasmic and Nuclear HDAC Activity Assays for the combinations of SFN and EGCG **107**

4.4.10. Reactive oxygen species and SOD may modulate AP-1 transactivation by the combinations of SFN and EGCG **108**

4.5. Discussion **108**

4.6. Acknowledgements **116**

CHAPTER 5 Regulation of gene expression by a combination of dietary factors sulforaphane and (-) epigallocatechin-3-gallate in PC-3 AP-1 human prostate adenocarcinoma cells and Nrf2-deficient murine prostate

5.1. Abstract **124**

5.2. Introduction **125**

5.3. Materials and Methods **130**

5.4. Results **138**

5.4.1. Diminished transactivation of AP-1 luciferase reporter by combinations of SFN and EGCG **138**

5.4.2. Viability of the PC-3 AP-1 cells with the combinations of SFN and EGCG **139**

5.4.3. Temporal gene expression profiles elicited by combinations of SFN and EGCG **139**

5.4.4. Comparative promoter analyses of NRF2 and AP-1, as well as ATF-2 and ELK-1, for conserved Transcription Factor Binding Sites (TFBS) **141**

5.4.5. Temporal microarray analyses of genes modulated by SFN+EGCG combination in the prostate of NRF2-deficient mice **142**

5.5. Discussion **143**

5.6. Acknowledgements **146**

CHAPTER 6 Regulatory potential for concerted modulation of Nrf2- and Nfkb1-mediated gene expression in inflammation and carcinogenesis

6.1. Abstract **157**

6.2. Introduction **158**

6.3. Materials and Methods **162**

6.4. Results **165**

6.4.1. Identification of microarray datasets bearing inflammation/injury or cancer signatures **165**

6.4.2. Comparative promoter analyses of Nrf2(Nfe2l2) and Nfkb1 for conserved Transcription Factor Binding Sites (TFBS) **166**

6.4.3. Multiple species alignment of Nrf2 (Nfe2l2) and Nfkb1 sequences **167**

6.4.4. Construction and validation of canonical first-generation regulatory network involving Nrf2(Nfe2l2) and Nfkb1 **168**

6.4.5. Putative model for Nrf2-Nfkb1 interactions in inflammation and carcinogenesis **169**

6.5. Discussion **170**

6.6. Acknowledgements **176**

CHAPTER 7 Pharmacogenomic investigation of potential prognostic biomarkers in human prostate cancer

7.1. Abstract **192**

7.2. Introduction **193**

7.3. Materials and Methods **196**

7.4. Results **199**

7.4.1. Genes modulated in human prostate cancer **199**

7.4.2. Biomarker filtration **199**

7.4.3. Metabolomics analyses **200**

7.4.4. Identification of TFBS-association signatures **201**

7.5. Discussion **202**

7.6. Acknowledgements **206**

CHAPTER 8 Differential regulatory networks elicited in androgen-dependent, androgen- and estrogen-dependent, and androgen-independent human prostate cancer cell lines

8.1. Abstract 215

8.2. Introduction 216

8.3. Materials and Methods 219

8.4. Results 222

8.4.1. Microarray analyses for cancerous and non-cancerous prostate cell lines **222**

8.4.2. Biological Networks in different prostate cancer cell lines **223**

8.4.3. Metabolomics analyses **224**

8.4.4. Regulatory element analyses **225**

8.5. Discussion 225

8.6. Acknowledgements 230

APPENDIX 253

REFERENCES 311

CURRICULUM VITA 332

LIST OF TABLES IN APPENDIX

Table 1.1. Major Phase II detoxifying/antioxidant genes upregulated by select dietary chemopreventive agents and downregulated by a toxicant via the redox-sensitive transcription factor Nrf2 — 254

Table 2.1. Oligonucleotide primers used in quantitative real-time PCR (qRT-PCR) — 255

Table 2.2. BHA-induced Nrf2-dependent genes in mouse small intestine and liver — 256-261

Table 2.3. BHA-suppressed Nrf2-dependent genes in mouse small intestine and liver — 262-265

Table 3.1. Oligonucleotide primers used in quantitative real-time PCR (qRT-PCR) — 266

Table 3.2. TM-induced Nrf2-dependent genes in mouse small intestine and liver — 267-271

Table 3.3. **TM-suppressed Nrf2-dependent genes in mouse small intestine and liver** **272-275**

Table 4.1. **Oligonucleotide primers used for quantitative real-time PCR (qRT-PCR)** **276**

Table 4.2. **Temporal gene expression profiles elicited by combinations of SFN and EGCG** **277-278**

Table 4.3. **Temporal gene expression profiles elicited by combinations of SFN and EGCG in the presence of SOD** **279-280**

Table 5.1.A. **Human and Murine Matrix Families conserved between Nrf2 and AP-1** **281**

Table 5.1.B. **Human and Murine Matrix Families conserved between ATF-2 and ELK1** **282**

Table 5.2. **Matrices with conserved regulatory sequences in promoter regions of human, or murine, NRF2 and AP-1** **283-289**

Table 5.3.	**Temporal microarray analyses of genes suppressed by SFN+EGCG combination in the prostate of NRF2-deficient mice**	**290-293**
Table 6.1.	**Microarray datasets bearing inflammation/injury or cancer signatures**	**294-295**
Table 6.2.	**Human and Murine Matrix Families conserved between Nrf2 and Nfkb1**	**296**
Table 6.3.A.	**Multiple species alignment for Nfe2l2**	**297**
Table 6.3.B.	**Multiple species alignment for Nfkb1**	**298**
Table 6.4.	**Canonical first-generation regulatory network members representing putative crosstalk between Nrf2(Nfe2l2) and Nfkb1 in inflammation-associated carcinogenesis**	**299**
Table 7.1.	**Major gene clusters modulated in human prostate cancer**	**300-302**

Table 8.1. Human prostate cell lines used in this study and their descriptors **303**

Table 8.2. Genes modulated in all prostate cancer cell lines **304-310**

LIST OF FIGURES

Figure 1.1. The Keap1-Nrf2 axis in redox signaling – Proposed model for Nrf2 redox signaling **29-30**

Figure 1.2. The Nrf2 paradigm in gene expression - Proposed model for a multimolecular coactivator-corepressor complex that elicits transcriptional events through the ARE **31-32**

Figure 2.1. Chemical Structure of Butylated hydroxyanisole (BHA) **56**

Figure 2.2. Schematic representation of experimental design **57**

Figure 2.3. Regulation of Nrf2-dependent gene expression by BHA in mouse small intestine and liver **58**

Figure 2.4. Correlation of microarray data with quantitative real-time PCR data **59**

Figure 3.1. Chemical Structure of Tunicamycin (TM) **84**

Figure 3.2. Schematic representation of experimental design **85**

Figure 3.3. Regulation of Nrf2-dependent gene expression by TM in mouse small intestine and liver 86

Figure 3.4. Correlation of microarray data with quantitative real-time PCR data 87

Figure 4.1. Transactivation of AP-1 luciferase reporter by combinations of SFN and EGCG, and attenuation by SOD 117

Figure 4.2. Isobologram analyses of synergy between combinations of SFN and EGCG 118

Figure 4.3. Viability of the HT-29 AP-1 cells with the combinations of SFN and EGCG 119

Figure 4.4. Inhibition of EGCG-induced senescence by the combinations of SFN and EGCG 120

Figure 4.5. Protein expression with the combinations of SFN and EGCG 121

Figure 4.6. **HDAC inhibitor Trichostatin A potentiates the synergism elicited by the low-dose combination of SFN and EGCG** **122**

Figure 4.7. **Reactive oxygen species and SOD may modulate AP-1 transactivation by the combinations of SFN and EGCG** **123**

Figure 5.1A. **Diminished transactivation of AP-1 luciferase reporter by combinations of SFN and EGCG** **147**

Figure 5.1B. **Viability of the PC-3 AP-1 cells with the combinations of SFN and EGCG** **148**

Figure 5.2. **Temporal gene expression profiles elicited by combinations of SFN and EGCG** **149-153**

Figure 5.3. **Conserved Transcription Factor Binding Sites (TFBS) in promoter regions of ATF-2 and ELK-1** **154-156**

Figure 6.1. **Conserved TFBS between murine Nfe2l2 and Nfkb1 (A) and human NFE2l2 and NFKB1 (B)** **177-179**

Figure 6.2. **Multiple species alignment for Nfe2l2 (A) and Nfkb1 (B) with phylogenetic tree (C) and conserved TFBS among top matching human sequences (D)** **180-184**

Figure 6.3. **Canonical regulatory network (A) for Nrf2-Nfkb1 interactions in inflammation-associated carcinogenesis and literature networks in human (B) or mouse (C) and functional crosstalk (D)** **185-189**

Figure 6.4. **Putative model for Nrf2-Nfkb1 interactions in inflammation and carcinogenesis** **190-191**

Figure 7.1. **Major gene clusters modulated in human prostate cancer** **207**

Figure 7.2. **Candidate biomarkers in human prostate cancer (A) and putative crosstalk between them (B)** **208-209**

Figure 7.3. **Functional biological networks in human prostate cancer including (A) Cell Death, Cellular Growth and Differentiation, Cellular Development Network, (B) Gene Expression, Cancer, Cellular Growth and Proliferation Network, and (C) Merged Network** **210-213**

Figure 7.4. Identification of TFBS-association signatures 214

Figure 8.1. Clustering of human prostate cell lines used in the study 231

Figure 8.2. Biological network (A) in androgen-dependent human prostate cancer 22Rv1 cells and sub-network structure in upper (B) and lower (C) panels 232-235

Figure 8.3. Biological network (A) in androgen- and estrogen-dependent human prostate cancer LNCaP cells and sub-network structure (B) 236-238

Figure 8.4. Biological network (A) in androgen-dependent human prostate cancer MDA PCa 2b cells and sub-network structure (B) 239-241

Figure 8.5. Biological network in androgen-independent human prostate cancer DU 145 cells 242

Figure 8.6. Biological network in androgen-independent human prostate cancer PC-3 cells 243

Figure 8.7. Cell Death, Cancer, Cellular Development Network 244

Figure 8.8. Cancer, Endocrine System Development and Function, Organ Development Network 245

Figure 8.9. Cancer, Cell Death, Cellular Movement Network 246

Figure 8.10. Gene Expression, Cell Cycle, Cancer Network 247

Figure 8.11. Comprehensive overview (A) of all Metabolomics Networks in prostate cancer cell lines and sub-network structure in upper (B) and lower (C) panels 248-251

Figure 8.12. Regulatory element analyses for identification of TFBS-association signatures 252

CHAPTER 1

INTRODUCTION

Natural Dietary Anti-cancer chemopreventive compounds: Redox-mediated Differential Signaling Mechanisms in Cytoprotection of Normal Cells Versus Cytotoxicity in Tumor Cells [1,2,3]

1.1. Abstract

Pharmacogenomic profiling of cancer has recently seen much activity with the accessibility of the newest generation of high-throughput platforms and technologies. To develop a comprehensive understanding of cancer pathogenesis, and potential for chemopreventive intervention with dietary factors, an integrated approach that encompasses both pharmacogenomic and mechanistic aspects is desirable. Many dietary phytochemicals exhibit health beneficial effects including prevention of diseases such as cancer, neurological, cardiovascular, inflammatory and metabolic. Evolutionarily, herbivorous and omnivorous animals have been ingesting plants. This interaction between "animal-plant" ecosystems has resulted in an elaborate system of detoxification

---

[1]Part of this chapter has been published as a review article – **Nair, S.,** Kong, A.-N. T., Acta Pharmacol Sin., 2007 Apr;28(4):459-72.

[2]**Keywords :** Redox, Nrf2, Keap1, NES, NLS, gene expression profiles

[3]**Abbreviations :** ROS, Reactive oxygen species; RNS, Reactive Nitrogen species; Nrf2, Nuclear Factor-E2-related factor 2; ARE, Antioxidant response element; Keap1, Kelch-like erythroid CNC homologue (ECH)-associated protein 1; BHA, Butylated hydroxyanisole; EGCG, epigallocatechin-3-gallate; SFN, Sulforaphane; ER, Endoplasmic reticulum; UPR, Unfolded protein response; NES, Nuclear export signal; NLS, Nuclear localization signal; CBP, CREB-binding protein; Ncor1, nuclear receptor co-repressor 1; Nrip1, nuclear receptor co-repressor interacting protein; Ncoa3, nuclear receptor co-activator 3; Ncoa5, nuclear receptor co-activator 5; P/CAF, P300/CBP-associated factor; MAPK, mitogen activated protein kinase.

and defense mechanisms evolved by animals including humans. Mammalian, including human, cells respond to these dietary phytochemicals by "non-classical receptor sensing" mechanism of electrophilic chemical-stress typified by 'thiol modulated" cellular signaling events primarily leading to gene expression of pharmacologically beneficial effects, but sometimes unwanted cytotoxicity. Our laboratory has been studying two groups of dietary phytochemical cancer chemopreventive compounds (isothiocyanates and polyphenols), which are effective in chemical-induced as well as genetically induced animal carcinogenesis models. These compounds typically generate "cellular stress" and modulate gene expression of Phase II detoxifying/antioxidant enzymes. Indeed, electrophiles, reactive oxygen species (ROS) and reactive nitrogen species (RNS) are known to act as second messengers in the modulation of many cellular signaling pathways leading to gene expression changes and pharmacological responses. Redox-sensitive transcription factors such as Nrf2, AP-1, NF-κB, to cite a few examples, sense and transduce changes in cellular redox status and modulate gene expression responses to oxidative and electrophilic stresses presumably via sulfhyrdryl modification of critical cysteine residues found on these proteins and/or other upstream redox-sensitive molecular targets. In the current review, we will explore dietary cancer chemopreventive phytochemicals, discuss the link between oxidative/electrophilic stresses and the redox circuitry and consider different redox-sensitive transcription factors. We will also discuss the Keap1-Nrf2 axis in redox signaling of induction of Phase II detoxifying/antioxidant defense mechanisms, an important target and preventive strategy for normal cells against carcinogenesis, and conversely inhibition of cell growth/inflammatory signaling pathways that would confer therapeutic intervention

in many types of cancers. Further, we will summarize the Nrf2 paradigm in gene expression, the pharmacotoxicogenomic relevance of redox-sensitive Nrf2, and the redox regulation of cell death mechanisms. Finally, we will discuss the relevance of an integrated systems biology approach to cancer chemoprevention.

1.2. Introduction

Many dietary phytochemicals exhibit beneficial effects to health including prevention of diseases such as cancer, as well as neurological, cardiovascular, inflammatory and metabolic diseases. Evolutionarily, herbivorous and omnivorous animals have been ingesting plants. This interaction between "animal-plant" ecosystems has resulted in an elaborate system of detoxification and defense mechanisms evolved by animals including humans. Indeed, the condition of stress generated by electrophiles or xenobiotics may be referred to as electrophilic stress. Mammalian, including human, cells respond to these dietary phytochemicals by "non-classical receptor sensing" mechanism of electrophilic chemical-stress typified by 'thiol modulated" cellular signaling events primarily leading to gene expression of pharmacologically beneficial effects, but sometimes unwanted cytotoxicity also. Our laboratory has been studying two groups of dietary phytochemical cancer chemopreventive compounds (isothiocyanates and polyphenols) (reviewed in references[1,2]), which are effective in chemical-induced as well as genetically-induced animal carcinogenesis models[3,4]. These compounds typically generate "cellular stress" and modulate gene expression of Phase II detoxifying/antioxidant enzymes.

Multicellullar organisms rely on highly organized pathways to orchestrate the many extracellular clues received by the cells and to convert them into specific physiological processes. The classical first step in this cascade of molecular events that are collectively referred to as signal transduction pathways is the specific interaction of an extracellular ligand with its receptor at the cell membrane[5]. Indeed, reactive oxygen species (ROS) and reactive nitrogen species (RNS) have been proposed as second messengers in the activation of several signaling pathways leading to mitogenesis or apoptosis[5]. Effective transmission of information requires specificity, and how ROS signaling occurs with specificity and without oxidative damage remains poorly understood[6]. In addition, gene expression responses to oxidative stress are necessary to ensure cell survival and are largely attributed to specific redox-sensitive transcription factors[7]. Redox-sensitive cysteine residues are known to sense and transduce changes in cellular redox status caused by the generation of ROS and the presence of oxidized thiols[8].

Sporn and Liby[9] noted that the principal need in the chemoprevention of cancer remains the discovery of new agents that are effective and safe, and the development of new dose-scheduling paradigms that will allow their beneficial use over relatively long periods of time (but not necessarily constantly) in a manner that is essentially free of undesirable side effects. It has been reported[10] that human cancers overexpress genes that are specific to a variety of normal human tissues, including normal tissues other than those from which the cancer originated suggesting that this general property of cancer cells plays a major role in determining the behavior of the cancers, including their metastatic potential. Surh[11] observed that disruption or deregulation of

intracellular-signalling cascades often leads to malignant transformation of cells, and it is therefore important to identify the molecules in the signalling network that can be affected by individual chemopreventive phytochemicals to allow for better assessment of their underlying molecular mechanisms. Conney[12] suggested that tailoring the chemopreventive regimen to the individual or to groups of individuals living under different environmental conditions, or with different mechanisms of carcinogenesis, may be an important aspect of cancer chemoprevention in human populations. Given the inability to guarantee the long-term safety of current chemopreventive regimens, Sporn[9] suggested two approaches- the more widespread use of low-dose combinations of chemopreventive agents, with the goal of achieving a therapeutic synergy between individual drugs while reducing their individual toxicities; or the use of intermittent, rather than constant, chronic dosing of chemopreventive agents.

In the current review, we will attempt to shed light on redox-mediated signaling translating into gene expression and *in vivo* pharmacological events. We will explore dietary cancer chemopreventive phytochemicals, discuss the link between oxidative/electrophilic stress and the redox circuitry and consider a brief overview of redox-sensitive transcription factors. We will then discuss the Keap1-Nrf2 axis in redox signaling, an important target for preventive and possibly therapeutic intervention in many types of cancers. We will also discuss the Nrf2 paradigm in gene expression, transcriptome profiling of disparate gene categories, and the pharmacotoxicogenomic relevance of redox-sensitive Nrf2. Finally, we will discuss the redox regulation of cell death mechanisms.

1.3. Natural dietary anti-cancer chemopreventive compounds

Because carcinogenesis comprises three different stages - initiation, promotion and progression - many potential cancer-protective (chemopreventive) agents can be categorized broadly as blocking agents (which impede the initiation stage) or suppressing agents (which arrest or reverse the promotion and progression of cancer), presumably by affecting or perturbing crucial factors that control cell proliferation, differentiation, senescence or apoptosis[2,13]. Dietary chemopreventive compounds functioning as detoxifying enzyme inducers primarily include phenolic and sulfur-containing compounds. Phenolic compounds may be classified into polyphenols and flavonoids, whereas sulfur-containing compounds may be classified into isothiocyanates and organosulfur compounds[1]. Representative examples of polyphenols include epigallocatechin-3-gallate (EGCG) from green tea, curcumin from turmeric, and resveratrol from grapes; whereas flavonoids are exemplified by quercetin from citrus fruits and genistein from soy. Isothiocyanates include, amongst others, sulforaphane (SFN) from broccoli, phenethyl isothiocyanate (PEITC) from turnips and watercress, and allyl isothiocyanate from brusssels sprouts. Organosulfur compounds chiefly include diallyl sulfides from garlic oil. Dietary isothiocyanates are derived *in vivo* from the hydrolysis of glucosinolates present in cruciferous vegetables.

Our laboratory has worked extensively towards understanding the molecular mechanisms *in vitro* and determining the chemopreventive efficacy *in vivo* of polyphenols (e.g., EGCG and curcumin), and isothiocyanates (e.g., SFN and PEITC), and combinations of these phytochemicals to elicit maximum efficacy in cancer cells/tumorigenic tissue with minimum toxicity to normal cells. It is indeed quite

puzzling how these compounds can differentiate between “normal” versus “abnormal tumor” cells in terms of signaling, gene expression and pharmacological effects. We have shown[14] that EGCG treatment in human colon HT-29 cancer cells causes damage to mitochondria, and that c-Jun N-terminal kinase (JNK) mediates EGCG-induced apoptotic cell death. Similarly, it was shown[15] that PEITC can induce apoptosis in HT-29 cells in a time- and dose-dependent manner via the mitochondrial caspase cascade, and that the “activation” of JNK appears to be critical for the initiation of the apoptotic processes. On the other hand, EGCG, Curcumin, SFN and PEITC appear to “inhibit” (instead of activate) lipopolysaccharide (LPS)-induced nuclear factor-kappaB (NFκB) activation in the same cell type - HT-29 cells - stably transfected with an NFκB luciferase reporter construct[16]. In addition, the mechanism of action of SFN was recently[17] attributed to the inhibition of p38 Mitogen-Activated Protein Kinase (MAPK) isoforms which contributed to the induction of Antioxidant Response Element (ARE)-mediated heme oxygenase-1 gene expression in human hepatoma HepG2 cells. Besides, extracellular signal-regulated protein kinase (ERK) and JNK pathways were activated[18] by PEITC treatment in human prostate cancer PC-3 cells. Interestingly, a combination of PEITC and curcumin was found to have an additive effect[19] in the induction of apoptosis in PC-3 cells stably transfected with an NFκB luciferase reporter construct and involved an inhibition of EGFR and its downstream signaling including PI3K and Akt. *In vivo*, PEITC and curcumin alone or in combination exhibited significant cancer-preventive activities in NCr immunodeficient (nu/nu) mice bearing subcutaneous xenografts of PC-3 cells[20]. It is tempting to speculate that “abnormal tumor” cells such as PC-3 and HT-29 cells require the

overexpressed or hyper-activated NF-κB and/or EGFR for cell survival/proliferation, whereas "normal" cells do not require these signaling molecules to do so. Blockade of NF-κB and/or EGFR signaling by these compounds would sensitize tumor cells to die but not the normal cells (but, instead, in normal cells, these compounds will redox-dependently affect the Nrf2-mediated cellular detoxifying/antioxidant defense enzymes, which will be discussed in greater detail later on), and hence the potential specificities between "abnormal tumor" versus "normal" cells. Recently, we[3] and others[21] showed that SFN inhibited adenoma formation in the gastrointestinal tract of genetically mutant ApcMin/+ mice, and that the concentrations of SFN and its metabolite SFN-GSH were found to be between 3 and 30 nmol/g (~ 3 – 30 μM), which concentrations resembled that of the *in vitro* cell culture systems[22]. Interestingly, under such conditions, using immunohistochemical (IHC) staining of the adenomas indicated that SFN significantly suppressed the expression of phosphorylated-c-Jun-N-terminal kinase (p-JNK), phosphorylated-extracellular signal-regulated kinases (p-ERK) and phosphorylated-Akt (p-Akt), which were found to be highly expressed in the adenomas of ApcMin/+ mice versus normal mucosa[3]. When the acute effect of SFN on the gene expression profiles was investigated in the small intestine polyps of the SFN-treated Apc+/Min mice by using Affymetrix microarray platforms, the results showed that genes involved in apoptosis, cell growth and maintenance rather than Phase II detoxifying genes were modulated in the polyps of the SFN-treated Apc+/Min mice. Some of the proapoptotic genes such as MBD4 and serine/threonine kinase 17b, tumor necrosis factor receptor superfamily member 7 and tumor necrosis factor (ligand) superfamily member 11 were up-regulated while some pro-survival genes such as

cyclin-D2, integrin β1 and Wnt 9A were significantly down regulated in adenomas treated with SFN. Importantly, two important genes involved in colorectal carcinogenesis, arachidonate 15-lipoxygenase (15-LOX) and COX-2 were found to be increased and decreased respectively by SFN[3]. Most recently, we found that in the colon of the Nrf2 -/- mice challenged with the classical inflammatory agent dextran sodium sulfate (DSS), the inflammatory proteins such as COX-2 and iNOS were overexpressed with a concomitant decreased expression of cellular antioxidant enzymes such as HO-1 and NQO1 [23]. These results imply that the induction of antioxidant enzymes by dietary cancer chemopreventive compounds could potentially counteract the oxidative/inflammatory signaling pathways as suggested by Dinkova-Kostova *et al* [24].

1.4. Redox-mediated signaling

1.4.1. Oxidative stress and redox circuitry

Although oxidants are constantly generated for essential biologic functions, excess generation or an imbalance between oxidants and antioxidants can produce a common pathophysiologic condition known as oxidative stress[25]. Mediators of oxidative stress, i.e., reactive oxygen species (ROS), also function as second messengers in signal transduction. In the light of this knowledge, *oxidative stress* has been very remarkably defined as *perturbations in redox circuitry*[6]. Indeed, proteins present on cell surfaces and located in extracellular fluids undergo oxidation in diverse pathophysiologic conditions, and a growing body of evidence suggests that the steady-state oxidation is responsive to diet[25].

Interestingly, redox compartmentation functions as a mechanism for specificity in redox signaling and oxidative stress, with the relative redox states[6] from most reducing to most oxidizing being mitochondria > nuclei > cytoplasm > endoplasmic reticulum > extracellular space. Hansen *et al* [6]noted that a circuitry model for redox signaling and control has been developed based on the observations that three major thiol/disulfide couples, namely glutathione (GSH)/glutathione disulfide (GSSG), reduced thioredoxin [Trx-$(SH)_2$]/oxidized thioredoxin (Trx-SS), and cysteine (Cys)/cystine (CySS) are not in redox equilibrium and therefore could function as control nodes for many different redox-sensitive processes. In this model, redox switches and pathways exist in parallel circuits, with electron flow from NADPH as a central electron donor to ROS and O_2 as electron acceptors.

Given the involvement of reactive oxygen species (ROS) and reactive nitrogen species (RNS) in a multiplicity of physiological responses through modulation of signaling pathways, studies on RONS (reactive oxygen and nitrogen species) signaling have received considerable attention in recent times. Forman[5] noted primarily that (i) antioxidant enzymes are essential "turn-off" components in signaling, (ii) spatial relationships are probably more important in RONS signaling thatn the overall 'redox state' of the cell, and (iii) deprotonation of the cysteine to form the thiolate, which can react with RONS, occurs in specific protein sites providing specificity in signaling. The bacterial transcription factor OxyR[8] mediates the cellular response to both ROS and RNS by controlling the expression of the OxyR regulon, which encodes proteins involved in H_2O_2 metabolism and the cytoplasmic thiol redox response. In budding yeast, the transcription factor Yap1 (yeast AP1), which is a basic leucine zipper (bZip)

transcription factor, confers the cellular response to redox stress by controlling the expression of the regulon that encodes most yeast antioxidant proteins[8]. Interestingly, Georgiou[26] noted that, in both bacteria and yeast, the redox control networks exemplified by OxyR and Yap1 respectively exhibit conserved dynamic features, namely autoregulation (which in yeast is accomplished via reduction of Yap1 by thioredoxin) and hysteresis. Indeed, the question of whether these features are intrinsic properties of the regulatory architecture required for proper adaptation to redox stress remains to be resolved. Jacob[27] observed that DSOs (disulfide-S-oxides) are formed from glutathione under oxidizing conditions and specifically modulate the redox status of thiols, indicating the existence of specialized cellular oxidative pathways. This supports the paradigm of oxidative signal transduction and provides a general pathway whereby ROS can convert thiols into disulfides.

1.4.2. Redox-sensitive transcription factors

Many transcription factors are redox-sensitive, including Activator protein-1 (AP-1), Nuclear Factor kappa B (NF-κB), Nuclear Factor-E2-related factor 2 (Nrf2), p53, glucocorticoid receptor, and others[6]. Such sensitivity involves at least two redox-sensitive steps, one in activation of the signaling cascade and another in DNA binding, and possibly additional redox-sensitive nuclear processes such as nuclear import and export[6]. Nuclear and cytoplasmic redox couples perform distinct functions during redox-sensitive transcription factor regulation.

AP-1 is responsive to low levels of oxidants resulting in AP-1/DNA binding and an increase in gene expression. AP-1 activation is due to the induction of JNK activity by

oxidants resulting in the phosphorylation of serine 63 and serine 73 in the c-Jun transactivation domain[7,28,29]. With high concentrations of oxidants, AP-1 is inhibited and gene expression is impeded. Inhibition of AP-1/DNA interactions is attributed to the oxidation of specific cysteine residues in c-Jun's DNA binding region, namely cysteine 252[7,30]. Xanthoudakis and Curran[31] reported that a DNA repair enzyme apurinic/apyrimidinic endoculease (APE), also termed redox factor-1 (Ref-1), possessed oxidoreductase activity and was responsible for the redox regulation of AP-1. Oxidized AP-1 could be effectively reduced by Ref-1, restoring DNA binding activity. Trx1 was shown to be a critical player in AP-1 regulation by virtue of its ability to reduce oxidized Ref-1[32]. Thus, for AP-1, a nuclear pathway to reduce the Cys of the DNA-binding domain is distinct[6] from the upstream redox events that activate the signaling kinase pathway.

Similarly, NF-κB contains a redox-sensitive critical cysteine residue (cysteine 62) in the p50 subunit that is involved in DNA binding[7,33]. NF-κB is normally sequestered in the cytoplasm by IκB, but under oxidative conditions, IκB is phosphorylated by IκB kinase (IKK), ubiquitinated and subsequently degraded. ROS production appears to be necessary to initiate the events leading to the dissociation of the NF-κB/IκB complex[6], but excessive ROS production (oxidative stress) results in the oxidation of cysteine 62 which does not affect its translocation to the nucleus but rather interferes with DNA binding and decreases gene expression[7,34]. Overexpression of Trx1 inhibited NF-κB activity, but overexpression of nuclear-targeted Trx1 enhanced NF-κB activity[35]. These findings suggested[6] that Trx1 plays distinct roles within the

cytoplasm (regulation of activation and dissociation of IκB), and within the nucleus (regulation of DNA binding).

Pivotal to the antioxidant response[36-39] typical in mammalian homeostasis and oxidative stress is the important transcription factor Nrf2 or Nuclear Factor-E2-related factor 2 that has been extensively studied by many research groups[1,36-43]. Nrf2 is indispensable to cellular defense against many chemical insults of endogenous and exogenous origin, which play major roles in the etiopathogenesis of many cancers and inflammation-related diseases such as inflammatory bowel disease[23] and Parkinson's disease[44]. The role of Nrf2 as a critical redox-sensitive transcription factor will be discussed in greater detail in the following section devoted to redox signaling with specific emphasis on the Keap1-Nrf2 axis.

1.4.3. The Keap1-Nrf2 axis in redox signaling

Under homeostatic conditions, Nrf2 is mainly sequestered in the cytoplasm by a cytoskeleton-binding protein called Kelch-like erythroid CNC homologue (ECH)-associated protein 1 (Keap1)[13,40,45]. Zhang and Hannink[46] have identified two critical cysteine residues in Keap1, namely, C273 and C288 that are required for Keap1-dependent ubiquitination of Nrf2 as shown in Figure 1.1. They have also identified[46] a third cysteine residue in Keap1, namely, C151, that is uniquely required for inhibition of Keap1-dependent degradation of Nrf2 (Figure 1.1) by sulforaphane and oxidative stress. It has also been shown[47] that Keap1 is a redox-regulated substrate adaptor protein for a Cul3-dependent ubiquitin ligase complex that controls steady-state levels of Nrf2 in response to cancer-preventive compounds and oxidative stress. Moreover, it

has been reported[48] that Keap1 regulates the oxidation-sensitive shuttling of Nrf2 into and out of the nucleus via an active Crm1/exportin-dependent nuclear export mechanism. When challenged with oxidative stress, Nrf2 is quickly released from Keap1 retention and translocates to the nucleus[40,49]. We have recently identified[40] a canonical redox-insensitive nuclear export signal (NES) (^{537}LKKQLSTLYL^{546}) located in the leucine zipper (ZIP) domain of the Nrf2 protein, as well as a redox-sensitive NES (^{173}LLSI-PELQCLNI^{186}) in the transactivation (TA) domain of Nrf2[50]. Once in the nucleus, Nrf2 not only binds to the specific consensus cis-element called antioxidant response element (ARE) present in the promoter region of many cytoprotective genes[43,45], but also to other trans-acting factors such as small Maf (MafG and MafK)[51] that can coordinately regulate gene transcription with Nrf2. We have also reported[41] that different segments of Nrf2 transactivation domain have different transactivation potential; and that different mitogen-activated protein kinases (MAPKs) have differential effects on Nrf2 transcriptional activity with ERK and JNK pathways playing an unequivocal role in positive regulation of Nrf2 transactivation domain activity[41]. To better understand the biological basis of signaling through Nrf2, it has also become imperative to identify possible interacting partners of Nrf2 such as coactivators or corepressors apart from trans-acting factors such as small Maf[51,52].

A salient feature of the canonical redox-insensitive Nrf2-NES ($NES_{zip,}$ ^{537}LKKQLSTLYL^{546}) alluded to above is its overlap with the leucine zipper domain. This overlap implies that when Nrf2 forms heterodimers via its leucine zipper with other bZIP proteins, such as its obligatory binding partner small MafG/K proteins, the

NES motif may be simultaneously masked[40]. Further, we observed[40] that Nrf2 heterodimerization via leucine zipper with MafG/K may not only enhance the DNA binding specificity of Nrf2 but may also effectively recruit Nrf2 into the nucleus by simultaneously masking the NES activity. Accumulating evidence shows that after fulfilling its transactivation function, Nrf2 is destined for proteasomal degradation in the cytoplasm, although some weak degradation activity may also exist within the nucleus. Hence, Nrf2 signaling may be turned on and off rapidly to match the rapid changes of the cellular redox status[40]. Interestingly, a bipartite nuclear localization signal (bNLS, ^{494}RRRGKQKVAANQCRKRK^{511}) as well as an NES (^{545}LKRRLSTLYL^{554}) have been identified[53] in the C terminus of Nrf2, further underscoring the importance of nuclear import and export in controlling the subcellular localization of Nrf2.

Unlike the NES_{zip}, the new functional redox-sensitive NES located in the transactivation (TA) domain of Nrf2 (NES_{TA}, ^{173}LLSIPELQCLNI^{186}) possesses a reactive cysteine residue (C183)[50] and exhibited a dosage-dependent nuclear translocation when treated with sulforaphane[50]. The NES_{TA} motif functions as a redox-sensitive switch that can be turned on/off by oxidative signals and determines the subcellular localization of Nrf2[50]. These discoveries suggest that Nrf2 may be able to transduce redox signals in a Keap-1 independent manner; however, Keap1 may provide additional regulation of Nrf2 both in basal and inducible conditions.

Li *et al* [50]have recently proposed a new model for Nrf2 redox signaling. As depicted in Figure 1.1, the Nrf2 molecule possesses multivalent NES/NLS motifs, and their relative driving forces are represented by the size and direction of the arrows. Under unstimulated conditions (to the left of Figure 1.1), the combined nuclear exporting

forces of NES_{TA} [50] and NES_{zip} [50]may counteract the nuclear importing force of the bNLS[53]. As a result, Nrf2 exhibits a predominantly whole cell distribution. While the majority of Nrf2 molecules remain in the cytoplasm, the residual nuclear Nrf2 may account for the basal or constitutive Nrf2 activities. The observation of a small percentage of cells exhibiting nuclear and cytosolic distribution of Nrf2 may reflect the hyper- and hypo-oxidative condition of individual cells respectively. When challenged with oxidative stress (to the right of Figure 1.1), the redox-sensitive NES_{TA} is disabled but the redox-insensitive NES_{zip} remains functional[40,50] and the bNLS motif may remain functionally uninterrupted[50,54]. Since the driving force of the NES_{zip} is weaker than that of the bipartite bNLS, the nuclear importing force mediated by the bNLS prevails and triggers Nrf2 nuclear translocation[50] as shown in Figure 1.1.

1.5. Gene expression and *in vivo* pharmacological effects

1.5.1. The Nrf2 paradigm in gene expression

Nrf2 knockout mice are greatly predisposed to chemical-induced DNA damage and exhibit higher susceptibility towards cancer development in several models of chemical carcinogenesis[43]. Observations that Nrf2-deficient mice are refractory to the protective actions of some chemopreventive agents[43], indeed, highlight the importance of the Keap1-Nrf2-ARE signaling pathway as a molecular target for prevention. Hence, several studies have focused on using these Nrf2-deficient mice for pharmacogenomic or toxicogenomic profiling of the transcriptome in response to dietary chemopreventive agents[52,55-58] and toxicants[59].

1.5.2. Transcriptome profiling of putative Nrf2 coactivators and corepressors

In recent times, there is a renewed interest in dissecting the interacting partners of Nrf2 such as coactivators and corepressors which are co-regulated with Nrf2 to better understand the biochemistry of Nrf2. In a recent microarray study[55] with Nrf2 knockout mice, it was reported that CREB-binding protein (CBP) was upregulated in mice liver on treatment with (-)epigallocatechin-3-gallate (EGCG) in an Nrf2-dependent manner. Katoh *et al* [60] showed that two domains of Nrf2 (Neh4 and Neh5) cooperatively bind CBP and synergistically activate transcription. It was also demonstrated[41] previously, using a Gal4-Luc reporter co-transfection assay system in HepG2 cells, that the nuclear transcriptional coactivator CBP, which can bind to Nrf2 transactivation domain and can be activated by extracellular signal-regulated protein kinase (ERK) cascade, showed synergistic stimulation with Raf on the transactivation activities of both the chimera Gal4-Nrf2 (1-370) and the full-length Nrf2. In a recent microarray study with butylated hydroxyanisole (BHA) treatment in Nrf2 knockout mice[52], we observed the upregulation of the trans-acting factor v-maf musculoaponeurotic fibrosarcoma oncogene family protein G avian (MafG), nuclear receptor co-repressor 1 (Ncor1) and nuclear receptor co-repressor interacting protein (Nrip1); as well as downregulation of the nuclear receptor co-activator 3 (Ncoa3) in an Nrf2-dependent manner. Similarly, in another transcriptome profiling study in Nrf2 knockout mice with the Endoplasmic Reticulum (ER) stress inducer Tunicamycin[59] that modulates the unfolded protein response (UPR), we observed the upregulation of the P300/CBP-associated factor (P/CAF), trans-acting factor v-maf musculoaponeurotic fibrosarcoma oncogene family, protein F (Maf F), nuclear receptor co-activator 5

(Ncoa5), nuclear receptor co-repressor interacting protein (Nrip1) and Smad nuclear interacting protein 1 (Snip1) ; as well as downregulation of the src family associated phosphoprotein 2 (Scap2) in an Nrf2-dependent manner. Although microarray expression profiling cannot provide evidence of binding between partners, this could potentially suggest[52] that co-repressors Ncor1 and Nrip1 and co-activator Ncoa3, such as CBP in the previous studies, may serve as putative BHA-regulated nuclear interacting partners of Nrf2 in eliciting the cancer chemopreventive effects of BHA; and that co-repressor Nrip1 and co-activators P/CAF and Ncoa5 may serve as putative Tunicamycin-regulated nuclear interacting partners of Nrf2 in eliciting the UPR-responsive events[59] *in vivo*. Furthermore, induction of Nrip1 was observed in both small intestine and liver with BHA suggesting that the Nrf2/ARE pathway may play an important role in BHA-elicited regulation of this gene. It has also been shown recently[61] that coactivator P/CAF could transcriptionally activate a chimeric Gal4-Nrf2-Luciferase system containing the Nrf2 transactivation domain in HepG2 cells. In addition, P/CAF which is known[62] to be a histoneacetyl transferase protein has recently been shown[63] to mediate DNA damage-dependent acetylation on most promoters of genes involved in the DNA-damage and ER-stress response, which validates the observation[59] of P/CAF induction *via* Nrf2 in response to Tunicamycin-induced ER stress.

Taken together, it is tempting to speculate that dietary chemopreventive agents such as BHA and EGCG and toxicants such as Tunicamycin may elicit their chemopreventive and pharmacological/toxicological events through the ARE by means of a multimolecular complex[52,59] of coactivators and corepressors that function in concert

with the redox-sensitive transcription factor Nrf2 as depicted in Figure 1.2. The putative multimolecular complex may involve Nrf2 along with the transcriptional co-repressors Ncor1 and Nrip1 and the transcriptional co-activators Ncoa3, Ncoa5, P/CAF and CBP, in addition to the currently known trans-acting factors such as MafG[51], with multiple interactions between the members of the putative complex as has been shown recently with the p160 family of proteins[61]. As shown in Figure 1.2, chemical signals generated by dietary chemopreventive agents or toxicants may cause Nrf2 nuclear translocation that sets in motion a dynamic machinery of coactivators and corepressors that may form a multimolecular complex with Nrf2 to modulate transcriptional response through the ARE. Further studies of a biochemical nature would be needed to substantiate this hypothesis and extend our current understanding of Nrf2 regulation in chemoprevention with BHA or EGCG and in Tunicamycin-mediated ER stress.

1.5.3. Coordinated regulation of Phase I, II and III drug metabolizing enzyme/transporter genes via Nrf2

Dietary chemopreventives such as BHA, EGCG and Curcumin could coordinately regulate the Phase I, II, and III xenobiotic metabolizing enzyme genes as well as antioxidative stress genes through Nrf2-dependent pathways *in vivo* [52,55,56]. Interestingly, a co-ordinated response involving Phase I, II and III genes was also observed *in vivo* on ER stress induction with the toxicant Tunicamycin in an Nrf2-dependent manner[59]. The array of genes coordinately[52] modulated included Phase I drug metabolizing enzymes, Phase II detoxification and antioxidant genes, and Phase III transporter genes. The regulation of these genes could have significant effects on

prevention of tumor initiation by enhancing the cellular defense system, preventing the activation of procarcinogens/reactive intermediates, and increasing the excretion/efflux of reactive carcinogens or metabolites[52,56]. Indeed, the induction of Phase II enzymes itself achieves protection against the toxic and neoplastic effects of many carcinogens. In addition to enzymes (that conjugate to functionalized xenobiotics) such as glutathione S-transferases and UDP-glucuronosyltransferases, a provisional and partial list of Phase II genes might include[64] NAD(P)H:quinone reductase, epoxide hydrolase, dihydrodiol dehydrogenase, gamma-glutamylcysteine synthetase, heme oxygenase-1, leukotriene B4 dehydrogenase, aflatoxin B1 dehydrogenase, and ferritin. The major Phase II genes modulated via Nrf2 by BHA, EGCG, Curcumin, Sulforaphane, PEITC and Tunicamycin are summarized in Table 1.1.

1.5.4. Spatial and temporal control of Nrf2-mediated gene expression

It has been observed that the regulation of Nrf2-mediated gene expression takes place at both spatial and temporal levels in the *in vivo* whole animals. For example, the dietary chemopreventive BHA did not modulate the transcription of NAD(P)H:quinine oxidoreductase (NQO1) at 3 hours; however, NQO1 was induced by BHA at 12 hours[52]. The relatively delayed induction of the NQO1 gene compared with the other Phase II genes in response to BHA points to the possibility of differential kinetics of BHA-regulated Phase II gene response with temporal or time-dependent specificity. However, many other genes were modulated differentially at 3 hours in response to BHA between small intestine and liver[52] indicating certain spatial or tissue/compartment-dependent control of gene expression. Similar phenomena were

also observed in microarray studies with EGCG[55], Curcumin[56], SFN [57] and PEITC[58]. This could be attributed to a complex of physiological factors including partitioning across the gastrointestinal tract, intestinal transit time, uptake into the hepatobiliary circulation, exposure parameters such as Cmax, Tmax and AUC, and the pharmacokinetics of disposition after oral administration[52]. Other potential complicating factor(s) could be the possibility of differential tissue/organ-dependent expression of endogenous Keap1 and Nrf2 in conjunction with other tissue-specific/general nuclear coregulators and corepressors[41,61,65] which could dynamically shift the equilibrium locally in favor of or against Nrf2-mediated transcription of different ARE-driven genes.

1.5.5. Pharmacotoxicogenomic relevance of redox-sensitive Nrf2

Recently, it was reported[66] that Nrf1, another member of the Cap' n' Collar (CNC) family of basic leucine zipper proteins that is structurally similar to Nrf2, is normally targeted to the ER membrane, and that ER stress induced by Tunicamycin *in vitro* may play a role in modulating Nrf1 function as a transcriptional activator. As a protein-folding compartment, the ER is exquisitely sensitive to alterations in homeostasis, and provides stringent quality control systems to ensure that only correctly folded proteins transit to the Golgi and unfolded or misfolded proteins are retained and ultimately degraded. A number of biochemical and physiological stimuli, including perturbation in redox status, can disrupt ER homeostasis and impose stress to the ER, subsequently leading to accumulation of unfolded or misfolded proteins in the ER lumen[67]. The ER has evolved highly specific signaling pathways called the unfolded protein response

(UPR) to cope with the accumulation of unfolded or misfolded proteins[67,68]. ER stress stimulus by Thapsigargin has also been shown[69] to activate the c-Jun N-terminal kinase (JNK) or stress-activated protein kinase (SAPK) that is a member of the mitogen-activated protein kinase (MAPK) cascade[70]. Moreover, it has been reported that the coupling of ER stress to JNK activation involves transmembrane protein kinase IRE1 by binding to an adaptor protein TRAF2, and that IRE1$\alpha^{-/-}$ fibroblasts were impaired in JNK activation by ER stress[71]. It has been previously reported that phenethyl isothiocyanate (PEITC), contained in large amounts in cruciferous vegetables such as watercress, activates JNK1[72] , and that the activation of the antioxidant response element (ARE) by PEITC involves both Nrf2 and JNK1[42] in HeLa cells. It has also been demonstrated that extracellular signal-regulated kinase (ERK) and JNK pathways play an unequivocal role in positive regulation of Nrf2 transactivation domain activity *in vitro* in HepG2 cells. Although there is a growing interest amongst researchers in targeting the UPR against cancerous tumor growth[73], there is currently little understanding of the role of Nrf2 in modulating the UPR *in vivo.* Interestingly, in a Nrf2-deficient murine model[59], glutathione peroxidase 3 (Gpx3) was upregulated and superoxide dismutase 1 (Sod1) were downregulated by Tunicamycin in an Nrf2-deficient manner, which can have important implications in oxidative stress-mediated[22] pathophysiology or ER stress caused by perturbations in redox circuitry[22,67,74]. The identification of novel molecular targets that are regulated by the toxicant Tunicamycin via Nrf2 *in vivo* raises possibilities for targeting the UPR proteins in future to augment or suppress the ER stress response and modulate disease progression. Future toxicogenomic/toxicokinetic studies may provide new biological

insights into the diverse cellular and physiological processes that may be regulated by the UPR signaling pathways in cancer pharmacology and toxicology and the role(s) of Nrf2 in these processes.

1.5.6. Redox regulation of cellular signaling molecules leading to cell death mechanisms

It has been demonstrated[75] that the redox regulation of platelet-derived growth factor receptor (PDGFr) tyrosine autophosphorylation and its signaling are related to NADPH oxidase activity through protein kinase C (PKC) and phosphoinositide-3-kinase (PI3K) activation and H_2O_2 production. Cheng and Liu[76] reported that lead (Pb) increased lipopolysaccharide (LPS)-induced liver damage in rats by modulation of tumor necrosis factor-alpha and oxidative stress through protein kinase C and P42/44 mitogen-activated protein kinase. Recently, it was shown[77] that Rac upregulated tissue inhibitor of metalloproteinase-1 expression by redox-dependent activation of extracellular signal-regulated kinase (ERK) signaling. It has been reported[78] that cancer chemoprevention by the nitroxide antioxidant tempol acts partially via the p53 tumor suppressor.

Trachootham *et al* [79] have recently demonstrated a selective killing of oncogenically transformed cells by PEITC via an ROS-mediated mechanism. Oncogenic transformation of ovarian epithelial cells with H-Ras(V12) or expression of Bcr-Abl in hematopoietic cells caused elevated ROS generation and rendered the malignant cells highly sensitive to PEITC, which effectively disabled the glutathione antioxidant system and caused severe ROS accumulation preferentially in the transformed cells due to their active ROS output resulting in oxidative mitochondrial damage, inactivation of

redox-sensitive molecules, and massive cell death[79]. Xu *et al* [80] demonstrated an inhibition by SFN and PEITC on NF-κB transcriptional activation as well as down-regulation of NF-κB-regulated VEGF, cyclin D1, and Bcl-X(L) gene expression primarily through the inhibition of IKK-beta phosphorylation, and the inhibition of IκB-alpha phosphorylation and degradation, and decrease of nuclear translocation of p65 in human prostate cancer PC-3 cells. Furthermore, in the same PC-3 cells, PEITC and curcumin substantially inhibited EGFR, PI3K as well as Akt activation/phosphorylation, and the combination of PEITC and curcumin were more effective in the inhibition[19]. These inhibitions can also be recapitulated *in vivo* in PC-3 transplanted athymic nude mice[20] Shen and Pervaiz[81] have noted a role for redox-dependent execution in TNF receptor superfamily-induced cell death. Moreover, oxidation of the intracellular environment of hepatocytes by ROS or redox-modulating agents has been recently shown[82] to sensitize hepatocytes to TNF-induced apoptosis that seems to occur only in a certain redox range (in which redox changes can inhibit NF-κB activity but not completely inhibit caspase activity) by interfering with NF-κB signaling pathways. Nitric oxide has been reported[83] to induce thioredoxin-1 nuclear translocation that may be associated with the p21Ras survival pathway. Also, p53-independent G1 cell cycle arrest of HT-29 human colon carcinoma cells by SFN was shown[84] to be associated with induction of $p21^{CIP1}$ and inhibition of expression of cyclin D1. A small dose (10 μM) of hydrogen peroxide has been shown[85] to enhance TNF alpha-induced cell apoptosis, upregulate Bax and downregulate Bcl-2 expression in human vascular endothelial cell line ECV304.

Recently, a new functional class of redox-reactive thalidomide analogs with distinct and selective anti-leukemic activity have been identified[86]. These agents activate nuclear factor of activated T-cells (NFAT) transcriptional pathways while simultaneously repressing NF-κB via a rapid intracellular amplification of ROS that is associated with caspase-independent cell death[86]. This cytotoxicity is highly selective for transformed lymphoid cells and preferentially targets cells in S-phase of the cell cycle[86]. Capsaicin has been shown[87] to selectively induce apoptosis in mitogen-activated or transformed T cells with rapid increase of ROS; however, neither production of ROS nor apoptosis was detected in capsaicin-treated resting T cells suggesting differential signaling between activated/transformed T cells versus resting T cells. As noted elsewhere, a combination of PEITC and curcumin has been reported[19] to suppress epidermal growth factor receptor (EGFR) phosphorylation as well as phosphorylation of IκB-alpha and Akt. Furthermore, Kim *et al* [22] reported that SFN, at low concentrations, showed strong induction of Phase II genes that could potentially protect cells from cytotoxic effects; however, at high concentrations (above 50μM), SFN induced cell death with activation of caspase 3 and JNK1/2, which could be blocked by exogenous glutathione. The extent of SFN-induced cellular stress may, thus, decide the direction of signaling between cell survival and cell death[22]. The formation of mixed disulfides with GSH, which is known as S-glutathionylation, is a posttranslational modification that is emerging as an important mode of redox signaling[88]. Indeed, redox-reactive compounds provide a new tool through which selective cellular properties of redox status and intracellular bioactivation of potential redox-sensitive molecular targets can be leveraged by rational combinatorial therapeutic strategies and

appropriate drug design to exploit cell-specific vulnerabilities for maximum drug efficacy[86].

1.5.7. Modulation of apoptosis and cell-cycle control genes via Nrf2

Several genes related to apoptosis and cell-cycle control that are critical in the etiopathogenesis of many cancers have been shown[52,55-59] to be regulated through Nrf2 in response to several dietary chemopreventive agents and toxicants, which are far too many to be discussed here at least in normal murine tissues. The reader is referred to references[52,55-59] for a comprehensive list of these genes. Future studies would ascertain whether Nrf2 would be required for regulation of these apoptosis and cell-cycle control genes in tumor tissues/cells.

1.6. Integrated systems biology approach to cancer chemoprevention

Rhodes and Chinnaiyan [89] noted that although microarray profiling can to some extent decipher the molecular heterogeneity of cancer, integrative analyses that evaluate cancer transcriptome data in the context of other data sources are more capable of extracting deeper biological insight from the data. Indeed, integrative computational and analytical approaches, including Transcription Factor Binding Site (TFBS)-association signature analyses and transcriptional network analyses are a step in this direction with the ultimate aim of enhancing our understanding of prognostic biomarkers and key signaling pathways that are important in cancer progression, thus delineating functionally relevant targets for chemopreventive or therapeutic intervention. Thus, the elucidation of several target hubs in the latent structure of

biological networks and the delineation of key TFBS-association signatures, would help enhance our understanding of regulatory nodes that might be central to identifying key players in cellular signal transduction cascades that are important in the pathogenesis of cancer.

1.7. Concluding Remarks

In summary, electrophilic stress, oxidative stress or perturbations in redox circuitry can have a profound influence on the direction of signaling between cell survival and cell death. The potential involvement of cellular redox-sensitive transcription factors can modulate gene expression events and pharmacotoxicologic responses in diseases like cancer, thus, providing new molecular targets for preventive or therapeutic intervention. Indeed, controlled nutritional studies in future may specifically utilize extracellular redox measurements to explore mechanistic links between diet, health status, and diseases[25]. Taken together, redox-mediated signaling is an important mechanism for the cancer chemopreventive effects elicited by dietary anti-cancer chemopreventive compounds. Future studies will likely provide additional insights into the intricacies of the redox paradigm in signal transduction pathways with respect to the etiopathogenesis of cancer and its potential for chemopreventive intervention.

In addition, pharmacogenomic profiling of cancer has recently seen much activity with the accessibility of the newest generation of high-throughput platforms and technologies. A myriad of mechanistic studies have been devoted to identifying dietary factors that can help prevent cancer, with evidence gleaned from epidemiologic studies revealing an inverse correlation between the intake of cruciferous vegetables and the

risk of certain types of cancer. To develop a comprehensive understanding of cancer pathogenesis, and potential for chemopreventive intervention with dietary factors, an integrated approach that encompasses both pharmacogenomic and mechanistic aspects is desirable.

1.8. Acknowledgements

The authors are grateful to all members of the Kong laboratory as well as researchers in the scientific community whose works have been cited here. The authors also regret the inability to include many other excellent relevant citations in the interests of comprehensive abridgement. Works described here were supported in part by RO1-CA094828, RO1-CA092515, RO1-CA073674 and R01-CA118947 to Ah-Ng Tony Kong from the National Institutes of Health (NIH).

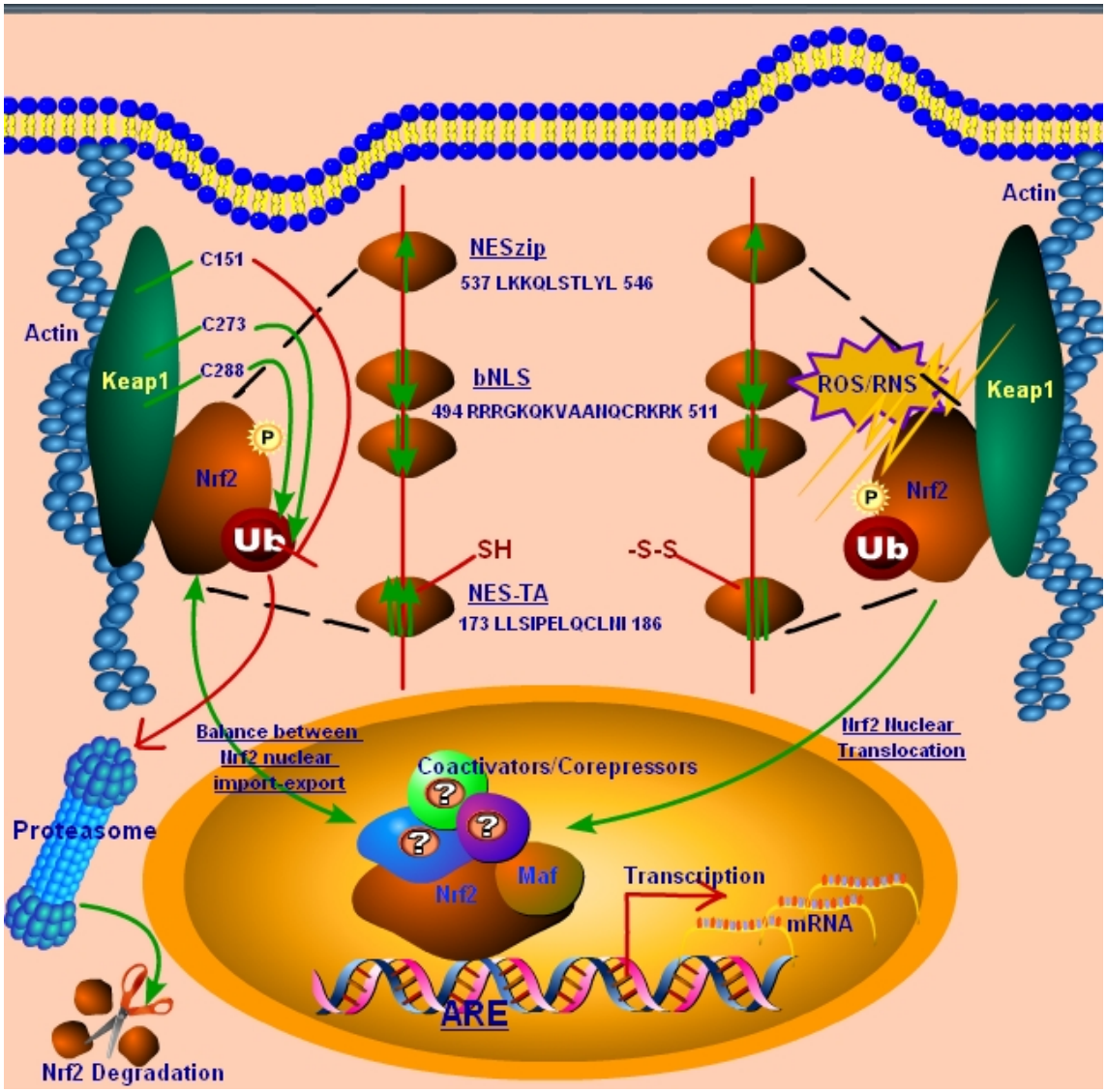

Figure 1.1. The Keap1-Nrf2 axis in redox signaling – Proposed model for Nrf2 redox signaling.

Nrf2 is sequestered to Keap1, a cytosolic actin-binding protein. Critical cysteine residues in Keap1 (C273[46] and C288[46]), are required for Keap1-dependent ubiquitination of Nrf2. A third cysteine residue in Keap1 (C151[46]), is uniquely required for inhibition of Keap1-dependent degradation of Nrf2. The Nrf2 molecule possesses multivalent NES/NLS motifs (dotted lines from Nrf2 molecule diverge to

encompass the dissected individual motifs), and their relative driving forces are represented by the size and direction of the arrows. Under unstimulated conditions (to the left of Figure 1), the combined nuclear exporting forces of NES_{TA} [50] and NES_{zip} [50] may counteract the nuclear importing force of the bNLS[53]. As a result, Nrf2 exhibits a predominantly whole cell distribution[50]. While the majority of Nrf2 molecules remain in the cytoplasm, the residual nuclear Nrf2 may account for the basal or constitutive Nrf2 activities. When challenged with oxidative stress (to the right of Figure 1), the redox-sensitive NES_{TA} is disabled but the redox-insensitive NES_{zip} remains functional[40,50] and the bNLS motif may remain functionally uninterrupted[50,54]. Since the driving force of the NES_{zip} is weaker than that of the bipartite bNLS, the nuclear importing force mediated by the bNLS prevails and triggers Nrf2 nuclear translocation as shown[50].

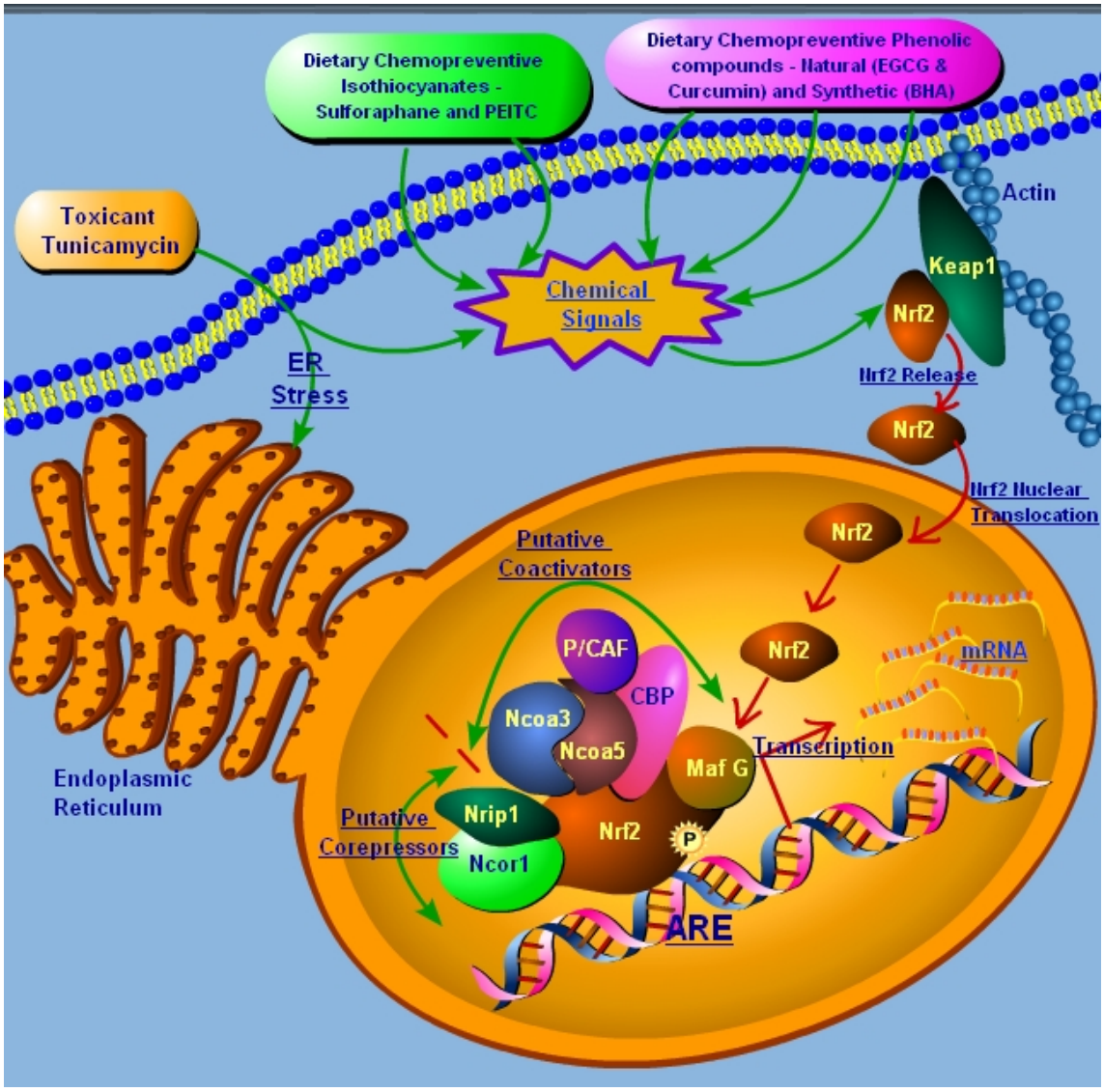

Figure 1.2. The Nrf2 paradigm in gene expression - Proposed model for a multimolecular coactivator-corepressor complex that elicits transcriptional events through the ARE.

Chemical signals generated by dietary chemopreventive agents or toxicants may cause Nrf2 nuclear translocation that sets in motion a dynamic machinery of coactivators and corepressors[52,59] that may form a multimolecular complex with Nrf2 to modulate transcriptional response through the ARE. The putative multimolecular complex may

involve the transcriptional co-repressors Ncor1[52] and Nrip1[52,59], and the transcriptional co-activators Ncoa3[52], Ncoa5[59], P/CAF[59], CBP[55], and MafG[52], with multiple interactions between the members of the putative complex that function in concert with the redox-sensitive transcription factor Nrf2 to elicit the chemopreventive and pharmacological/toxicological events through the ARE.

CHAPTER 2

Pharmacogenomics of Phenolic Antioxidant Butylated hydroxyanisole (BHA) in the Small Intestine and Liver of Nrf2 Knockout and C57BL/6J Mice[4,5,6]

2.1. Abstract

This objective of this study was to investigate the pharmacogenomics and the spatial regulation of global gene expression profiles elicited by cancer chemopreventive agent butylated hydroxyanisole (BHA) in mouse small intestine and liver as well as to identify BHA-modulated Nuclear Factor-E2-related factor 2 (Nrf2)–dependent genes. C57BL/6J (+/+; wildtype) and C57BL/6J/Nrf2(–/–; knockout) mice were administered a single 200 mg/kg oral dose of BHA or only vehicle. Both small intestine and liver were collected at 3 h after treatment and total RNA was extracted. Gene expression profiles were analyzed using 45,000 Affymetrix mouse genome 430 2.0 array and GeneSpring 7.2 software. Microarray results were validated by quantitative real-time reverse transcription-PCR analyses. Clusters of genes that were either induced or suppressed more than two-fold by BHA treatment compared with vehicle in C57BL/6J/Nrf2(-/-; knockout) and C57BL/6J/Nrf2(+/+; wildtype) mice genotypes were identified. Amongst

---

[4]Work described in this chapter has been published as **Nair, S**., Kong, A.-N. T., Pharm Res. 2006 Nov;23(11):2621-37.

[5]**Keywords** : Butylated hydroxyanisole, Nuclear Factor-E2-related factor 2, microarray, chemoprevention, global gene expression profiles.

[6]**Abbreviations :** BHA, Butylated hydroxyanisole; Nrf2, Nuclear Factor-E2-related factor 2; Mapk, Mitogen-activated protein kinase; ARE, Antioxidant response element.

these, in small intestine and liver, 1490 and 493 genes respectively were identified as Nrf2-dependent and upregulated, and 1090 and 824 genes respectively as Nrf2-dependent and downregulated. Based on their biological functions, these genes can be categorized into ubiquitination/proteolysis, apoptosis/cell cycle, electron transport, detoxification, cell growth/differentiation, transcription factors/interacting partners, kinases and phosphatases, transport, biosynthesis/metabolism, RNA/protein processing and nuclear assembly, and DNA replication genes. Phase II detoxification/antioxidant genes as well as novel molecular target genes, including putative interacting partners of Nrf2 such as nuclear corepressors and coactivators, were also identified as Nrf2-dependent genes. The identification of BHA-regulated and Nrf2-dependent genes not only provides potential novel insights into the gestalt biological effects of BHA on the pharmacogenomics and spatial regulation of global gene expression profiles in cancer chemoprevention, but also points to the pivotal role of Nrf2 in these biological processes.

2.2. Introduction

The phenolic antioxidant butylated hydroxyanisole (BHA) is a commonly used food preservative with broad biological activities [90], including protection against acute toxicity of chemicals, modulation of macromolecule synthesis and immune response, induction of phase II detoxifying enzymes, and, indeed, its potential tumor-promoting activities. Whereas the potential cytotoxicity of BHA has been partially attributed to reactive intermediates [90,91], BHA has also been shown to shift cell death from necrosis to apoptosis [92,93] and to inhibit mitochondrial complex I and lipoxygenases

[92]. A chemopreventive role for BHA is reiterated by the induction of A5 subunit of GST in rat liver immunoblotting experiments [94]. BHA has also been reported to increase the levels of liver glutathione and the activity of hepatic cytosolic gamma-glutamylcysteine synthetase [92]. Moreover, BHA has been shown to be an effective inhibitor of 7,12-dimethylbenz(a) anthracene-induced mammary carcinogenesis [95] in Sprague-Dawley rats; and is effective in the chemoprevention [96] of 1,2-dimethylhydrazine-induced large bowel neoplasms. In addition, BHA in diet has been demonstrated [97] to inhibit the initiation phase of 2-acetylaminofluorene and aflatoxin B1 hepatocarcinogenesis in rats. We have previously demonstrated [98] that the cytotoxicity of BHA is due to the induction of apoptosis that is mediated by the direct release of cytochrome c and the subsequent activation of caspases.

Pivotal to the antioxidant response [36-39] typical in mammalian homeostasis and oxidative stress is the important transcription factor Nrf2 or Nuclear Factor-E2-related factor 2 that has been extensively studied by many research groups [36-39] including this laboratory [1,40-42]. Under homeostatic conditions, Nrf2 is mainly sequestered in the cytoplasm by a cytoskeleton-binding protein called Kelch-like erythroid CNC homologue (ECH)-associated protein 1 (Keap1) [13,40,45]. When challenged with oxidative stress, Nrf2 is quickly released from Keap1 retention and translocates to the nucleus [40,49]. We have recently identified [40] a canonical redox-insensitive nuclear export signal (NES) (^{537}LKKQLSTLYL^{546}) located in the leucine zipper (ZIP) domain of the Nrf2 protein. Once in the nucleus, Nrf2 not only binds to the specific consensus cis-element called antioxidant response element (ARE) present in the promoter region of many cytoprotective genes [41,43,45], but also to other trans-acting factors such as

small Maf (MafG and MafK) [51] that can coordinately regulate gene transcription with Nrf2. We have previously demonstrated [90,99] that BHA is capable of activating distinct mitogen-activated protein kinases (MAPKs) such as extracellular signal-regulated protein kinase 2 (ERK2), and c-Jun N-terminal kinase 1 (JNK1). We have also reported [41] that different segments of Nrf2 transactivation domain have different transactivation potential; and that different MAPKs have differential effects on Nrf2 transcriptional activity with ERK and JNK pathways playing an unequivocal role in positive regulation of Nrf2 transactivation domain activity [41]. To better understand the biological basis of signaling through Nrf2, it has also become imperative to identify possible interacting partners of Nrf2 such as coactivators or corepressors apart from trans-acting factors such as small Maf [51].

Nrf2 knockout mice are greatly predisposed to chemical-induced DNA damage and exhibit higher susceptibility towards cancer development in several models of chemical carcinogenesis [43]. Observations that Nrf2-deficient mice are refractory to the protective actions of some chemopreventive agents [43], indeed, highlight the importance of the Keap1-Nrf2-ARE signaling pathway as a molecular target for prevention. In the present study, we have investigated, by microarray expression profiling, the global gene expression profiles elicited by oral administration of BHA in small intestine and liver of Nrf2 knockout (C57BL/6J/Nrf2-/-) and wild type (C57BL/6J) mice to enhance our understanding of BHA-regulated cancer chemopreventive effects mediated through Nrf2. We have identified clusters of BHA-modulated genes that are Nrf2-dependent in small intestine and liver and categorized them based on their biological functions. The identification of BHA-regulated Nrf2-

dependent genes will yield valuable insights into the role of Nrf2 in BHA-modulated gene regulation and cancer chemopreventive effects. This study also enables the identification of novel molecular targets for BHA-mediated chemoprevention that are regulated by Nrf2. The current study is also the first to investigate the global gene expression profiles elicited by BHA in an *in vivo* murine model where the role of Nrf2 is also examined.

2.3. Materials and Methods

Animals and Dosing : The protocol for animal studies was approved by the Rutgers University Institutional Animal Care and Use Committee (IACUC). Nrf2 knockout mice Nrf2 (-/-) (C57BL/SV129) have been described previously.[100] Nrf2 (-/-) mice were backcrossed with C57BL/6J mice (The Jackson Laboratory, ME USA). DNA was extracted from the tail of each mouse and genotype of the mouse was confirmed by polymerase chain reaction (PCR) by using primers (3'-primer, 5'-GGA ATG GAA AAT AGC TCC TGC C-3'; 5'-primer, 5'-GCC TGA GAG CTG TAG GCC C-3'; and lacZ primer, 5'-GGG TTT TCC CAG TCA CGA C-3'). Nrf2(-/-) mice-derived PCR products showed only one band of ~200bp, Nrf2 (+/+) mice-derived PCR products showed a band of ~300bp while both bands appeared in Nrf2(+/-) mice PCR products. Female C57BL/6J/Nrf2(-/-) mice from third generation of backcrossing were used in this study. Age-matched female C57BL/6J mice were purchased from The Jackson Laboratory (Bar Harbor, ME). Mice in the age-group of 9-12 weeks were housed at Rutgers Animal Facility with free access to water and food under 12 h light/dark cycles. After one week of acclimatization, the mice were put on AIN-76A

diet (Research Diets Inc. NJ USA) for another week. The mice were then administered BHA (Sigma-Aldrich, St.Louis, MO) at a dose of 200 mg/kg (dissolved in 50% PEG 400 solution at a concentration of 20 mg/ml)) by oral gavage. The control group animals were administered only vehicle (50% PEG 400 solution). Each treatment was administered to a group of four animals for both C57BL/6J and C57BL/6J/Nrf2(-/-) mice. Mice were sacrificed 3h after BHA treatment or 3 h after vehicle treatment (control group). Livers and small intestines were retrieved and stored in RNA Later (Ambion, Austin,TX) solution.

Sample Preparation for Microarray Analyses: Total RNA from liver and small intestine tissues were isolated by using a method of TRIzol (Invitrogen, Carlsbad, CA) extraction coupled with the RNeasy kit from Qiagen (Valencia, CA). Briefly, tissues were homogenized in trizol and then extracted with chloroform by vortexing. A small volume (1.2 ml) of aqueous phase after chloroform extraction and centrifugation was adjusted to 35% ethanol and loaded onto an RNeasy column. The column was washed, and RNA was eluted following the manufacturer's recommendations. RNA integrity was examined by electrophoresis, and concentrations were determined by UV spectrophotometry.

Microarray Hybridization and Data Analysis: Affymetrix (Affymetrix, Santa Clara, CA) mouse genome 430 2.0 array was used to probe the global gene expression profiles in mice following BHA treatment. The mouse genome 430 2.0 Array is a high-density oligonucleotide array comprised of over 45,101 probe sets representing over

34,000 well-substantiated mouse genes. The library file for the array is available at http://www.affymetrix.com/support/technical/libraryfilesmain.affx. After RNA isolation, all the subsequent technical procedures including quality control and concentration measurement of RNA, cDNA synthesis and biotin-labeling of cRNA, hybridization and scanning of the arrays, were performed at CINJ Core Expression Array Facility of Robert Wood Johnson Medical School (New Brunswick, NJ). Each chip was hybridized with cRNA derived from a pooled total RNA sample from four mice per treatment group, per organ, and per genotype (a total of eight chips were used in this study) (Figure 2.2). Briefly, double-stranded cDNA was synthesized from 5 μg of total RNA and labeled using the ENZO BioArray RNA transcript labeling kit (Enzo Life Sciences, Inc.,Farmingdale, NY, USA) to generate biotinylated cRNA. Biotin-labeled cRNA was purified and fragmented randomly according to Affymetrix's protocol. Two hundred microliters of sample cocktail containing 15 μg of fragmented and biotin-labeled cRNA was loaded onto each chip. Chips were hybridized at 45°C for 16 h and washed with fluidics protocol EukGE-WS2v5 according to Affymetrix's recommendation. At the completion of the fluidics protocol, the chips were placed into the Affymetrix GeneChip Scanner where the intensity of the fluorescence for each feature was measured. The expression value (average difference) for each gene was determined by calculating the average of differences in intensity (perfect match intensity minus mismatch intensity) between its probe pairs. The expression analysis file created from each sample (chip) was imported into GeneSpring 7.2 (Agilent Technologies, Inc., Palo Alto, CA) for further data characterization. Briefly, a new experiment was generated after importing data from the same organ in which data was

normalized by array to the 50th percentile of all measurements on that array. Data filtration based on flags present in at least one of the samples was first performed, and a corresponding gene list based on those flags was generated. Lists of genes that were either induced or suppressed more than two fold between treated versus vehicle group of same genotype were created by filtration-on-fold function within the presented flag list. By use of color-by-Venn-Diagram function, lists of genes that were regulated more than two fold only in C57BL/6J mice in both liver and small intestine were created. Similarly, lists of gene that were regulated over two fold regardless of genotype were also generated.

Quantitative Real-time PCR for Microarray Data Validation: To validate the microarray data, 13 genes of interest were selected from various categories for quantitative real-time PCR analyses. Glyceraldehyde-3-phosphate-dehydrogenase (GAPDH) served as the "housekeeping" gene. The specific primers for these genes listed in Table 2.1 were designed by using Primer Express 2.0 software (Applied Biosystems, Foster City, CA) and were obtained from Integrated DNA Technologies, Coralville, IA. The specificity of the primers was examined by a National Center for Biotechnology Information Blast search of the mouse genome. Instead of using pooled RNA from each group, RNA samples isolated from individual mice as described earlier were used in real-time PCR analyses. For the real-time PCR assays, briefly, first-strand cDNA was synthesized using 4μg of total RNA following the protocol of SuperScript III First-Strand cDNA Synthesis System (Invitrogen) in a 40 μl reaction volume. The PCR reactions based on SYBR Green chemistry were carried out using 100 times

diluted cDNA product, 60 nM of each primer, and SYBR Green master mix (Applied Biosystems, Foster City, CA) in 10 µl reactions. The PCR parameters were set using SDS 2.1 software (Applied Biosystems, Foster City, CA) and involved the following stages : 50°C for 2min, 1 cycle; 95°C for 10 mins, 1 cycle; 95°C for 15 secs → 55 °C for 30 secs →72°C for 30 secs, 40 cycles; and 72°C for 10 mins, 1 cycle. Incorporation of the SYBR Green dye into the PCR products was monitored in real time with an ABI Prism 7900HT sequence detection system, resulting in the calculation of a threshold cycle (C_T) that defines the PCR cycle at which exponential growth of PCR products begins. The carboxy-X-rhodamine (ROX) passive reference dye was used to account for well and pipetting variability. A control cDNA dilution series was created for each gene to establish a standard curve. After conclusion of the reaction, amplicon specificity was verified by first-derivative melting curve analysis using the ABI software and the integrity of the PCR reaction product and absence of primer dimers was ascertained. The gene expression was determined by normalization with control gene GAPDH.

Statistics : In order to validate the results, the correlation between corresponding microarray data and real-time PCR data was evaluated by the 'coefficient of determination', $\mathbf{r^2} = 0.89$.

2.4. Results

2.4.1. BHA-Modulated Gene Expression Patterns in Mouse Small Intestine and Liver

Subsequent to data normalization, 50.5% (22,779) of the probes passed the filtration based on flags present in at least one of four small intestine sample arrays depicted in Figure 2.2. Amongst these probes, 13.86% and 11.69% of probes were induced and suppressed over two fold respectively regardless of genotype. Expression levels of 2580 probes were either elevated (1490) or suppressed (1090) over two fold by BHA only in the wild-type mice, while 3243 probes were either induced (1669) or inhibited (1574) over two fold by BHA only in the Nrf2(–/–) mice small intestine (Figure 2.3A). Similarly, changes in gene expression profiles were also observed in mice liver. Overall, the expression levels of 52.79% (23,809) probes were detected in least in one of four liver sample arrays depicted in Figure 2.2. Amongst these probes, 6.29% and 5.94% of probes were induced and suppressed over two fold respectively regardless of genotype. In comparison with the results from small intestine sample arrays, a smaller proportion (1317) of well-defined genes were either elevated (493) or suppressed (824) over two fold by BHA in wild-type mice liver alone; whereas 1596 well-defined genes were induced (1005) or inhibited (591) in Nrf2(–/–) mice liver. (Figure 2.3B).

2.4.2. Quantitative Real–Time PCR Validation of Microarray Data

To validate the data generated from the microarray studies, several genes from different categories (Table 2.1) were selected to confirm the BHA-regulative effects by the use of quantitative real-time PCR analyses as described in detail under Materials and Methods.

After ascertaining the amplicon specificity by first-derivative melting curve analysis, the values obtained for each gene were normalized by the values of corresponding GAPDH expression levels. The fold changes in expression levels of treated samples over control samples were computed by assigning unit value to the control (vehicle) samples. Computation of the correlation statistic showed that the data generated from the microarray analyses are well-correlated with the results obtained from quantitative real-time PCR (coefficient of determination, $r^2 = 0.89$, Figure 2.4).

2.4.3. BHA-Induced Nrf2-Dependent Genes in Small Intestine and Liver

Genes that were induced only in wild-type mice, but not in Nrf2(–/–) mice, by BHA were designated as BHA-induced Nrf2-dependent genes. Based on their biological functions, these genes were classified into categories, including ubiquitination and proteolysis, electron transport, detoxification enzymes, transport, apoptosis and cell cycle control, cell adhesion, kinases and phosphatases, transcription factors and interacting partners, RNA/Protein processing and nuclear assembly, biosynthesis and metabolism, cell growth and differentiation, and G protein-coupled receptors (Table 2.2 lists a subset of these genes relevant to our interest).

Gene expression in small intestine in response to BHA treatment was more sensitive than that elicited in the liver with a larger number of Nrf2-dependent genes being upregulated in the former. The category of transcription factors and interacting partners predominated the upregulated genes followed by kinases and phosphatases. In the former category, a number of interesting transcription factors were identified as BHA-regulated Nrf2-dependent genes. In the small intestine, these primarily included insulin-

like growth factor 2 *(Igf2)*, Jun oncogene *(Jun)*, Notch gene homolog 4 (Drosophila) *(Notch 4)*, nuclear receptor co-repressor *(Ncor1)*, nuclear receptor interacting protein 1 *(Nrip1)*, serum response factor binding protein 1 *(Srfbp1)*, Spred-1 *(Spred1)*, suppressor of cytokine signaling 5 *(Socs5)*, thyroid hormone receptor beta *(Thrb)*, transforming growth factor, beta receptor 1*(Tgfbr1)*, transducer of ERBB2, 2 *(Tob2)*, members 19 and 23 of tumor necrosis factor superfamily *(Tnfrsf19 and Tnfrsf23)*, v-maf musculoaponeurotic fibrosacroma oncogene family, protein G (avian) *(MafG)*, and wingless-type MMTV integration site 9B *(Wnt9b)*. Similarly, the major BHA-regulated Nrf2-dependent transcription factors identified in the liver included Activating signal cointegrator 1 complex subunit 2 (Ascc2), Eph receptor A3 (Epha3), Eph receptor B1 (Ephb1), fos-like antigen 2 (Fosl2), insulin-like growth factor 2 receptor (Igf2r), nuclear receptor interacting protein 1 *(Nrip1)*, RAB4A member RAS oncogene family (Rab4a), reticuloendotheliosis oncogene (Rel), and transcription factor AP-2 beta (Tcfap2b). Interestingly, induction of Nrip1 was observed in both small intestine and liver suggesting that the Nrf2/ARE pathway may play a dominant role in BHA-elicited regulation of this gene.

Amongst the kinases and phosphatases in small intestine, the highest expression was seen with microtubule associated serine/threonine kinase-like (Mastl). Several important members of the mitogen-activated protein kinase (Mapk) pathway activating the Nrf2/ARE signaling were also induced in the small intestine including Mapk8, Mapk6, Map3k9, Map4k4 and Map4k5 with strongest induction seen with Mapk8. Moreover, induction was also observed of Janus kinase 2 (Jak2), types 1 and 2 of neurotrophic tyrosine kinase, receptor (Ntrk1 and Ntrk2), tyrosine kinase, non-

receptor,1 (Tnk1). Comparable expression was noted of different isoforms of protein kinases including epsilon, eta, and cAMP dependent regulatory, type II alpha (Prkce, Prkch and Prkar2a respectively). Regulatory subunits of protein phosphatase 1 (Ppp1r14a) and 2 (Ppp2r5e) and catalytic subunit of protein phosphatase 3, beta isoform (Ppp3cb) were also upregulated in the small intestine as BHA-regulated and Nrf2-dependent genes. In the liver, the genes induced in the same category included diacylglycerol kinase kappa (Dagkκ) , inhibitor of kappaB kinase gamma (Iκbkg), protein kinase, cAMP dependent regulatory, type I, alpha (Prkar1a), protein tyrosine phosphatase (Ptp), and putative membrane-associated guanylate kinase 1 (Magi-1) mRNA, alternatively spliced c form (Baiap1).

Representative genes induced by BHA in an Nrf2-dependent manner in the category of apoptosis and cell cycle control genes included members of the caspase cascade as well as cyclins G1 and T2 in small intestine; and growth arrest and DNA-damage-inducible 45 alpha (Gadd45a) in liver. Several important Nrf2-dependent detoxifying genes were also upregulated by BHA including glutamate-cysteine ligase, catalytic subunit (Gclc) in both small intestine and liver, glutathione S-transferase, mu 1 (Gstm1) and mu 3 (Gstm3) isoforms in small intestine and liver respectively, and heme oxygenase (decycling) 1 (Hmox1) in liver. BHA could also modulate many other important categories of genes in an Nrf2-dependent manner. Salient amongst them were the biosynthesis and metabolism genes, G-protein coupled receptors, RNA/protein processing and nuclear assembly, ubiquitination and proteolysis, and transport genes. Major transporters induced included the multidrug resistance associated proteins Mrp1

and 3 and Mdr1. Also induced were the sodium/glucose cotransporter (Slc5a12) and ion channels for sodium, potassium and chloride ions.

2.4.4. BHA-Suppressed Nrf2-Dependent Genes in Small Intestine and Liver

As shown in Table 2.3, which lists a subset of genes relevant to our interest, BHA treatment also inhibited the expression of many genes falling into similar functional categories in an Nrf2-dependent manner, although the number of genes was smaller. Notably, the category of transcription factors and interacting partners remained the largest amongst these genes with Nuclear receptor coactivator 3 (Ncoa3), and src family associated phosphoprotein 1 (Scap1) being among the genes suppressed by BHA and co-regulated with Nrf2 in small intestine; and epidermal growth factor receptor pathway substrate 15 (Eps15) and Hypoxia inducible factor 1, alpha subunit (Hif1a) being suppressed in the liver.

Amongst the kinases and phosphatases, BHA suppressed, in small intestine, the expression of G protein-coupled receptor kinase 5 (Grk5), glycogen synthase kinase 3 beta (Gsk3β), Mapk-activated protein kinase 5 (Mapkapk5), Mapk associated protein 1 (Mapkap1), p21-activated kinase 3 (Pak3), and ribosomal protein S6 kinase, polypeptide 4 (Rps6ka4). In the liver, BHA suppressed, in an Nrf2-dependent manner, genes such as Map2k7, phosphoinositide-3-kinase, regulatory subunit 5, p101 (Pik3r5), Ribosomal protein S6 kinase, polypeptide 5 (Rps6ka5) and microtubule associated serine/threonine kinase family member 4 (Mast4) amongst others.

Major genes down-regulated by BHA in an Nrf2-dependent manner in the category of apoptosis and cell cycle control included B-cell leukemia/lymphoma 2 (Bcl2), breast

cancer 1 (Brca1), and Cyclin I in liver. Among the transport genes, the fatty acid binding protein 6, ileal (gastrotropin) (Fabp6) was suppressed in small intestine by BHA. In the category of electron transport genes, representative genes included the cytochrome c oxidase, subunit VIIa 1 (Cox7a1) which was inhibited in both small intestine and liver, and thioredoxin reductase 2 (Txnrd2) which was suppressed in liver. Besides, members of the cytochrome P450 family such as Cyp3a44 in small intestine, and Cyp21a1 and Cyp7a1 in liver were also down-regulated by BHA in an Nrf2-dependent manner in the same category. Other categories of BHA-suppressed genes including ubiquitination and proteolysis, RNA/protein processing and nuclear assembly, biosynthesis and metabolism, and cell growth and differentiation were also identified as regulated through Nrf2.

2.5. Discussion

Since BHA was first introduced as a food preservative back in the 1960s, it has attracted a lot of attention and debate because of its potentially diverse biological effects on the health of humans including its potential cancer chemopreventive effects. Although extensive studies have been conducted to define the biological activities of BHA, and a growing body of evidence has been accumulated, a comprehensive definition of the potential cellular targets of BHA that trigger important signal transduction pathways remains a challenge that has yet to be undertaken. Indeed, the molecular basis and the mechanisms of action of BHA are not quite yet fully understood [90]. Transcription factor Nrf2 or Nuclear Factor-E2 -related factor 2 is indispensable to cellular defense against many chemical insults of endogenous and exogenous origin[43], which play

major roles in the etiopathogenesis of many cancers. Pivotal to this role of Nrf2 is the antioxidant response element (ARE) present in the promoter regions of many cytoprotective genes [43,45]. Indeed, Nrf2 (-/-; deficient) mice, which are highly susceptible to cancer development, are known to be refractory to the protective actions of some cancer chemopreventive agents [43]. It is, therefore, of interest to investigate the role of Nrf2 in BHA-elicited global gene expression profiles *in vivo* in order to extend the latitude of current understanding on the Nrf2-ARE signaling pathway that has emerged as an important molecular target for cancer chemoprevention. To our knowledge, this is the first attempt to elucidate, by microarray expression profiling, the gestalt genomic basis of BHA-regulated Nrf2-dependent cancer chemoprevention *in vivo* in an Nrf2-deficient murine model.

In the continuing quest to unravel the complex secrets of the biology of Nrf2 in cancer chemoprevention, there is renewed interest in dissecting the interacting partners of Nrf2 such as coactivators and corepressors which are co-regulated with Nrf2. In a recent microarray study [55], we have reported that CREB-binding protein (CBP) was upregulated in mice liver on treatment with (-)epigallocatechin-3-gallate (EGCG) in an Nrf2-dependent manner. We have also demonstrated [41] previously, using a Gal4-Luc reporter co-transfection assay system in HepG2 cells, that the nuclear transcriptional coactivator CBP, which can bind to Nrf2 transactivation domain and can be activated by extracellular signal-regulated protein kinase (ERK) cascade, showed synergistic stimulation with Raf on the transactivation activities of both the chimera Gal4-Nrf2 (1-370) and the full-length Nrf2. In the current study, we observed the upregulation of the trans-acting factor v-maf musculoaponeurotic fibrosarcoma oncogene family, protein G,

avian (MafG), nuclear receptor co-repressor 1 (Ncor1) and nuclear receptor co-repressor interacting protein (Nrip1); as well as downregulation of the nuclear receptor co-activator 3 (Ncoa3) in an Nrf2-dependent manner. Although microarray expression profiling cannot provide evidence of binding between partners, this is the first investigation to potentially suggest that co-repressors Ncor1 and Nrip1 and co-activator Ncoa3, such as CBP in our previous studies, may serve as putative BHA-regulated nuclear interacting partners of Nrf2 in eliciting the cancer chemopreventive effects of BHA. Furthermore, induction of Nrip1 was observed in both small intestine and liver suggesting that the Nrf2/ARE pathway may play an important role in BHA-elicited regulation of this gene. Taken together, it is tempting to speculate that the BHA-regulated chemopreventive effects through the ARE may be regulated by a multimolecular complex, which involves Nrf2 along with the transcriptional co-repressors Ncor1 and Nrip1 and the transcriptional co-activator Ncoa3, in addition to the currently known trans-acting factors such as MafG [51], with multiple interactions between the members of the putative complex as we have shown recently with the p160 family of proteins [101]. Further studies of a biochemical nature would be needed to substantiate this hypothesis and extend our current understanding of Nrf2 regulation in chemoprevention with BHA.

The major detoxification genes induced in this study included glutamate-cysteine ligase, catalytic subunit (Gclc) in both small intestine and liver, glutathione S-transferase, mu 1 (Gstm1) and mu 3 (Gstm3) isoforms in small intestine and liver respectively, and heme oxygenase (decycling) 1 (Hmox1) in liver. Since Nrf2 binds to the cis-acting ARE and induces the expression of many important Phase II detoxification and antioxidant genes

[36,43,45,49], and since BHA is known to induce Phase II genes, the current study on spatial regulation in small intestine and liver of BHA-regulated chemopreventive effects *via* Nrf2 showing the upregulation of Phase II detoxification genes is, indeed, consistent with previous reports[37,102-105] and also validates our results from a biological perspective. Indeed, we were able to detect the presence of NAD(P)H:quinine oxidoreductase (NQO1) gene induction in qRT-PCR experiments performed in another study at a 12 hour time-point (data not shown) suggesting that there may be a relatively delayed induction of the NQO1 gene compared with the other Phase 2 genes in response to BHA and possible differential kinetics of BHA-regulated Phase 2 gene response. Interestingly, genes involved in Phase I drug metabolism as well as Phase III drug transport were also regulated by BHA *via* Nrf2. The Phase I drug-metabolizing enzymes (DME's) identified here included cytochrome P450 family members Cyp7a1 and Cyp21a1 suppressed in liver and Cyp3a44 suppressed in small intestine. The roles played by these Phase I DME's in BHA-elicited cancer chemopreventive effects, however, remain presently unknown. Several transport-related genes were also identified in this study for the first time as both BHA-regulated and Nrf2-dependent. Amongst the upregulated transporters were the ATP-binding cassette superfamily members belonging to MDR/TAP, MRP or ALD subfamilies such as MDR1a/P-glycoprotein (Abcb1a) and MRP 1 (Abcc1) in small intestine; and MRP3 (Abcc3) in the liver. The ALD member responsible for peroxisomal import [106] of fatty acids (Abcd3) was upregulated in the liver, whereas the fatty acid binding protein 6, ileal (gastrotropin) (Fabp6) was suppressed in small intestine, suggesting a putative role for BHA and Nrf2 co-regulation of lipid pathways in chemoprevention that has never been

examined. Also identified for the first time as transport genes upregulated by BHA *via* Nrf2 were members of the solute carrier family such as genes encoding for zinc transport, sodium/glucose cotransport, sodium-dependent phosphate transport and organic anion transport (Slc39a10, Slc5a12, Slc20a2 and Slco2a1 respectively). Although the involvement of water channels (aquaporins) in cell migration, fat metabolism, epidermal biology and neural signal transduction point to a role in the pathophysiology of cancers [107], the current study is the first to show BHA-elicited regulation *via* Nrf2 of aquaporins 1, 3 and 8 which may play a role in the overall cancer chemopreventive effects of BHA. Taken together, the current study suggests that BHA could coordinately regulate the Phase I, II, and III xenobiotic metabolizing enzyme genes as well as antioxidative stress genes through Nrf2-dependent pathways *in vivo*. The regulation of these genes could have significant effects on prevention of tumor initiation by enhancing the cellular defense system, preventing the activation of procarcinogens/reactive intermediates, and increasing the excretion/efflux of reactive carcinogens or metabolites [56].

Bone morphogenetic proteins (BMPs) are multifunctional signaling molecules regulating growth, differentiation, and apoptosis in various target cells [108,109]. BMP receptor 1A (Bmpr1a) is a serine/threonine kinase receptor that mediates the osteogenic effects of the BMPs and is co-ordinately regulated with transforming growth factor, beta (Tgfβ) *in vitro* [110]. Here, we show that Bmpr1a was upregulated along with a strong induction of Tgfβ (>14-fold) in an Nrf2-dependent manner in small intestine. Therefore, the current study is the first to identify a role for Nrf2 in co-regulation of BMP and Tgfβ pathways in BHA-elicited chemopreventive effects *in vivo* which may

be, in part, due to induction of apoptosis caused by activation of BMP [108]. Interestingly, Bmp6 was suppressed in the liver suggesting a spatial regulation of BHA-regulated chemoprevention via Nrf2 in the liver and small intestine. A recent study [111] reported that BMP-2 modulates the expression of molecules involved in Wnt signaling, and activates the canonical Wnt pathway in normal human keratinocytes. In our study, we also observed an Nrf2-dependent upregulation of wingless-type MMTV integration site 9B (Wnt9b) along with a down-regulation of skin hornerin (Hrnr) in small intestine, and an upregulation (greater than 5-fold) of stratum corneum (epidermis) development genes such as keratin associated protein 6-1 (Krtap6-1) and keratin complex 2, basic, gene 18 (Krt2-18) in liver. Since BMP-2 and Wnt are involved in the development of skin and skin appendages [111] as morphogens, and since Nrf2 has been implicated in hyperproliferation of keratinocytes [112], our results are the first identification of a putative *in vivo* cross-talk regulated by Nrf2 and modulated by BHA between BMP and Wnt pathway members in the etiopathophysiology and chemoprevention of skin cancers. Further studies in an appropriate *in vivo* model as well as *in vitro* mechanistic studies will be necessary to enhance our current understanding of regulation of skin cancer by Nrf2.

We have demonstrated previously [90] *in vitro* that BHA is capable of activating distinct mitogen-activated protein kinases (MAPKs) including extracellular signal-regulated protein kinase 2 (ERK2), and c-Jun N-terminal kinase 1 (JNK1). The current study elucidates the Nrf2-dependent, BHA-modulated regulation *in vivo* of many members of the MAPK family including Mapk6, Mapk8, Map3k9, Map4k4, Map4k5, Map2k7, Mapkap1, and Mapkapk5; as well as the Jun oncogene, thus, validating the

physiological relevance of our results. BHA could also alter the expression of many important signaling biomolecules in discrete signal transduction pathways in an Nrf2-dependent manner including those of the JAK/STAT pathway (Janus kinase 2, *Jak2*, and protein inhibitor of activated Stat4, *Pias4*). In mammalian cells, insulin-induced PI3K (phosphoinositide 3-kinase) activation, generates the lipid second messenger PtdIns (P_3), which is thought [113] to play a key role in triggering the activation of p70 ribosomal S6 protein kinase (S6K). The identification in the current study of phosphoinositide-3-kinase, regulatory subunit 5, p101 (Pik3r5), insulin-like growth factor 1 (Igf1), Insulin-like growth factor 2 receptor (Igf2r), and Ribosomal protein S6 kinase, polypeptide 5 (Rps6ka5) as Nrf2-dependent and BHA-regulated genes is interesting as this is the first identification of Igf2r as a target of BHA *in vivo*, and may be another putative mechanism by which BHA elicits its Nrf2-mediated chemopreventive effects. We also observed a BHA-elicited, Nrf2-dependent stimulation of Diacylglycerolkinase kappa, and epsilon and eta isoforms of protein kinase C (Prkce and Prkch respectively) which is consistent with reports of PKC-activation by BHA and diacylglycerol [114,115]. In addition, G protein-coupled receptor kinase 5 (GRK5) and glycogen synthase kinase 3 beta (Gsk3β), which were down-regulated in small intestine in an Nrf2-dependent manner, were identified for the first time as putative targets for BHA-mediated chemoprevention.

BHA could also modulate the expression of many genes involved in apoptosis and cell cycle control in an Nrf2-dependent manner including cyclin G1 (Ccng1), cyclin T2 (Ccnt2), cyclin I (Ccni), G0/G1 switch gene 2 (G0s2), growth arrest and DNA-damage-inducible 45 alpha and beta (Gadd45a, Gadd45b), CASP8 and FADD-like apoptosis

regulator (Cflar), growth arrest specific 1 (Gas1), G1 to S phase transition 1 (Gspt1), breast cancer 1 (Brca1), and p21 (CDKN1A)-activated kinase 3 (Pak3). Several other important categories of genes were identified as Nrf2-dependent and BHA-regulated such as cell adhesion, biosynthesis and metabolism, ubiquitination and proteolysis, RNA/protein processing and nuclear assembly, cell growth and differentiation, DNA replication and G-protein coupled receptors. The current study, thus, addresses the spatial regulation in mouse small intestine and liver of global gene expression profiles elicited by BHA in exerting its chemopreventive effects *via* Nrf2. Since a greater number of genes in this study were altered in the small intestine as compared to the liver, and since the phenolic compound BHA (Fig.1) is a lipophilic molecule with a KowWin (http://www.syrres.com/Esc/est_kowdemo.htm) estimated log octanol/water partitition coefficient (log P) as high as 3.50, the spatial regulation of gene expression profiles may be attributed to a complex of physiological factors including partitioning across the gastrointestinal tract, intestinal transit time, uptake into the hepatobiliary circulation, exposure parameters such as Cmax, Tmax and AUC, and pharmacokinetics of disposition after oral administration of BHA. Further studies will be necessary to address the effect(s) of temporal dependence on pharmacokinetic parameters and gene expression profiles to further enhance our current understanding of BHA-mediated chemoprevention mechanisms.

In conclusion, our microarray expression profiling study provides some novel insights into the pharmacogenomics and spatial regulation of global gene expression profiles elicited in the mouse small intestine and liver by BHA in an Nrf2-dependent manner from a gestalt biological perspective. Amongst these BHA-regulated genes, clusters of

Nrf2-dependent genes were identified by comparing gene expression profiles between C57BL/6J Nrf2(+/+) and C57BL/6J/Nrf2(–/–) mice. The identification of novel molecular targets that are regulated by BHA *via* Nrf2 underscores the ineluctable importance of the Nrf2/ARE signaling pathway in cancer chemoprevention. This study clearly extends the current latitude of thought on the molecular mechanisms underlying BHA's cancer chemopreventive effects as well as the role(s) of Nrf2 in its biological functions. Future *in vivo* and *in vitro* mechanistic studies exploring the germane molecular targets or signaling pathways as well as Nrf2-dependent genes related to the significant functional categories uncovered in the current study would inexorably extend our current understanding of cancer chemoprevention.

2.6. Acknowledgements

The authors are deeply grateful to Mr. Curtis Krier at the Cancer Institute of New Jersey (CINJ) Core Expression Array Facility for his expert assistance with the microarray analyses. The authors are also deeply indebted to Ms. Donna Wilson of the Keck Center for Collaborative Neuroscience, Rutgers University as well as the staff of the Human Genetics Institute of New Jersey at Rutgers University for their great expertise and help with the quantitative real-time PCR analyses. This work was supported in part by NIH grant R01-CA094828.

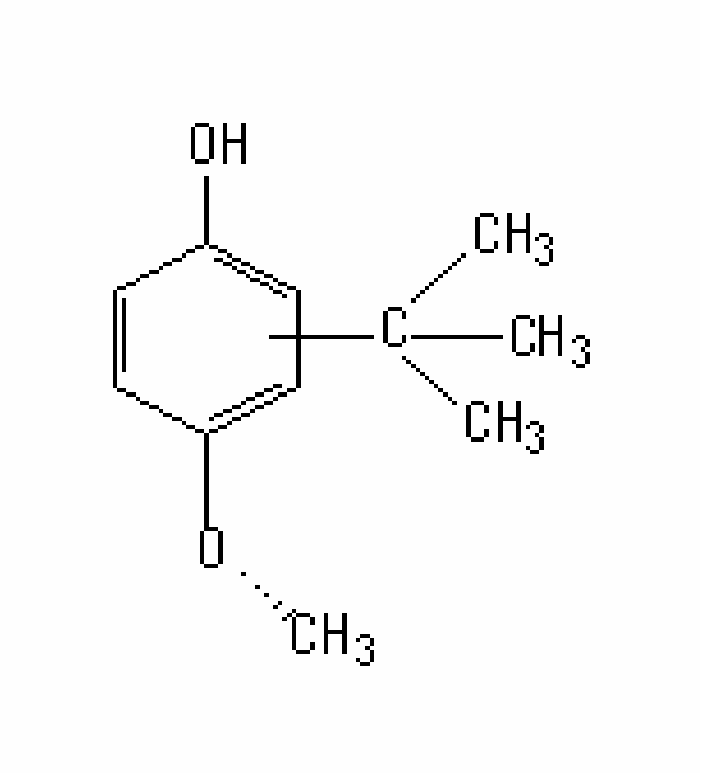

Figure 2.1. Chemical Structure of Butylated hydroxyanisole (BHA)

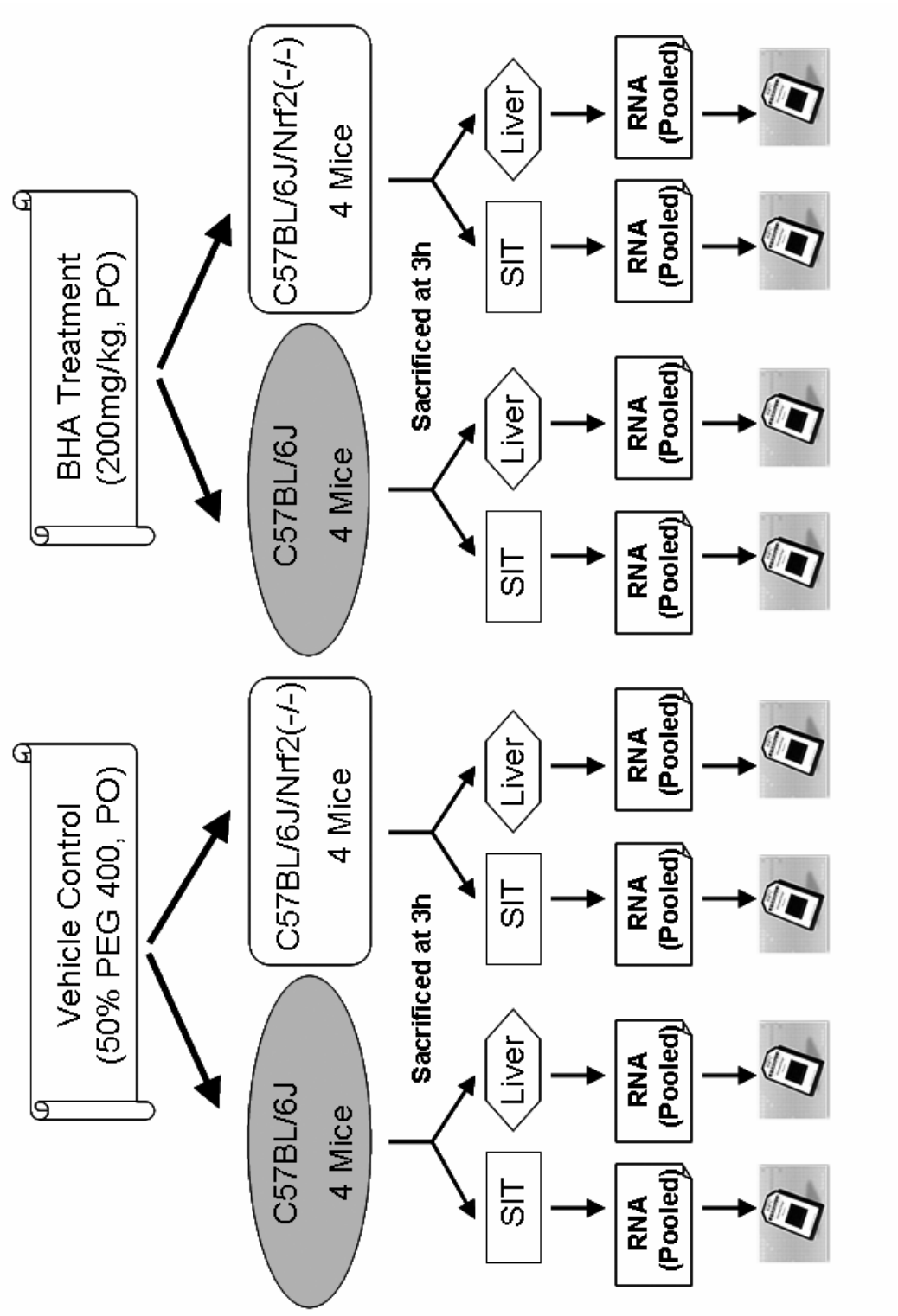

Figure 2.2. Schematic representation of experimental design; *SIT*, Small Intestine.

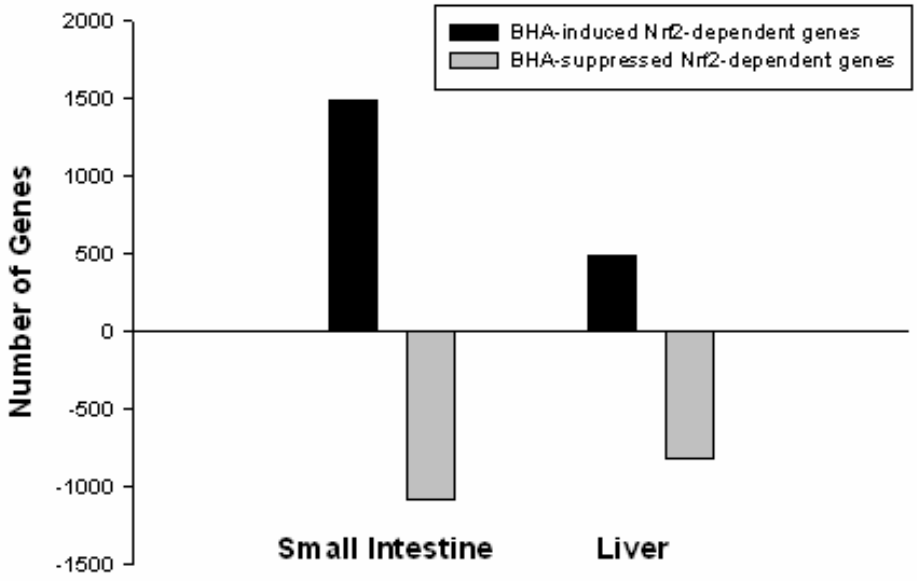

Figure 2.3. Regulation of Nrf2-dependent gene expression by BHA in mouse small intestine and liver. Gene expression patterns were analyzed at 3h after administration of a 200mg/kg single oral dose of BHA; Nrf2-dependent genes that were either induced or suppressed over two fold were listed. The positive numbers on the *y-axis* refer to the number of genes being induced; the negative numbers on the *y-axis* refer to the number of genes being suppressed.

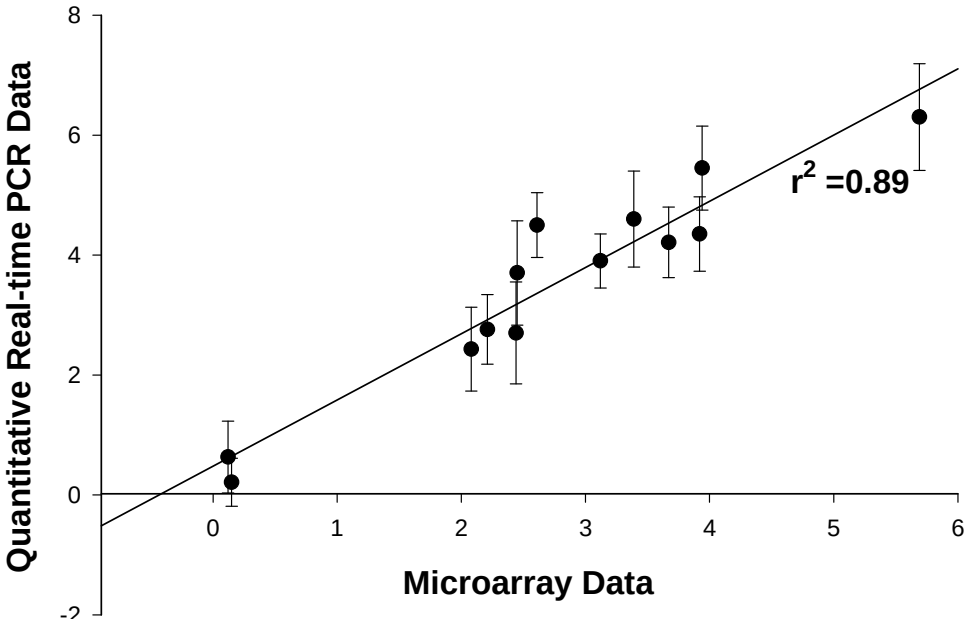

Figure 2.4. Correlation of microarray data with quantitative real-time PCR data. Fold changes in gene expression measured by quantitative real-time PCR for each sample in triplicate (n=3) were plotted against corresponding fold changes from microarray data (coefficient of determination, $r^2 = 0.89$).

CHAPTER 3

Toxicogenomics of Endoplasmic Reticulum stress inducer Tunicamycin in the Small Intestine and Liver of Nrf2 Knockout and C57BL/6J Mice[7.8.9]

3.1. Abstract

This objective of this study was to investigate the toxicogenomics and the spatial regulation of global gene expression profiles elicited by Endoplasmic Reticulum (ER) stress inducer Tunicamycin (TM) in mouse small intestine and liver as well as to identify TM-modulated Nuclear Factor-E2-related factor 2 (Nrf2)–dependent genes. Gene expression profiles were analyzed using 45,000 Affymetrix mouse genome 430 2.0 array and GeneSpring 7.2 software. Microarray results were validated by quantitative real-time reverse transcription-PCR analyses. Clusters of genes that were either induced or suppressed more than two fold by TM treatment compared with vehicle in C57BL/6J/Nrf2(–/–; knockout)and C57BL/6J Nrf2 (+/+; wildtype) mice genotypes were identified. Amongst these, in small intestine and liver, 1291 and 750 genes respectively were identified as Nrf2-dependent and upregulated, and 1370 and

---

[7]Work described in this chapter has been published as **Nair, S**., Kong, A.-N. T., Toxicol Lett. 2007 Jan 10;168(1):21-39.

[8]**Keywords** : Tunicamycin, endoplasmic reticulum stress, Nuclear Factor-E2-related Factor 2, Microarray, Global Gene Expression Profiles.

[9]**Abbreviations :** TM, Tunicamycin; Nrf2, Nuclear Factor-E2-related factor 2; ER, Endoplasmic Reticulum; UPR, Unfolded Protein Response; Mapk, Mitogen-activated protein kinase; ARE, Antioxidant response element.

943 genes respectively as Nrf2-dependent and downregulated. Based on their biological functions, these genes can be categorized into molecular chaperones and heat shock proteins, ubiquitination/proteolysis, apoptosis/cell cycle, electron transport, detoxification, cell growth/differentiation, signaling molecules/interacting partners, kinases and phosphatases, transport, biosynthesis/metabolism, nuclear assembly and processing, and genes related to calcium and glucose homeostasis. Phase II detoxification/antioxidant genes as well as putative interacting partners of Nrf2 such as nuclear corepressors and coactivators, were also identified as Nrf2-dependent genes. The identification of TM-regulated and Nrf2-dependent genes in the unfolded protein response to ER stress not only provides potential novel insights into the gestalt biological effects of TM on the toxicogenomics and spatial regulation of global gene expression profiles in cancer pharmacology and toxicology, but also points to the pivotal role of Nrf2 in these biological processes.

3.2. Introduction

The endoplasmic reticulum (ER) is an important organelle in which newly synthesized secretory and membrane-associated proteins destined to the extracellular space, plasma membrane, and the exo/endocytic compartments are correctly folded and assembled [116,117]. An imbalance between the cellular demand for protein synthesis and the capacity of the ER in promoting protein maturation and transport can lead to an accumulation of unfolded or malfolded proteins in the ER lumen. This condition has been designated “ER stress” [117,118]. Interestingly, the accumulation of misfolded protein in the ER triggers an adaptive stress response – termed the unfolded protein

response (UPR) – mediated by the ER transmembrane protein kinase and endoribonuclease inositol-requiring enzyme-1α (IRE1α) [68]. The glucosamine-containing nucleoside antibiotic, Tunicamycin (TM, Figure 3.1), produced by genus Streptomyces, is an inhibitor of N-linked glycosylation and the formation of N-glycosidic protein-carbohydrate linkages [119]. It specifically inhibits dolichol pyrophosphate-mediated glycosylation of asparaginyl residues of glycoproteins [120] and induces "ER stress".

Pivotal to the antioxidant response [36-39] typical in mammalian homeostasis and oxidative stress is the important transcription factor Nrf2 or Nuclear Factor-E2-related factor 2 that has been extensively studied by many research groups cited above as well as this laboratory [1,40-42]. Under homeostatic conditions, Nrf2 is mainly sequestered in the cytoplasm by a cytoskeleton-binding protein called Kelch-like erythroid CNC homologue (ECH)-associated protein 1 (Keap1) [13,40,45]. When challenged with oxidative stress, Nrf2 is quickly released from Keap1 retention and translocates to the nucleus [40,49]. We have recently identified [40] a canonical redox-insensitive nuclear export signal (NES) (^{537}LKKQLSTLYL^{546}) located in the leucine zipper (ZIP) domain of the Nrf2 protein as well as a redox-sensitive NES (^{173}LLSI-PELQCLNI^{186}) in the transactivation (TA) domain of Nrf2 [121]. Once in the nucleus, Nrf2 not only binds to the specific consensus cis-element called antioxidant response element (ARE) present in the promoter region of many cytoprotective genes [41,43,45], but also to other trans-acting factors such as small Maf (MafG and MafK) [51] that can coordinately regulate gene transcription with Nrf2. We have previously reported [41] that different segments of Nrf2 transactivation domain have different transactivation potential; and that

different MAPKs have differential effects on Nrf2 transcriptional activity, with ERK and JNK pathways playing an unequivocal role in positive regulation of Nrf2 transactivation domain activity. To better understand the biological basis of signaling through Nrf2, it has also become imperative to identify possible interacting partners of Nrf2 such as coactivators or corepressors apart from trans-acting factors such as small Maf .

Recently, it was reported [122] that Nrf1, another member of the Cap' n' Collar (CNC) family of basic leucine zipper proteins that is structurally similar to Nrf2, is normally targeted to the ER membrane, and that ER stress induced by TM *in vitro* may play a role in modulating Nrf1 function as a transcriptional activator. We sought to investigate the potential role of ER stress in modulating Nrf2 function as a transcriptional activator *in vivo*. Nrf2 knockout mice are greatly predisposed to chemical-induced DNA damage and exhibit higher susceptibility towards cancer development in several models of chemical carcinogenesis [43]. In the present study, we have investigated, by microarray expression profiling, the global gene expression profiles elicited by oral administration of TM in small intestine and liver of Nrf2 knockout (C57BL/6J/Nrf2-/-) and wild type (C57BL/6J) mice to enhance our understanding of TM-regulated toxicological effects mediated through Nrf2. We have identified clusters of TM-modulated genes that are Nrf2-dependent in small intestine and liver and categorized them based on their biological functions. The identification of TM-regulated Nrf2-dependent genes will yield valuable insights into the role of Nrf2 in TM-modulated gene regulation with respect to cancer pharmacology and toxicology. This study also enables the identification of novel molecular targets that are regulated by TM *via* Nrf2. The current

study is also the first to investigate the global gene expression profiles elicited by TM in an *in vivo* murine model where the role of Nrf2 is also examined.

3.3. Materials and Methods

Animals and Dosing : The protocol for animal studies was approved by the Rutgers University Institutional Animal Care and Use Committee (IACUC). Nrf2 knockout mice Nrf2 (-/-) (C57BL/SV129) have been described previously.[100]. Nrf2 (-/-) mice were backcrossed with C57BL/6J mice (The Jackson Laboratory, ME USA). DNA was extracted from the tail of each mouse and genotype of the mouse was confirmed by polymerase chain reaction (PCR) by using primers (3'-primer, 5'-GGA ATG GAA AAT AGC TCC TGC C-3'; 5'-primer, 5'-GCC TGA GAG CTG TAG GCC C-3'; and lacZ primer, 5'-GGG TTT TCC CAG TCA CGA C-3'). Nrf2(-/-) mice-derived PCR products showed only one band of ~200bp, Nrf2 (+/+) mice-derived PCR products showed a band of ~300bp while both bands appeared in Nrf2(+/-) mice PCR products. Female C57BL/6J/Nrf2(-/-) mice from third generation of backcrossing were used in this study. Age-matched female C57BL/6J mice were purchased from The Jackson Laboratory (Bar Harbor, ME). Mice in the age-group of 9-12 weeks were housed at Rutgers Animal Facility with free access to water and food under 12 h light/dark cycles. After one week of acclimatization, the mice were put on AIN-76A diet (Research Diets Inc. NJ USA) for another week. The mice were then administered TM (Sigma-Aldrich, St.Louis, MO) at a dose of 2 mg/kg (dissolved in 50% PEG 400 aqueous solution) by oral gavage. The control group animals were administered only vehicle (50% PEG 400 aqueous solution). Each treatment was administered to a group

of four animals for both C57BL/6J and C57BL/6J/Nrf2(-/-) mice. Mice were sacrificed 3h after TM treatment or 3 h after vehicle treatment (control group). Livers and small intestines were retrieved and stored in RNA Later (Ambion, Austin,TX) solution.

Sample Preparation for Microarray Analyses : Total RNA from liver and small intestine tissues were isolated by using a method of TRIzol (Invitrogen, Carlsbad, CA) extraction coupled with the RNeasy kit from Qiagen (Valencia, CA). Briefly, tissues were homogenized in trizol and then extracted with chloroform by vortexing. A small volume (1.2 ml) of aqueous phase after chloroform extraction and centrifugation was adjusted to 35% ethanol and loaded onto an RNeasy column. The column was washed, and RNA was eluted following the manufacturer's recommendations. RNA integrity was examined by electrophoresis, and concentrations were determined by UV spectrophotometry.

Microarray Hybridization and Data Analysis : Affymetrix (Affymetrix, Santa Clara, CA) mouse genome 430 2.0 array was used to probe the global gene expression profiles in mice following TM treatment. The mouse genome 430 2.0 Array is a high-density oligonucleotide array comprised of over 45,101 probe sets representing over 34,000 well-substantiated mouse genes. The library file for the above-mentioned oligonucleotide array is readily available at http://www.affymetrix.com/support/technical /libraryfilesmain.affx. After RNA isolation, all the subsequent technical procedures including quality control and concentration measurement of RNA, cDNA synthesis and biotin-labeling of cRNA, hybridization and scanning of the arrays, were performed at

CINJ Core Expression Array Facility of Robert Wood Johnson Medical School (New Brunswick, NJ). Each chip was hybridized with cRNA derived from a pooled total RNA sample from four mice per treatment group, per organ, and per genotype (a total of eight chips were used in this study) (Fig.2). Briefly, double-stranded cDNA was synthesized from 5 μg of total RNA and labeled using the ENZO BioArray RNA transcript labeling kit (Enzo Life Sciences, Inc.,Farmingdale, NY, USA) to generate biotinylated cRNA. Biotin-labeled cRNA was purified and fragmented randomly according to Affymetrix's protocol. Two hundred microliters of sample cocktail containing 15 μg of fragmented and biotin-labeled cRNA was loaded onto each chip. Chips were hybridized at 45°C for 16 h and washed with fluidics protocol EukGE-WS2v5 according to Affymetrix's recommendation. At the completion of the fluidics protocol, the chips were placed into the Affymetrix GeneChip Scanner where the intensity of the fluorescence for each feature was measured. The expression value (average difference) for each gene was determined by calculating the average of differences in intensity (perfect match intensity minus mismatch intensity) between its probe pairs. The expression analysis file created from each sample (chip) was imported into GeneSpring 7.2 (Agilent Technologies, Inc., Palo Alto, CA) for further data characterization. Briefly, a new experiment was generated after importing data from the same organ in which data was normalized by array to the 50th percentile of all measurements on that array. Data filtration based on flags present in at least one of the samples was first performed, and a corresponding gene list based on those flags was generated. Lists of genes that were either induced or suppressed more than two fold between treated versus vehicle group of same genotype were created by filtration-on-

fold function within the presented flag list. By use of color-by-Venn-Diagram function, lists of genes that were regulated more than two fold only in C57BL/6J mice in both liver and small intestine were created. Similarly, lists of gene that were regulated over two fold regardless of genotype were also generated.

Quantitative Real-time PCR for Microarray Data Validation : To validate the microarray data, several genes of interest were selected from various categories for quantitative real-time PCR analyses. Glyceraldehyde-3-phosphate-dehydrogenase (GAPDH) served as the "housekeeping" gene. The specific primers for these genes listed in Table 3.1 were designed by using Primer Express 2.0 software (Applied Biosystems, Foster City, CA) and were obtained from Integrated DNA Technologies, Coralville, I A. The specificity of the primers was examined by a National Center for Biotechnology Information Blast search of the mouse genome. Instead of using pooled RNA from each group, RNA samples isolated from individual mice as described earlier were used in real-time PCR analyses. For the real-time PCR assays, briefly, first-strand cDNA was synthesized using 4μg of total RNA following the protocol of SuperScript III First-Strand cDNA Synthesis System (Invitrogen) in a 40 μl reaction volume. The PCR reactions based on SYBR Green chemistry were carried out using 100 times diluted cDNA product, 60 nM of each primer, and SYBR Green master mix (Applied Biosystems, Foster City, CA) in 10 μl reactions. The PCR parameters were set using SDS 2.1 software (Applied Biosystems, Foster City, CA) and involved the following stages : 50°C for 2min, 1 cycle; 95°C for 10 mins, 1 cycle; 95°C for 15 secs → 55 °C for 30 secs →72°C for 30 secs, 40 cycles; and 72°C for 10 mins, 1 cycle. Incorporation

of the SYBR Green dye into the PCR products was monitored in real time with an ABI Prism 7900HT sequence detection system, resulting in the calculation of a threshold cycle (C_T) that defines the PCR cycle at which exponential growth of PCR products begins. The carboxy-X-rhodamine (ROX) passive reference dye was used to account for well and pipetting variability. A control cDNA dilution series was created for each gene to establish a standard curve. After conclusion of the reaction, amplicon specificity was verified by first-derivative melting curve analysis using the ABI software; and the integrity of the PCR reaction product and absence of primer dimers was ascertained. The gene expression was determined by normalization with control gene GAPDH. In order to validate the results, the correlation between corresponding microarray data and real-time PCR data was evaluated by the statistical 'coefficient of determination', $\mathbf{r^2}$=0.97.

3.4. Results

3.4.1. TM-Modulated Gene Expression Patterns in Mouse Small Intestine and Liver

Subsequent to data normalization, 48.76% (21,991) of the probes passed the filtration based on flags present in at least one of four small intestine sample arrays depicted in Figure 3.2. Expression levels of 1291 probes were elevated or of 1370 probes were suppressed over two fold by TM only in the wild-type mice, while 3471 probes were induced or 2024 probes were inhibited over two fold by TM only in the Nrf2(–/–) mice small intestine (Figure 3.3a). Similarly, changes in gene expression profiles were also observed in mice liver. Overall, the expression levels of 51.495% (23,225) probes were

detected in least in one of four liver sample arrays depicted in Figure 3.2. In comparison with the results from small intestine sample arrays, a smaller proportion of well-defined genes were either elevated (750) or suppressed (943) over two fold by TM in wild-type mice liver alone; whereas 39 well-defined genes were induced or 3170 genes were inhibited in Nrf2(–/–) mice liver. (Figure 3.3b).

3.4.2. Quantitative Real–Time PCR Validation of Microarray Data

To validate the data generated from the microarray studies, several genes from different categories (Table 3.1) were selected to confirm the TM-regulative effects by the use of quantitative real-time PCR analyses as described in detail under Materials and Methods. After ascertaining the amplicon specificity by first-derivative melting curve analysis, the values obtained for each gene were normalized by the values of corresponding GAPDH expression levels. The fold changes in expression levels of treated samples over control samples were computed by assigning unit value to the control (vehicle) samples. Computation of the correlation statistic showed that the data generated from the microarray analyses are well-correlated with the results obtained from quantitative real-time PCR (coefficient of determination, $r^2 = 0.97$, Figure 3.4).

3.4.3. TM-Induced Nrf2-Dependent Genes in Small Intestine and Liver

Genes that were induced only in wild-type mice, but not in Nrf2(–/–) mice, by TM were designated as TM-induced Nrf2-dependent genes. Based on their biological functions, these genes were classified into categories, including ubiquitination and proteolysis, electron transport, chaperones and unfolded protein response genes, detoxification

enzymes, transport, apoptosis and cell cycle control, cell adhesion, kinases and phosphatases, transcription factors and interacting partners, glucose-related genes, ER and Golgi-related genes, translation factors, RNA/Protein processing and nuclear assembly, biosynthesis and metabolism, cell growth and differentiation, and G protein-coupled receptors (Table 3.2 lists genes relevant to our interest).

In response to TM-induced ER stress, several unfolded protein response genes were identified as Nrf2-regulated including, amongst others, heat shock protein, alpha-crystallin-related, B6 (Hspb6) in liver, heat shock protein family, member 7,cardiovascular (Hspb7) in small intestine, and stress 70 protein chaperone, microsome-associated, human homolog (Stch) in both liver and small intestine. A large number of apoptosis and cell-cycle related genes were also upregulated in response to TM treatment. Representative members included B-cell leukemia/lymphoma 2 (Bcl2), CASP8 and FADD-like apoptosis regulator (Cflar), Epiregulin (Ereg), Growth arrest specific 2 (Gas2) and synovial apoptosis inhibitor 1, synoviolin (Syvn1). Interestingly, several important transcription/translation factors and interacting partners were identified as Nrf2-dependent and TM-regulated. These included P300/CBP-associated factor (Pcaf), Smad nuclear interacting protein 1 (Snip1), nuclear receptor coactivator 5 (Ncoa5), nuclear receptor interacting protein 1 (Nrip1), nuclear transcription factor, X-box binding-like 1 (Nfxl1), eukaryotic translation initiation factors 1α 2, 4e and 5 (Eif 1a2, 4e and 5), Erbb2 interacting protein (Erbb2ip), cAMP responsive element binding protein 3-like 2 (Creb3l2) and Jun oncogene (Jun).

Other categories of genes induced by TM in an Nrf2-dependent manner included cell adhesion (cadherins 1, 2, and 10), glucose-related genes (hexokinase 2), transport

(solute carrier family members Slc13a1, Slc22a3, Slc8a1 and others), and ubiquitination and proteolysis (Constitutive photomorphogenic protein and carboxypeptidase A4). The glutathione peroxidase 3 (Gpx3) gene was also upregulated in liver in an Nrf2-dependent manner in response to TM treatment.

3.4.4. TM-Suppressed Nrf2-Dependent Genes in Small Intestine and Liver

As shown in Table 3.3 which lists genes relevant to our interest, TM treatment also inhibited the expression of many genes falling into similar functional categories in an Nrf2-dependent manner. Major Phase II detoxifying genes identified as Nrf2-regulated and TM-modulated included several isoforms of Glutathione-S-transferase (Gst), and glutamate cysteine ligase, modifier subunit (Gclm). Additionally, Phase I genes such as cytochrome P450 family members Cyp3a44, Cyp39a1 and Cyp8b1 were also downregulated in response to TM-treatment in an Nrf2-dependent manner. Moreover, many transport genes, which may be regarded as Phase III genes, including members of solute carrier family (Slc23a2, Slc23a1, Slc37a4, Slc4a4, Slc40a1, Slc9a3) and multidrug-resistance associated proteins (Abcc3) were also downregulated *via* Nrf2 and regulated through TM. Thus, a co-ordinated response involving Phase I, II and III genes was observed on TM treatment in an Nrf2-dependent manner.

Other categories of genes affected included apoptosis and cell cycle-related genes (Caspases 6 and 11, growth arrest and DNA-damage-inducible 45 β), electron transport (Cyp450 members and NADH dehydrogenase isoforms), kinases and phosphatases (mitogen activated protein kinase family members, ribosomal protein S6 kinase), transcription factors and interacting partners (inhibitor of kappa B kinase gamma and

src family associated phosphoprotein 2), and glucose-related genes (glucose-6-phosphatase, catalytic, fructose bisphosphatase 1, and glucose phosphate isomerase 1). Superoxide dismutase (Sod1) was also identified as an Nrf2-regulated and TM-modulated gene that was suppressed. Furthermore, cell adhesion genes (cadherin 22), ubiquitination and proteolysis genes (Usp25 and Usp34), and some unfolded protein response genes (heat shock proteins 1B and 3) were also observed to be downregulated in response to TM treatment *via* Nrf2.

3.5. Discussion

The major goal of this study was to identify toxicant Tunicamycin-regulated Nrf2-dependent genes in mice liver and small intestine by using C57BL/6J Nrf2 (+/+; wildtype) and C57BL/6J/Nrf2(–/–; knockout) mice and genome-scale microarray analyses. We sought to investigate by transcriptome expression profiling the potential role of ER stress stimulus in modulating Nrf2 function as a transcriptional activator *in vivo*. As a protein-folding compartment, the ER is exquisitely sensitive to alterations in homeostasis, and provides stringent quality control systems to ensure that only correctly folded proteins transit to the Golgi and unfolded or misfolded proteins are retained and ultimately degraded. A number of biochemical and physiological stimuli, such as perturbation in calcium homeostasis or redox status, elevated secretory protein synthesis, expression of misfolded proteins, sugar/glucose deprivation, altered glycosylation, and overloading of cholesterol can disrupt ER homeostasis, impose stress to the ER, and subsequently lead to accumulation of unfolded or misfolded proteins in the ER lumen [67]. The ER has evolved highly specific signaling pathways called the

unfolded protein response (UPR) to cope with the accumulation of unfolded or misfolded proteins [67,68]. ER stress stimulus by Thapsigargin has also been shown [69] to activate the c-Jun N-terminal kinase (JNK) or stress-activated protein kinase (SAPK) that is a member of the mitogen-activated protein kinase (MAPK) cascade [70]. Moreover, it has been reported that the coupling of ER stress to JNK activation involves transmembrane protein kinase IRE1 by binding to an adaptor protein TRAF2, and that IRE1$\alpha^{-/-}$ fibroblasts were impaired in JNK activation by ER stress [71]. We have previously reported that phenethyl isothiocyanate (PEITC) from cruciferous vegetables activates JNK1 [72] and that the activation of the antioxidant response element (ARE) by PEITC involves both Nrf2 and JNK1 [42] in HeLa cells. We have also reported [41] that extracellular signal-regulated kinase (ERK) and JNK pathways play an unequivocal role in positive regulation of Nrf2 transactivation domain activity *in vitro* in HepG2 cells. Recently, it was shown [122] that Nrf1, another member of the Cap' n' Collar (CNC) family of basic leucine zipper proteins that is structurally similar to Nrf2, is normally targeted to the ER membrane, and that ER stress induced by TM *in vitro* may play a role in modulating Nrf1 function as a transcriptional activator. Here, we investigated the role of Nrf2 in modulating transcriptional response to ER stress stimulus by TM *in vivo* in an Nrf2 (-/-; deficient) murine model, thus providing new biological insights into the diverse cellular and physiological processes that may be regulated by the UPR in cancer pharmacology and toxicology.

Interestingly, a co-ordinated response involving Phase I, II and III genes that has not been demonstrated earlier was observed *in vivo* on ER stress induction with TM in an Nrf2-dependent manner. Phase I drug-metabolizing enzymes (DMEs) such as

cytochrome P450 family members Cyp3a44, Cyp39a1 and Cyp8b1 were downregulated in response to TM-treatment in an Nrf2-dependent manner. Additionally, major Phase II detoxifying genes identified as Nrf2-regulated and TM-modulated included several isoforms of Glutathione-S-transferase (Gst), and glutamate cysteine ligase, modifier subunit (Gclm). Moreover, many transport genes, which may be regarded as Phase III genes, including members of solute carrier family (Slc23a2, Slc23a1, Slc37a4, Slc4a4, Slc40a1, Slc9a3) and multidrug-resistance associated proteins (Abcc1, Abcc3 and Mdr1b or Abcb1b) were also downregulated *via* Nrf2 and regulated through TM. The co-ordinated regulation of these genes could have significant effects in toxicology by enhancing the cellular defense system, preventing the activation of procarcinogens/reactive intermediates, and increasing the excretion/efflux of reactive carcinogens or metabolites.

There could be two possible outcomes of prolonged ER stress: (1) an adaptive response promoting cell survival; or (2) the induction of apoptotic cell death [118]. Indeed, several genes related to apoptosis and cell cycle control were modulated in response to TM stimulus *in vivo* in an Nrf2-dependent manner. The major genes upregulated in this category included the anti-apoptotic B-cell leukemia/lymphoma 2 (Bcl2) family gene, CASP8 and FADD-like apoptosis regulator (Cflar), Epiregulin (Ereg), Growth arrest specific 2 (Gas2), cyclin T2 (Ccnt2) and cyclin-dependent kinase 7 (Cdk7) all in small intestine apart from mucin 20 (Muc20) and synovial apoptosis inhibitor 1, synoviolin (Syvn1) in liver ; whereas genes downregulated in this category included cyclin-dependent kinase 6 (Cdk6) and Bcl2 in liver, baculoviral inhibitor of apoptosis (IAP)-repeat containing 6 (Birc6) and Caspases 6 and 11 in small intestine, and growth arrest

and DNA-damage-inducible 45 – β (Gadd45b), and gamma interacting protein 1 (Gadd45gip1) - in liver and small intestine respectively amongst others. To our knowledge, this is the first report *in vivo* of apoptosis and cell cycle-related genes that are both modulated by the ER stress inducer TM and regulated *via* Nrf2. Moreover, it has been noted [123] that although the basic machinery to carry out apoptosis appears to be present in essentially all mammalian cells at all times, the activation of the suicide program is regulated by many different signals that originate from both the intracellular and the extracellular milieu. Notably, transcription factor NF-κB is critical for determining cellular sensitivity to apoptotic stimuli by regulating both mitochondrial and death receptor apoptotic pathways. Recently, it was reported [57] that autocrine tumor necrosis factor alpha links ER stress to the membrane death receptor pathway through IRE1alpha-mediated NF-κB activation and down-regulation of TRAF2 expression. In our study, we saw a downregulation of inhibitor of kappaB kinase gamma (Iκbkg or IKKγ) in liver in an Nrf2-dependent manner in response to TM-induced ER stress. Since the catalytic subunits, IKKα and IKKß, require association with the regulatory IKKγ (NEMO) component to gain full basal and inducible kinase activity and since tetrameric oligomerization of IκB Kinase γ (IKKγ) is obligatory for IKK Complex activity and NF-κB activation [124], our results appear to be validated from a functional standpoint and underscore the complexity of factors involved in making the decision between cell survival and cell death in response to TM-mediated ER stress *in vivo*, not excluding the possibility of potential cross-talk between Nrf2/ARE pathway and other signaling pathways that may converge at multiple levels in the cell.

Interestingly, impaired proteasome function through pharmacological inhibition, or by accumulation of malfolded protein in the cytoplasm, can ultimately block ER-associated degradation (ERAD) [125] which is important for eviction of malfolded proteins from the ER to the cytoplasm where they are subsequently ubiquitinated and degraded *via* the proteasome. In our study, several genes associated with the ubiquitin/proteasome pathway were regulated in response to TM in an Nrf2-dependent manner. These included, amongst others, constitutive photomorphogenic protein (Cop1), carboxypeptidase A4 (Cpa4), ubiquitin-specific peptidase 34 (Usp34), and ubiquitin-specific processing protease (Usp25). Furthermore, UPR genes such as various heat shock proteins (Hspb3, Hspb6, Hspb7, Hspa1B) and molecular chaperones and folding enzymes, e.g., stress 70 protein chaperone (Stch) were also seen to be regulated by TM-induced ER stress and modulated by Nrf2. Since the UPR directs gene expression important for remediating accumulation of malfolded protein in the ER, the identification of UPR-responsive genes in our study validates our results from a biological perspective. Moreover, important genes related to glycosylation modifications (e.g., galactosyltransferase, B3galt1), ER to Golgi transport (ADP-ribosylation factor GTPase activating protein 3, Arfgap3; coatomer protein complex subunit alpha, Copa; Lectin, mannose-binding 1,Lman1), and intra-Golgi transport (Golgi associated, gamma adaptin ear containing, ARF binding protein 2, Gga2) were also seen to be regulated by TM in an Nrf2-dependent manner. Genes related to biogenesis of ribosomes on rough ER where proteins are synthesized from mRNA, e.g., brix domain containing 2 (Bxdc2) and ribosomal protein S6 kinase, polypeptides 1 (Rps6ka1) and 4 (Rps6ka4), were also regulated *via* Nrf2 and modulated by TM

treatment. To our knowledge, this is the first *in vivo* investigation examining the potential role of Nrf2 and TM-induced ER stress in the simultaneous modulation of UPR-responsive genes, clearance by the ubiquitin/proteasome pathway members, and cellular biosynthetic-secretory pathway involving ribosomal biogenesis genes and ER to Golgi transport genes.

Additionally, many genes related to glucose biosynthesis and metabolism including glucose phosphate isomerase 1 (gluconeogenesis/glycolysis), fructose bisphosphatase 1(gluconeogenesis), glucose-6-phosphatase (glycogen biosynthesis), hexokinase 2 (glycolysis), adiponectin (glucose metabolism), lectins (galactose- and mannose-binding) and the solute carrier family member Slc 35b1 (sugar porter) were all seen to be regulated through Nrf2 and modulated by TM-induced ER stress. The simultaneous modulation of genes encoding for insulin like growth factor receptors 1 and 2 point to a potential role for glucose- and ER stress-mediated insulin resistance [126] wherein the potential role of Nrf2 has never been examined earlier.

In recent times, there is a renewed interest in dissecting the interacting partners of Nrf2 such as coactivators and corepressors which are co-regulated with Nrf2 to better understand the biochemistry of Nrf2. In a recent microarray study [55], we have reported that CREB-binding protein (CBP) was upregulated in mice liver on treatment with (-)epigallocatechin-3-gallate (EGCG) in an Nrf2-dependent manner. We have also demonstrated [41] previously, using a Gal4-Luc reporter co-transfection assay system in HepG2 cells, that the nuclear transcriptional coactivator CBP, which can bind to Nrf2 transactivation domain and can be activated by extracellular signal-regulated protein kinase (ERK) cascade, showed synergistic stimulation with Raf on the transactivation

activities of both the chimera Gal4-Nrf2 (1-370) and the full-length Nrf2. In the current study, we observed the upregulation of the P300/CBP-associated factor (P/CAF), trans-acting factor v-maf musculoaponeurotic fibrosarcoma oncogene family, protein F (Maf F), nuclear receptor co-activator 5 (Ncoa5), nuclear receptor co-repressor interacting protein (Nrip1) and Smad nuclear interacting protein 1 (Snip1) ; as well as downregulation of the src family associated phosphoprotein 2 (Scap2) in an Nrf2-dependent manner. Although microarray expression profiling cannot provide evidence of binding between partners, this is the first investigation to potentially suggest that co-repressor Nrip1 and co-activators P/CAF and Ncoa5, similar to CBP in our previous studies, may serve as putative TM-regulated nuclear interacting partners of Nrf2 in eliciting the UPR-responsive events *in vivo*. We have also shown recently [61] that coactivator P/CAF could transcriptionally activate a chimeric Gal4-Nrf2-Luciferase system containing the Nrf2 transactivation domain in HepG2 cells. In addition, P/CAF which is known [62] to be a histoneacetyl transferase protein has recently been shown [63] to mediate DNA damage-dependent acetylation on most promoters of genes involved in the DNA-damage and ER-stress response, which validates our observation of P/CAF induction *via* Nrf2 in response to TM-induced ER stress. Taken together, it is tempting to speculate that the TM-regulated pharmacological and toxicological effects may be regulated by a multimolecular complex, which involves Nrf2 along with the transcriptional co-repressor Nrip1 and the transcriptional co-activators P/CAF and Ncoa5, in addition to the currently known trans-acting factors such as small Maf [51], with multiple interactions between the members of the putative complex as we have shown recently with the p160 family of proteins [61]. Indeed, further studies of a

biochemical nature would be needed to substantiate this hypothesis and extend our understanding of Nrf2 regulation in TM-mediated ER stress.

Many important transcription factors affecting diverse signaling pathways were identified as regulated through Nrf2 and modulated by TM treatment. For example, Jun oncogene, platelet-derived growth factor, metallothionein 1 and 2, transforming growth factor beta 1 and ErbB2 interacting protein were upregulated ; whereas hypoxia-inducible factor 1, alpha subunit inhibitor, peroxisome proliferator activated receptor binding protein, v-erb-b2 erythroblastic leukemia viral oncogene homolog 3 (avian) and protein kinase C binding protein 1 were downregulated *via* Nrf2 in response to TM. Since these transcription factors can modulate the expression of many different gene transcripts encoding various proteins, their identification as Nrf2-regulated and ER-stress- or TM-modulated would be important in enhancing our current understanding of UPR responsive genes and in providing new biological insights into the diverse cellular and physiological processes that may be regulated by the UPR in Nrf2-regulated cancer pharmacology and toxicology.

In the category of kinases and phosphatases, several members of the MAPK cascade such as Map2k7, Mapk14, Mapk8, Map3k7 as well as MAPK-activated protein kinase 5 (Mapkapk5) were identified as regulated by TM *via* Nrf2. Moreover, members of the calcium/calmodulin signaling pathway such as calcium/calmodulin-dependent - protein kinase I gamma (Camkg), -protein kinase 1D (Camk1d) and -protein kinase IV (Camk4) were shown to be regulated by TM in an Nrf2-dependent manner. Interestingly, glutathione peroxidase 3 (Gpx3) was upregulated and superoxide dismutase 1 (Sod1) was downregulated by TM *via* Nrf2 which can have important

implications in oxidative stress-mediated [22] pathophysiology or ER stress caused by perturbations in redox circuitry [22,67,74]

Indeed, there is a growing interest amongst researchers in targeting the UPR in cancerous tumor growth [73]. Recently, it was shown [127] that the proteasomal inhibitor bortezomib induces a unique type of ER stress characterized by an absence of eif2alpha phosphorylation, ubiquitylated protein accumulation, and proteotoxicity in human pancreatic cancer cells. It was also reported [128] that malignant B cells may be highly dependent on ER-Golgi protein transport and that targeting and inhibiting this process by brefeldin A may be a promising therapeutic strategy for B-cell malignancies, especially for those that respond poorly to conventional treatments, e.g., fludarabine resistance in chronic lymphocytic leukemia (CLL). However, the role of Nrf2 in modulating the UPR *in vivo* has never been examined before.

The current study, thus, addresses the spatial regulation in mouse small intestine and liver of global gene expression profiles elicited by TM-mediated ER stress *via* Nrf2. Several common clusters of genes such as that for ubiquitin/proteasome, cell adhesion, transcription factors were observed in this study that were also observed in previous studies with Nrf2 activators [38,52,55,56,129] which validates our studies from a functional standpoint. In addition, three clusters of genes – calcium homeostasis, ER/Golgi transport & ER/Golgi biosynthesis/metabolism genes, and glucose homeostasis genes – were uniquely observed as modulated via Nrf2 in response to TM-mediated ER stress that were not discernible in previous studies with Nrf2 activators. Indeed, the involvement of the three clusters mentioned above is a rational response to alteration in the homeostatic environment brought about by the toxicant TM-induced

ER stress, and is reflective of their potential role in the UPR to ER stress that is naturally not observed in previous studies on cancer chemoprevention with Nrf2 activators that do not induce ER stress. The presence of the three unique clusters as mentioned above that relate to the putative role of these genes in the UPR is an effect that appears to be elicited in a toxicant-specific manner. In addition, classical Phase II genes such as Gst isoforms and Gclm were downregulated in a Nrf2-dependent fashion in response to the toxicant TM at 3 hours in this study. We were able to see the downregulation of classical Phase II genes in qRT-PCR experiments performed at a 12 hour time-point (data not shown) with the extent of downregulation being more pronounced at 12 hours than at 3 hours in response to the toxicant TM. Interestingly, this contrasts with the delayed response reported for the classical Phase II gene NQO1 in response to Nrf2 activator BHA (Butylated hydroxyanisole) wherein the induction of the gene peaked at 12 hours [52] with no gene induction at 3 hours. Taken together, the downregulation of classical Phase II genes in response to TM-induced ER stress should be viewed in the light of a complex of physiological factors including partitioning across the gastrointestinal tract, intestinal transit time, uptake into the hepatobiliary circulation, exposure parameters such as Cmax, Tmax and AUC, and pharmacokinetics of disposition after oral administration of TM. Further studies will be necessary to address the effect(s) of temporal dependence on pharmacokinetic parameters and gene expression profiles to further enhance our current understanding of TM-mediated ER stress response, the complexity of kinetics of Phase II gene expression response to a toxicant and the role of Nrf2.

In conclusion, our microarray expression profiling study provides some novel insights into the pharmacogenomics and spatial regulation of global gene expression profiles elicited in the mouse small intestine and liver by TM in an Nrf2-dependent manner from a biological perspective. Amongst these TM-regulated genes, clusters of Nrf2-dependent genes were identified by comparing gene expression profiles between C57BL/6J Nrf2(+/+) and C57BL/6J/Nrf2(–/–) mice. The identification of novel molecular targets that are regulated by TM *via* Nrf2 *in vivo* raises possibilities for targeting the UPR proteins in future to augment or suppress the ER stress response and modulate disease progression. This study clearly extends the current latitude of thought on the molecular mechanisms underlying TM-mediated UPR effects as well as the role(s) of Nrf2 in its biological functions. Future *in vivo* and *in vitro* mechanistic studies exploring the germane molecular targets or signaling pathways as well as Nrf2-dependent genes related to the significant functional categories uncovered in the current study would greatly extend our understanding of the diverse cellular and physiological processes that may be regulated by the UPR in cancer pharmacology and toxicology, and the potential role of ER stress in modulating Nrf2 function as a transcriptional activator.

3.6. Acknowledgements

The authors are deeply grateful to Mr. Curtis Krier at the Cancer Institute of New Jersey (CINJ) Core Expression Array Facility for his expert assistance with the microarray analyses. The authors are also deeply indebted to Ms. Donna Wilson of the Keck Center for Collaborative Neuroscience, Rutgers University as well as the staff of the Human

Genetics Institute of New Jersey at Rutgers University for their great expertise and help with the quantitative real-time PCR analyses. This work was supported in part by NIH grant R01- 094828.

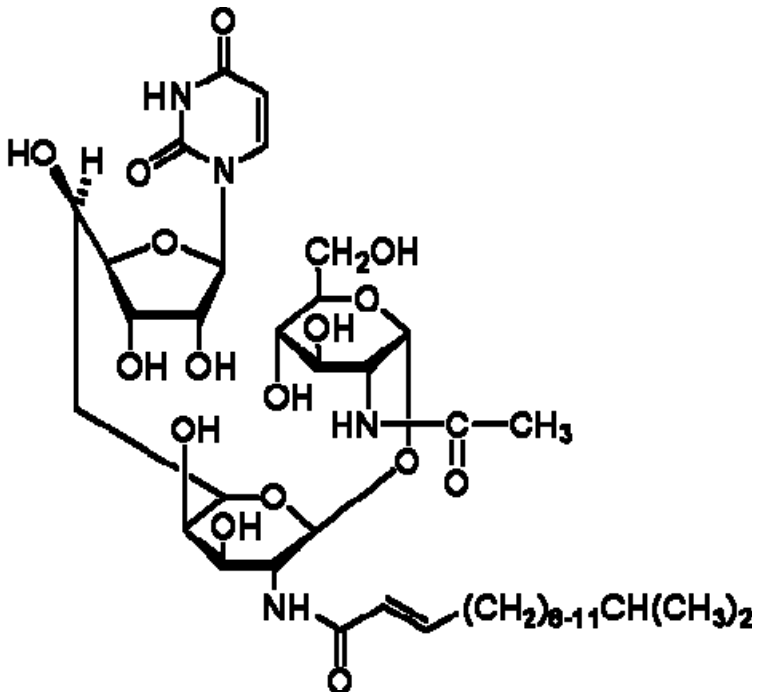

Figure 3.1. Chemical Structure of Tunicamycin (TM).

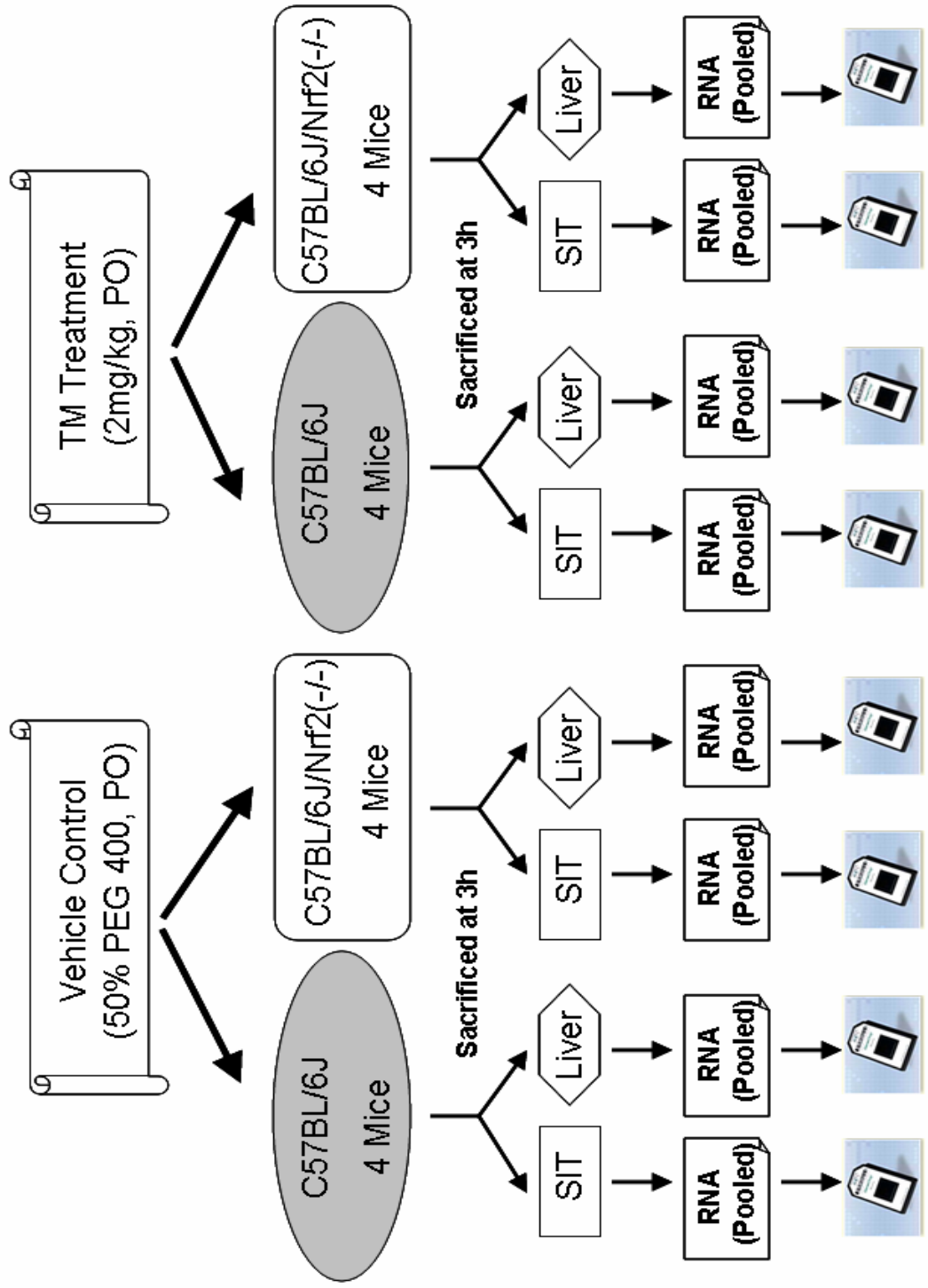

Figure 3.2. Schematic representation of experimental design; *SIT*, Small Intestine.

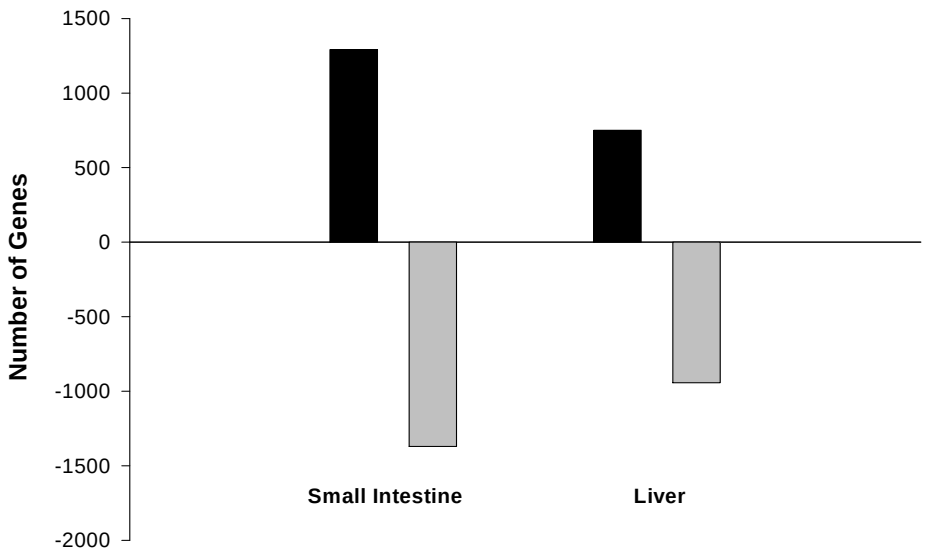

Figure 3.3. Regulation of Nrf2-dependent gene expression by TM in mouse small intestine and liver. Gene expression patterns were analyzed at 3h after administration of a 2mg/kg single oral dose of TM; Nrf2-dependent genes that were either induced or suppressed over two fold were listed. The positive numbers on the *y-axis* refer to the number of genes being induced; the negative numbers on the *y-axis* refer to the number of genes being suppressed.

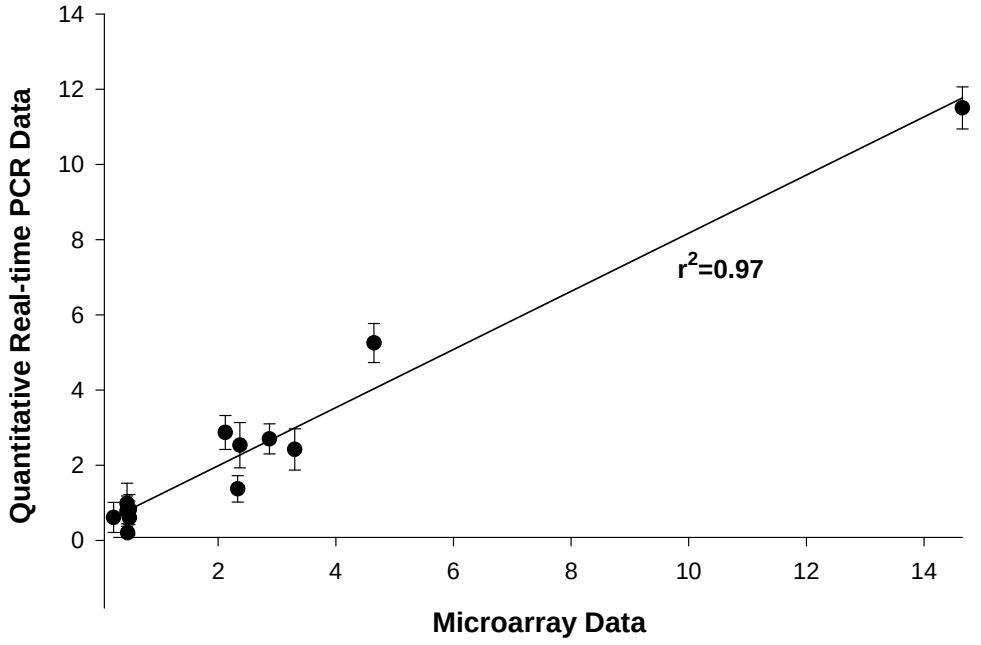

Figure 3.4. Correlation of microarray data with quantitative real-time PCR data. Fold changes in gene expression measured by quantitative real-time PCR for each sample in triplicate (n=3) were plotted against corresponding fold changes from microarray data (coefficient of determination, $r^2 = 0.97$).

CHAPTER 4

Synergistic effects of a combination of dietary factors sulforaphane and (-) epigallocatechin-3-gallate in HT-29 AP-1 human colon carcinoma cells[10,11,12]

4.1. Abstract

The objective of this study was to investigate combinations of two chemopreventive dietary factors: EGCG 20 μM (or 100 μM) and SFN (25 μM) in HT-29 AP-1 human colon carcinoma cells. After exposure of HT-29 AP-1 cells to SFN and EGCG, individually or in combination, we performed AP-1 luciferase reporter assays, cell viability assays, isobologram analyses, senescence staining, quantitative real-time PCR (qRT-PCR) assays, western blotting, and assays for HDAC activity and hydrogen peroxide. In some experiments, we exposed cells to superoxide dismutase (SOD) or Trichostatin A (TSA) in addition to the treatment with dietary factors. The combinations of SFN and EGCG dramatically enhanced transcriptional activation of AP-1 reporter in HT-29 cells (46-fold with 25 μM SFN and 20 μM EGCG; and 175-fold with 25 μM SFN and 100 μM EGCG). Isobologram analysis showed synergistic activation for the combinations with combination index, CI<1. Interestingly,

---

[10]Work described in this chapter has been published as **Nair, S.,** Kong, A.-N. T., Pharm Res. 2007 Jul 27; [Epub ahead of print].

[11]**Keywords :** Isothiocyanate, sulforaphane, EGCG, colon cancer, AP-1, combination.

[12]**Abbreviations :** SFN, sulforaphane; EGCG, (-) epigallocatechin-3-gallate; MAPK, mitogen-activated protein kinase; SOD, superoxide dismutase; HDAC, histone deacetylase; TSA, Trichostatin A; qRT-PCR, quantitative real-time PCR; AP-1, activator protein-1.

co-treatment with 20units/ml of SOD, a free radical scavenger, attenuated the synergism elicited by the combinations (2-fold with 25 μM SFN and 20 μM EGCG; and 15-fold with 25 μM SFN and 100 μM EGCG). Cell viability assays showed that the low-dose combination decreased cell viability to 70% whereas the high-dose combination decreased cell viability to 40% at 48 hrs, with no significant change in cell viability at 24 hours as compared to control cells. In addition, 20 μM and 100 μM EGCG, but not 25 μM SFN, showed induction of senescence in the HT-29 AP-1 cells subjected to senescence staining. However, both low- and high-dose combinations of SFN and EGCG attenuated the cellular senescence induced by EGCG alone. There was no significant change in the protein levels of phosphorylated forms of ERK, JNK, p38, and Akt-Ser473 or Akt-Thr308. Besides, qRT-PCR assays corroborated the induction of the luciferase gene seen with the combinations in the reporter assay. Relative expression levels of transcripts of many other genes known to be either under the control of the AP-1 promoter or involved in cell cycle regulation or cellular influx-efflux such as cyclin D1, cMyc, ATF-2, Elk-1, SRF, CREB5, SLCO1B3, MRP1, MRP2 and MRP3 were also quantified by qRT-PCR in the presence and absence of SOD at both 6hr and 10hr. In addition, pre-treatment with 100ng/ml TSA, a potent HDAC inhibitor, potentiated (88-fold) the synergism seen with the low-dose combination on the AP-1 reporter transcriptional activation. Cytoplasmic and nuclear fractions of treated cells were tested for HDAC activity at 2hr and 12 hr both in the presence and absence of TSA, however, there was no significant change in their HDAC activity. In addition, the H_2O_2 produced in the cell system was about 2 μM for the low-dose combination which was scavenged to about 1 μM in the presence of SOD. Taken together, the synergistic

activation of AP-1 by the combination of SFN and EGCG that was potentiated by HDAC inhibitor TSA and attenuated by free radical scavenger SOD point to a possible multifactorial control of colon carcinoma that may involve a role for HDACs, inhibition of cellular senescence, and SOD signaling.

4.2. Introduction

Colorectal cancer (cancer of the colon or rectum), according to the Centers for Disease Control and Prevention (CDC) [130], is the second leading cause of cancer-related deaths and the third most common cancer in men and in women in the United States. In addition, the National Cancer Institute (NCI)'s Surveillance Epidemiology and End Results (SEER) Statistics Fact Sheets [131] show that, based on rates from 2001-2003, 5.56% of men and women born today will be diagnosed with cancer of the colon and rectum during their lifetime, i.e., 1 in 18 men and women in the United States are at a lifetime risk of developing colorectal cancer. Since colorectal cancer is initiated in colonic crypts, a succession of genetic mutations or epigenetic changes can lead to homeostasis in the crypt being overcome, and subsequent unbounded growth [132]. Using mathematical models of tumorigenesis through failure of programmed cell death or differentiation, it was predicted [133] that exponential growth in cell numbers does sometimes occur, usually when stem cells fail to die or differentiate. At other times, exponential growth does not occur, instead, the number of cells in the population reaches a new, higher equilibrium which may explain many aspects of tumor behavior including early premalignant lesions such as cervical intraepithelial neoplasia [133]. The development of colon cancer results from the sequential accumulation of activating

mutations in oncogenes, such as *ras*, and inactivating mutations, truncations, or deletions in the coding sequence of several tumor suppressor genes, including *p53* and *adenomatous polyposis coli* (*APC*), together with aberrant activity of molecules controlling genomic stability [134,135].

Epidemiological studies have revealed an inverse correlation between the intake of cruciferous vegetables and the risk of certain types of cancer [136,137]. It has also been reported [138] that because elevated vegetable consumption has been associated with a lower risk of colorectal cancer, vegetables may have a stronger role in preventing the progression of adenomas to carcinomas rather than in preventing the initial appearance of adenomas. Isothiocyanates are a chemical class of compounds that are not naturally present in cruciferous vegetables, such as broccoli and cauliflower, but are nevertheless generated from hydrolysis of secondary metabolites known as glucosinolates by the enzyme myrosinase during the process of vegetable crushing or mastication [139] . Also, they may be produced in the intestines where resident microflora can promote the hydrolysis of glucosinolates to isothiocyanates [140]. Sulforaphane (SFN), an isothiocyanate compound found at high levels in broccoli and broccoli sprouts, is a potent inducer of phase 2 detoxification enzymes and inhibits tumorigenesis in animal models [141]. Indeed, sulforaphane has been implicated in a variety of anti-carcinogenic mechanisms including effects on cell cycle checkpoint controls and cell survival and/or apoptosis in various cancer cells [141], however, epidemiological studies indicate [142] that the protective effects in humans may be influenced by individual genetic variation (polymorphisms) in the metabolism and elimination of isothiocyanates from the body. Recently, we reported [17] that SFN induces

hemoxygenase-1 (HO-1) by activating the antioxidant response element (ARE) through the induction of Nrf2 protein in HepG2 cells and that overexpression of all four p38 mitogen-activated protein kinase (MAPK) isoforms negatively regulated the constitutive and inducible ARE-dependent gene expression. Myzak et al [141] have also reported inhibition of histone deacetylase (HDAC) as a novel mechanism of chemoprotection by SFN.

Green tea polyphenol (-) epigallocatechin-3-gallate (EGCG) is noted to suppress colonic tumorigenesis in animal models and epidemiological studies. The water-extractable fraction of green tea contains abundant polyphenolic compounds, in which EGCG is the major constituent (>50% of polyphenolic fraction) [143]. It has been reported that EGCG, when administered to rats, inhibited azoxymethane-induced colon tumorigenesis [144], and also blocked the formation of 1,2-dimethylhydrazine-induced colonic aberrant crypt foci [145], which is a typical precursor lesion of chemical-initiated colon cancer. Recently [146], EGCG was reported to inhibit inflammation-associated angiogenesis by targeting inflammatory cells, mostly neutrophils, and also inhibit the growth of the highly angiogenic Kaposi's sarcoma tumor cells (KS-Imm) in nude mice. We have observed [14] that EGCG treatment causes damage to mitochondria, and that c-jun N-terminal kinase (JNK) mediates EGCG-induced apoptotic cell death in HT-29 human colon cancer cells. EGCG is also reported [147,148] to inhibit DNA methyltransferase with demethylation of the CpG islands in the promoters, and to reactivate methylation-silenced genes such as p16INK4a, retinoic acid receptor beta, O6-methylguanine methyltransferase, human mutL homolog 1, and glutathione S-transferase-pi in human colon cancer HT-29 cells, esophageal cancer

KYSE 150 cells, and prostate cancer PC3 cells. These activities could be enhanced by the presence of HDAC inhibitors or by a longer-term treatment [148].

Transcription factor activator protein-1 (AP-1) is a redox-sensitive transcription factor that senses and transduces changes in cellular redox status and modulates gene expression responses to oxidative and electrophilic stresses presumably via sulfhydryl modification of critical cysteine residues found on this protein and/or other upstream redox-sensitive molecular targets [149]. In budding yeast, the transcription factor Yap1 (yeast AP1), which is a basic leucine zipper (bZip) transcription factor, confers the cellular response to redox stress by controlling the expression of the regulon that encodes most yeast antioxidant proteins [8]. AP-1 is responsive to low levels of oxidants resulting in AP-1/DNA binding and an increase in gene expression. AP-1 activation is typically due to the induction of JNK activity by oxidants resulting in the phosphorylation of serine 63 and serine 73 in the c-Jun transactivation domain [7,28,29]. With high concentrations of oxidants, AP-1 is inhibited and gene expression is impeded. Inhibition of AP-1/DNA interactions is attributed to the oxidation of specific cysteine residues in c-Jun's DNA binding region, namely cysteine 252 [7,30]. Indeed, for AP-1, a nuclear pathway to reduce the Cys of the DNA-binding domain is apparently distinct from the upstream redox events that activate the signaling kinase pathway [6].

The fate of cancer chemopreventive strategies relies largely on the ability to maximally exploit the intrinsic anti-carcinogenic potential of chemopreventive agents, both singly and in combination, without incurring undue toxicity. Targeting multiple signal transduction pathways involved in different stages of carcinogenesis by use of

combinatorial approaches would ideally empower the clinician to better manage or delay the progression of the disease. Given the abundance of literature on the multifarious anti-carcinogenic mechanisms of SFN and EGCG, we investigated the combinations of these two dietary factors and the role(s) mediated by redox transcription factor AP-1 in modulating the anti-cancer potential of this putative chemopreventive combination for the management of colon cancer.

4.3. Materials and Methods

Cell culture and Reagents : Human colon carcinoma HT-29 cells were stably transfected with an Activator Protein (AP-1) luciferase reporter construct, and are referred to as HT-29 AP-1 cells. The cells were cultured in Minimum Essential Medium (MEM) containing 10% Fetal Bovine Serum (FBS) and 1% Penicillin-Streptomycin. Twelve hours prior to experimental treatments, the cells were exposed to MEM containing 0.5% FBS. Sulforaphane (SFN) was obtained from LKT Labs, (-) epigallocatechin-3-gallate (EGCG), superoxide dismutase (SOD) were obtained from Sigma-Aldrich Co., and Trichostatin A (TSA) was obtained from Biomol. SFN, EGCG and TSA were dissolved in dimethylsulfoxide (DMSO, Sigma), whereas SOD was dissolved in 1X phosphate-buffered saline (PBS).

Reporter gene assays : HT-29 AP-1 cells were seeded in six-well culture plates and treated in duplicate with dimethylsulfoxide (control), 20 μM EGCG, 100 μM EGCG, 25 μM SFN, 20 μM EGCG + 25 μM SFN, or 100 μM EGCG + 25 μM SFN for 24 hours. Thereafter, the supernatant medium was aspirated on ice, cells were washed

thrice with ice-cold 1X PBS, treated with 1X Luciferase Reporter Lysis Buffer (Promega) and subjected to one cycle of snap freeze-thaw at -80 °C. Cell lysates were harvested with sterile RNAse-free and DNAse-free cell scrapers into microcentrifuge tubes that were immediately placed on ice. They were then centrifuged at 4 °C for ten minutes at 13000 x g and returned to ice. Twenty microliters of supernatant solution was analyzed for relative luciferase activity using a Sirius Luminometer (Berthold Detection Systems). The relative luciferase activities were normalized by protein concentrations of individual samples as described below.

Protein Assays : Protein concentrations of samples were determined by the bicinchonic acid-based BCA Protein Assay Kit (Pierce) according to the manufacturer's instructions using a 96-well plate. Standard curves were constructed using bovine serum albumin (BSA) as a standard. The sample readings were obtained on a μQuant microplate reader (Bio-tek Instruments, Inc.) at 560nm.

Western blotting : HT-29 AP-1 cells were subjected to treatment with different dietary factors for one or two hours and harvested on ice with either 1X Whole Cell Lysis Buffer or 1X MAPK Buffer. Protein (20 μg) was boiled with sample loading buffer containing β-mercaptoethanol and loaded onto 18-well Criterion Pre-cast gels (Bio-Rad) with Precision Plus Dual Color Protein Marker (Bio-Rad). Electrophoresis was performed at 200 V and semi-dry transfer of each gel was effected onto a polyvinylidine difluoride (PVDF) membrane in an electroblotter at 130mA for 1.5 hours. The membranes were then blocked with 5% BSA in TBST for one hour, washed

thrice for ten minutes each with 1X TBST, and incubated with primary antibodies against ERK, JNK, p38, AKT Ser473, AKT Thr308, and Actin (Cell Signaling Inc.) in 3% BSA in TBST (1:2000 antibody dilutions, except beta-actin which was 1:1000) for one hour at room temperature with gentle agitation. After further three washes with 1X TBST, the membranes were incubated with appropriate secondary antibodies in 3% BSA in TBST (1:2000 for P-ERK and P-JNK, 1:5000 for P-p-38 and beta-actin, and 1:10,000 for phosphorylated forms of Akt) overnight at 4 °C with gentle rocking. The following day, the membranes were washed again thrice with 1X TBST and treated with ECL chemiluminescence reagent (Pierce) and visualized using a Bio-Rad Imaging Station. The protein expression was normalized against that of actin as a control.

Cell Viability Assays : The cell viability assays were performed in 24-well cell culture plates using MTS Assay Kit (Promega) according to the manufacturer's instructions. Cell viability was determined at both 24 and 48 hours after treatment with dietary factors. The absorbance readings were obtained on an μQuant microplate reader (Bio-tek Instruments, Inc.) at recommended wavelength of 490nm.

RNA Extraction and Assessment of RNA Integrity : HT-29 AP-1 cells were subjected to treatment with different dietary factors in triplicate for 6hours or 10 hours. RNA was harvested using the RNeasy Mini Kit (Qiagen) according to the manufacturer's instructions. RNA integrity was assessed using formaldehyde gels in 1X MOPS buffer and RNA concentration was determined by the 260/280 ratio on a DU 530 UV/Visible spectrophotometer (Beckman).

Quantitative Real-time PCR Assays : Several genes of interest including luciferase gene as well as genes known to be either under the control of the AP-1 promoter or involved in cell cycle regulation or cellular influx-efflux such as cyclin D1, cMyc, ATF-2, Elk-1, SRF, CREB5, MDR1, SLCO1B3, MRP1, MRP2 and MRP3 were selected for quantitative real-time PCR analyses both in the presence or absence of SOD treatment. Beta-actin served as the "housekeeping" gene. The specific primers for these genes listed in Table 4.1 were designed by using Primer Express 2.0 software (Applied Biosystems, Foster City, CA) and were obtained from Integrated DNA Technologies, Coralville, IA. The specificity of the primers was examined by a National Center for Biotechnology Information Blast search of the human genome. For the real-time PCR assays, briefly, after the RNA extraction and assessment of RNA integrity, first-strand cDNA was synthesized using 4μg of total RNA following the protocol of SuperScript III First-Strand cDNA Synthesis System (Invitrogen) in a 40 μl reaction volume. The PCR reactions based on SYBR Green chemistry were carried out using 100 times diluted cDNA product, 60 nM of each primer, and SYBR Green master mix (Applied Biosystems, Foster City, CA) in 10 μl reactions. The PCR parameters were set using SDS 2.1 software (Applied Biosystems, Foster City, CA) and involved the following stages : 50°C for 2min, 1 cycle; 95°C for 10 mins, 1 cycle; 95°C for 15 secs → 55 °C for 30 secs →72°C for 30 secs, 40 cycles; and 72°C for 10 mins, 1 cycle. Incorporation of the SYBR Green dye into the PCR products was monitored in real time with an ABI Prism 7900HT sequence detection system, resulting in the calculation of a threshold cycle (C_T) that defines the PCR cycle at which exponential growth of PCR products

begins. The carboxy-X-rhodamine (ROX) passive reference dye was used to account for well and pipetting variability. A control cDNA dilution series was created for each gene to establish a standard curve. After conclusion of the reaction, amplicon specificity was verified by first-derivative melting curve analysis using the ABI software; and the integrity of the PCR reaction product and absence of primer dimers was ascertained. The gene expression was determined by normalization with control gene beta-actin.

Hydrogen Peroxide Assays : The levels of hydrogen peroxide in the cell-free medium was ascertained by the Amplex Red Hydrogen Peroxide Assay Kit (Molecular Probes/Invitrogen) according to the manufacturer's instructions. Briefly, a working solution of 100 μM Amplex Red reagent and 0.2U/ml HRP was prepared, of which 50 μl was added to each microplate well containing the positive control (10 μM H_2O_2), negative control (1X Reaction Buffer without H_2O_2) and test samples. The fluorescence signal was measured on a FLx-800 microplate fluorescent reader (Bio-tek Instruments, Inc.) at excitation wavelength of 560 nm and emission wavelength of 590 nm.

HDAC Activity Assays : Cytoplasmic and nuclear fractions of cells treated with dietary factors, both in the presence and absence of 100ng/ml TSA, were extracted using the Ne-Per extraction kit (Pierce). The HDAC activity was determined using a Fluor-de-Lys HDAC Fluorescent Activity Assay Kit (Biomol) according to the manufacturer's instructions. Briefly, incubations were performed at 37°C for 10 min with HeLa nuclear cell extracts containing known HDAC activity that were provided by the manufacturer. The HDAC reaction was initiated by the addition of Fluor-de-Lys

substrate. After 10 min, the reaction was quenched by adding the Fluor-de-Lys Developer, and the mixture was incubated for another 10 min at ambient temperature. The fluorescence signal was measured using a FLx-800 microplate fluorescent reader (Bio-tek Instruments, Inc.) at excitation wavelength of 360 nm and emission wavelength of 460 nm.

Senescence Staining : HT-29 AP-1 cells were grown on cover slips and treated with DMSO (control), individual dietary factors, or combinations of dietary factors. The X-gal-based staining was performed using the Senescence Assay Kit (Sigma-Aldrich Co.) according to the manufacturer's instructions. Bluish-green stain was positive for senescence-associated beta-galactosidase activity. The slides were fixed and images were obtained using a Nikon Eclipse E600 microscope (Micron-Optics, Cedar Knolls, NJ) equipped with DXM 1200 Nikon Digital Camera.

Statistical Analyses : Data are expressed as mean ± standard deviation, and comparisons among treatment groups were made using one-way analysis of variance (ANOVA) followed by a post hoc test for multiple comparisons – the Tukey's Studentized Range Honestly Significant Difference (HSD) test. In all these multiple comparisons, $P < 0.05$ was considered statistically significant. When only two groups of treatment means were evaluated, we employed paired, two-tailed Student's t-test ($P<0.01$ was considered significant) or paired, one-tailed Student's t-test ($P<0.05$ was considered significant) as indicated in the text where applicable. Statistical analyses

were performed using SAS 9.1 software (SAS Institute Inc, NC) licensed to Rutgers University.

4.4. Results

4.4.1. Transactivation of AP-1 luciferase reporter by combinations of SFN and EGCG

As shown in Figure 4.1, treatment of HT-29 AP-1 cells for 24 hours with either SFN 25 μM, EGCG 20 μM or EGCG 100 μM individually resulted in about five-fold induction of AP-1 luciferase activity as compared to control cells that were treated with DMSO. Surprisingly, a low-dose combination of SFN 25 μM + EGCG 20 μM elicited a dramatic induction of AP-1 luciferase activity (over 45-fold). In addition, a high-dose combination of SFN 25 μM + EGCG 100 μM further potentiated the induction of AP-1 luciferase activity to about 175-fold. We also investigated the effects of pre-treatment on the induction of AP-1 luciferase activity. In these experiments (data not shown), we first pre-treated the HT-29 AP-1 cells for six hours with EGCG (20 μM or 100 μM), then washed off the EGCG thrice with phosphate-buffered saline (PBS) and treated the cells with SFN 25 μM for an additional 18 hours before assaying for luciferase activity. Alternatively, we also pre-treated the cells with SFN 25 μM for 6 hours before washing with PBS as above and treating with EGCG (20 μM or 100 μM) for an additional 18 hours. It was observed that there was no significant difference in induction of AP-1 luciferase activity in these pre-treatment experiments (data not shown) as compared to when the two agents were co-treated as shown in Figure 4.1. This enabled us to rule out any physicochemical interaction between the two agents in cell culture when co-treated

that may have otherwise produced any experimental artifacts in the luciferase assay. Hence, since the effects of the combinations when co-treated were not physicochemical, but potentially modulated at a mechanistic level, we continued all our experiments by co-treating both agents together for 24 hours for ease of experimentation without confounding variables.

4.4.2. SOD attenuates the synergism elicited by combinations of SFN and EGCG

Since EGCG is known to produce oxidative stress [14], we also investigated whether the effects of the SFN and EGCG combinations on AP-1 luciferase induction were mediated, in part, by the free radical scavenger SOD. Accordingly, we also co-treated the combinations with 20U/ml of SOD before assaying for AP-1 luciferase activity. Interestingly, the co-treatment with SOD significantly attenuated the induction observed with the SFN + EGCG combinations in the HT-29 AP-1 cells. The relative luciferase activity of the SFN 25 μM + EGCG 20 μM combination (over 45-fold) was attenuated to about 2-fold in the presence of SOD; whereas the relative luciferase activity of the SFN 25 μM + EGCG 100 μM combination (175-fold) was attenuated to about 15-fold in the presence of SOD as shown in Figure 4.1 indicating that SOD signaling may play a role in modulation of AP-1 luciferase activity by these chemopreventive combinations.

4.4.3. Isobologram analyses and combination indices for the combinations of SFN and EGCG

In order to confirm the synergistic interaction observed in the luciferase assays with the combinations of SFN and EGCG, we performed isobologram analyses as reported by Zhao et al [150]. Twenty-five combinations of SFN (2.5 μM, 5 μM, 7.5 μM, 10 μM, 12.5 μM) with EGCG (2.5 μM, 5 μM, 7.5 μM, 10 μM, 12.5 μM) were tested in addition to the SFN 25 μM + EGCG 20 μM combination. Nine of these combinations that showed same effect as individual agents in terms of five-fold induction of AP-1 luciferase activity were selected for isobologram analyses. Under the conditions of the analyses, all the combinations tested showed synergistic interaction in the isobologram analyses as shown in Figure 4.2. This confirmed the synergistic nature of the interaction between the combinations and indicated that lower doses of SFN with EGCG would also be able to elicit synergistic transactivation of the AP-1 luciferase reporter although to a lesser degree. In addition, as reported by Zhao et al [150], we evaluated the combination indices that were generated by these combinations in these analyses, and it was observed that, in conformity with the general consensus, all the synergistic combinations had a value of combination index <1 (ranging from 0.325 to 0.7, data not shown) which further confirmed the synergistic interaction between the combinations of SFN with EGCG.

4.4.4. Viability of the HT-29 AP-1 cells with the combinations of SFN and EGCG

In order to ascertain the effects of the combinations of SFN and EGCG on the cell viability of the HT-29 AP-1 cells, we used the MTS assay with treatment durations of

24 hours and 48 hours. As shown in Figure 4.3, there was no significant change in cell viability at 24 hours between the combination treatments and the individual agent treatments relative to the control cells showing that the doses used were non-toxic to the cells at 24 hours. At 48 hours, however, the viability of cells treated with combinations comprising SFN 25 μM + EGCG 20 μM and SFN 25 μM + EGCG 100 μM decreased to 70% and 40% respectively relative to control cells indicating that the low-dose combination of SFN 25 μM + EGCG 20 μM may be more appropriate to pursue in longer duration in vitro studies or potential in vivo studies without seemingly toxic effects a priori, and at the same time not compromising on the synergistic efficacy elicited by the combination of these two chemopreventive agents.

4.4.5. Inhibition of EGCG-induced senescence by the combinations of SFN and EGCG

Since EGCG is known to inhibit telomerase and induce senescence in leukemic cells [151], we also investigated the effects of the combinations of SFN and EGCG on senescence-associated beta-galactosidase activity by a standard staining procedure as described in Materials and Methods. As shown in Figure 4.4, HT-29 AP-1 cells, when cultured on cover slips and exposed to individual treatment of EGCG (20 μM or100 μM) for 24 hours, showed induction of senescence which was not observed in the case of SFN 25 μM. Interestingly, on combining EGCG with SFN, the EGCG-associated senescence was attenuated. Both combinations comprising SFN 25 μM + EGCG 20 μM, and, SFN 25 μM + EGCG 100 μM attenuated the cellular senescence induced by EGCG suggesting that the synergistic effects of the combination on AP-1

transactivation may also be potentially mediated in part via inhibition of cellular senescence pathways.

4.4.6. Temporal gene expression profiles elicited by combinations of SFN and EGCG and attenuation by SOD

We performed quantitative real-time PCR (qRT-PCR) experiments with primers (Table 4.1) for the luciferase gene to corroborate the synergism elicited with the combinations of SFN and EGCG in the luciferase protein assay with mRNA levels in qRT-PCR. As shown in Table 4.2, the temporal expression (at 6 hrs and 10 hrs) of luciferase gene in qRT-PCR assays was significantly higher ($P<0.01$ at 6hrs by a two-tailed, paired Student's t-test ; and $P<0.05$ at 10hrs by a one-tailed, paired Student's t-test) for the combinations of SFN and EGCG as compared to individual dietary factor treatments in consonance with our data in the luciferase protein assays. The treatment means for all the treatment groups at a specific time point (6 hrs or 10 hrs) were significantly different from each other ($P<0.05$ by ANOVA and post hoc Tukey's test for multiple comparisons to detect significantly different means). In addition, co-treatment with SOD attenuated the synergism elicited with the combinations of SFN and EGCG at both 6 hrs and 10 hrs as shown in Table 4.3 which also further validated our luciferase data. We also determined by qRT-PCR the relative expression levels of transcripts of many genes that were known to be either under the control of the AP-1 promoter or involved in cell cycle regulation or cellular influx-efflux such as cyclin D1, cMyc, ATF-2, Elk-1, SRF, CREB5, SLCO1B3, MRP1, MRP2 and MRP3 in the absence of SOD (Table 4.2) and in the presence of SOD (Table 4.3).

The low- and high-dose combinations of SFN and EGCG in this study elicited the downregulation of positive cell cycle regulator cyclin D1 expression (Table 4.2) that was further decreased by SOD (Table 4.3) as compared with individual dietary factors. There was, however, no appreciable change in expression of cell proliferation-related cMyc except for its downregulation in the high-dose combination in the presence of SOD. In addition, transcription factors/coactivators that are known to be under the control of the AP-1 promoter such as activating transcription factor (ATF-2), Ets-like transcription factor (Elk-1), serum response factor (SRF) and cyclic AMP response element binding protein 5 (CREB5) were also studied in the absence and presence of SOD (Tables 4.2 and 4.3 respectively). Interestingly, the expression of ATF-2 with the low-dose combination of SFN and EGCG was similar to that of the SFN-only treatment. The activation of Elk-1 that was observed in our qRT-PCR studies (Table 4.2) was similar for the combinations as well as individual agents which complemented our results for phosphorylated ERK1/2 protein (Figure 4.5). Interestingly, the low-dose combination of SFN and EGCG inhibited the transcriptional activation of SRF as compared to individual dietary factors; this inhibition was reversed on co-treatment with SOD at both time points. The combinations had no effect on transcriptional expression of CREB5 as compared to individual agents. Since exogenous stress can potentially stimulate the influx-efflux machinery of cells, we also investigated some key transporter genes (Table 4.2). In this study, we observed the induction of the SLCO1B3 gene, which encodes for the organic anion transporter protein OATP1B3, by EGCG-alone treatments which was reversed by treatment with the combinations of SFN and EGCG (Table 4.2). Interestingly, the combinations of SFN and EGCG greatly induced

the expression of the efflux transporter MRP2 as shown in Table 4.2. In addition, the expression of influx transporters MRP1 and MRP3 was lower for the combination-treated cells as compared to the individual agent-treated cells.

4.4.7. Protein expression with the combinations of SFN and EGCG

We investigated the effects of the combinations on protein expression of major mitogen-activated protein kinase (MAPK) pathway members including ERK, JNK and p38 as well as the Akt pathway (Figure 4.5). Interestingly, although the expression of c-jun N-terminal kinase (JNK) was greater for the combinations relative to the control, it was not greater than the JNK expression of individual agents, suggesting that the SFN+EGCG combination-mediated activation of AP-1 reporter may occur by cellular mechanisms that are exclusive of JNK activation. Similarly, there was no significant change in protein expression of extracellular signal regulated kinase (ERK), p38 or Akt Ser and Akt Thr for the combination-treated cells as compared to the individual agent-treated cells.

4.4.8. HDAC inhibitor Trichostatin A potentiates the synergism elicited by the low-dose combination of SFN and EGCG

Since inhibition of histone deacetylase (HDAC) has been reported [141] as a novel mechanism of chemoprotection by the isothiocyanate SFN, we investigated the effects of HDAC inhibitor Trichostatin A (TSA) on the transactivation potential of the combinations by pre-treatment of HT-29 AP-1 cells with 100ng/ml TSA for four hours followed by treatment with dietary factors for 24 hours. Interestingly, as shown in

Figure 4.6, pre-treatment with HDAC inhibitor TSA potentiated (about 20-fold) the transactivation of the AP-1 luciferase reporter by SFN 25 μM alone, suggesting that activation of AP-1 luciferase activity in this cell system may possibly relate to HDAC inhibition. Similarly, a strong potentiation of AP-1 transactivation (about 88-fold) was also observed with the low-dose combination of SFN 25 μM + EGCG 20 μM suggesting that maximal transcriptional activation of the AP-1 reporter genes may potentially be achieved by combining TSA with this synergistic combination. On the other hand, transactivation by both EGCG 20 μM and EGCG 100 μM was not potentiated by TSA inhibition. Interestingly, the high-dose combination of SFN 25 μM + EGCG 100 μM attenuated (about 93-fold) the synergism elicited with this combination which may be attributed to toxicity caused by exposure to TSA in addition to the high-dose combination.

4.4.9. Cytoplasmic and Nuclear HDAC Activity Assays for the combinations of SFN and EGCG

HDAC activity assays for cytoplasmic and nuclear fractions of cells treated with dietary factors were conducted as described under Materials and Methods at both 2 hours and 12 hours after treatment, as well as after first pre-treating the cells with 100ng/ml TSA before treatment with dietary factors for 2 or 12 hours. Interestingly, there was no significant change in HDAC activity of cytoplasmic or nuclear fractions of dietary factor-treated cells relative to vehicle control (data not shown).

4.4.10. Reactive oxygen species and SOD may modulate AP-1 transactivation by the combinations of SFN and EGCG

Since EGCG is known to induce oxidative stress, we investigated the potential role of reactive oxygen species (ROS) such as hydrogen peroxide (H_2O_2) along with the free radical scavenger SOD in modulating the transcriptional events through the AP-1-responsive reporter. Accordingly, we performed assays for H_2O_2 in cell-free media using an assay kit as described in Materials and Methods. Consistent with the ability of EGCG to induce oxidative stress, we quantified a production of 2 μM H_2O_2 at 15 minutes in HT-29 AP-1 cells treated with 20 μM EGCG alone. Presence of SFN in the SFN 25 μM + EGCG 20 μM combination did not affect the amount of H_2O_2 produced by EGCG. However, co-treatment with 20 U/ml of SOD decreased the amount of H_2O_2 detected at 15 minutes by half to 1 μM, which result was consistent in the case of both EGCG 20 μM alone or SFN 25 μM + EGCG 20 μM as shown in Figure 4.7. The amount of H_2O_2 detected decreased in a generally time-dependent manner thereafter for most dietary factor treatments. In addition, about 4 μM H_2O_2 was produced at 15 minutes in HT-29 AP-1 cells treated with 100 μM EGCG alone or SFN 25 μM + EGCG 100 μM. However, co-treatment with 20 U/ml SOD was not able to significantly scavenge the H_2O_2 produced at the high dose of EGCG or by the high-dose combination of SFN 25 μM + EGCG 100 μM.

4.5. Discussion

Colorectal cancer has a natural history of transition from precursor to malignant lesion that spans, on average, 15-20 years, providing a window of opportunity for effective

interventions and prevention [152]. Data accumulating in recent years have suggested that aspirin, non-steroidal anti-inflammatory drugs, and selective cycloxygenase (COX-2) inhibitors all have a potential to reduce both colorectal cancer and colorectal adenomas [153], however, issues of safety and therapeutic indices have come up as barriers to the use of some of these agents. Many dietary phytochemicals exhibit beneficial effects to health including prevention of diseases such as cancer. Mammalian, including human, cells respond to these dietary phytochemicals by "non-classical receptor sensing" mechanism of electrophilic chemical-stress typified by "thiol modulated" cellular signaling events primarily leading to gene expression of pharmacologically beneficial effects, but sometimes unwanted cytotoxicity [149]. Indeed, with the ultimate goal of preventing cancer, science has advanced greatly in better understanding cancer biology as also in identifying chemotherapeutic/chemopreventive agents that would inhibit or delay the progression of this disease. However, the need to maximally exploit the preventive or therapeutic efficacy of agents without incurring toxicity to normal cells remains challenging. A combinatorial approach to cancer therapy/prevention is being widely recognized as an alternative strategy to potentially improve treatment success rates. Recently [154], a Phase I Trial of sorafenib in combination with IFN α-2a was conducted in patients with unresectable and/or metastatic renal cell carcinoma or malignant melanoma. Besides, combination therapy of an orthotopic renal cell carcinoma model using intratumoral vector-mediated costimulation and systemic interleukin-2 was recently reported [155]. Interestingly, Adhami et al [156] recently reported combined inhibitory effects of green tea polyphenols and selective COX-2 inhibitors on the growth of human prostate cancer

cells both in vitro and in vivo. Our laboratory has been studying two groups of dietary phytochemical cancer chemopreventive compounds (isothiocyanates and polyphenols) [1,2], which are effective in chemical-induced as well as genetically-induced animal carcinogenesis models [3,157]. We decided to pursue the current study on colon cancer prevention by examining the biologic modulation via AP-1 which is a group of dimeric transcription factors composed of Jun, Fos, and ATF family proteins [158]. Notably, in the present study, we investigated the combinations of two dietary factors – isothiocyanate SFN and green tea polyphenol EGCG - and the role(s) mediated by redox transcription factor AP-1 in modulating the anti-cancer potential of this putative chemopreventive combination in stably transfected HT-29 AP-1 human colon carcinoma cells.

We investigated the transactivation of the AP-1 luciferase reporter in our colon cancer cell system by individual treatments with SFN and EGCG and with combinatorial treatments of these two dietary factors (Fig. 1). Indeed, both low-dose and high-dose combinations of SFN and EGCG synergistically induced transactivation of the AP-1 reporter as compared to individual dietary factors. This observation correlated with a corresponding trend of luciferase gene induction in the quantitative real-time PCR (qRT-PCR) assays (Table 4.2). We also confirmed the synergistic interaction in the luciferase assays by testing various combinations of SFN and EGCG by isobologram analyses and determining combination index values as reported by Zhao et al [150] as shown in Figure 4.2. Studies in genetically modified mice and cells have highlighted a crucial role for AP-1 in a variety of cellular events involved in normal development or neoplastic transformation causing cancer [159]. Both gain- and loss-of-function studies

have revealed specific roles for individual AP-1 components in cell proliferation, differentiation, apoptosis, and other biological processes [158]. Recently, Maurer et al [160] observed that in tumors with long necessary follow-up, such as colorectal cancer, early-risk predictors would be needed, and provided first evidence for early prognostic relevance of transcription factors including AP-1 differentially bound to the promoter of the invasion-related gene u-PAR, and their molecular inducers, in colorectal cancer. The synergistic transcriptional activation of the AP-1 reporter that we observe with the combinations of SFN and EGCG in the present study may be seen in the light of the above evidence that point to a singular role for AP-1 mediated transcriptional control of potentially critical genes mediating cancer initiation and progression. This translates into potentially greater efficacy, of the combination of SFN and EGCG in chemoprevention of cancer. Interestingly, co-treatment with free radical scavenger SOD attenuated the synergism elicited by the combinations. This observation also corroborated with a corresponding attenuation of luciferase gene transcript in the qRT-PCR assays (Table 4.3). Indeed, assays for H_2O_2 in cell-free media (Figure 4.7) revealed that SOD co-treatment decreased the amount of H_2O_2 noted with the low-dose combination of SFN and EGCG by half. Taken together, these above observations point to a potential role for SOD signaling in modulating the pharmacologic activity of the combination of SFN and EGCG. Additional studies are necessary to better understand and delineate the specific pathway cross-talk with AP-1 signaling.

The downregulation of cyclin D1 by the SFN and EGCG combinations may be related to the intrinsic ability of SFN to induce G1 cell cycle arrest in HT-29 cells as we have reported earlier [84]. ATF-2 can form a heterodimer with c-jun and controls the

induction of c-jun in an AP-1 independent manner, however, both ATF-2 and c-jun can be activated by c-Jun N-terminal kinases (JNK) [161]. The absence of major ATF-2 activation with the combinations in our study may thus also relate to the absence of JNK activation that we observed with the combinations as compared to individual dietary factors (Figure 4.5). Biochemical studies have indicated that Elk-1 is a good substrate for ERKI/ERK2 in vitro, and that the kinetics of its modification correlated well with MAPK activation in vivo [162]. Thus, the limited transcriptional (Table 4.2) and translational (Figure 4.5) activation of Elk-1 and ERK1/2 respectively that we see in this study may potentially be inter-related, although additional biochemical studies will be necessary to substantiate this hypothesis. Because the influx-efflux machinery of cells could be potentially turned on by exogenous stress, we also investigated some key transporter genes (Table 4.2). Using Hagenbuch and Meier's new nomenclature [163], the gene encoding for the organic anion transporter protein OATP1B3 (old name OATP8) is known as the SLCO1B3 (old nomenclature SLC21A8). OATP1B3 has been shown to be expressed in various human cancer tissues as well as in different tumor cell lines derived from gastric, colon, pancreas, gallbladder, lung and brain cancers [163]. The induction of SLCO1B3 that we observed with EGCG-alone treatments which was reversed by treatment with the combinations of SFN and EGCG (Table 4.2) may be relevant since the intracellular, pharmacologically active concentration of any drug is the balance between uptake and neutralizing pathways, either by biotransformation or extrusion from the targeted cells [164], although the pathobiological significance of expression of this gene is not yet fully understood [163]. Interestingly, the combinations of SFN and EGCG greatly induced the expression of the efflux transporter MRP2

(Table 4.2) but downregulated the expression of influx transporters MRP1 and MRP3. Since the combination treatment of SFN and EGCG would impose exogenous stress on the cellular environment, the induction of MRP2 may be related to a cellular defense response purported to increase the excretion/efflux of the xenobiotics or their metabolites.

Cell senescence is broadly defined as the physiological program of terminal growth arrest, which can be triggered by alterations of telomeres or by different forms of stress [165]. Although senescent cells do not proliferate, they remain metabolically active and produce secreted proteins with both tumor-suppressing and tumor-promoting activities [165]. Besides apoptosis, cell proliferation could, thus, be limited by senescence [166]. In fact, it seems that activation of the senescence program and consequent permanent growth arrest significantly contributes to the loss of the clonogenic capacity of tumor cells and probably to tumor regression after anticancer therapy [166,167]. EGCG is known to inhibit telomerase and induce senescence in leukemic cells [151] and we were able to confirm this in HT-29 AP-1 cells as shown in Figure 4.4. Interestingly, the combinations of SFN and EGCG inhibited the EGCG-induced senescence (Figure 4.4) of HT-29 AP-1 cells. Recently [3], we demonstrated that ApcMin/+ mice fed with SFN-supplemented diet developed significantly less and smaller polyps with higher apoptotic and lower proliferative indices in their small intestine, in a SFN dose-dependent manner. SFN also regulated different sets of genes involving apoptosis, cell growth/maintenance and inflammation in the small intestinal polyps of ApcMin/+ mice [168]. SFN also induced G(1) phase cell cycle arrest in HT-29 cells [84]. We have also shown that EGCG treatment causes damage to mitochondria, and induces apoptotic cell

death [14].Thus, the inhibition of cellular senescence we observed with the combinations of SFN and EGCG may relate to the ability of SFN and EGCG to activate apoptotic pathways that predominate over the senescence pathways induced by EGCG. The viability (Figure 4.3) of the HT-29 AP-1 cells at 48 hours was about 70% and 40% with the low- and high-dose combinations respectively since the low-dose combination was not toxic to the cells as compared with the high-dose combination of SFN and EGCG.

The effects of the combinations on protein expression (Figure 4.5) of major mitogen-activated protein kinase (MAPK) pathway members including ERK, JNK and p38 as well as the Akt pathway was not dramatic as compared to individual agents, suggesting that the SFN+EGCG combination-mediated activation of AP-1 may occur by cellular mechanisms that are exclusive of JNK activation. Since inhibition of histone deacetylase (HDAC) has been reported [141] as a novel mechanism of chemoprotection by the isothiocyanate SFN, we investigated the effects of HDAC inhibitor Trichostatin A (TSA) on the transactivation potential of the combinations. Interestingly, TSA potentiated (Figure 4.6) the synergism elicited by the low-dose combination of SFN and EGCG leading us to speculate whether the strong AP-1 induction may relate to HDAC inhibition. However, there was no significant change in HDAC activity of cytoplasmic or nuclear fractions of dietary factor-treated cells (data not shown). Indeed, maximal transcriptional activation of the AP-1 reporter genes may potentially be achieved by combining TSA with the synergistic low-dose combination of SFN and EGCG. In contrast, the synergism elicited with the high-dose combination was attenuated by TSA (Figure 4.6) which may be attributed to toxicity caused by exposure to the high-dose

combination together with TSA. Further empirical and heuristic studies are necessary to elucidate the exact biochemical mechanisms and the nature of potential cross-talk between AP-1 and HDAC from a physiological perspective.

We have previously reported [169] that the peak plasma concentration (Cmax) achievable with SFN in rats was 20 μM after oral administration. In addition, we have reported [22] that SFN 50 μM was toxic to HepG2 C8 cells, whereas SFN 25 μM was suboptimal in its efficacy. Since a desirable objective of using combinatorial approaches is to reduce the dose of the administered agents thereby reducing toxic side-effects, our dose selection of 25 μM of SFN for the current study was guided by its proximity to the observed Cmax and its suboptimal effectiveness in eliciting transcriptional effects as compared to higher doses of SFN. Besides, in most studies, the concentrations needed to observe the activities of EGCG typically range from 1 to 100 μM; these are, in reality, concentrations that exceed those found in rodent and human plasma by 10- to 100-fold [170,171]. However, the uptake of EGCG in HT-29 cells has also been shown to be concentration-dependent in the range of 20-600 μM [170]. In addition, we have also previously reported [14] that EGCG inhibited HT-29 cell growth with an IC50 of approximately 100 μM. Accordingly, we elected to test two doses of EGCG (20 μM and 100 μM) in the current study in combination with the 25 μM dose of SFN.

In summary, it is necessary to evolve and to justify alternative strategies to develop agents that modulate multiple targets simultaneously with the aim of enhancing efficacy or improving safety relative to agents that address only a single molecular target. Combinatorial approaches to cancer chemoprevention lend themselves to the cause of maximally exploiting the intrinsic ant-carcinogenic potential of known dietary factors

with already proven beneficial effects individually. Taken together, the synergistic activation of the AP-1 reporter that was potentiated by HDAC inhibitor TSA and attenuated by free radical scavenger SOD point to a possible multifactorial control of colon carcinoma that may involve a role for HDACs, inhibition of cellular senescence, and SOD signaling. Future studies to delineate the complex regulation in biological systems, as well as in vivo studies, would be useful in elucidating the effects of combining dietary factors SFN and EGCG to better appreciate the pharmacological benefits of this synergy in cancer prevention.

4.6. Acknowledgements

Sujit Nair is extremely grateful to Ms. Donna Wilson at the Keck Center for Collaborative Neuroscience, Rutgers University, for exhaustive training and extensive discussions that were very helpful in optimizing and validating the quantitative real-time PCR assays. This work was supported in part by RO1-CA073674 and RO1-CA092515 to Ah-Ng Tony Kong from the National Institutes of Health (NIH).

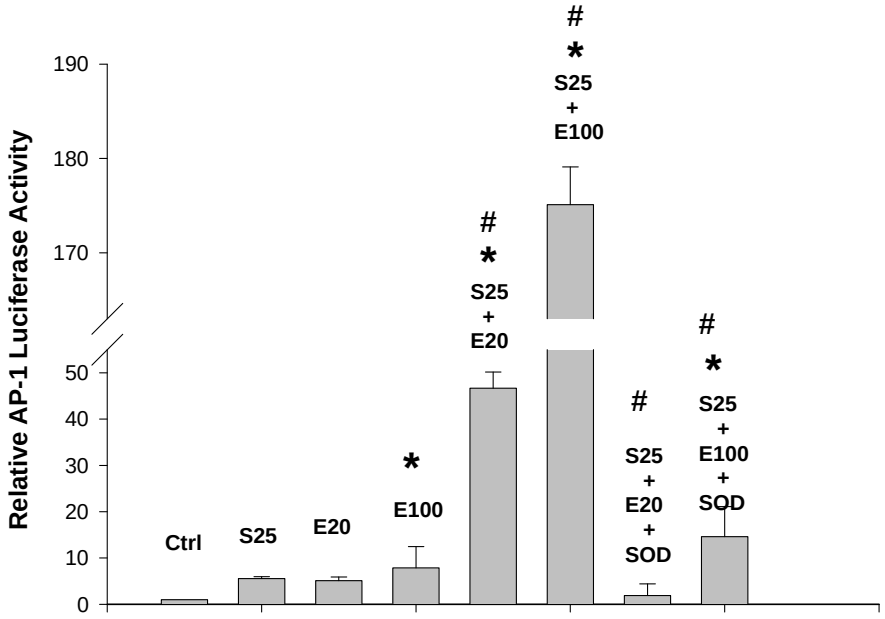

Figure 4.1. Transactivation of AP-1 luciferase reporter by combinations of SFN and EGCG, and attenuation by SOD

HT-29 AP-1 cells were seeded in six-well plates and treated with individual dietary factors or with combinations of SFN and EGCG, as indicated, in the absence or presence of 20U/ml SOD. The AP-1 luciferase activity was measured relative to vehicle control (DMSO) after 24 hours of incubation and normalized against protein concentration. Values represent mean ± standard deviation for three replicates, and are representative of seven independent experiments. * $P < 0.05$, significantly different from vehicle control (Ctrl) ; # $P < 0.05$, significantly different from each other.

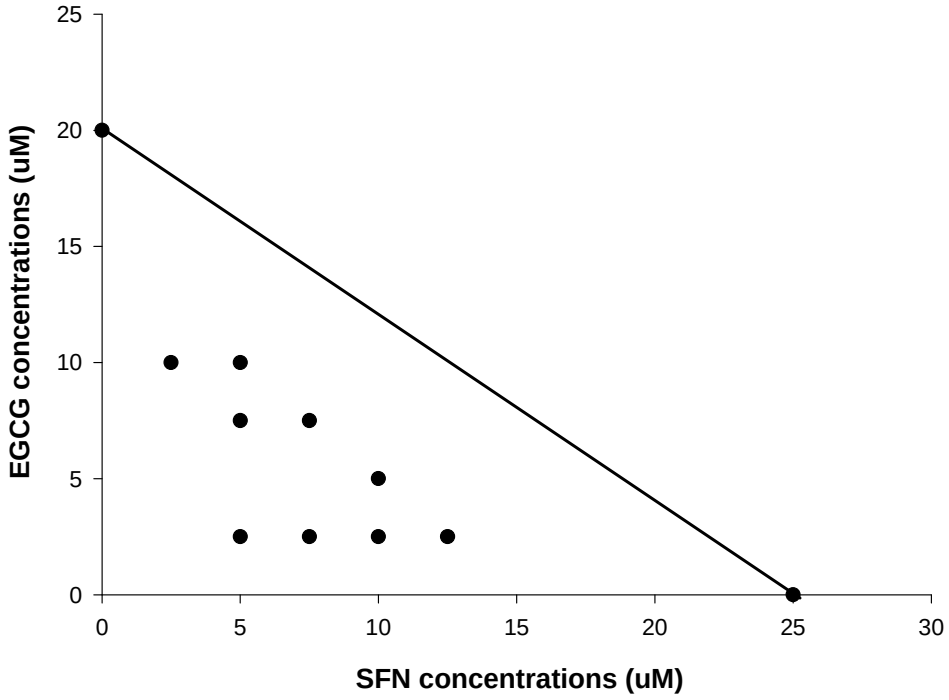

Figure 4.2. Isobologram analyses of synergy between combinations of SFN and EGCG.

Several combinations of individual dietary factors SFN and EGCG were analyzed for synergy by the method of isobologram analysis as described elsewhere [150] and were confirmed as synergistic. Data points are described by concentrations (in μM) of SFN and EGCG reflected on x- and y-axes respectively, and are representative of three independent experiments. The corresponding combination indices ranged from 0.325 to 0.7 (data not shown) which further confirmed the synergy between the combinations of SFN and EGCG.

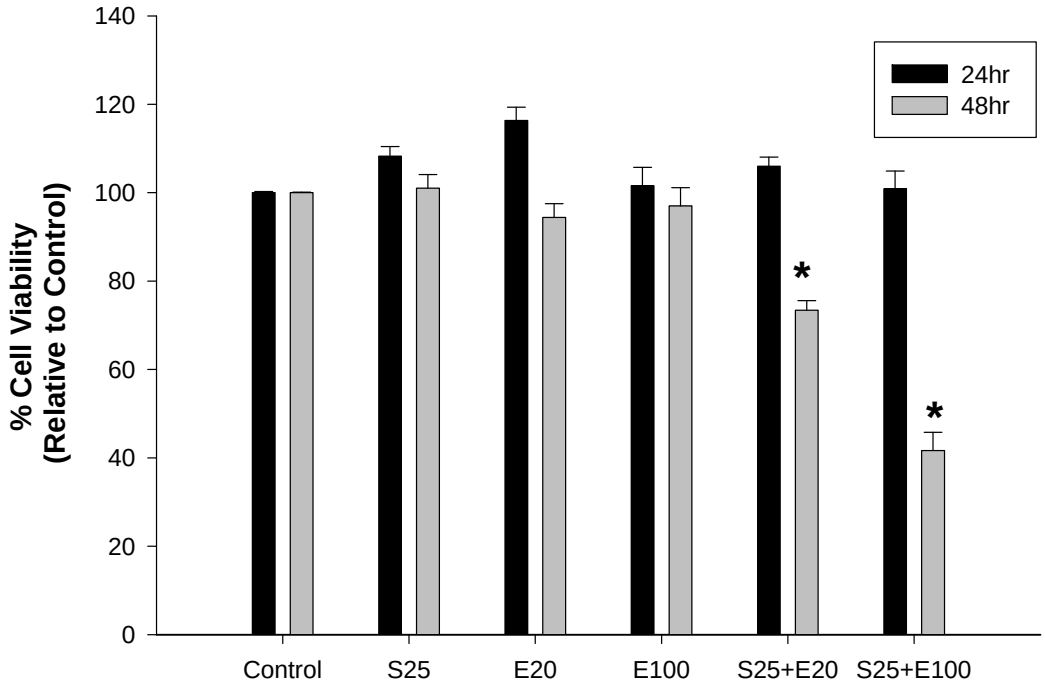

Figure 4.3. Viability of the HT-29 AP-1 cells with the combinations of SFN and EGCG

HT-29 AP-1 cells were treated with individual dietary factors or with combinations of SFN and EGCG for 24 hr or 48 hr as indicated and treated with MTS assay reagent to ascertain cell viability. Values represent mean ± standard deviation for six replicates, and are representative of three independent experiments. * $P < 0.05$, significantly different from control.

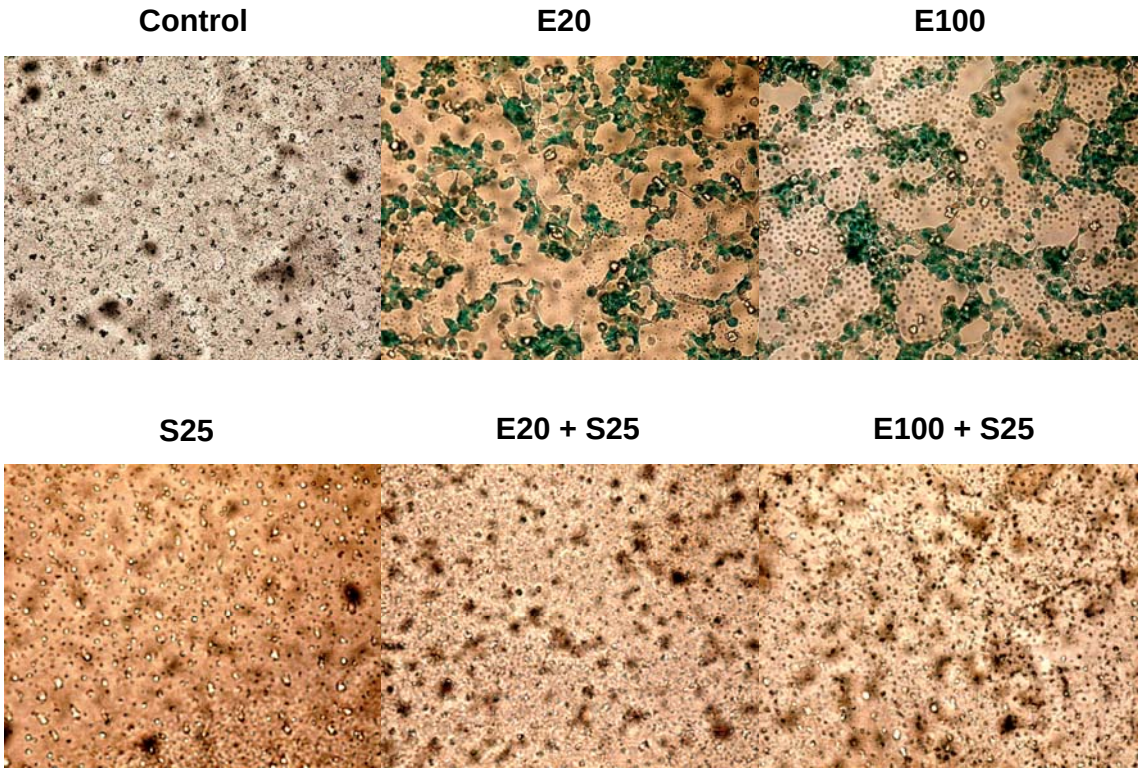

Figure 4.4. Inhibition of EGCG-induced senescence by the combinations of SFN and EGCG

HT-29 AP-1 cells were cultured on cover slips and treated with individual dietary factors or with combinations of SFN and EGCG for 24 hr. The cells were then fixed and subjected to a histochemical stain for β-galactosidase activity following which they were examined microscopically for senescence. Images are representative of three independent experiments.

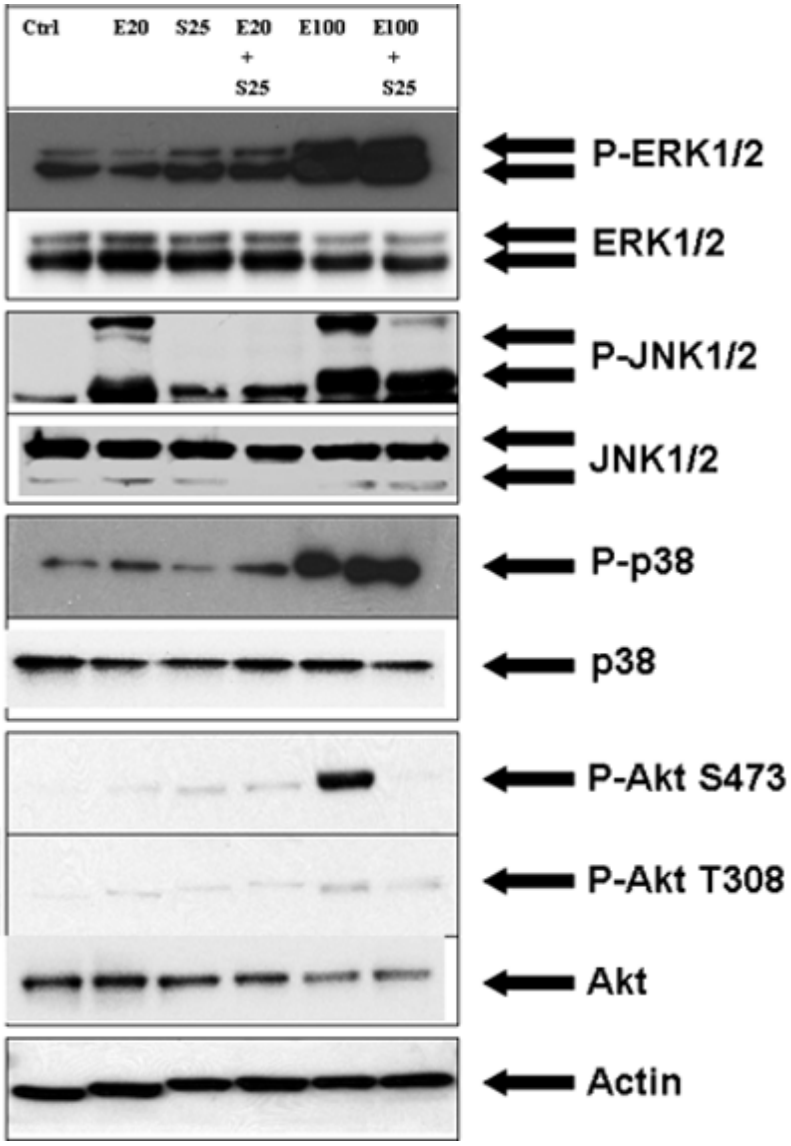

Figure 4.5. Protein expression with the combinations of SFN and EGCG

HT-29 AP-1 cells were treated with individual dietary factors or with combinations of SFN and EGCG as indicated for 1 hr. Protein was harvested using a MAPK lysis buffer for phosphorylated MAPK or with a whole cell lysis buffer for other proteins. The proteins were immunoblotted using specific antibodies as indicated using actin as the control. Blots are representative of three independent experiments.

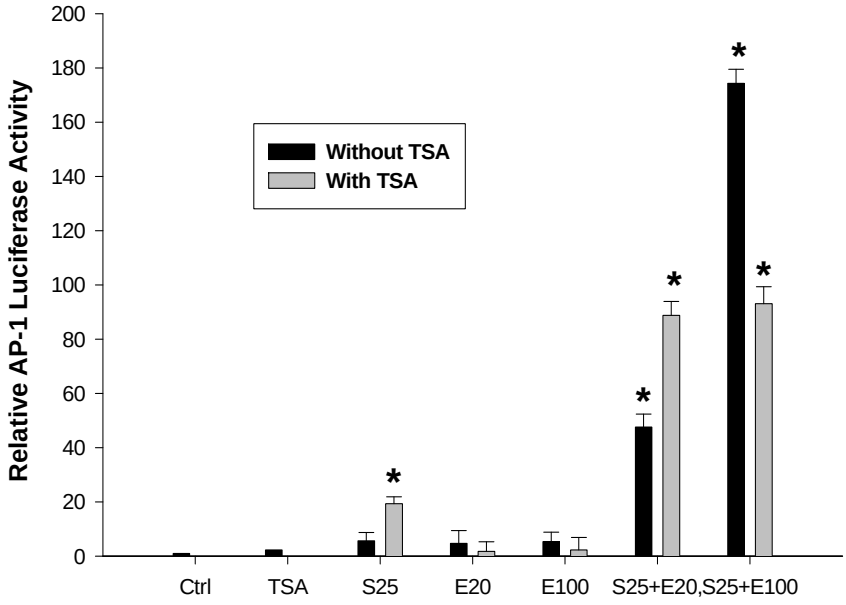

Figure 4.6. HDAC inhibitor Trichostatin A potentiates the synergism elicited by the low-dose combination of SFN and EGCG

HT-29 AP-1 cells were seeded in six-well plates and pre-treated with 100ng/ml TSA for 4 hrs. Thereafter, they were additionally treated with individual dietary factors or with combinations of SFN and EGCG as indicated for another 24 hrs. The AP-1 luciferase activity was measured relative to vehicle control (DMSO) and normalized against protein concentration. Values represent mean ± standard deviation for three replicates, and are representative of three independent experiments. * $P < 0.05$, significantly different from vehicle control (Ctrl).

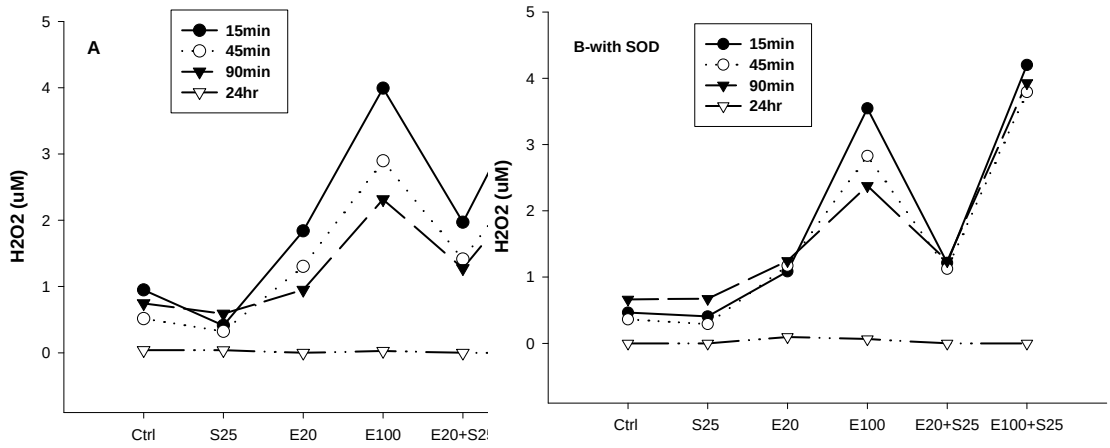

Figure 4.7. Reactive oxygen species and SOD may modulate AP-1 transactivation by the combinations of SFN and EGCG

HT-29 AP-1 cells were treated with individual dietary factors or with combinations of SFN and EGCG as indicated both in the absence (7A) and presence (7B) of co-treatment with 20U/ml SOD. Cell-free media were tested for H_2O_2 levels using only H_2O2 (10 μM) as a positive control in a fluorescence-based assay. For clarity of presentation, only mean values of three replicates are shown that are representative of three independent experiments.

CHAPTER 5

Regulation of gene expression by a combination of dietary factors sulforaphane and (-) epigallocatechin-3-gallate in PC-3 AP-1 human prostate adenocarcinoma cells and Nrf2-deficient murine prostate[13,14,15]

5.1. Abstract

Although previous studies have addressed the role(s) of NRF2 or AP-1 in prostate cancer, the potential for crosstalk between these two important transcription factors in the etiopathogenesis of prostate cancer has not been explored thus far. We posited that putative crosstalk may exist between NRF2 and AP-1 in prostate cancer on treatment with dietary factors sulforaphane and (-) epigallocatechin-3-gallate in combination. We performed in vitro studies in PC-3 AP-1 human prostate adenocarcinoma cells, in vivo temporal (3 hr and 12 hr) microarray studies in the prostate of NRF2-deficient mice, and in silico bioinformatic analyses to delineate conserved binding sites or regulatory motifs in the promoter regions of NRF2 and AP-1, as well as coregulated genes including ATF-2 and ELK-1. Downregulation (3 fold to around 35-fold) of key genes identified as NRF2-dependent appeared to be the dominant response to oral administration of the SFN+EGCG combination at both 3 hr and 12 hr, which was in

---

[13]Work described in this chapter is under consideration for publication as **Nair, S**., Cai, L., Kong AN.

[14]**Keywords:** sulforaphane, EGCG, Nrf2, AP-1, microarray, prostate cancer

[15]**Abbreviations :** NRF2, Nuclear Factor-E2-related factor 2; AP-1, activator protein-1; ATF-2, activating transcription factor 2; SFN, sulforaphane; EGCG, (-) epigallocatechin-3-gallate; MAPK, mitogen-activated protein kinase; qRT-PCR, quantitative real-time PCR.

consonance with the diminished induction of the AP-1 luciferase reporter by the SFN+EGCG combination seen in our in vitro studies. Our current transcriptional regulation study identifying NRF2- and AP-1-coregulated genes provides a discursive framework for appreciating putative crosstalk between NRF2 and AP-1 on treatment with the SFN+EGCG combination in prostate cancer and may help to identify new markers for screening or targets for therapy. Taken together, it appears a priori that the combination of SFN+EGCG may hold promise for patients in the management of prostate cancer via concerted modulation of NRF2 and AP-1 pathways.

5.2. Introduction

Prostate cancer, according to the Centers for Disease Control and Prevention (CDC) [130], is the second leading cause of cancer deaths among men in the United States, and the seventh leading cause of deaths overall for men. The incidence of prostate cancer in the United States has increased by 1.1% per year from 1995–2003 [130,172]. In addition, the National Cancer Institute (NCI)'s Surveillance Epidemiology and End Results (SEER) Statistics Fact Sheets [173] show that, based on rates from 2002–2004, 16.72% of men born today will be diagnosed with cancer of the prostate at some time during their lifetime, i.e., 1 in 6 men in the United States are at a lifetime risk of developing prostate cancer. In a recent study [174], the prostate-specific antigen (PSA) nadir while intermittently taking a testosterone-inactivating pharmaceutical agent was determined to be the best predictor of prostate cancer-specific mortality. Nevertheless, despite the considerable attention given to PSA as a screening test for prostate cancer, it

is needle biopsy, and not the PSA test result, that actually establishes the diagnosis of prostate cancer [175].

Pivotal to the antioxidant response [36-39] typical in mammalian homeostasis and oxidative stress is the important transcription factor Nrf2 or Nuclear Factor-E2-related factor 2 that has been extensively studied by many investigators including us as noted elsewhere [149,176]. Nrf2 is indispensable to cellular defense against many chemical insults of endogenous and exogenous origin, which play major roles in the etiopathogenesis of many cancers as well as inflammatory bowel disease [177] and Parkinson's disease [44]. Rushmore et al [178] were the first to identify a core antioxidant response element (core ARE or cARE) sequence 5′–RGTGACNNNGC–3′ responsible for transcriptional activation by xenobiotics, that was later expanded by Wasserman and Fahl [179] giving rise to an expanded ARE (eARE) sequence described by 5'-TMAnnRTGAYnnnGCRwwww-3'. Recently, Nerland [180] noted that nucleotides previously considered to be degenerate also contribute to the binding of the Nrf2 heterodimer to the response element. We observed [18] that the induction of antioxidant response element (ARE)-regulated genes in vitro in human prostate cancer PC-3 cells upon treatment with phenethyl isothiocyanate (PEITC) is associated with the activation of extracellular signal-regulated kinase (ERK) and c-jun N-terminal kinase (JNK) resulting in the phosphorylation and nuclear translocation of Nrf2. More recently, Watai et al [181] showed that endogenous Keap1, which acts as a regulator of Nrf2 activity through an interaction with the Nrf2 Neh2 domain, remains mostly in the cytoplasm, and electrophiles promote nuclear accumulation of Nrf2 without altering the

subcellular localization of Keap1. Thus, the Keap1-Nrf2-ARE axis potentially has an important role to play in various forms of cancer including that of the prostate.

Transcription factor activator protein-1 (AP-1) regulates a wide range of cellular processes, including cell proliferation, death, survival and differentiation [182]. AP-1 is a redox-sensitive transcription factor that senses and transduces changes in cellular redox status and modulates gene expression responses to oxidative and electrophilic stresses presumably *via* sulfhydryl modification of critical cysteine residues found on this protein and/or other upstream redox-sensitive molecular targets [149]. AP-1 is composed of heterodimeric protein complexes of members of the basic leucine zipper (bZIP) protein families, including the Jun (c-Jun, JunB and JunD) and Fos (c-Fos, FosB, Fra-1 and Fra-2) families, Maf (c-Maf, MafB, MafA, Maf G/F/K and Nrl), Jun dimerization partners (JDP1 and JDP2) and the closely related activation transcription factor (ATF; ATF2, LRF1/ATF3 and B-ATF) subfamilies [182-184] which recognize either 12-*O*-tetradecanoylphorbol-13-acetate (TPA) response elements (TRE, 5'-TGAG/CTCA-3') or cAMP response elements (CRE, 5'-TGACGTCA-3') [185]. Recently, we showed that ERK and JNK signaling pathways are involved in the regulation of AP-1 and cell death elicited by three isothiocyanates (SFN; PEITC; and allyl isothiocyanate, AITC) in human prostate cancer PC-3 cells [184].

Evidence gleaned from epidemiological studies has revealed an inverse correlation between the intake of cruciferous vegetables and the risk of certain types of cancer [136]. Isothiocyanates are a chemical class of compounds that are not naturally present in cruciferous vegetables, such as broccoli and cauliflower, but are nevertheless generated from hydrolysis of secondary metabolites known as glucosinolates by the

enzyme myrosinase during the process of vegetable crushing or mastication [139]. They may also be produced in the intestines where resident microflora can promote the hydrolysis of glucosinolates to isothiocyanates [140]. Sulforaphane (SFN), a dietary phytochemical obtained from broccoli, has been implicated in several physiological processes consistent with anticarcinogenic activity, including enhanced xenobiotic metabolism, cell cycle arrest, and apoptosis [186]. Epigenetic changes associated with inhibition of histone deacetylase (HDAC) activity [187] constitute one mechanism of cancer chemoprevention by SFN. Indeed, SFN has been shown [188] to retard the growth of human PC-3 xenografts and inhibit HDAC activity in human subjects. Recently, we reported [17] that SFN induces hemoxygenase-1 (HO-1) by activating the antioxidant response element (ARE) through the induction of Nrf2 protein in HepG2 cells, and that overexpression of all four p38 mitogen-activated protein kinase (MAPK) isoforms negatively regulated the constitutive and inducible ARE-dependent gene expression. It has also been reported [189] that SFN-induced cell death in PC-3 and DU145 human prostate cancer cells is initiated by reactive oxygen species and that induction of autophagy [190] represents a defense mechanism against SFN-induced apoptosis in PC-3 and LNCaP human prostate cancer cells. In addition, we have observed [80] that SFN suppresses the transcriptional activation of NFkappaB as well as NFkappaB-regulated gene expression in PC-3 cells via inhibition of IKKbeta phosphorylation as well as IkappaBalpha phosphorylation and degradation.

The water-extractable fraction of green tea contains abundant polyphenolic compounds, in which (-) epigallocatechin-3-gallate (EGCG) is the major constituent (>50% of polyphenolic fraction) [143]. We have observed [14] that EGCG treatment causes

damage to mitochondria, and that JNK mediates EGCG-induced apoptotic cell death in HT-29 human colon cancer cells. EGCG is also reported [147,148] to inhibit DNA methyltransferase with demethylation of the CpG islands in the promoters, and to reactivate methylation-silenced genes such as p16INK4a, retinoic acid receptor beta, O6-methylguanine methyltransferase, human mutL homolog 1, and glutathione S-transferase-pi in human colon cancer HT-29 cells, esophageal cancer KYSE 150 cells, and prostate cancer PC-3 cells. Recently, it was noted [191] that EGCG suppresses early stage, but not late stage, prostate cancer in TRAMP (Transgenic Adenocarcinoma Mouse Prostate) animals without incurring undue toxicity. EGCG has also been shown to induce growth arrest and apoptosis in NRP-152 and NRP-154 rat prostate epithelial cells [192]. Besides, EGCG has been reported [193] to modulate the phosphatidylinositol-3-kinase/protein kinase B- and MAPK-pathways in DU145 and LNCaP human prostate cancer cells, and to have combined inhibitory effects with selective cyclooxygenase-2 inhibitors [156] on the growth of human prostate cancer cells both in vitro and in vivo. We have also shown [55] that a greater number of Nrf2-regulated genes are modulated in murine liver on oral administration of EGCG than in small intestine.

Nrf2 knockout mice are greatly predisposed to chemical-induced DNA damage and exhibit higher susceptibility towards cancer development in several models of chemical carcinogenesis [43]. In the present study, we investigated via transcriptome profiling the gene expression changes induced by a combination of dietary factors SFN and EGCG in Nrf2-deficient mice, the in vitro effects of this combination in PC-3 AP-1 cells, and in silico bioinformatic analyses to delineate conserved binding sites or regulatory motifs in

the promoter regions of NRF2 and AP-1, as well as coregulated genes including ATF-2 and ELK-1. We demonstrate that the effects of the combination of SFN+EGCG in prostate cancer may be mediated via concerted modulation of NRF2 and AP-1 pathways.

5.3. Materials and Methods

Cell culture and Reagents : Human prostate cancer PC-3 cells were stably transfected with an Activator Protein (AP-1) luciferase reporter construct, and are referred to as PC-3 AP-1 cells or PC-3 C9 cells. The cells were cultured in Minimum Essential Medium (MEM) containing 10% Fetal Bovine Serum (FBS) and 1% Penicillin-Streptomycin. Twelve hours prior to experimental treatments, the cells were exposed to MEM containing 0.5% FBS. Sulforaphane (SFN) was obtained from LKT Labs (St. Paul, MN) ; whereas (-) epigallocatechin-3-gallate (EGCG) and superoxide dismutase (SOD) were obtained from Sigma-Aldrich (St.Louis, MO). Both SFN and EGCG were dissolved in dimethylsulfoxide (DMSO, Sigma), whereas SOD was dissolved in 1X phosphate-buffered saline (PBS).

Reporter gene assays : PC-3 AP-1 cells were seeded in six-well culture plates and treated in duplicate with dimethylsulfoxide (control), 20 μM EGCG, 100 μM EGCG, 25 μM SFN, 20 μM EGCG + 25 μM SFN, or 100 μM EGCG + 25 μM SFN for 24 hours. Thereafter, the supernatant medium was aspirated on ice, cells were washed thrice with ice-cold 1X PBS, treated with 1X Luciferase Reporter Lysis Buffer (Promega) and subjected to one cycle of snap freeze-thaw at -80 °C. Cell lysates were

harvested with sterile RNAse-free and DNAse-free cell scrapers into microcentrifuge tubes that were immediately placed on ice. They were then centrifuged at 4 °C for ten minutes at 13000 x g and returned to ice. Twenty microliters of supernatant solution was analyzed for relative luciferase activity using a Sirius Luminometer (Berthold Detection Systems). The relative luciferase activities were normalized by protein concentrations of individual samples as described below.

Protein Assays : Protein concentrations of samples were determined by the bicinchonic acid-based BCA Protein Assay Kit (Pierce) according to the manufacturer's instructions using a 96-well plate. Standard curves were constructed using bovine serum albumin (BSA) as a standard. The sample readings were obtained on a μQuant microplate reader (Bio-tek Instruments, Inc.) at 560nm.

Cell Viability Assays : The cell viability assays were performed in 24-well cell culture plates using MTS Assay Kit (Promega) according to the manufacturer's instructions. Cell viability was determined at both 24 and 48 hours after treatment with dietary factors. The absorbance readings were obtained on an μQuant microplate reader (Bio-tek Instruments, Inc.) at recommended wavelength of 490nm.

RNA Extraction and Assessment of RNA Integrity : PC-3 AP-1 cells were subjected to treatment with different dietary factors in triplicate for 6hours or 10 hours. RNA was harvested using the RNeasy Mini Kit (Qiagen) according to the manufacturer's instructions. RNA integrity was assessed using formaldehyde gels in 1X

MOPS buffer and RNA concentration was determined by the 260/280 ratio on a DU 530 UV/Visible spectrophotometer (Beckman).

Quantitative Real-time PCR Assays : Several genes of interest including luciferase gene as well as genes known to be either under the control of the AP-1 promoter or involved in cell cycle regulation or cellular influx-efflux such as cyclin D1, cMyc, ATF-2, Elk-1, SRF, CREB5, MDR1, SLCO1B3, MRP1, MRP2 and MRP3 were selected for quantitative real-time PCR analyses. Beta-actin served as the "housekeeping" gene. The specific primers for these genes as we have reported previously [194] were designed using Primer Express 2.0 software (Applied Biosystems, Foster City, CA) and were obtained from Integrated DNA Technologies, Coralville, IA. The specificity of the primers was examined by a National Center for Biotechnology Information Blast search of the human genome. For the real-time PCR assays, briefly, after the RNA extraction and assessment of RNA integrity, first-strand cDNA was synthesized using 4μg of total RNA following the protocol of SuperScript III First-Strand cDNA Synthesis System (Invitrogen) in a 40 μl reaction volume. The PCR reactions based on SYBR Green chemistry were carried out using 100 times diluted cDNA product, 60 nM of each primer, and SYBR Green master mix (Applied Biosystems, Foster City, CA) in 10 μl reactions. The PCR parameters were set using SDS 2.1 software (Applied Biosystems, Foster City, CA) and involved the following stages : 50°C for 2min, 1 cycle; 95°C for 10 mins, 1 cycle; 95°C for 15 secs → 55 °C for 30 secs →72°C for 30 secs, 40 cycles; and 72°C for 10 mins, 1 cycle. Incorporation of the SYBR Green dye into the PCR products was monitored in real time with an ABI

Prism 7900HT sequence detection system, resulting in the calculation of a threshold cycle (C_T) that defines the PCR cycle at which exponential growth of PCR products begins. The carboxy-X-rhodamine (ROX) passive reference dye was used to account for well and pipetting variability. A control cDNA dilution series was created for each gene to establish a standard curve. After conclusion of the reaction, amplicon specificity was verified by first-derivative melting curve analysis using the ABI software; and the integrity of the PCR reaction product and absence of primer dimers was ascertained. The gene expression was determined by normalization with control gene beta-actin.

Promoter Analyses for Transcription Factor Binding Sites (TFBS) : The promoter analyses were performed in the laboratory of Dr. Li Cai (Department of Biomedical Engineering, Rutgers University) using Genomatix MatInspector [195,196]. Briefly, human promoter sequences of NRF2, AP-1, ATF-2 and ELK-1, or corresponding murine promoter sequences, were retrieved from Gene2Promoter (Genomatix). Comparative promoter analyses were then performed by input of these sequences in FASTA format into MatInspector using optimized default matrix similarity thresholds. The similar and/or functionally related TFBS were grouped into 'matrix families' and graphical representations of common TFBS were generated. The 'V$' prefixes to the individual matrices are representative of the Vertebrate MatInspector matrix library. We also elucidated common regulatory sequences in promoter regions of human, or murine, NRF2 and AP-1. The 'core sequence' of a matrix is defined as the (usually four) highest conserved positions of the matrix that is provided in upper case letters in our Tables. The maximum core similarity of 1.0 is only

reached when the highest conserved bases of a matrix match exactly in the sequence. Only matches that contain the "core sequence" of the matrix with a score higher than the core similarity are listed in the output.

Animals and Dosing : The protocol for animal studies was approved by the Rutgers University Institutional Animal Care and Use Committee (IACUC). Nrf2 knockout mice Nrf2 (-/-) (C57BL/SV129) have been described previously [100]. Nrf2 (-/-) mice were backcrossed with C57BL/6J mice (The Jackson Laboratory, ME USA). DNA was extracted from the tail of each mouse and genotype of the mouse was confirmed by polymerase chain reaction (PCR) by using primers (3'-primer, 5'-GGA ATG GAA AAT AGC TCC TGC C-3'; 5'-primer, 5'-GCC TGA GAG CTG TAG GCC C-3'; and lacZ primer, 5'-GGG TTT TCC CAG TCA CGA C-3'). Nrf2(-/-) mice-derived PCR products showed only one band of ~200bp, Nrf2 (+/+) mice-derived PCR products showed a band of ~300bp while both bands appeared in Nrf2(+/-) mice PCR products. Male C57BL/6J/Nrf2(-/-) mice from third generation of backcross were used in this study. Age-matched male C57BL/6J mice were purchased from The Jackson Laboratory (Bar Harbor, ME). Mice in the age-group of 9-12 weeks were housed at Rutgers Animal Facility with free access to water and food under 12 h light/dark cycles. After one week of acclimatization, the mice were put on AIN-76A diet (Research Diets Inc. NJ USA) for another week. The mice were then administered both SFN (LKT Labs, St. Paul, MN) and EGCG (Sigma-Aldrich, St.Louis, MO) at doses of 45 mg/kg and 100mg/kg respectively (dissolved in 50% PEG 400 aqueous solution) by oral gavage. The control group animals were administered only vehicle (50% PEG 400

aqueous solution). Each treatment was administered to a group of four animals for both C57BL/6J and C57BL/6J/Nrf2(-/-) mice. Mice were sacrificed at either 3h or 12hr after dietary factor treatment or vehicle administration (control group). The prostates of the animals were retrieved and stored in RNA Later (Ambion, Austin,TX) solution.

Microarray Sample Preparation and Hybridization : Total RNA from prostate tissues was isolated by using TRIzol (Invitrogen, Carlsbad, CA) extraction coupled with the RNeasy kit from Qiagen (Valencia, CA). Briefly, tissues were homogenized in trizol and then extracted with chloroform by vortexing. A small volume (1.2 ml) of aqueous phase after chloroform extraction and centrifugation was adjusted to 35% ethanol and loaded onto an RNeasy column. The column was washed, and RNA was eluted following the manufacturer's recommendations. RNA integrity was examined by electrophoresis, and concentrations were determined by UV spectrophotometry. Affymetrix (Affymetrix, Santa Clara, CA) mouse genome 430 2.0 array was used to probe the global gene expression profiles in mice following SFN+EGCG treatment. The mouse genome 430 2.0 Array is a high-density oligonucleotide array comprised of over 45,101 probe sets representing over 34,000 well-substantiated mouse genes. The library file for the above-mentioned oligonucleotide array is readily available at http://www.affymetrix.com/support/technical/libraryfiles.main.affx. After RNA isolation, the subsequent technical procedures including quality control and estimation of RNA concentration, cDNA synthesis and biotin-labeling of cRNA, hybridization and scanning of the arrays, were performed at CINJ Core Expression Array Facility of Robert Wood Johnson Medical School (New

Brunswick, NJ). Each chip was hybridized with cRNA derived from a pooled total RNA sample from four mice per treatment group, per time-point, and per genotype (a total of eight chips were used in this study). Briefly, double-stranded cDNA was synthesized from 5 μg of total RNA and labeled using the ENZO BioArray RNA transcript labeling kit (Enzo Life Sciences, Inc.,Farmingdale, NY, USA) to generate biotinylated cRNA. Biotin-labeled cRNA was purified and fragmented randomly according to Affymetrix's protocol. Two hundred microliters of sample cocktail containing 15 μg of fragmented and biotin-labeled cRNA was loaded onto each chip. Chips were hybridized at 45°C for 16 h and washed with fluidics protocol EukGE-WS2v5 according to Affymetrix's recommendation. At the completion of the fluidics protocol, the chips were placed into the Affymetrix GeneChip Scanner where the intensity of the fluorescence for each feature was measured.

Microarray Data Analyses : The microarray data analyses were performed in the laboratory of Dr. Li Cai (Department of Biomedical Engineering, Rutgers University). The CEL file created from each sample (chip) was first imported into dChip software [197,198] for further data characterization. Briefly, a gene information file with current annotations and functional gene ontology was generated and the Affymetrix Chip Description File (CDF) was specified. The data were then normalized in dChip and the expression value for each gene was determined by calculating the average of differences in intensity (perfect match intensity minus mismatch intensity) between its probe pairs. The expression values were imported into GeneSpring 7.2 (Agilent Technologies, Inc., Palo Alto, CA) followed by data filtration based on flags

present in at least one of the samples, and a corresponding gene list based on those flags was generated. Lists of genes that were either induced or suppressed more than three fold between treated versus vehicle group of same genotype were created by filtration-on-fold function within the presented flag list. By use of Venn Diagram function, lists of genes that were regulated more than three fold only in prostate of C57BL/6J mice but not in prostate of C57BL/6J/Nrf2(-/-) mice at both 3h and 12h were generated, and were designated as Nrf2-dependent genes. Using a Unix-based program at Dr. Li Cai's laboratory, the Affymetrix Probe Set IDs for the Nrf2-dependent genes thus identified were matched against the "all genes" expression values list for these set of samples, and expression values for these Affymetrix Probe Set IDs were retrieved. This 'external data' was then imported into dChip whereupon Clustering and Enrichment Analysis was performed to obtain hierarchical tree clustering diagrams for the Nrf2-dependent genes. This clustering provided functional classification of Affymetrix Probe Set IDs and gene descriptions that were then matched with the GeneSpring-generated Nrf2-dependent Affymetrix Probe Set IDs with fold-change values. Quantitative real-time PCR assays as described earlier were performed on several genes to validate the microarray results.

Statistical Analyses : Data are expressed as mean ± standard deviation, and comparisons among treatment groups were made using one-way analysis of variance (ANOVA) followed by a post hoc test for multiple comparisons – the Tukey's Studentized Range Honestly Significant Difference (HSD) test. In all these multiple comparisons, $P < 0.05$ was considered statistically significant. In order to validate the

microarray results, the correlation between corresponding microarray data and real-time PCR data was evaluated by the statistical 'coefficient of determination', $\mathbf{r^2} = 0.96$. Statistical analyses were performed using SAS 9.1 software (SAS Institute Inc, NC) licensed to Rutgers University.

5.4. Results

5.4.1. Diminished transactivation of AP-1 luciferase reporter by combinations of SFN and EGCG

As shown in Figure 4.1A, treatment of PC-3 AP-1 cells for 24 hours with either EGCG 20 μM, EGCG 100 μM or SFN 25 μM individually, resulted in variable induction of AP-1 luciferase activity as compared to control cells that were treated with DMSO. Surprisingly, a low-dose combination of SFN 25 μM + EGCG 20 μM elicited a diminished induction of AP-1 luciferase activity (less than 5-fold). In addition, a high-dose combination of SFN 25 μM + EGCG 100 μM further diminished the induction of the AP-1 luciferase reporter. We also investigated the effects of pre-treatment on the induction of AP-1 luciferase activity. In these experiments (data not shown), we first pre-treated the PC-3 AP-1 cells for six hours with EGCG (20 μM or 100 μM), then washed off the EGCG thrice with phosphate-buffered saline (PBS) and treated the cells with SFN 25 μM for an additional 18 hours before assaying for luciferase activity. Alternatively, we also pre-treated the cells with SFN 25 μM for 6 hours before washing with PBS as above and treating with EGCG (20 μM or 100 μM) for an additional 18 hours. It was observed that there was no significant difference in induction of AP-1 luciferase activity in these pre-treatment experiments (data not shown) as compared to

when the two agents were co-treated as shown in Figure 4.1A. This enabled us to rule out any physicochemical interaction between the two agents in cell culture, when co-treated, that may have otherwise produced any experimental artifacts in the luciferase assay. Hence, since the effects of the combinations when co-treated were not physicochemical, but potentially modulated at a mechanistic level, we continued co-treating both agents together for a duration of 24 hours for ease of experimentation without confounding variables.

5.4.2. Viability of the PC-3 AP-1 cells with the combinations of SFN and EGCG

In order to ascertain the effects of the combinations of SFN and EGCG on the cell viability of the PC-3 AP-1 cells, we used the MTS assay with treatment durations of 24 hours and 48 hours. As shown in Figure 4.1B, the cell viability at 24 hours for the low-dose combination treatment of SFN 25 μM + EGCG 20 μM was about 75 to 80 %, whereas it was about 60% for the high-dose combination of SFN 25 μM + EGCG 100 μM. The low-dose combination of SFN 25 μM + EGCG 20 μM may be more appropriate to pursue in longer duration in vitro studies or potential in vivo studies without seemingly toxic effects a priori, and at the same time not compromising on the efficacy elicited by the combination of these two chemopreventive agents.

5.4.3. Temporal gene expression profiles elicited by combinations of SFN and EGCG

We performed quantitative real-time PCR (qRT-PCR) experiments with primers for the luciferase gene to corroborate the synergism elicited with the combinations of SFN and

EGCG in the luciferase protein assay with mRNA levels in qRT-PCR. As shown in Figure 5.2, the temporal expression (at 6 hrs and 10 hrs) of luciferase gene in qRT-PCR assays was lower for the combinations of SFN and EGCG as compared to individual dietary factor treatments in consonance with our data in the luciferase protein assays. The treatment means for all the treatment groups at a specific time point (6 hrs or 10 hrs) were significantly different from each other ($P<0.05$ by ANOVA and post hoc Tukey's test for multiple comparisons to detect significantly different means). We also determined by qRT-PCR the relative expression levels of transcripts of many genes that were known to be either under the control of the AP-1 promoter or involved in cell cycle regulation or cellular influx-efflux such as cyclin D1, cMyc, ATF-2, ELK-1, SRF, CREB5, SLCO1B3, MRP1, MRP2 and MRP3 (Figure 5.2).

The low- and high-dose combinations of SFN and EGCG in this study elicited the downregulation of positive cell cycle regulator cyclin D1 expression as compared with individual dietary factors especially at 10 hr. There was, however, no appreciable change in expression of cell proliferation-related cMyc Binding Protein. In addition, transcription factors/coactivators that are known to be under the control of the AP-1 promoter such as activating transcription factor (ATF-2), Ets-like transcription factor (ELK-1), serum response factor (SRF) and cyclic AMP response element binding protein 5 (CREB5) were also studied. Interestingly, both ATF-2 and ELK-1 were significantly downregulated by the combinations of SFN and EGCG as compared to individual dietary factors. Besides, the low-dose combination of SFN and EGCG at 6hr (and the high-dose combination at 10hr) inhibited the expression of SRF as compared to individual dietary factors. Similarly, the combinations inhibited the expression of

CREB5 as compared to individual agents. Since exogenous stress can potentially stimulate the influx-efflux machinery of cells, we also investigated some key transporter genes (Figure 5.2). In this study, we observed that the combinations of SFN and EGCG inhibited the expression of the SLCO1B3 gene, which encodes for the organic anion transporter protein OATP1B3, whereas the combinations did not have any significant effect on the expression of MDR1 gene. Interestingly, the combinations of SFN and EGCG greatly induced the expression of the efflux transporter MRP2 as compared to individual agents as shown in Figure 5.2. In addition, the expression of influx transporters MRP1 and MRP3 was not significantly different for the combination-treated cells as compared to the individual agent-treated cells.

5.4.4. Comparative promoter analyses of NRF2 and AP-1, as well as ATF-2 and ELK-1, for conserved Transcription Factor Binding Sites (TFBS)

We performed comparative analyses of NRF2 and AP-1 human promoter sequences as described in Materials and Methods. We also studied Nrf2 and AP-1 murine promoter sequences similarly. Table 5.1A is an alphabetical listing of the conserved vertebrate (V$) matrix families between these two transcription factors. The major human families included Activator protein 4 and related proteins, cell cycle regulators, E-box binding factors, human and murine ETS1 factors, fork head domain factors, hypoxia inducible factor, myc-associated zinc fingers, nuclear respiratory factor 1, serum response element binding factor, and signal transducer and activator of transcription amongst others. Interestingly, nuclear factor kappa B (NFkB) was conserved in human sequences of Nrf2 and AP-1. We also performed comparative promoter analyses on ATF-2 and

ELK-1, which we had previously identified (Figure 5.2) as AP-1-regulated genes. Table 5.1B alphabetically lists the conserved vertebrate (V$) matrix families between ATF-2 and ELK-1 that have been pictorially represented in Figure 5.3. Some key conserved matrix families included AP-1, cyclic AMP-responsive element binding proteins, estrogen response elements, human and murine ETS1 factors, fork head domain factors, farnesoid-X-activated receptor response elements, human acute myelogenous leukemia factors, Ikaros zinc finger family, myc-associated zinc fingers, nuclear factor of activated T-cells, nuclear factor kappa B (NFkB), peroxisome proliferators-activated receptor, ras-responsive element binding protein, serum response element binding factor, signal transducer and activator of transcription, and X-box binding factors amongst others. Interestingly, as is evident from Tables 5.1A and 5.1B, several key matrix families were conserved not just between NRF2 and AP-1, or between the AP-1-regulated genes ATF-2 and ELK-1, in either human or murine species, but there was also some degree of overlap between TFBS identified in Tables 5.1A and 5.1B. Furthermore, as shown in Table 5.2, we identified matrices (individual matrix family members) with conserved regulatory sequences in promoter regions of NRF2 and AP-1 in either human or murine species. Multiple matches that were elicited with the same core sequence have also been grouped together and listed in Table 5.2.

5.4.5. Temporal microarray analyses of genes modulated by SFN+EGCG combination in the prostate of NRF2-deficient mice

Table 5.3 lists the genes that were downregulated at both 3hr and 12 hr by the SFN+EGCG combination in the prostate of NRF2-deficient mice according to their

biological functions. Interestingly, downregulation of genes appeared more important in the prostate of these mice, since the upregulation of genes was negligible (data not shown). Indeed, a strong degree of downregulation ranging from 3 to around 35 fold was observed in vivo. This was also in consonance with our in vitro results in Figure 5.1 where the combination of SFN+EGCG elicited diminished activation of the luciferase reporter. Furthermore, several genes that were downregulated in our in vivo study were also common to our regulatory comparative promoter analyses between NRF2 and AP-1, and ATF-2 and ELK-1, as described earlier. These included Ikaros family zinc fingers, forkhead box members, and ATF-2 amongst others. Interestingly, several coactivators and corepressors of NRF2, as well as NRF3, and the adenomatosis polyposis coli (Apc) gene, were also shown to be modulated via NRF2 in response to the combination of SFN+EGCG.

5.5. Discussion

Expression profiling and proteomics have the potential to transform the management of prostate cancer, identifying new markers for screening, diagnosis, prognosis, monitoring and targets for therapy [199]. Although several studies have addressed the putative role(s) of either NRF2 or AP-1 per se in prostate cancer, the potential for putative crosstalk between these two important transcription factors in the etiopathogenesis of prostate cancer has not been explored thus far. We have used a multi-pronged approach consisting of in vitro studies in prostate cancer PC-3 AP-1 cells, in vivo studies in the prostate of NRF2-deficient mice, and bioinformatic tools to elucidate conserved motifs in the promoter regions of these transcription factors, as well

as genes coregulated by them. We, thus, demonstrate the potential for putative crosstalk between NRF2 and AP-1 in prostate cancer on treatment with dietary factors SFN and EGCG in combination.

Interestingly, from our in vitro data in PC-3 AP-1 cells (Figure 5.1A), we observed a diminished induction of the luciferase reporter on treatment with a combination of SFN+EGCG that was dose-dependent. We observed similar trends in our in vivo microarray data in NRF2-deficient mice (Table 5.3), where downregulation (3 fold to around 35-fold) of key genes identified as NRF2-dependent appeared to be the dominant response to oral administration of the SFN+EGCG combination at both 3 hr and 12 hr. Quantitative real-time PCR analyses in our in vitro system (Figure 5.2) confirmed that several genes including ATF-2 and ELK-1 were regulated by AP-1. Bioinformatic analyses of the promoter regions of NRF2 and AP-1, as well as ATF-2 and ELK-1, revealed an interesting group of conserved TFBS (Tables 5.1A, 5.1B and Figures 5.3A, 5.3B) in both human and murine promoters. Furthermore, we were able to identify genes with conserved regulatory sequences in the promoter regions of human, or murine, NRF2 and AP-1 as shown in Table 5.2. Indeed, microarray analyses in Nrf2-deficient mice (Table 5.3) confirmed that genes identified as Nrf2-dependent, including ATF-2, were coregulated with genes elicited from our AP-1 in vitro studies as well as the comparative analyses of promoter regions of NRF2 and AP-1 using bioinformatic analyses. It has been noted [199] that a majority of prostate cancers contain fusion genes that result in regulation via ETS family transcription factors. Our in silico results (Tables 5.1A, 5.1B and 5.2) as well as our in vitro data (Figure 5.2) also demonstrate a

role for ETS family members including ELK-1 which is, thus, in consonance with previous reports.

The identification of conserved TFBS for pro-survival transcription factor NFkB in the promoter regions of NRF2 and AP-1 (Tables 5.1A, 5.1B, 5.2 and Figures 5.3A, 5.3B) raises an important question as to whether there could be any possible crosstalk between NRF2, AP-1 and NFkB in concert that may contribute to the overall effects of the SFN+EGCG combination in prostate cancer. Indeed, further studies would be necessary to explore this possibility in greater detail. The identification of several key MAPK genes in our microarray studies (Table 5.3) as NRF2-dependent is in congruence with the known role(s) of MAPKs in NRF2 phosphorylation and activation. Besides, the downregulation of NRF3, a negative regulator of ARE-mediated gene expression [200] with substantial homology to NRF2, in our microarray data (Table 5.3) reinforces the putative chemopreventive potential of the SFN+EGCG combination. Furthermore, the elucidation of several coactivators and corepressors as NRF2-dependent including nuclear receptor coactivators 1 and 7 (Ncoa1 and Ncoa7) and nuclear receptor corepressor 1 (Ncor1) indicate that these cofactors may have a potentially significant role to play in the ability of NRF2 to crosstalk with AP-1 in vivo.

We have demonstrated recently [194] that a combination of SFN+EGCG resulted in a synergistic transactivation of the AP-1 reporter in HT-29 human colon carcinoma cells that was mediated by histone deacetylases, inhibition of cellular senescence and SOD signaling. Surprisingly, our current results show that the same combination of SFN+EGCG results in a downregulation of the AP-1 reporter as well as key genes in prostate cancer. Indeed, this leads to the intriguing possibility that dietary

chemopreventive agents such as SFN+EGCG, when used in combination, may exert different multifactorial mechanisms in different forms of cancer. Our current transcriptional regulation study addresses this question in terms of providing a discursive framework for understanding putative crosstalk between NRF2 and AP-1 in prostate cancer that may potentially explain the behavior of the combination of SFN+EGCG that we have observed in the current study. It is tempting to speculate that, when extrapolated to a clinical setting, one would have to face the additional confounding factor of idiosyncratic behavior in patient sub-populations. However, it appears a priori that the combination of SFN+EGCG may hold promise for patients with early-grade prostate cancer via concerted modulation of NRF2 and AP-1 pathways. Further studies focusing on the specific signaling intermediates, as well as clinical studies, would be necessary to better appreciate the putative chemopreventive efficacy of the combination of SFN+EGCG in the management of prostate cancer.

5.6. Acknowledgements

Sujit Nair is extremely grateful to Dr. Li Cai for his patient training, expertise and extensive help with the bioinformatic approaches used in this study. Sujit Nair also thanks Avantika Barve, Tin-Oo Khor, Guoxiang Shen and Wen Lin for their help with animal handling. This work was supported in part by RO1-CA073674, RO1-CA092515, R01-CA118947 and RO1-CA094828 to Ah-Ng Tony Kong from the National Institutes of Health (NIH).

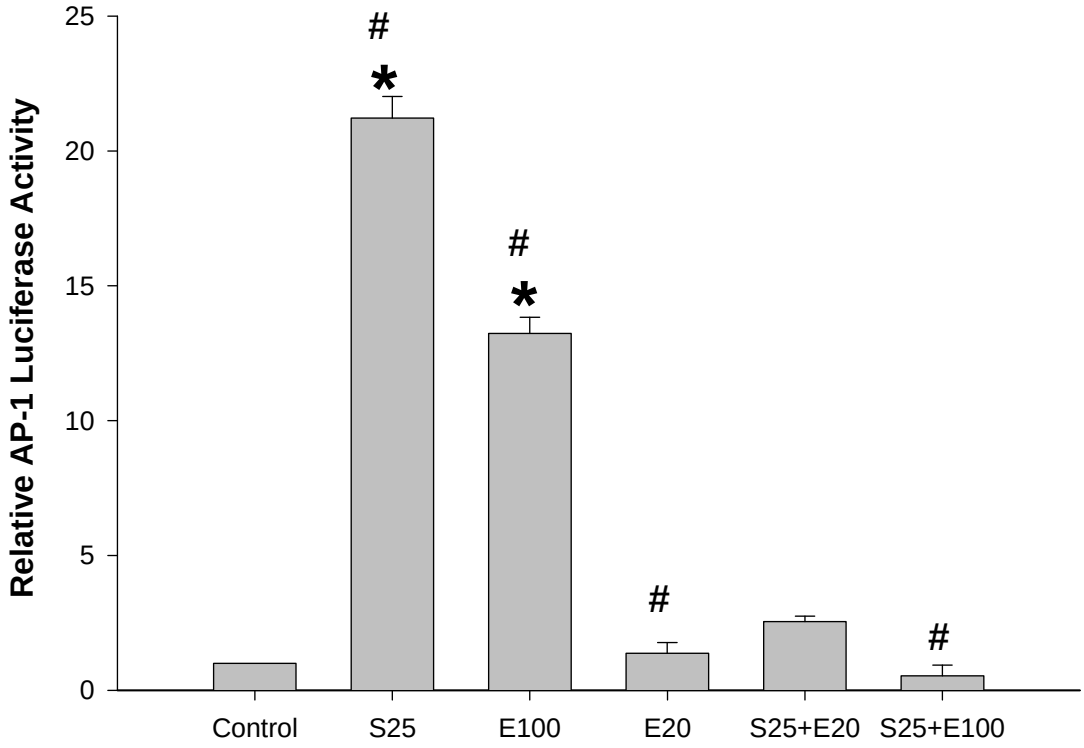

Figure 5.1A. Diminished transactivation of AP-1 luciferase reporter by combinations of SFN and EGCG

PC-3 AP-1 cells were seeded in six-well plates and treated with individual dietary factors, or with combinations of SFN and EGCG, as indicated. The AP-1 luciferase activity was measured relative to vehicle control (DMSO) after 24 hours of incubation and normalized against protein concentration. Values represent mean ± standard deviation for three replicates, and are representative of seven independent experiments. * $P < 0.05$, significantly different from vehicle control (Ctrl) ; # $P < 0.05$, significantly different from each other.

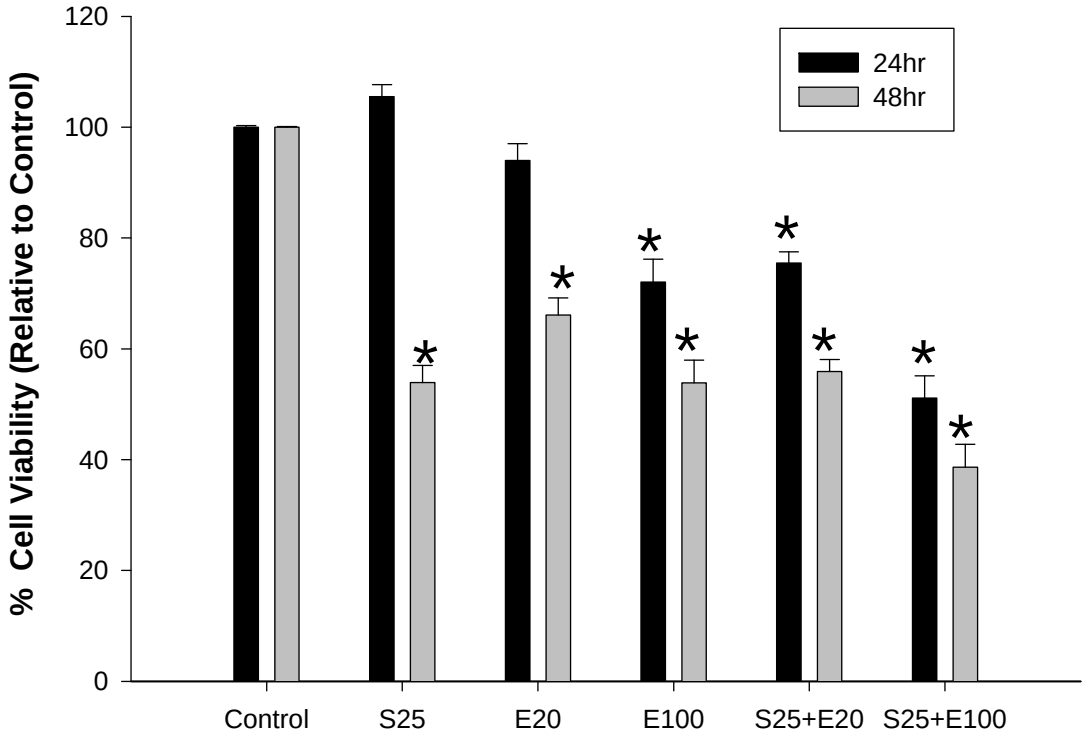

Figure 5.1B. Viability of the PC-3 AP-1 cells with the combinations of SFN and EGCG

PC-3 AP-1 cells were treated with individual dietary factors or with combinations of SFN and EGCG for 24 hr or 48 hr, as indicated, and treated with MTS assay reagent to ascertain cell viability. Values represent mean ± standard deviation for six replicates, and are representative of three independent experiments. * $P < 0.05$, significantly different from control.

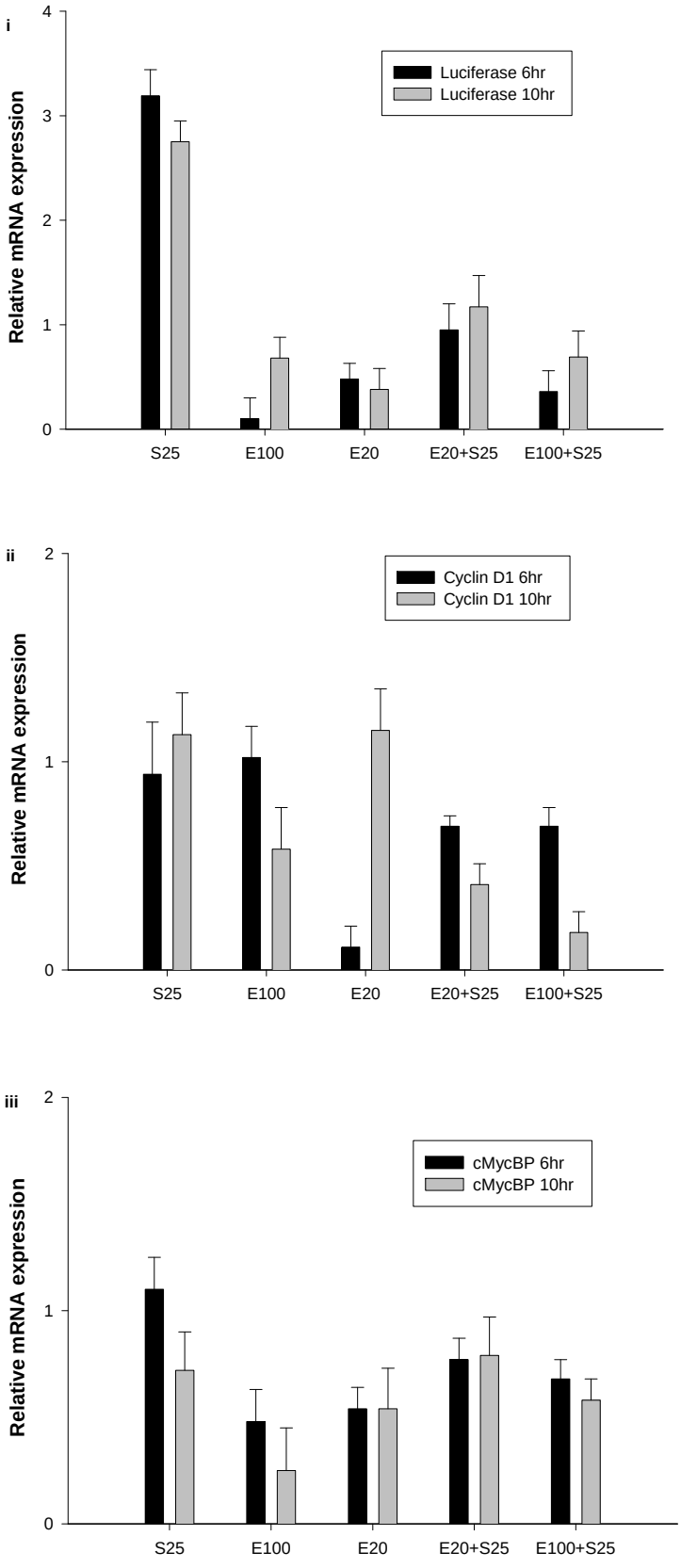
i
Relative mRNA expression
Luciferase 6hr
Luciferase 10hr
S25
E100
E20
E20+S25
E100+S25
ii
Relative mRNA expression
Cyclin D1 6hr
Cyclin D1 10hr
S25
E100
E20
E20+S25
E100+S25
iii
Relative mRNA expression
cMycBP 6hr
cMycBP 10hr
S25
E100
E20
E20+S25
E100+S25

Figure 5.2.a.

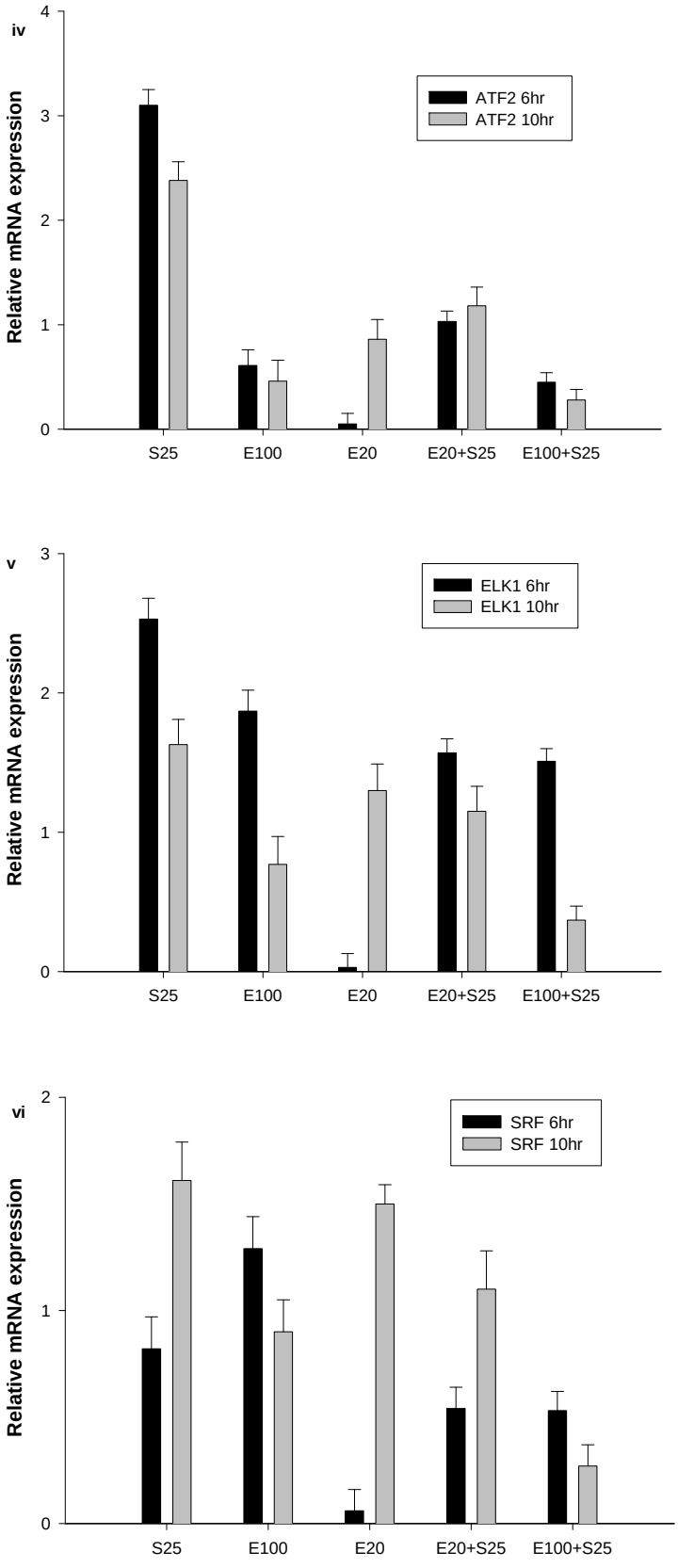
iv
Relative mRNA expression
ATF2 6hr
ATF2 10hr
S25
E100
E20
E20+S25
E100+S25
v
Relative mRNA expression
ELK1 6hr
ELK1 10hr
S25
E100
E20
E20+S25
E100+S25
vi
Relative mRNA expression
SRF 6hr
SRF 10hr
S25
E100
E20
E20+S25
E100+S25

Figure 5.2.b.

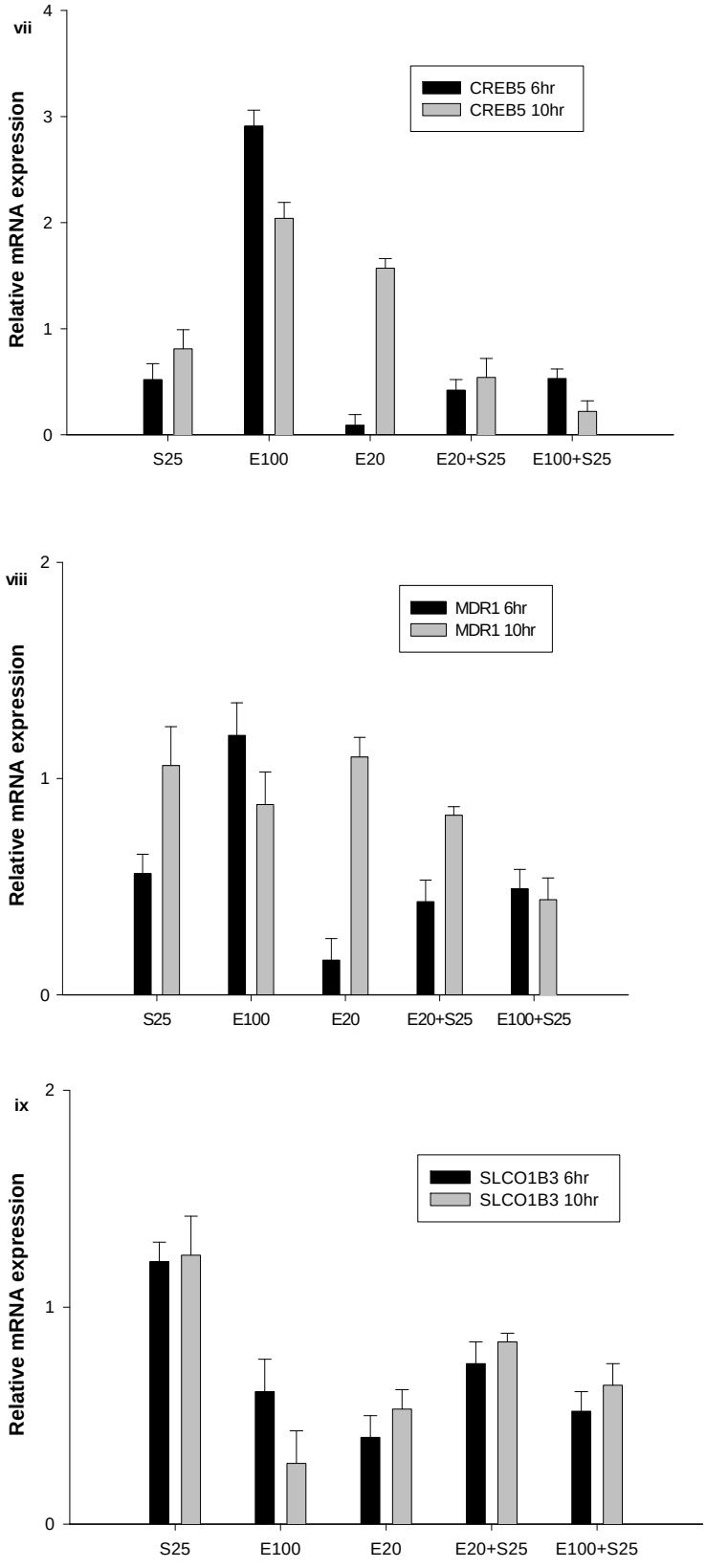
vii
Relative mRNA expression
CREB5 6hr
CREB5 10hr
S25
E100
E20
E20+S25
E100+S25
viii
Relative mRNA expression
MDR1 6hr
MDR1 10hr
S25
E100
E20
E20+S25
E100+S25
ix
Relative mRNA expression
SLCO1B3 6hr
SLCO1B3 10hr
S25
E100
E20
E20+S25
E100+S25

Figure 5.2.c.

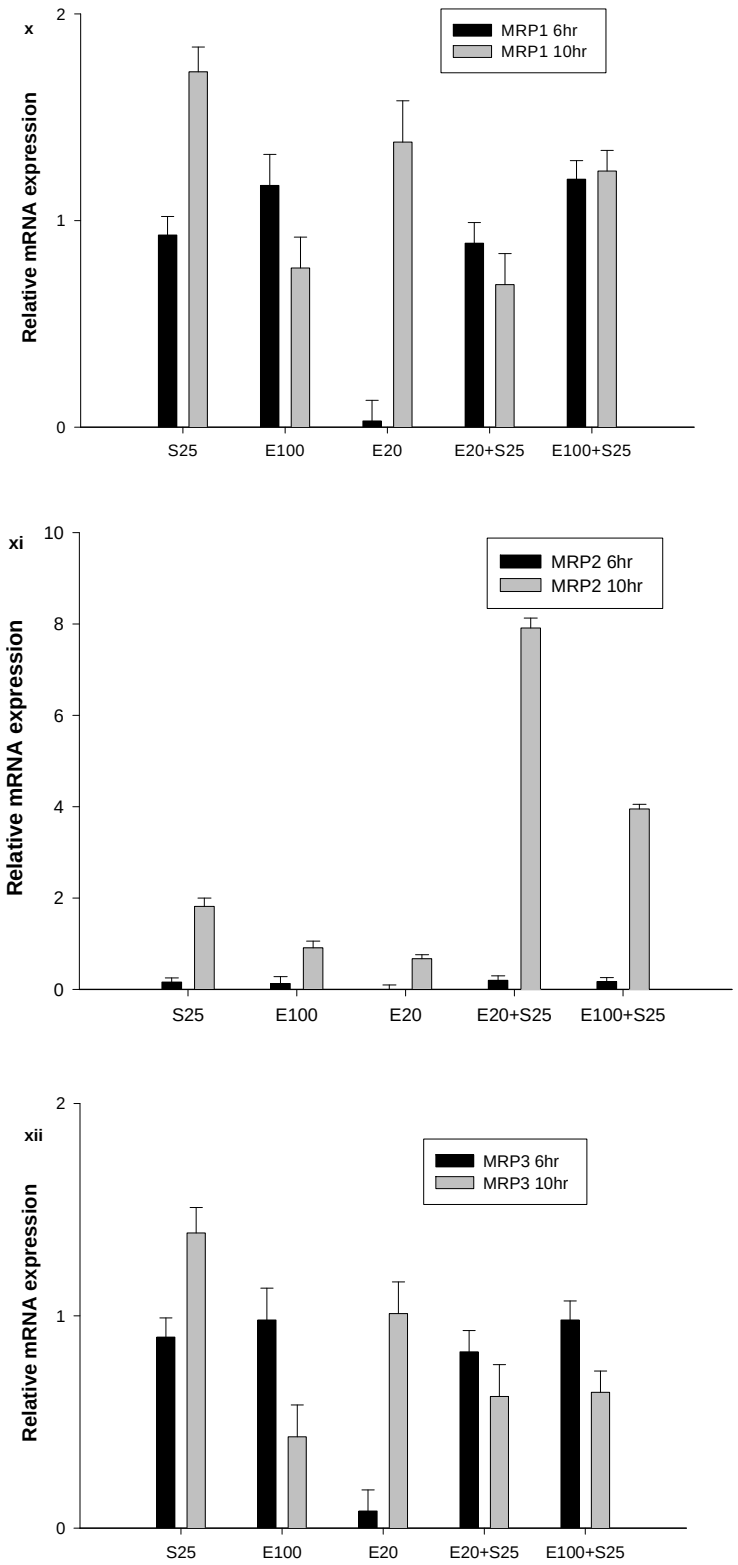
x
Relative mRNA expression
MRP1 6hr
MRP1 10hr
0
1
2
S25
E100
E20
E20+S25
E100+S25
xi
Relative mRNA expression
MRP2 6hr
MRP2 10hr
0
2
4
6
8
10
S25
E100
E20
E20+S25
E100+S25
xii
Relative mRNA expression
MRP3 6hr
MRP3 10hr
0
1
2
S25
E100
E20
E20+S25
E100+S25

Figure 5.2.d.

Figure 5.2. Temporal gene expression profiles elicited by combinations of SFN and EGCG

PC-3 AP-1 cells were treated for 6 hr or 10 hr with individual dietary factors, or combinations of SFN and EGCG, as indicated. RNA was extracted, transcribed into cDNA after ascertaining RNA integrity, and quantitative real-time PCR assays were performed for twelve genes (i- xii, above) at both time-points, as indicated, using beta-actin as the housekeeping gene. Values represent mean ± standard deviation for three replicates of each gene, and are representative of two independent experiments.

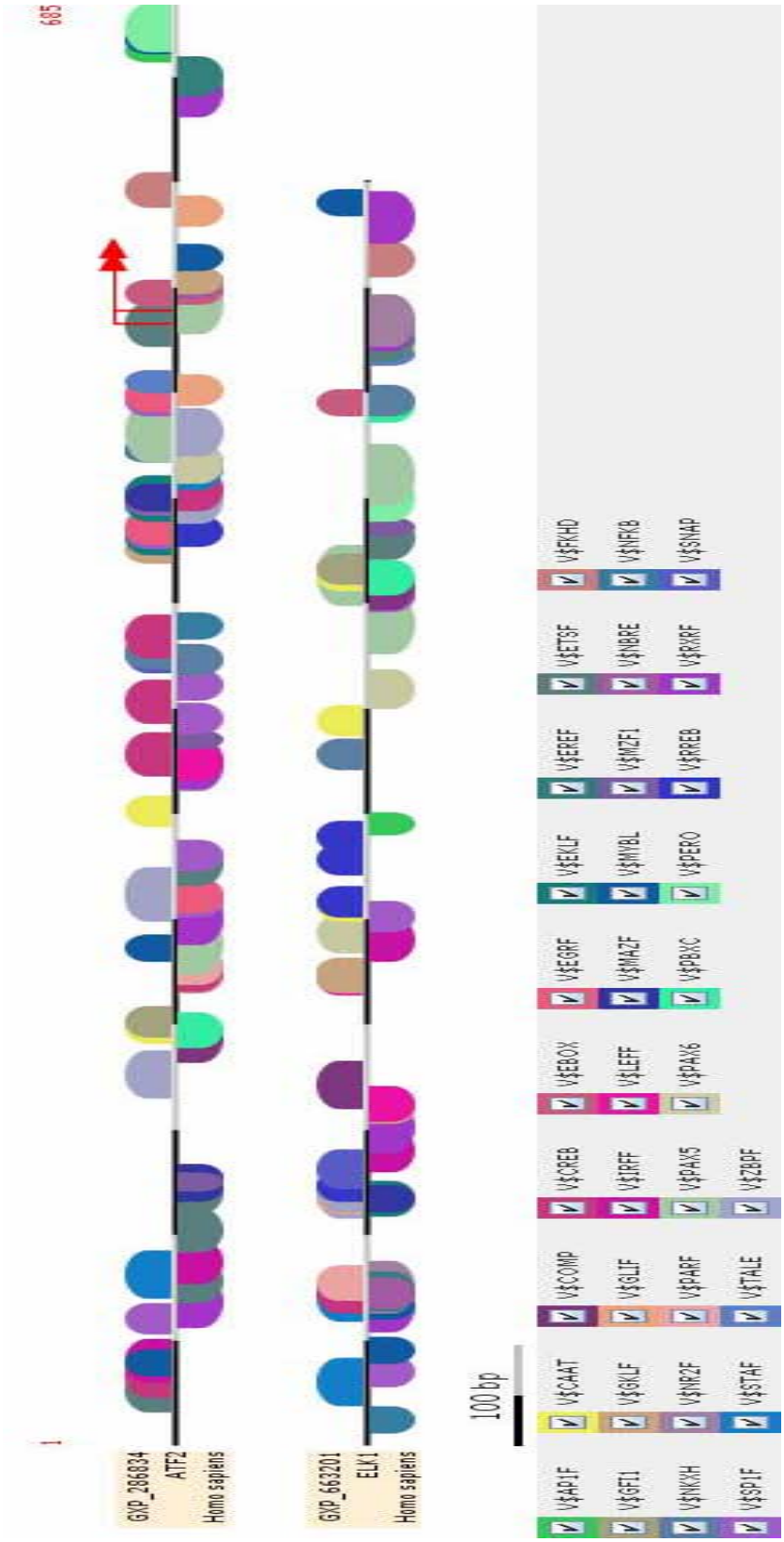
685
1
GXP_2866834
ATF2
Homo sapiens
GXP_6632201
ELK1
Homo sapiens
100 bp
V$AP1F
V$GFI1
V$NKXH
V$SP1F
V$CAAT
V$GKLF
V$NR2F
V$STAF
V$COMP
V$GLIF
V$PARF
V$TALE
V$CREB
V$TRFF
V$PAX5
V$ZBPF
V$EBOX
V$LEFF
V$PAX6
V$E6RF
V$MAZF
V$PBXC
V$EKLF
V$MYBL
V$PERO
V$EREF
V$MZF1
V$RREB
V$ETSF
V$NBRE
V$RXRF
V$FKHD
V$NFKB
V$SNAP

Figure 5.3.A.

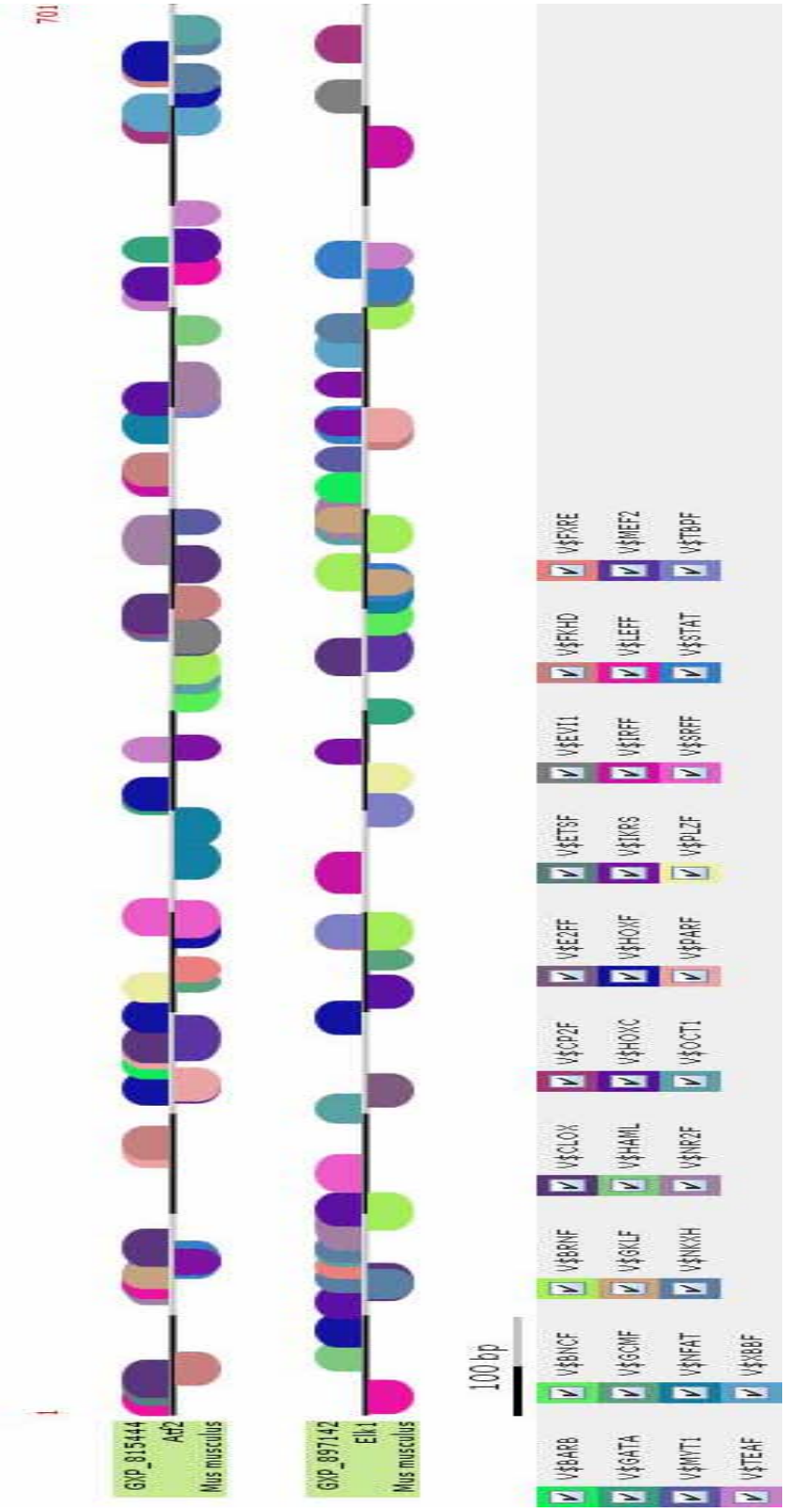
701
1
GXP_815444
Ah2
Mus musculus
GXP_897142
Elk1
Mus musculus
100 bp
V$ARB
V$GATA
V$MYT1
V$TEAF
V$BNCF
V$GCMF
V$NFAT
V$X8BF
V$BRNF
V$GKLF
V$NKXH
V$GLOX
V$HAML
V$NR2F
V$GP2F
V$HOXC
V$OCT1
V$E2FF
V$HOXF
V$PAXF
V$ETSF
V$EKRS
V$PLZF
V$EVI1
V$IRFF
V$SRFF
V$FKHD
V$LEFF
V$STAT
V$FXRE
V$MEF2
V$TBPF

Figure 5.3.B.

Figure 5.3. Conserved Transcription Factor Binding Sites (TFBS) in promoter regions of ATF-2 and ELK-1

Human promoter sequences of ATF-2 and ELK-1, or corresponding murine promoter sequences, were retrieved from Gene2Promoter (Genomatix). Comparative promoter analyses were then performed by input of these sequences in FASTA format into MatInspector using optimized default matrix similarity thresholds. The similar and/or functionally related TFBS were grouped into 'matrix families' and graphical representations of common TFBS were generated (Figure 5.3A, human ATF-2 and ELK-1; Figure 5.3B, murine Atf-2 and Elk-1). The 'V$' prefixes to the individual matrices are representative of the Vertebrate MatInspector matrix library.

CHAPTER 6

Regulatory potential for concerted modulation of Nrf2- and Nfkb1-mediated gene expression in inflammation and carcinogenesis[16,17,18].

6.1. Abstract

Many studies have implicated Nrf2 (Nfe2l2) in cancer and inflammation-associated diseases such as colitis or inflammatory bowel disease; and Nfkb1 in inflammation and cancer. However, despite a growing recognition of the important role(s) played by Nrf2 and Nfkb1, the regulatory potential for crosstalk between these two important transcription factors in inflammation and carcinogenesis has not been explored. To delineate conserved transcription factor binding sites (TFBS) signatures, we performed in silico bioinformatic analyses on the promoter regions of human and murine Nrf2 and Nfkb1, as well as coregulated genes. In order to investigate conserved biological features, we performed multiple sequence alignment of Nrf2 and Nfkb1 genes in five mammalian species – human, chimpanzee, dog, mouse and rat. We identified key regulatory genes in distinct inflammation/cancer signatures and constructed a canonical regulatory network for concerted modulation of Nrf2 and Nfkb1 involving several

---

[16]Work described in this chapter is under consideration for publication as **Nair, S**., Kong, AN., Cai, L.

[17]**Keywords** : Nrf2, Nfkb1, regulatory network, inflammation, carcinogenesis

[18]**Abbreviations** : BHA, butylated hydroxyanisole; EGCG, epigallocatechin-3-gallate; MAPK, mitogen-activated protein kinase; Nrf2 (Nfe2l2), Nuclear Factor-E2-related factor 2; Nfkb1, Nuclear Factor-κB1; NCSRS, Non-Coding Sequence Retrieval System; SFN, sulforaphane; TFBS, Transcription Factor Binding Sites.

members of the mitogen-activated protein kinase (MAPK) family. The identification of conserved TFBS and biological features across mammalian species, along with coregulation of several MAPKs with Nrf2 and Nfkb1, underscore putative crosstalk between these two critical transcription factors modulated via the MAPK cascade that may influence inflammation-associated etiopathogenesis of cancer. We present a canonical model for concerted modulation of Nrf2 and Nfkb1 in inflammation/carcinogenesis. Taken together, the elucidation of potential relationships among these two pivotal transcription factors may help to better understand transcriptional regulation, as well as transcription factor networks, associated with the etiopathogenesis of inflammation and cancer.

6.2. Introduction

The National Cancer Institute (NCI) Inflammation and Cancer Think Tank in Cancer Biology [201] has recognized that epidemiologic and clinical research corroborates an increased risk of certain cancers in the setting of chronic inflammation. Indeed, chronic inflammation, because of both infectious and non-infectious etiologies, has been associated with an increased risk of cancer development at a number of organ sites, with infectious agents estimated to be responsible for the development of 18% of all new cancer cases worldwide [202]. Infectious agents linked to cancer include Hepatitis B virus and liver cancer, Helicobacter pylori and stomach cancer, and liver fluke infection and cholangiocarcinoma. Additionally, a number of inflammatory conditions without an infectious etiology result in a significantly increased cancer risk. Examples include chronic gastroesophageal reflux-induced esophageal cancer, proliferative inflammatory

atrophy-induced prostate cancer and chronic ulcerative colitis-associated colorectal cancer. Activation of inflammatory cells is accompanied by an increase in the release of reactive oxygen species (ROS) at the site of inflammation. Excess levels of ROS, due to chronic inflammation, may contribute to carcinogenesis by reacting with DNA to form oxidative DNA adducts possibly leading to mutagenesis and impaired regulation of cellular growth [202]. Many of the processes involved in inflammation (e.g., leukocyte migration, dilatation of local vasculature with increased permeability and blood flow, angiogenesis), when found in association with tumors, are more likely to contribute to tumor growth, progression, and metastasis than to elicit an effective host anti-tumor response [201]. Recently, it has been shown [203] that signals downstream of the receptor for advanced glycation end-products (RAGE) can fuel chronic inflammation, creating a microenvironment that is ideal for tumor formation in a mouse model of skin cancer.

Nuclear Factor-E2-related factor 2 (Nrf2 or Nfe2l2) is indispensable to cellular defense against many chemical insults of endogenous and exogenous origin, which play major roles in the etiopathogenesis of many cancers and inflammation-related diseases such as inflammatory bowel disease, and Parkinson's disease [149]. Under basal conditions, Nrf2 - a member of the Cap-N-Collar family of transcription factors - is sequestered in the cytoplasm by Keap1 resulting in enhanced proteasomal degradation of Nrf2. In conditions of oxidative stress, Nrf2 is released from Keap1 either by direct oxidative modification of Keap1 or after phosphorylation by redox sensitive protein kinases, translocates to the nucleus and, in combination with other transcription factors, activates transcription of genes containing an antioxidant response element (ARE) in their

promoter regions resulting in a cytoprotective adaptive response. This adaptive response is characterized by upregulation of a battery of antioxidative enzymes and decreased sensitivity to oxidative damage and cytotoxicity. These antioxidative enzymes have also been shown to attenuate inflammatory damage and neutralize ROS implicated in inflammatory signaling pathways. We have also reported [177] that Nrf2 could play an important role in protecting intestinal integrity, through regulation of proinflammatory cytokines and induction of phase II detoxifying enzymes. Besides, we have demonstrated [204] that mitogen activated protein kinase (MAPK) pathways such as extracellular signal-regulated kinase (ERK) and c-jun N-terminal kinase (JNK) signaling pathways played important and positive roles in chemopreventive agent butylated hydroxyanisole (BHA)-induced and Nrf2-dependent regulation of ARE-mediated gene expression, as well as the nuclear translocation of Nrf2 in HepG2 cells. We have observed previously [205] that activation of MAPK pathways induces ARE-mediated gene expression via a Nrf2-dependent mechanism. In addition, we have also shown [41] that different segments of the Nrf2 transactivation domain have different transactivation potential and that different MAPK have differential effects on Nrf2 transcriptional activity with ERK and JNK pathways playing an unequivocal role in the positive regulation of Nrf2 transactivation domain activity [41,149].

Importantly, recent mouse studies provide strong and direct genetic evidence that the classical, IKK-β (inhibitor-of-NFκB kinase-β)-dependent Nuclear Factor-κB (NF-κB)-activation pathway, which was proposed several years ago to be the molecular link between inflammation and carcinogenesis, is a crucial mediator of tumour promotion [206]. Indeed, several pro-inflammatory cytokines and chemokines — such as TNF, IL-

1, IL-6 and CXC-chemokine ligand 8 (CXCL8; also known as IL-8), all of which are encoded by target genes of the IKK-β-dependent NF-κB-activation pathway — are associated with tumour development and progression in humans and mice. It has, thus, been hypothesized that activation of NF-κB by the classical, IKK-β-dependent pathway is a crucial mediator of inflammation-induced tumour growth and progression, as well as an important modulator of tumour surveillance and rejection [206]. We have also demonstrated [80] that the suppression of NF-κB and NF-κB-regulated gene expression (VEGF, cyclin D1 and Bcl-XL) by chemopreventive isothiocyanates sulforaphane (SFN) and phenethyl isothiocyanate (PEITC) is mainly mediated through the inhibition of IKK phosphorylation, particularly IKK-β, and the inhibition of IκB-α phosphorylation and degradation, as well as the decrease of nuclear translocation of p65 in human prostate cancer PC-3 cells. Recently, it has been observed [207] that PEITC suppresses receptor activator of NF-κB ligand (RANKL)-induced osteoclastogenesis by blocking activation of ERK1/2 and p38 MAPK in RAW264.7 macrophages. Besides, HL60 cells treated with fisetin presented high expression of NFkappaB, activation of p38 MAPK and an increase of phosphoprotein levels [208].

In this study, we explored the potential for putative crosstalk between Nrf2 and NF-κB signaling pathways in inflammation/injury and carcinogenesis. We performed in silico bioinformatic analyses to delineate conserved transcription factor binding sites (TFBS) or regulatory motifs in the promoter regions of human and murine Nrf2 and Nfkb1, as well as coregulated genes. We performed multiple sequence alignment of Nrf2 and Nfkb1 genes in five mammalian species and studied conserved biological features. We also looked at microarray data from public repositories such as Oncomine [209], Gene

Expression Omnibus (GEO), Public Expression Profiling Resource (PEPR) as well as datasets from the Kong Laboratory, in order to dissect the role(s) of key regulatory genes in these select inflammation/cancer signatures and constructed a regulatory network for concerted modulation of Nrf2 and Nfkb1 involving several members of the MAPK family. Our in silico analyses show that concerted modulation of Nrf2 and NF-κB signaling pathways, and putative crosstalk involving multiple members of the MAPK family, may be potential molecular events governing inflammation and carcinogenesis.

6.3. Materials and Methods

Identification of microarray datasets bearing inflammation/injury or cancer signatures : We perused several microarray datasets from public repositories such as Oncomine, GEO, PEPR, as well as datasets from the Kong Laboratory. We selected thirteen datasets that presented distinct signatures of inflammation or injury or carcinogenesis. Specifically, these studies reflected data on prostate cancer, spinal trauma, inflammatory response to injury; and genes modulated by chemopreventive agents/toxicants in Nrf2-deficient animal models. These studies encompassed three mammalian species – human, mouse and rat – and exhibited modulation of both Nrf2 (Nfe2l2) and Nfkb1 genes as well as coregulated genes.

Promoter Analyses for Transcription Factor Binding Sites (TFBS) : The promoter analyses were performed in the laboratory of Dr. Li Cai (Department of Biomedical Engineering, Rutgers University) using Genomatix MatInspector [195,196].

Briefly, human promoter sequences of NFE2L2 and NFKB1, or corresponding murine promoter sequences, were retrieved from Gene2Promoter (Genomatix). Comparative promoter analyses were then performed by input of these sequences in FASTA format into MatInspector using optimized default matrix similarity thresholds. The similar and/or functionally related TFBS were grouped into 'matrix families' and graphical representations of common TFBS were generated. The 'V$' prefixes to the individual matrices are representative of the Vertebrate MatInspector matrix library. Similarly, we also elucidated common TFBS amongst the three topmost conserved human regulatory sequences after multiple alignment (as described below) of NRF2 and NFKB1 sequences.

Multiple species alignment of Nrf2 (Nfe2l2) and Nfkb1 sequences : Non-coding sequences of Nfe2l2 and Nfkb1 genes in five mammalian species – human, chimpanzee, dog, mouse, and rat – were retrieved using the Non-Coding Sequence Retrieval System (NCSRS) for comparative genomic analysis of gene regulatory elements that has been previously developed and published [210] by the Cai Laboratory, and is readily available at http://cell.rutgers.edu/ncsrs/. Multiple sequence alignment was performed by submitting the non-coding sequences to MLAGAN (Multi-LAGAN, Multi-Limited Area Global Alignment of Nucleotides) [211] that is compatible with the VISTA visualization tool. The MLAGAN alignments were, thus, visualized using VISTA by projecting them to pairwise alignments with respect to one reference sequence (human) as baseline. The common TFBS between Nfe2l2 and Nfkb1 between the top biological features that were conserved in multiple species were

then determined using Genomatix MatInspector as described earlier in Materials and Methods under Promoter Analyses for TFBS.

Construction and validation of canonical first-generation regulatory network involving Nrf2 (Nfe2l2) and Nfkb1 : A putative regulatory network for Nrf2 (Nfe2l2) and Nfkb1 representing 59 nodes and 253 potential interactions was constructed using Cytoscape 2.5.2 software [212]. Further, we validated our network using PubGene [213], a literature network where connections are a strong indicator of biological interaction. Additional validation was achieved by the generation of a biological network with these gene identifiers through the use of Ingenuity Pathways Analysis (Ingenuity® Systems, www.ingenuity.com). For this purpose, a dataset containing gene identifiers was uploaded into the application. Each gene identifier was mapped to its corresponding gene object in the Ingenuity Pathways Knowledge Base. These genes, called focus genes, were overlaid onto a global molecular network developed from information contained in the Ingenuity Pathways Knowledge Base. Networks of these focus genes were then algorithmically generated based on their connectivity.

Putative model for Nrf2-Nfkb1 interactions in inflammation and carcinogenesis : A pictorial model for Nrf2-Nfkb1 interactions was generated using Pathway Builder Tool 2.0 available from Protein Lounge, San Diego, CA.

6.4. Results

6.4.1. Identification of microarray datasets bearing inflammation/injury or cancer signatures

In order to investigate distinct signatures of inflammation/ injury or carcinogenesis, we perused several microarray datasets from public repositories such as Oncomine, GEO, PEPR, as well as microarray datasets from the Kong Laboratory. As summarized in Table 6.1, we selected thirteen datasets that presented distinct signatures of inflammation/injury or carcinogenesis. Specifically, these studies reflected data on prostate cancer, spinal trauma, inflammatory response to injury; and genes modulated by chemopreventive agents/toxicants in Nrf2-deficient animal models. These studies encompassed three mammalian species – human, mouse and rat – and exhibited modulation of both Nrf2 (or Nrf2-dependent) and Nfkb1 genes as well as coregulated genes. In other words, all these studies presented modulation of both Nrf2 (Nfe2l2) and Nfkb1 genes in concert, except for the studies with Nrf2-deficient animal models where Nrf2-dependent genes were elucidated. Interestingly, these datasets exhibited modulation of several key members of the MAPK family as well as cofactors of Nrf2 and Nfkb1. This literature pre-screen encouraged us to investigate further the regulatory potential for concerted modulation of Nrf2- and Nfkb1-mediated gene expression in inflammation and carcinogenesis using an in silico bioinformatic approach.

6.4.2. Comparative promoter analyses of Nrf2 (Nfe2l2) and Nfkb1 for conserved Transcription Factor Binding Sites (TFBS)

To identify conserved TFBS signatures, we performed comparative analyses of Nrf2 and Nfkb1 murine promoter sequences (Figure 6.1A) using Genomatix MatInspector [195,196] as described in Materials and Methods. We also studied NRF2 and NFKB1 human promoter sequences (Figure 6.1B) similarly. Table 6.2 includes, as indicated, an alphabetical listing of the conserved vertebrate (V$) matrix families between these two transcription factors. The major human matrix families included Activator protein 4 and related proteins, Ccaat/Enhancer Binding Protein, Camp-responsive element binding proteins, E2F-myc activator/cell cycle regulator, E-box binding factors, Basic and erythroid krueppel like factors, Fork head domain factors, Myc associated zinc fingers, Nuclear receptor subfamily 2 factors, p53 tumor suppressor, RXR heterodimer binding sites, SOX/SRY-sex/testis determining and related HMG box factors, Signal transducer and activator of transcription, X-box binding factors, Zinc binding protein factors, and Two-handed zinc finger homeodomain transcription factors, amongst others. Some key conserved murine matrix families included AHR-arnt heterodimers and AHR-related factors, Activator protein 2, Activator protein 4 and related proteins, E2F-myc activator/cell cycle regulator, E-box binding factors, Basic and erythroid krueppel like factors, Farnesoid X - activated receptor response elements, Heat shock factors, Ikaros zinc finger family, Myc associated zinc fingers, Nuclear factor kappa B/c-rel, Nuclear receptor subfamily 2 factors, Nuclear respiratory factor 1, p53 tumor suppressor, Pleomorphic adenoma gene, RXR heterodimer binding sites, SOX/SRY-sex/testis determining and related HMG box factors, Serum response element binding factor,

Tata-binding protein factor, Zinc binding protein factors, amongst others. Indeed, as evident from Table 6.2, several matrix families were conserved between Nrf2 and Nfkb1 in both human and murine promoters.

6.4.3. Multiple species alignment of Nrf2 (Nfe2l2) and Nfkb1 sequences

With the objective of investigating conserved biological features across different mammalian species, we performed multiple species alignment of Nrf2 (Nfe2l2) and Nfkb1 sequences as described in Materials and Methods. We used the Non-Coding Sequence Retrieval System (NCSRS) for comparative genomic analysis of gene regulatory elements that has been previously developed and published [210] by the Cai Laboratory, and is readily available at http://cell.rutgers.edu/ncsrs/ and retrieved non-coding sequences of Nfe2l2 and Nfkb1 genes in five mammalian species – human, chimpanzee, dog, mouse, and rat. As shown in Figures 6.2A and 6.2B, we performed multiple sequence alignment using MLAGAN (Multi-LAGAN, Multi-Limited Area Global Alignment of Nucleotides) [211] for Nfe2l2 and Nfkb1 genes respectively, with respect to one reference sequence (human) as baseline. The phylogenetic tree for Nfe2l2 and Nfkb1 in the five species under consideration was constructed (Figure 6.2C). The conserved biological features across species for each of Nfe2l2 and Nfkb1 genes were perused, and the top five features for Nfe2l2 and the top three features for Nfkb1, as numbered in Figures 6.2A and 6.2B, are listed in Tables 6.3A and 6.3B respectively. Sequence 4 for Nfe2l2 and Sequence 1 for Nfkb1 exhibited the highest degree of conservation across species at 98.86% and 86.58% respectively. In addition, the top three conserved sequences in the human sequences of both these genes (Sequences 4, 3,

and 2 for Nfe2l2 in that order, and Sequences 1, 2, and 3 for Nfkb1 in that order) as evident from Tables 6.3A and 6.3B were submitted to Genomatix MatInspector. The common TFBS between Nfe2l2 and Nfkb1 between these biological features that were conserved in multiple species were then determined (Figure 2D) and tabulated along with the other TFBS results for comparative promoter analyses in Table 6.2 discussed earlier.

6.4.4. Construction and validation of canonical first-generation regulatory network involving Nrf2 (Nfe2l2) and Nfkb1

In order to construct a canonical first-generation biological network for Nrf2-Nfkb1 interactions, we streamlined our study to five datasets summarized in Table 6.4 which were representative of the most distinct inflammation/injury and cancer signatures from the thirteen datasets perused earlier. We obtained gene expression values for 59 genes, as shown in Table 6.4, including Nrf2 (Nfe2l2), Nfkb1, several cofactors, and many members of the MAPK family from these datasets. As shown in Figure 6.3A, we constructed a putative first-generation regulatory network for Nrf2 (Nfe2l2) and Nfkb1 representing 59 nodes and 253 potential interactions using Cytoscape 2.5.2 software [212]. Further, we validated our network by submitting 20 representative genes from Table 6.4 to PubGene [213], a literature network where connections are a strong indicator of biological interaction, and retrieved biological networks in human (Figure 6.3B) and mouse (Figure 6.3C), thus delineating gene signatures that validated the putative biological role(s) of the genes elucidated in the current in silico study that served as the source and target nodes in our regulatory network. We further validated

our network by querying Ingenuity Pathways Analysis (Ingenuity Systems®, www.ingenuity.com) application with the 59 gene identifiers forming the basis of our network, and obtained a biological network (Figure 6.3D) with a high degree of functional crosstalk based on the Ingenuity Knowledge Base reiterating the potential for crosstalk between multiple members of the MAPK family that might modulate the Nrf2-Nfkb1 interactions as indicated in our canonical network (Figure 6.3A).

6.4.5. Putative model for Nrf2-Nfkb1 interactions in inflammation and carcinogenesis

Based on the extensive experience [40,50,149,204,205,214] of the Kong Laboratory with Nrf2-Keap1 pathway and role(s) of MAPK/dietary chemopreventives/toxicants, our many microarray studies [52,55,56,58,215-218] in Nrf2-deficient mice, our studies [16,80] on NF-κB pathway and chemopreventive agents, and the gene signatures elicited in inflammation and carcinogenesis in the current in silico study using our data as well as publicly-available data from other research groups as indicated earlier, we generated a pictorial model (Figure 6.4) for Nrf2-Nfkb1 interactions using Pathway Builder Tool 2.0 available from Protein Lounge, San Diego, CA. In essence, chemical signals generated by dietary chemopreventive agents or toxicants, or inflammatory signals, may cause Nrf2 nuclear translocation that sets in motion a dynamic machinery of co-activators and co-repressors that may form a multi-molecular complex with Nrf2 to modulate transcriptional response through the antioxidant response element, ARE. Inflammation may also cause release of Nfκb1 from IκB and stimulate Nfκb1 nuclear translocation to modulate transcriptional response through the Nfκb1 response element,

Nfκb-RE, along with cofactors of Nfκb1. Several members of the MAPK family may act in concert with Nrf2 and Nfkb1 with multiple interactions between the members of the putative complex to elicit the chemopreventive and pharmacotoxicological events in inflammation and carcinogenesis.

6.5. Discussion

Karin and Greten [206] succinctly noted that carcinogenesis may be divided into three mechanistic phases: initiation (which involves stable genomic alterations), promotion (which involves the proliferation of genetically altered cells) and progression (which involves an increase in the size of the tumor, the spreading of the tumor and the acquisition of additional genetic changes). In 1863, Rudolf Virchow observed leucocytes in neoplastic tissues and suggested [219] that the “lymphoreticular infiltrate” reflected the origin of cancer at sites of chronic inflammation. Besides, persistent and recurrent episodes of inflammation [220] mediated by aberrant activation of innate and acquired immunity characterize a wide spectrum of idiopathic and infectious chronic inflammatory disorders. In response to tissue injury [221], a multifactorial network of chemical signals initiate and maintain a host response designed to 'heal' the afflicted tissue involving activation and directed migration of leukocytes (neutrophils, monocytes and eosinophils) from the venous system to sites of damage, and tissue mast cells also play a significant role. Interestingly, inflammation and innate immunity most commonly exert pro-tumorigenic effects [206] mediated through different types of leukocytes, including normal tissue macrophages, tumor-associated macrophages, dendritic cells, neutrophils, mast cells and T cells, which are recruited to the tumor microenvironment

through interactions with local stromal cells and malignant cells. These leukocytes produce cytokines, and growth and angiogenic factors, as well as matrix-degrading proteases (such as the matrix metalloproteinases MMP1, MMP3 and MMP9) and their inhibitors which allow tumor cells to proliferate, invade and metastasize [206]. Although the causal relationship between inflammation, innate immunity and cancer is more widely accepted, many of the molecular and cellular mechanisms mediating this relationship remain unresolved [221]. Many studies have implicated Nrf2 (Nfe2l2) in cancer [9,149,222-224] or inflammation-associated diseases such as colitis [177,202], and Parkinson's disease [225]; and NF-κB in inflammation [226-228] and cancer [80,229-231]. Indeed, the identification of combinatorial, or synergistic, transcription factors and the elucidation of relationships among them are of great importance for understanding transcriptional regulation as well as transcription factor networks [232]. However, despite a growing recognition of the important role(s) played by these two pivotal transcription factors, the regulatory potential for crosstalk between these two important transcription factors in inflammation and carcinogenesis has not been explored.

The perusal of several microarray datasets from public repositories such as Oncomine, GEO, PEPR, as well as datasets from the Kong Laboratory, facilitated the identification of thirteen datasets (Table 6.1) presenting distinct signatures of inflammation/injury or carcinogenesis that served as our literature pre-screen for concerted modulation of Nrf2 and Nfkb1 genes. The comparative analyses of TFBS in these two gene promoters revealed that many matrix families were conserved between human NRF2 and NFKB1 promoters, and between murine Nrf2 and Nfkb1 promoter regions (Figure 6.1 and Table

6.2). Furthermore, as elucidated in Table 6.2, several functionally important matrix families were also found to be common across human and murine species, including activator protein 4, E2F-myc activator/cell cycle regulators (V$E2FF), E box binding factors, basic and erythroid krueppel like factors, p53 tumor suppressor, and RXR heterodimer binding sites (V$RXRF), amongst others. The identification of V$E2FF is significant because disruption of retinoblastoma protein (pRb), a key controller of E2F activity and G1/S transition in the cell cycle, can alter the growth-inhibitory potential of TGF-β in the inflammatory milieu of chronic liver disease and contribute to cancer development [233]. Inflammatory conditions can enhance the genotoxic effects of carcinogenic polycyclic aromatic hydrocarbons such as benzo[a]pyrene (BaP) through upregulation of CYP1B1 expression associated with increased phosphorylation of p53 tumor suppressor at Ser-15 residue, enhanced accumulation of cells in the S-phase of the cell cycle and potentiation of BaP-induced apoptosis [234]. Thus, the presence of conserved p53 TFBS in Nrf2/Nfkb1 promoters may point to a critical role for inflammation in the etiopathogenesis of cancer, and underscore the relevance of crosstalk between these two transcription factors. The identification of V$RXRF is important since RXR physically interacts with peroxisome proliferator activated receptor (PPAR-α), a major player in lipid metabolism and inflammation, and PPAR-α agonists like fenofibrate inhibit NF-κB DNA-binding activity [235]. In addition, a conserved TFBS for NF-κB itself (Table 6.2) was found to be present in murine promoter regions of Nrf2 and Nfkb1 strengthening the potential for crosstalk between these two transcription factors. Our multiple sequence alignments (Figures 6.2A,B and Tables 6.3A,B) enabled the study of conserved biological features for each gene across

five mammalian species and the construction of a phylogenetic tree (Figure 6.2C). Interestingly, several key biological features were elicited on subjecting the top three conserved human sequences of each gene to comparative promoter analyses (Figure 6.2D and Table 6.2). Notably, autoimmune regulatory element binding factors (V$AIRE) and PPAR (or V$PERO) were conserved in these promoters. Recently, a cyclopentenonic prostaglandin 15-Deoxy-Delta(12,14)-prostaglandin J(2) has been shown to inhibit tumor necrosis factor (TNF)-related apoptosis-inducing ligand (TRAIL) mRNA expression by downregulating the activity of its promoter in T lymphocytes with NFκB being identified as a direct target of this prostanoid that is also regulated by activation of PPAR-γ [236]. The identification of PPAR in the promoter regions of Nrf2 and Nfkb1 in the current study, thus, reinforces the significance of these transcription factors and provides a possible mechanistic pathway for crosstalk in inflammation and cancer. Interestingly, a recent study [237] has reported that treatment of human brain astrocytes with double-stranded RNA induced interferon regulatory factor 3 (IRF3) phosphorylation and nuclear translocation followed by activation of signal transducer and activator of transcription 1 (STAT1) along with a concomitant activation of NFκB and MAPK cascade members (p38, JNK and ERK). In this study, we identified interferon regulatory factors (IRFF) and STAT as being conserved in Nrf2 and Nfkb1 promoters, as well as MAPK members in our regulatory network (Figure 6.3A), which agrees with mechanistic evidence from the brain astrocyte study. It has been observed [238] that stimulation with pro-inflammatory cytokines of CD38, known to be responsible for lung airway inflammation, rendered it insensitive to treatment with glucocorticoids such as fluticasone, dexamethasone or budesonide by inhibiting steroid-

induced glucocorticoid-responsive element (GRE)-dependent gene transcription. We also identified conserved GRE in the Nrf2/Nfkb1 promoters that further validated our results as biologically relevant. In addition, cell cycle regulators, heat shock factors, and several other matrices, were found to be conserved between the two genes, thus, underscoring the biological relevance, and the intrinsic complexity, of Nrf2/Nfkb1 crosstalk from a functional standpoint.

Further, we streamlined our study to five datasets (Table 6.4) which were representative of the most distinct inflammation/injury and cancer signatures of interest and constructed a canonical first-generation regulatory network (Figure 6.3A) for Nrf2 (Nfe2l2) and Nfkb1 representing 59 nodes and 253 potential interactions. We generated functionally relevant PubGene literature networks in human (Figure 6.3B) and mouse (Figure 6.3C), and using the Ingenuity Knowledge Base (Figure 6.3D), thus delineating gene signatures that validated the biological role(s), and potential for crosstalk, of the genes elucidated in the current in silico study. Our future work includes the expansion of our current study objectives to generate more detailed second-generation or third-generation regulatory networks for Nrf2 and Nfkb1 as more functional data emerges on these gene targets of interest and their interactions with coactivator/corepressor modules that associate with them. Interestingly, as shown in our current first-generation network (Figure 6.3A), several MAPKs play a central role in mediating the transcriptional effects of Nrf2 and Nfkb1. This is, indeed, in consonance with the known role of MAPKs in potentiating Nrf2-mediated ARE-activation [41,204,205] and their role in modulating NF-κB [207,208], thus, further underscoring the biological applicability of our results. Finally, we present a gestalt pictorial overview (Figure 6.4) of our current

knowledge of concerted modulation of Nrf2 and Nfkb1 based on the data from this study and our extensive experience in cancer chemoprevention.

The results from our current in silico study may strengthen the possibility that scientists could, in the future, consider pursuing Nrf2, Nfkb1 and MAPKs as potential targets in early drug discovery screens for the management of inflammation and cancer. In contemporary times, systems biology has interfaced with the drug discovery process to enable high-throughput screening of multiple drug targets and target-based leads. Indeed, a combination of high-throughput screening, kinase-specific libraries and structure-based drug design has facilitated the discovery of selective kinase inhibitors [239]. Needless to add, the benefits of applying molecular profiling to drug discovery and development include much lower failure rates at all stages of the drug development pipeline, faster progression from discovery through to clinical trials and more successful therapies for patient subgroups [240]. Thus, development of specific inhibitors that might regulate the specific crosstalk between the two central pleiotropic transcription factors Nrf2 and Nfkb1, and with the associated family of kinases, may serve as one of many strategies that might aid in the drug discovery process. Taken together, our study provides a canonical framework to understand the regulatory potential for concerted modulation of Nrf2 and Nfkb1 in inflammation and cancer. Further studies addressing this question with specific emphasis on cofactor modules binding to these transcription factors and coregulation with upstream signaling molecules in the MAPK cascade will enable a better appreciation of the emerging key role(s) of, and the crosstalk between, these two transcription factors in inflammation and carcinogenesis.

6.6. Acknowledgements

Sujit Nair is very grateful to Sung Tae Doh for his expert help with the multiple species alignment, and to Dr. Li Cai for the gracious training on the bioinformatic approaches used in this study. This work was supported in part by RO1 CA-094828 to Ah-Ng Tony Kong from the National Institutes of Health (NIH).

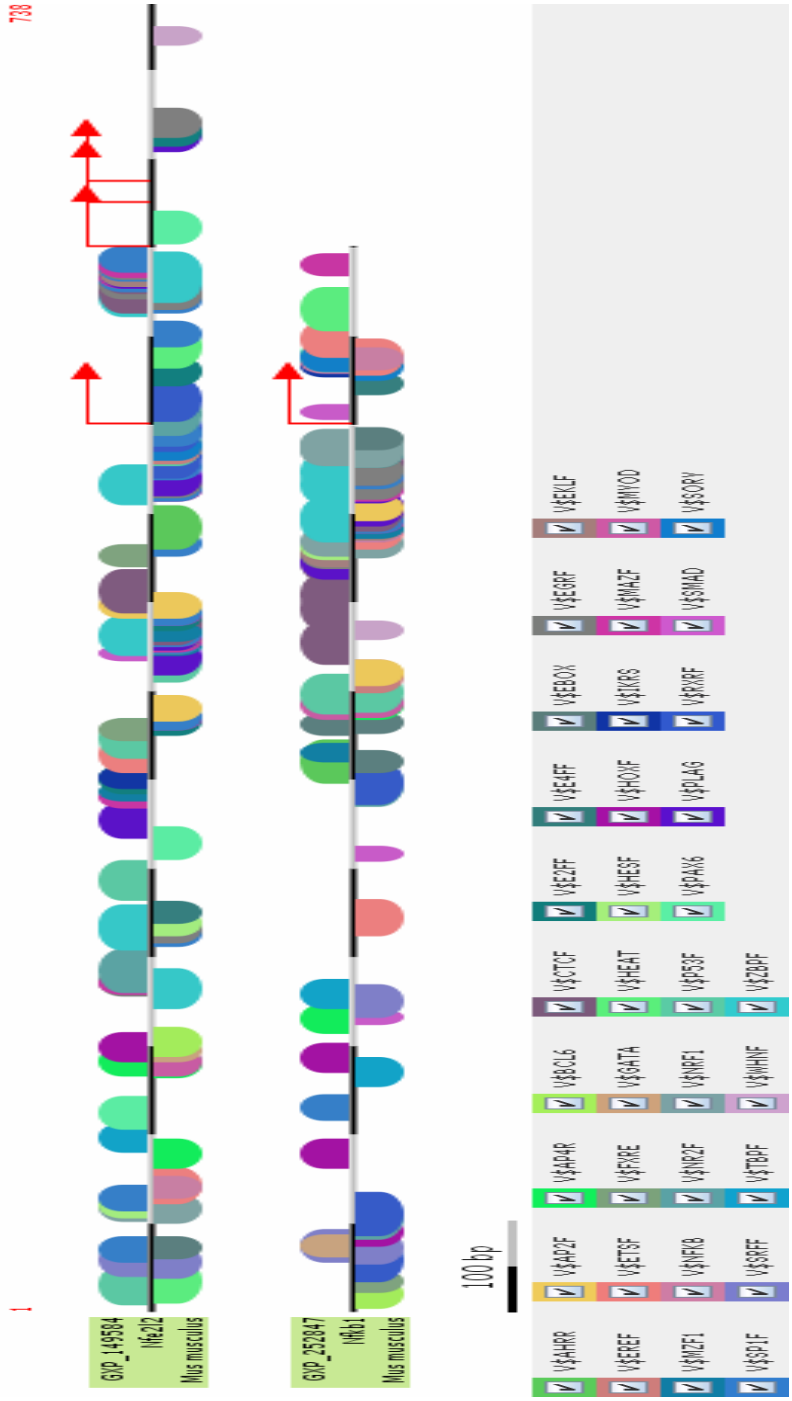
738
1
GVP_149584
Mus musculus
GVP_2528477
Mus musculus
100 bp

Figure 6.1. A.

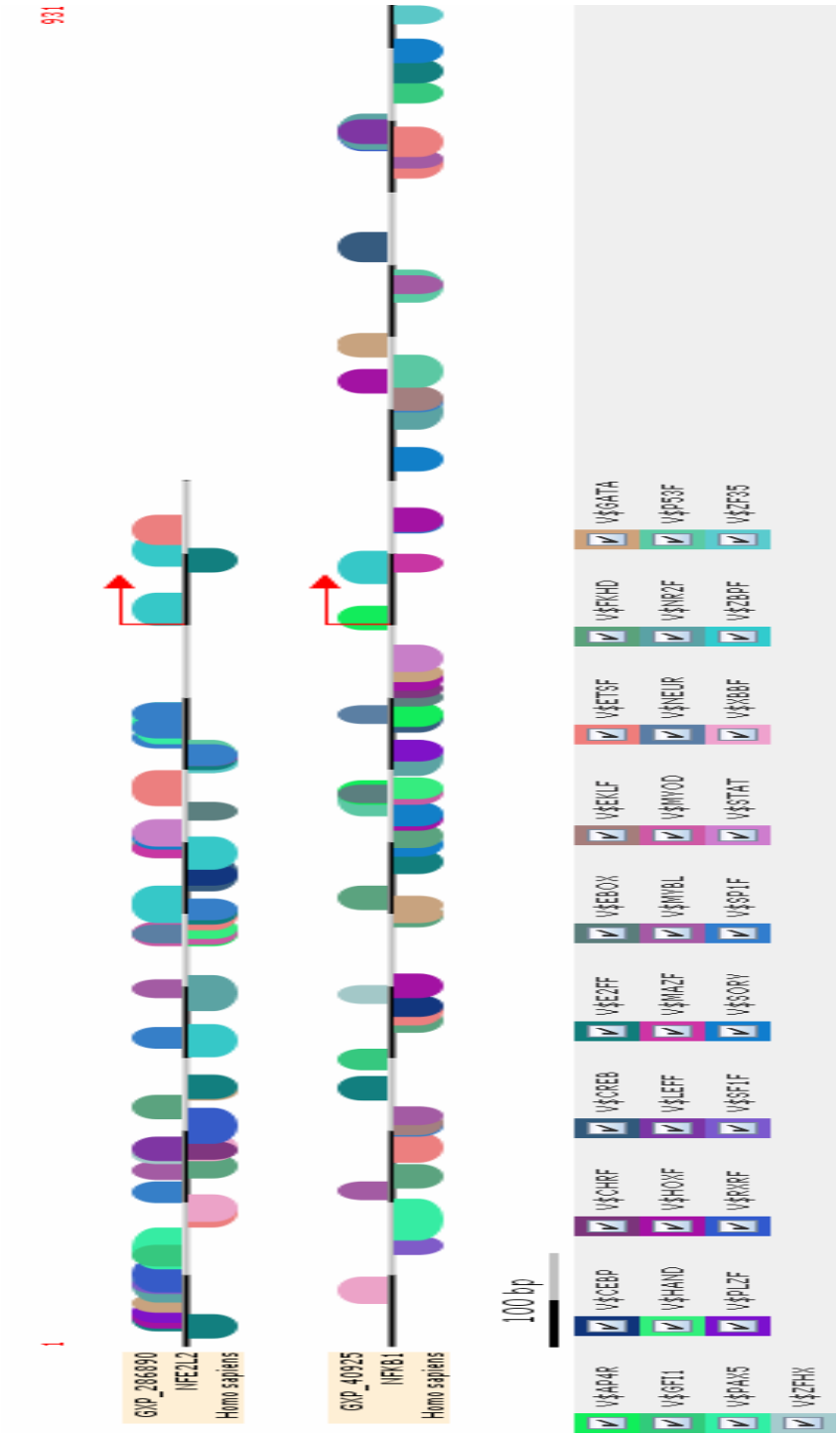
931
1
GVP_286890
NFE2L2
Homo sapiens
GVP_40225
NFYB1
Homo sapiens
100 bp

Figure 6.1. B.

Figure 6.1. Conserved TFBS between Nfe2l2 and Nfkb1

Vertebrate (V$) matrix families conserved between murine (or human) Nfe2l2 and Nfkb1 promoter regions were identified using Genomatix MatInspector.

6.1. A. Conserved TFBS between murine Nfe2l2 and Nfkb1**; 6.1.B.** Conserved TFBS between Human NFE2L2 and NFKB1.

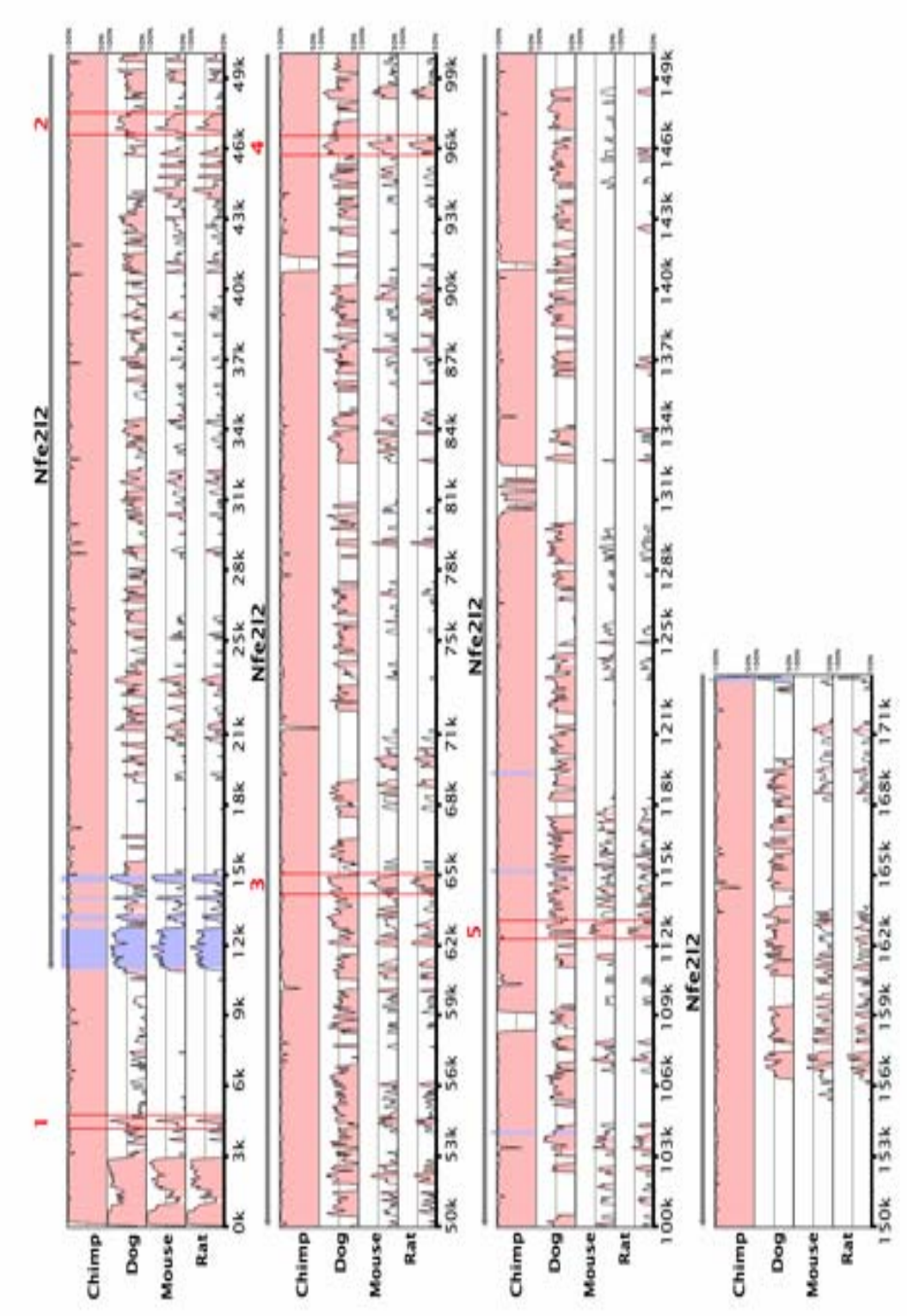
Nfe2l2
Chimp
Dog
Mouse
Rat
1
2
3
4
5
0k 3k 6k 9k 12k 15k 18k 21k 25k 28k 31k 34k 37k 40k 43k 46k 49k
50k 53k 56k 59k 62k 65k 68k 71k 75k 78k 81k 84k 87k 90k 93k 96k 99k
100k 103k 106k 109k 112k 115k 118k 121k 125k 128k 131k 134k 137k 140k 143k 146k 149k
150k 153k 156k 159k 162k 165k 168k 171k

Figure 6.2. A.

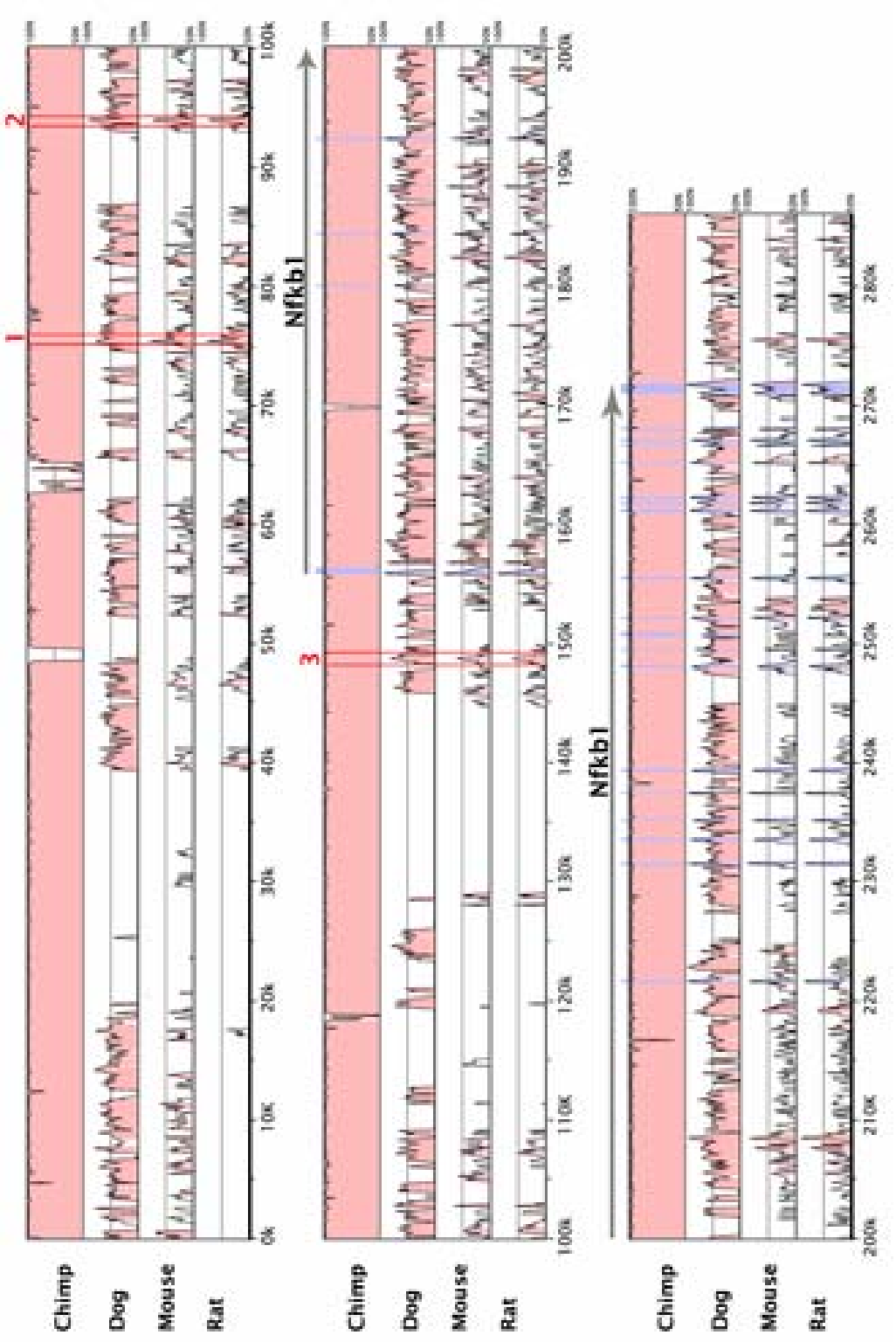
Nfkbl
Nfkbl
Chimp
Dog
Mouse
Rat
Chimp
Dog
Mouse
Rat
Chimp
Dog
Mouse
Rat

Figure 6.2. B.

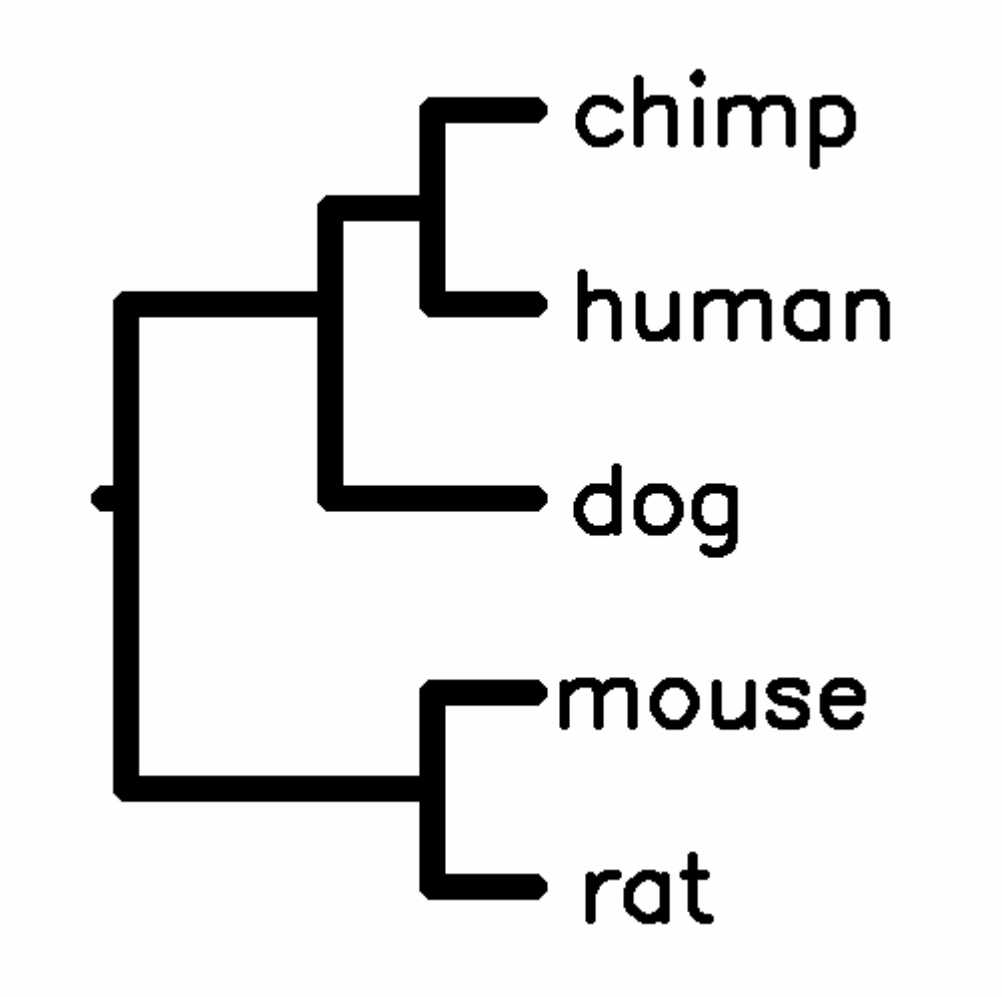

Figure 6.2. C.

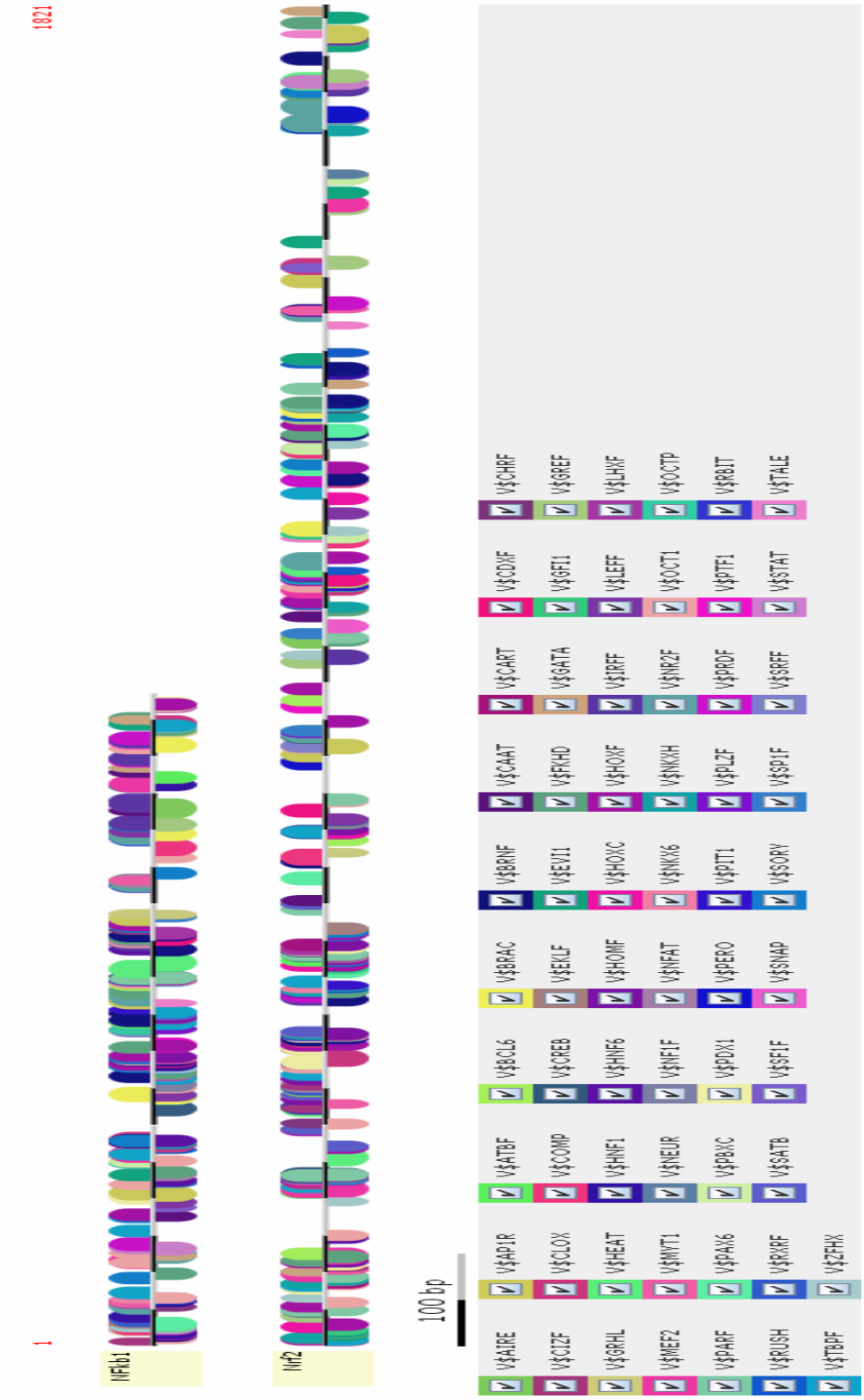
1821
1
NFkb1
Nrf2
100 bp
V$AIRE
V$AP1R
V$ATBF
V$BCL6
V$BRAC
V$BRNF
V$CAAT
V$CART
V$CDXF
V$CHRF
V$CIZF
V$CLOX
V$COMP
V$CREB
V$EKLF
V$EVI1
V$FKHD
V$GATA
V$GFI1
V$GREF
V$GRHL
V$HEAT
V$HNF1
V$HNF6
V$HOMF
V$HOXC
V$HOXF
V$IRFF
V$LEFF
V$LHXF
V$MEF2
V$MYT1
V$NEUR
V$NF1F
V$NFAT
V$NKX6
V$NKXH
V$NR2F
V$OCT1
V$OCTP
V$PARF
V$PAX6
V$PBXC
V$PDX1
V$PERO
V$PIT1
V$PLZF
V$PRDF
V$PTF1
V$RBJT
V$RUSH
V$RXRF
V$SATB
V$SF1F
V$SNAP
V$SOXW
V$SP1F
V$STAT
V$TBPF
V$ZFHX
V$TALE

Figure 6.2. D.

Figure 6.2. Multiple species alignment

Non-coding sequences of Nfe2l2 and Nfkb1 genes in five mammalian species – human, chimpanzee, dog, mouse, and rat – were retrieved using the Non-Coding Sequence Retrieval System (NCSRS) for comparative genomic analysis of gene regulatory elements. Multiple sequence alignment was performed by submitting the non-coding sequences to MLAGAN, and visualized by projecting them to pairwise alignments with respect to one reference sequence (human) as baseline [Pink regions, Conserved Non-Coding Sequences (CNS); Dark blue regions, Exons]. The numbers indicate CNS that were identified across species.

6.2. A. Multiple species alignment for Nfe2l2; **6.2. B.** Multiple species alignment for Nfkb1; **6.2. C.** Phylogenetic Tree for Nfe2l2 and Nfkb1; **6.2. D.** Conserved TFBS between NFE2L2 and NFKB1 among top matching human sequences

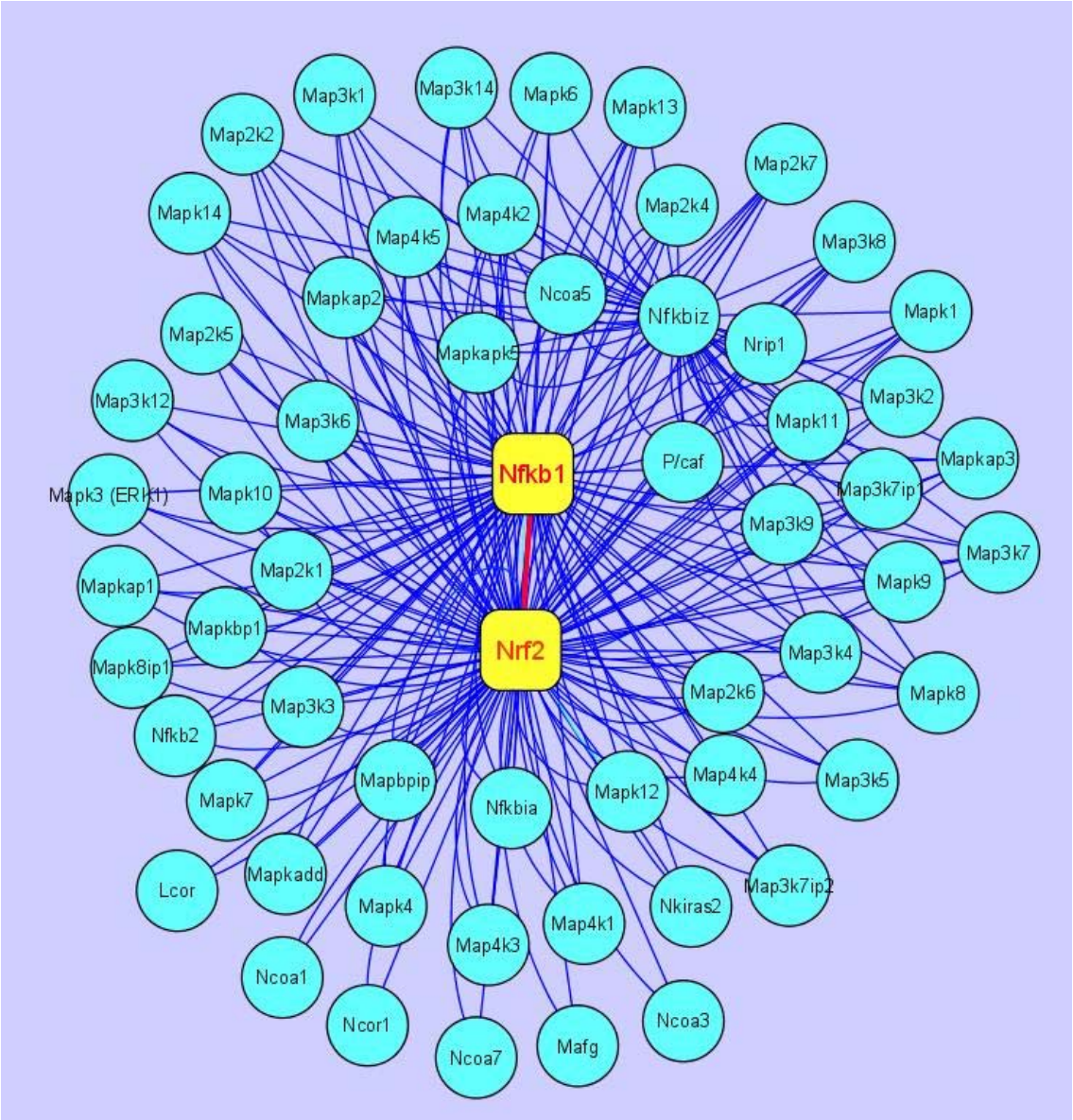
Map3k1
Map3k14
Mapk6
Mapk13
Map2k2
Map2k7
Mapk14
Map4k2
Map2k4
Map4k5
Map3k8
Mapkap2
Ncoa5
Nfkbiz
Mapk1
Map2k5
Mapkapk5
Nrip1
Map3k12
Map3k2
Map3k6
Mapk11
Nfkb1
P/caf
Mapkap3
Mapk3 (ERK1)
Mapk10
Map3k7ip1
Map3k9
Map3k7
Map2k1
Mapkap1
Mapk9
Mapkbp1
Nrf2
Map3k4
Mapk8ip1
Map2k6
Mapk8
Map3k3
Nfkb2
Mapbpip
Map4k4
Map3k5
Mapk7
Nfkbia
Mapk12
Lcor
Mapkadd
Map3k7ip2
Mapk4
Nkiras2
Map4k1
Map4k3
Ncoa1
Ncor1
Ncoa3
Ncoa7
Mafg

Figure 6.3. A.

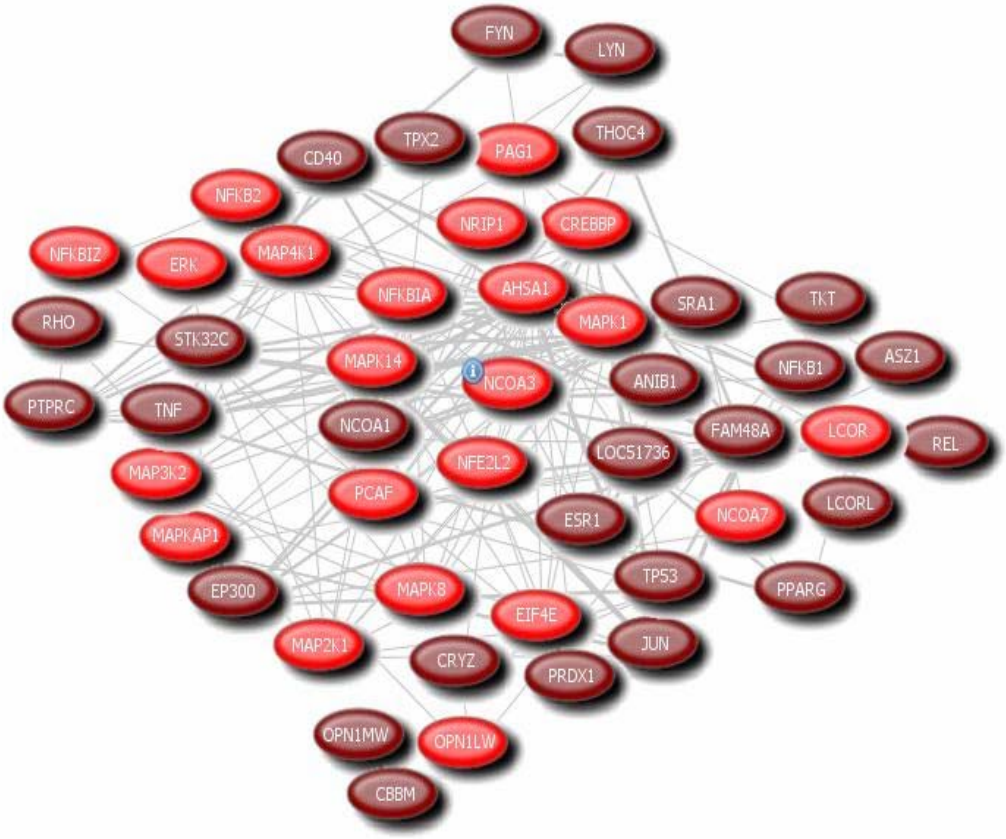
FYN
LYN
CD40
TPX2
PAG1
THOC4
NFKB2
NRIP1
CREBBP
NFKBIZ
ERK
MAP4K1
NFKBIA
AHSA1
SRA1
TKT
RHO
STK32C
MAPK1
MAPK14
NCOA3
ANIB1
NFKB1
ASZ1
PTPRC
TNF
NCOA1
FAM48A
LCOR
REL
LOC51736
MAP3K2
NFE2L2
PCAF
ESR1
NCOA7
LCORL
MAPKAP1
TP53
EP300
MAPK8
EIF4E
PPARG
MAP2K1
JUN
CRYZ
PRDX1
OPN1MW
OPN1LW
CBBM

Figure 6.3. B.

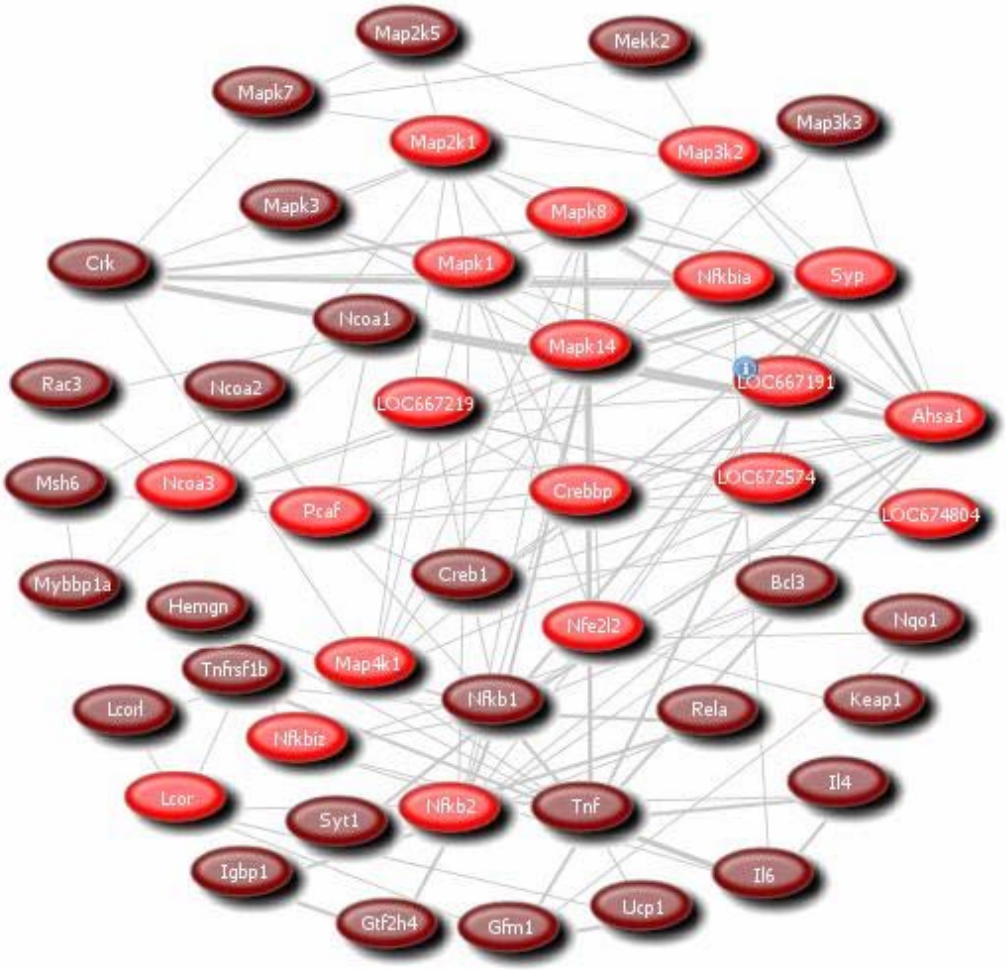
Map2k5
Mekk2
Mapk7
Map3k3
Map2k1
Map3k2
Mapk3
Mapk8
Crk
Mapk1
Nfkbia
Syp
Ncoa1
Mapk14
Rac3
Ncoa2
LOC667191
LOC667219
Ahsa1
Msh6
Ncoa3
LOC672574
Crebbp
Pcaf
LOC674804
Mybbp1a
Creb1
Bcl3
Hemgn
Nfe2l2
Nqo1
Tnfrsf1b
Map4k1
Lcorl
Nfkb1
Rela
Keap1
Nfkbiz
Il4
Lcor
Syt1
Nfkb2
Tnf
Igbp1
Il6
Ucp1
Gtf2h4
Gfm1

Figure 6.3. C.

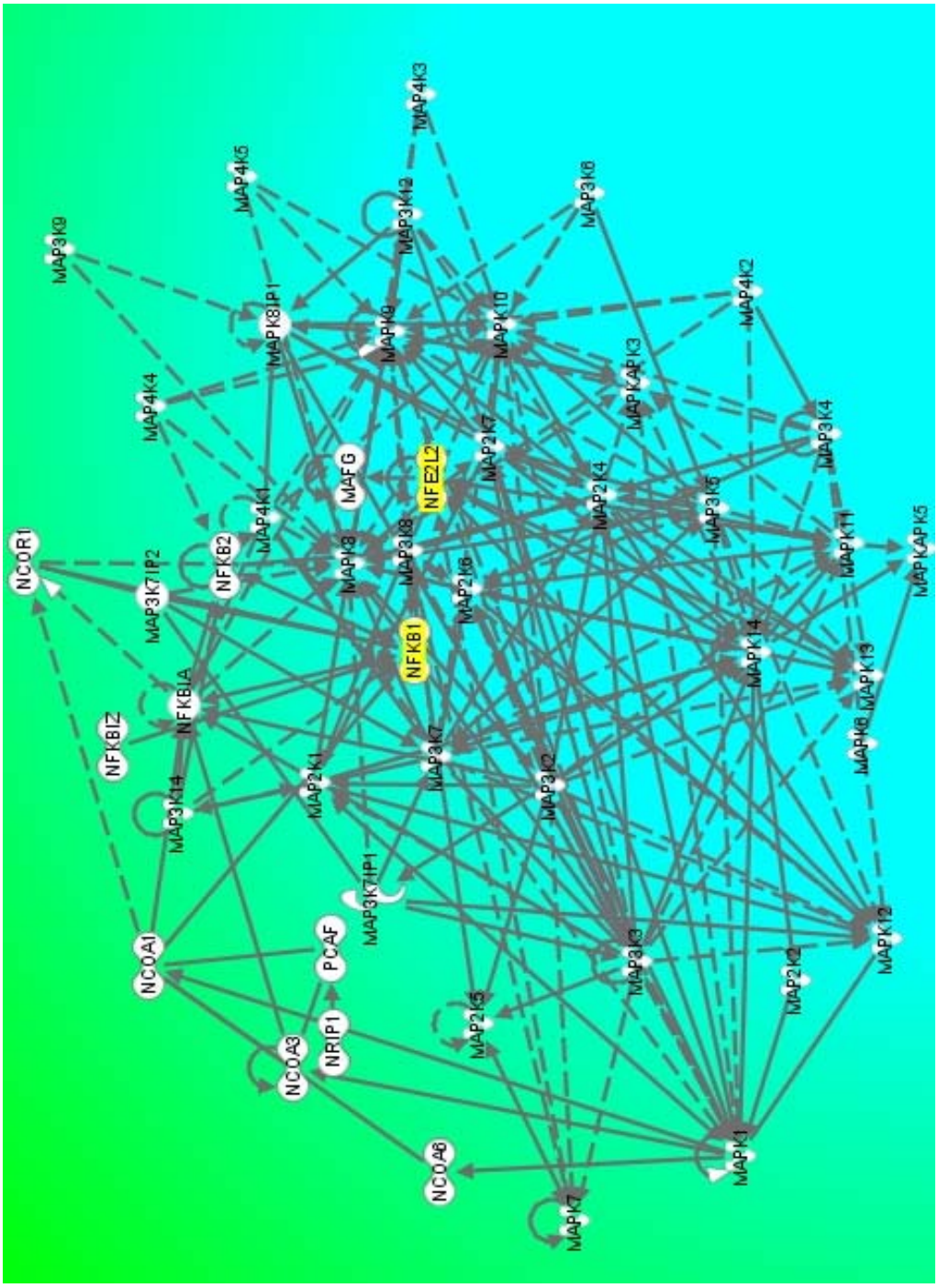
MAP3K9
MAP4K5
MAP4K3
MAP3K12
MAP3K6
MAP4K2
MAPK8IP1
MAPK8
MAPK10
MAPKAPK3
MAP4K4
MAP2K7
MAP3K4
MAFG
NFE2L2
MAP2K4
MAP3K5
MAP4K1
NCOR1
NFKB2
MAP3K8
MAPK11
MAPKAPK5
MAP3K7IP2
MAP2K6
NFKB1
MAPK14
NFKBIA
MAPK13
NFKBIZ
MAPK6
MAP3K7
MAP2K1
MAP3K14
MAP3K2
MAP3K7IP1
NCOA1
PCAF
MAPK12
MAP3K3
MAP2K2
NRIP1
MAP2K5
NCOA3
MAPK1
NCOA6
MAPK7

Figure 6.3. D.

Figure 6.3. Canonical regulatory networks for Nrf2-Nfkb1 interactions in inflammation-associated carcinogenesis

6.3. A. A putative regulatory network for Nrf2 (Nfe2l2) and Nfkb1 representing 59 nodes and 253 potential interactions implicating several members of the MAPK family; **6.3. B.** Literature network in human; **6.3. C.** Literature network in mouse; **6.3. D.** Functional crosstalk in biological network of Nfe2l2, Nfkb1 and various members of the MAPK cascade.

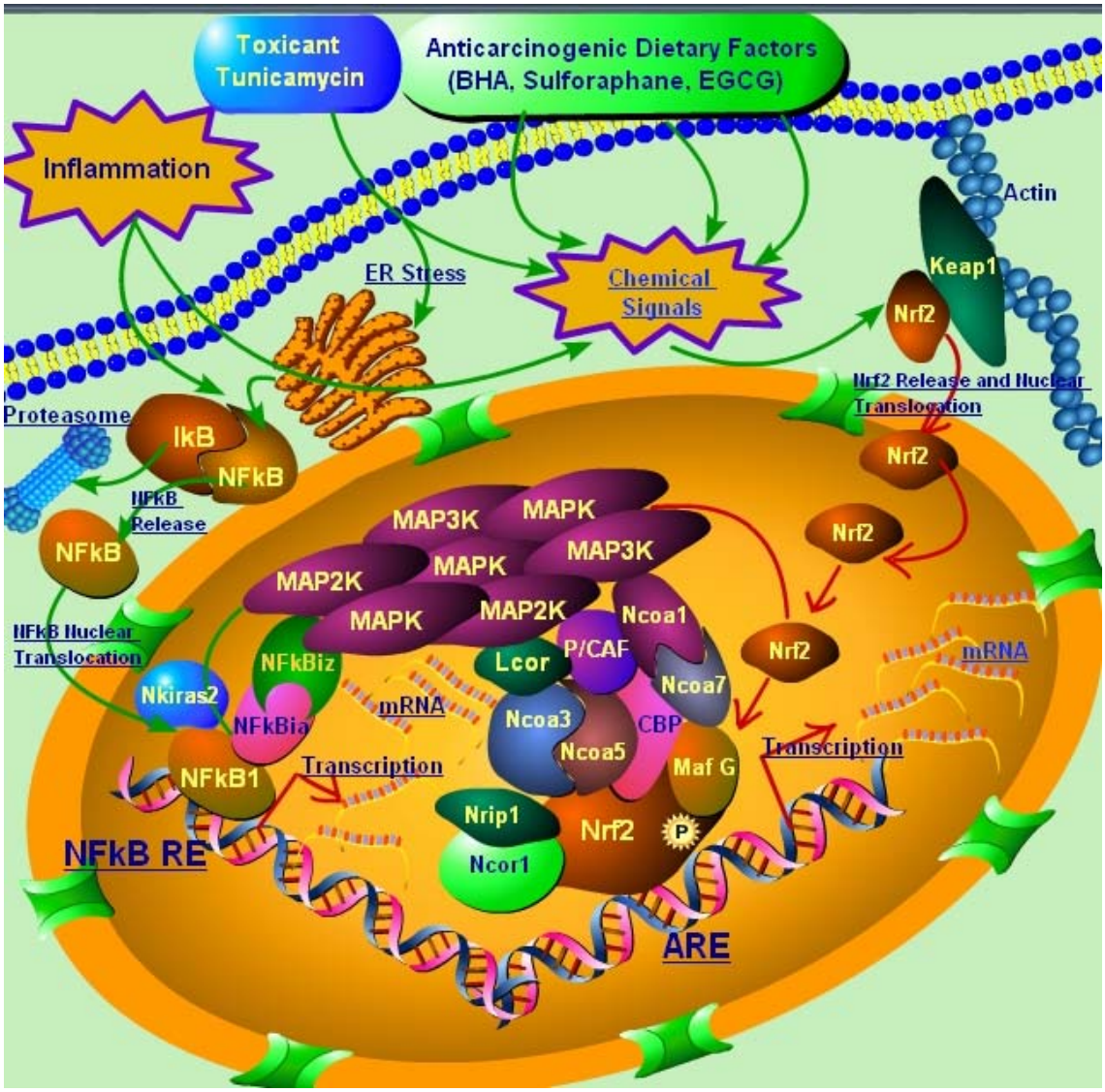

Figure 6.4. Putative Model for Nrf2-Nfkb1 interactions in inflammation and carcinogenesis

Chemical signals generated by dietary chemopreventive agents or toxicants, or inflammatory signals, may cause Nrf2 nuclear translocation that sets in motion a dynamic machinery of co-activators and co-repressors that may form a multi-molecular complex with Nrf2 to modulate transcriptional response through the antioxidant

response element, ARE. Inflammation may also cause release of NF-κB from IκB and stimulate NF-κB nuclear translocation to modulate transcriptional response through the NF-κB response element, NF-κB-RE, along with cofactors of NF-κB. Several members of the MAPK family may act in concert with Nrf2 and Nfkb1 with multiple interactions between the members of the putative complex to elicit the chemopreventive and pharmacotoxicological events in inflammation and carcinogenesis.

CHAPTER 7

Pharmacogenomic investigation of potential prognostic biomarkers in human prostate cancer[19,20,21]

7.1. Abstract

Prostate cancer is the second leading cause of cancer deaths among men in the United States, and the seventh leading cause of deaths overall for men. The objective of this study was to identify candidate biomarkers for human prostate cancer that could be important for chemopreventive or therapeutic intervention, thus resulting in a delay in advancement to clinical diagnosis of cancer. The development of rational chemopreventive strategies requires knowledge of the mechanisms of prostate carcinogenesis and crosstalk between important signaling pathways that are relevant in prostate cancer. We used microarray analyses to identify genes that are upregulated or downregulated at least five-fold in human prostate cancer. We generated functionally relevant signaling pathways that are important in prostate cancer through metabolomics analyses. Further, we identified TFBS-association signatures in the regulatory elements of representative biomarkers. The identification of key target hubs such as p38 MAPK, PPAR gamma, ESR2, VIP, Rb1 and others in the signaling networks, and of key

---

[19]Work described in this chapter is under consideration for publication as **Nair, S**., Cai, L., Kong, AN.

[20]**Keywords:** Human prostate cancer, microarray, bioinformatics, biomarkers, TFBS.

[21]**Abbreviations :** MAPK, mitogen-activated protein kinase; NRF2, nuclear factor (erythroid-derived-2)-related factor-2; TFBS, Transcription Factor Binding Sites.

transcription factors including NRF2 in the regulatory analysis, is a first step to identifying key biomarkers in prostate cancer. Taken together, using our systems biology approach, we were able to identify several candidate biomarkers and signaling networks that could be important target hubs for the development of chemopreventive strategies that target one or more of the identified biomarkers, alone or in combination, in order to improve the efficacy of chemoprevention in prostate cancer and enhance patient survival.

7.2. Introduction

The incidence of prostate cancer in the United States has increased by 1.1% per year from 1995–2003 [130,172]. According to the Centers for Disease Control and Prevention (CDC) [130], prostate cancer is the second leading cause of cancer deaths among men in the United States, and the seventh leading cause of deaths overall for men. Interestingly, the National Cancer Institute (NCI)'s Surveillance Epidemiology and End Results (SEER) Statistics Fact Sheets [173] show that, based on rates from 2002–2004, 16.72% of men born today will be diagnosed with cancer of the prostate at some time during their lifetime, i.e., 1 in 6 men in the United States are at a lifetime risk of developing prostate cancer. In addition, evidence from studies examining the association between adult body mass index (BMI) and the risk of prostate cancer is inconclusive with several cohort studies suggesting a positive association whereas other studies report no association, although there is some indication that the positive association is limited to fatal or more aggressive tumors [241].

Two different types of precursors of prostate cancer can be found in the prostate gland, for example, dysplastic areas termed prostatic intraepithelial neoplasia (PIN) [242,243] and proliferative inflammatory atrophy (PIA) lesions. PIA lesions can be found near adenocarcinomas and they can merge with high-grade PIN areas [243,244]. The detection of prostate cancer, recurrence, or metastatic disease is often determined using the serum prostate specific antigen (PSA) test. PSA is a serine protease that is synthesized by both normal and malignant epithelial cells of the human prostate. PSA expressed by malignant cells, however, is released into the serum at an increased level, which can be detected to diagnose and monitor prostate cancer [245]. In a recent study [246], the PSA nadir while intermittently taking a testosterone-inactivating pharmaceutical agent was determined to be the best predictor of prostate cancer-specific mortality. Nevertheless, despite the considerable attention given to PSA as a screening test for prostate cancer, it is needle biopsy, and not the PSA test result, that actually establishes the diagnosis of prostate cancer [175]. Garmey et al [247] noted that although hormone-based therapies generally result in rapid responses, virtually all patients ultimately develop androgen-independent progressive disease, and it is among these men with hormone-refractory prostate cancer that the role of chemotherapy continues to be investigated. To date, three drugs (estramustine, mitoxantrone, and docetaxel) have been approved by the US Food and Drug Administration (FDA) for first-line chemotherapy in hormone-refractory prostate cancer [247], with other agents and combinations now under evaluation in ongoing clinical trials.

Epidemiological research on prostate cancer risk in men throughout the world has identified significant correlations between dietary habits and prostate cancer occurrence.

These studies have served as a catalyst for exploration of the potential of dietary substances to act as chemopreventive agents, the tested agents including green tea catechins, lycopene, soy isoflavones, pomegranate phenolics, selenium, vitamins E and D, curcumin and resveratrol [248]. Indeed, prostate cancer is an ideal candidate disease for chemoprevention because it is typically diagnosed in the elderly population with a relatively slower rate of growth and progression, and therefore, even a modest delay in the development of cancer, achieved through pharmacologic or nutritional intervention, could result in substantial reduction in the incidence of clinically detectable disease [249]. The development of rational chemopreventive strategies requires knowledge of the mechanisms of prostate carcinogenesis and identification of agents that interfere with these mechanisms. Because of the long time period for prostate carcinogenesis and the large size of the cohort required for an evaluable study, identification and characterization of early intermediate biomarkers and their validation as surrogate endpoints for cancer incidence are essential for chemopreventive agent development [250] .

Using microarray technology, we compared the transcriptomic profiles in cancerous human prostate with that in normal prostate human tissue. We generated lists of genes that were greatly upregulated or downregulated (at least five-fold) in tumor as compared to normal. We then applied bioinformatic techniques and metabolomics analysis to indentify potential biomarkers that might be important in prostate cancer, as well as functional biological networks that might be critical in the etiopathogenesis of prostate cancer. The candidate biomarkers in the networks identified in this study could be important targets for chemoprevention research in prostate cancer.

7.3. Materials and Methods

Human prostate RNA : FirstChoice® Human Prostate Tumor/Normal Adjacent Tissue RNA (Catalog No. AM7288) was procured from Ambion (Applied Biosystems/Ambion, Austin, TX). The FirstChoice® RNA was total RNA isolated from an individual tumor (7288T) and the normal adjacent tissue (NAT, 7288N).

Assessment of RNA Integrity : RNA integrity was assessed using formaldehyde gels in 1X MOPS buffer and RNA concentration was determined by the 260/280 ratio on a DU 530 UV/Visible spectrophotometer (Beckman).

Microarray Sample Preparation and Hybridization : Affymetrix (Affymetrix, Santa Clara, CA) human genome U133 Plus 2.0 array was used to probe the global gene expression profiles in prostate RNA. The cDNA synthesis and biotin-labeling of cRNA, hybridization and scanning of the arrays, were performed at CINJ Core Expression Array Facility of Robert Wood Johnson Medical School (New Brunswick, NJ). Each chip was hybridized with cRNA derived from either cancerous or normal prostate. Briefly, double-stranded cDNA was synthesized from 5 μg of total RNA and labeled using the ENZO BioArray RNA transcript labeling kit (Enzo Life Sciences, Inc.,Farmingdale, NY, USA) to generate biotinylated cRNA. Biotin-labeled cRNA was purified and fragmented randomly according to Affymetrix's protocol. Two hundred microliters of sample cocktail containing 15 μg of fragmented and biotin-labeled cRNA was loaded onto each chip. Chips were hybridized at 45°C for 16 h and washed with fluidics protocol EukGE-WS2v5 according to Affymetrix's recommendation. At the

completion of the fluidics protocol, the chips were placed into the Affymetrix GeneChip Scanner where the intensity of the fluorescence for each feature was measured.

dChip Data Analyses : The CEL files created from each sample (chip) were first imported into dChip software [197,198] for further data characterization. Briefly, a gene information file with current annotations and functional gene ontology was generated and the Affymetrix Chip Description File (CDF) was specified. The data were then normalized in dChip and the expression value for each gene was determined by calculating the average of differences in intensity (perfect match intensity minus mismatch intensity) between its probe pairs. A list of genes that were modulated at least five-fold in cancerous prostate as compared to normal prostate was generated. Thereafter, Clustering and Enrichment Analysis was performed to obtain hierarchical tree clustering diagrams that provided functional classification of Affymetrix Probe Set IDs and gene descriptions.

Biomarker and Metabolomics Analyses : Functional analyses, biomarker filtration, and metabolomics analyses were performed through the use of Ingenuity Pathways Analysis (Ingenuity® Systems, www.ingenuity.com). Starting with the list of genes that were regulated at least five-fold in the dChip analyses described earlier, we performed functional analyses by associating them with biological functions in the Ingenuity Pathways Knowledge Base. Using Ingenuity's Biomarker Filter, we identified representative biomarkers that were greatly modulated (at least five-fold) in cancerous prostate as compared to normal. The criteria used for the filter were disease

state (cancer), tissue type (prostate gland) and species (human). The candidate biomarkers were toggled to their subcellular localization. Further, we subjected these candidate biomarkers to Ingenuity's Metabolomics analysis and identified biologically relevant signaling networks in prostate cancer. Briefly, a data set containing gene identifiers (GenBank Accession IDs) and corresponding expression values (obtained earlier from our dChip analyses) was uploaded into in the application. Each gene identifier was mapped to its corresponding gene object in the Ingenuity Pathways Knowledge Base. An expression value cut-off of 1.0 was set to identify all genes whose expression was significantly differentially regulated. These genes, called focus genes, were overlaid onto a global molecular network developed from information contained in the Ingenuity Pathways Knowledge Base. Networks of these focus genes were then algorithmically generated based on their connectivity.

Identification of TFBS-association signatures : The co-regulated potential biomarkers were now additionally investigated for Transcription Factor Binding Site (TFBS)-association signatures using NCBI's DiRE (Distant Regulatory Elements of co-regulated genes) at the DiRE server for the identification of distant regulatory elements of coregulated genes (http://dire.dcode.org) and the top ten transcription factors were identified. DiRE's unique feature is the detection of regulatory elements outside of proximal promoter regions, as it takes advantage of the full gene locus to conduct the search. Function-specific regulatory elements consisting of clusters of specifically-associated TFBSs were predicted, and the association of individual transcription factors with the biological function shared by the group of input genes were scored.

7.4. Results

7.4.1. Genes modulated in human prostate cancer

In order to identify important gene clusters that are modulated in human prostate cancer, we performed dChip analysis of our microarray data as described in detail in Materials and Methods. 408 genes that were modulated (upregulated or downregulated) at least five-fold in cancerous prostate (7288T) over normal adjacent tissue (7288N) were identified. The clustering analysis revealed ten significant gene clusters as shown in Figure 7.1 including cell adhesion, cell division and cell cycle, enzymatic activity, extracellular region, kinases and phosphatases, proteinaceous extracellular matrix, phosphate transport, regulation of transcription, transcription factor activity, and transporters. Major members of these important gene clusters that were all modulated at least five-fold in human prostate cancer are listed in Table 7.1 along with their GenBank Accession IDs and fold change values.

7.4.2. Biomarker filtration

To further identify functionally relevant biomarkers in prostate cancer, we used a biomarker filter as described earlier under Materials and Methods and identified 21 candidate biomarkers that passed the filter. We toggled these biomarkers to their subcellular localization as shown in Figure 7.2.A. The biomarkers included (i) VIP (vasoactive intestinal polypeptide, 24.3 fold); (ii) SFTPD (surfactant, pulmonary-associated protein D, -9.13 fold); (iii) BMP5 (bone morphogenetic protein 5, 12.55 fold); (iv) SHBG (sex hormone-binding globulin, 16.9 fold); (v) DLL 1 (delta-like 1 (Drosophila), -7.42 fold); (vi) FGF18 (Fibroblast growth factor 18, -20.06 fold); (vii)

GRIA1 (glutamate receptor, ionotropic, AMPA 1, 7.06 fold); (viii) TJP3 (tight junction protein 3 (zona occludens 3), -11.64 fold); (ix) ACVR1B (activin A receptor, type IB, 10.45 fold); (x) CXADR (coxsackie virus and adenovirus receptor, 24.8 fold); (xi) NUDT3 (Nudix (nucleoside diphosphate linked moiety X)-type motif 3, 9.42 fold); (xii) MSC (musculin (activated B-cell factor-1), -14.48 fold); (xiii) MBD1 (methyl-CpG binding domain protein 1, -7.48 fold); (xiv) NR1I2 (nuclear receptor subfamily 1, group I, member 2, 8.62 fold); (xv) ESR2 (estrogen receptor 2 (ER beta), 9.12 fold); (xvi) TOP2A (topoisomerase (DNA) II alpha 170kDa, 19.24 fold); (xvii) RGS12 (regulator of G-protein signaling 12, 7.19 fold); (xviii) NR1H4 (nuclear receptor subfamily 1, group H, member 4, 9.94 fold); (xix) TNNC2 (troponin C type 2 (fast), -22.55); (xx) MYH14 (myosin, heavy chain 14, 7.49); and, (xxi) ASNS (Asparagine synthetase, 7.49 fold). We searched for crosstalk between these potential biomarkers and deciphered a few connections as shown in Figure 7.2.B. All the above biomarkers were representative of different gene clusters that we had elicited in our microarray study and were considered as focal nodes for further analysis.

7.4.3. Metabolomics analyses

To generate biologically relevant signaling networks and to identify biomarker targets that are relevant specifically in prostate cancer pathogenesis, we subjected the 21 representative biomarkers identified earlier to Metabolomics analyses as described in Materials and Methods. Two simplified networks were derived from the Metabolomics analysis for the human prostate tumor biomarkers (i) Cell Death, Cellular Growth and Differentiation, and Cellular Development (Figure 7.3.A), and (ii) Gene Expression,

Cancer, Cellular Growth and Proliferation (Figure 7.3.B). These networks included p38 MAP Kinase, other MAP Kinases, HNF signaling molecules, LDL, Ncoa1, PPAR gamma, and estrogen receptor, amongst other important signaling molecules. In order to appreciate the complexity of the signaling networks that might be relevant in prostate cancer, we merged these two simplified networks as shown in Figure 7.3.C. We were thus able to identify major "target hubs" through which a greater number of connections traversed as is evident from these networks.

7.4.4. Identification of TFBS-association signatures

To investigate TFBS-association signatures in the promoter regions of the 21 representative biomarkers obtained after filtration, we submitted these gene sequences to DiRE analyses as described in Materials and Methods. The top ten TFBS-association signatures were identified with respect to occurrence and importance as shown in Figure 7.4. These TFBS included (i) SPZ1, spermatogenic leucine zipper (ii)TATA, TATA box (iii)IRF7, interferon regulatory factor 7 (iv)TAL1, T-cell acute lymphocytic leukemia 1 (v) OSF2, osteoblast-specific transcription factor (vi)NRF2, nuclear factor (erythroid-derived-2)-related factor-2 (vii)HNF3, hepatocyte nuclear factor 3 (viii)TEF, transcriptional enhancer factor (ix)TBP, TATA-binding protein, and (x)SEF1, SL3-3 enhancer factor 1.

7.5. Discussion

The Prostate Cancer Prevention Trial (PCPT) demonstrated that finasteride reduces the prevalence of prostate cancer by 24.8 % (risk reduction), however, cost-effectiveness analyses recently showed [251] that its use may be cost-effective only in high-risk populations when taking into consideration adjustments for the impact on quality of life. Nevertheless, prostate cancer is highly indicated for chemopreventive intervention due to its inherent characteristics [248] which include (i) frequent discovery of latent carcinoma, even in countries with low incidences of clinical cancer; (ii) very long time to clinically significant cancer; (iii) few patients under 50 years of age (primarily a disease of elderly men); (iv) strong influences of environmental factors such as food; (v) temporal effectiveness of androgen deprival therapy; and (vi) no effective therapeutic approaches once hormone-refractory neoplasms have developed. In drug discovery, attempts have been made to use functional genomics in target identification and validation, lead selection and optimization, and in preclinical studies to predict clinical outcome [252]. Knowledge of the genetics and genomics of drug metabolizing enzymes (DMEs) allows us to better understand and predict enzyme regulation and its effects on exogenous (pharmacokinetics) and endogenous pathways as well as biochemical processes (pharmacology) [253]. The identification of new drug targets for therapeutic or preventive intervention is, thus, of great importance and would be greatly assisted by recent developments in systems biology research.

In the current study, we provide a proof-of-concept demonstration of identification of human prostate cancer biomarkers by bioinformatic approaches. To identify relevant genes that were highly upregulated or downregulated in cancerous prostate as compared

to normal prostate, we performed microarray analyses and clustered the genes that were modulated at least five-fold into various functionally relevant gene categories as shown in Figure 7.1 and listed in Table 7.1. In order to identify important signaling networks in prostate cancer, we initially restricted ourselves to 21 potential biomarkers that passed our biomarker filter. These biomarkers were representative of the gene clusters identified in our microarray study. We then performed metabolomics analyses with these representative biomarkers and generated functional signaling networks that would be relevant in prostate cancer.

From our network in Figure 7.3.A, it is evident that p38 MAPK (mitogen-activated protein kinase) is a major target hub with several connections pointing to or leading away from this molecule. We have shown previously [254] that p38 MAPK negatively regulates the induction of phase II DMEs that detoxify carcinogens, thus the involvement of p38 MAPK as a major target hub in our network is in consonance with our previous findings on the role of p38 in cancer chemoprevention. The retinoblastoma tumor suppressor protein (Rb), a critical mediator of cell cycle progression, is functionally inactivated in the majority of human cancers, including prostatic adenocarcinoma, with 25% to 50% of prostatic adenocarcinomas harboring aberrations in Rb pathway. Thus, the identification of Rb1 in both our signaling networks in Figures 7.3.A and 7.3.B underscores its relevance as an important biomarker in prostate cancer. Furthermore, we identified NCOA1 (nuclear receptor coactivator 1) in Figures 7.3.A and 7.3.B which we have previously reported [52] as a potential NRF2-dependent binding partner, and also identified MAP2K6 in Figure 7.3.A. Since MAPK cascades have differential effects on NRF2 transactivation domain activity, and since NCOA1 is

an NRF2-dependent cofactor, the role of NRF2 as an important biomarker for prostate cancer must be considered. We also noted the presence of VIP (vasoactive intestinal polypeptide) and HNF4A (hepatocyte nuclear factor 4A) as major target hubs in both networks in Figures 7.3.A and 7.3.B. This is important because receptors for VIP and the human epidermal growth factor family of tyrosine kinase receptors (HER) are potent promoters of cell proliferation, survival, migration, adhesion and differentiation in prostate cancer [255]. Recently, a far module was found to support constitutive expression of CYP3A4 (cytochrome P450 3A4), that is involved in the metabolism of more than 50% of drugs and other xenobiotics, with the far module (like the distal module) being structurally clustered by a PXR response element (F-ER6) and elements recognized by HNF-4A. Thus, the identification of HNF-4A may relate to a heightened potential for CYP3A4-mediated metabolism of any interventive agent for prostate cancer prevention that must be taken note of. Interestingly, combined therapy against both growth factor and steroid receptor signaling appears very challenging in the era of optimization of therapeutic effect, and is currently under clinical investigation [256,257]. A very promising application of this concept is reported [258] in experiments that combined a pure-antiestrogen (Faslodex) and a tyrosine kinase inhibitor targeted to EGFR (Iressa), giving rise to an additive suppression of growth and VEGF secretion in NIH-H23 NSCLC and MCF-7 cells, through MAPK inhibition [256,258]. The identification of estrogen receptor (ESR2) in our signaling network (Figure 7.3.B) underscores the importance of steroid receptor signaling in hormone-refractory prostate cancer. We also identified TGF-beta in Figure 7.3.B that is in agreement with a recent report [259] on the relevance of TGF-beta related signaling markers in breast and

prostate cancer patients with bone metastasis. To obtain a comprehensive overview of crosstalk between major signaling networks that may be relevant in human prostate cancer, we merged the generated networks as shown in Figure 7.3.C. Several major target hubs including p38 MAPK, PPAR gamma, ESR2, VIP, Rb1, amongst others, were identified as key regulatory points in prostate cancer. The development of chemopreventive agents that would target these major signaling molecules alone or in combination may be pursued to further the cause of prostate cancer prevention.

Furthermore, our data on TFBS-association signatures in the regulatory elements of the representative biomarkers revealed interesting transcription factors as shown in Figure 7.4. Notably, the identification of NRF2 was in corroboration with the identification of NRF2-dependent gene NCOA1 as well as members of the MAPK family, including p38 MAPK, MAP2K6 and others in our metabolomics analyses. This is also in agreement with our previous reports [18,216] on the role of NRF2 in prostate cancer, thus underscoring the validity of pursing NRF2 as an additional biomarker target for prostate cancer chemopreventive intervention.

In summary, we have identified genes that are modulated at least five-fold in human prostate cancer. We were also able to generate functionally relevant signaling pathways that are important in prostate cancer through metabolomics analyses. We also identified TFBS-association signatures in the regulatory elements of representative biomarkers. The identification of key target hubs such as p38 MAPK, PPAR gamma, ESR2, VIP, Rb1 and others in the signaling networks, and of key transcription factors including NRF2 in the regulatory analysis, is a first step to identifying key biomarkers in prostate cancer. Using our systems biology approach, the development of chemopreventive

strategies that target one or more of the identified biomarkers, alone or in combination, would greatly reduce the time needed for development of new drugs, and eliminate false leads, in the drug discovery paradigm for prostate cancer.

7.6. Acknowledgements

Sujit Nair is very grateful to Dr. Li Cai for his excellent training on the bioinformatics approaches used in this study. This work was supported in part by RO1 CA 118947 to Ah-Ng Tony Kong from the National Institutes of Health (NIH).

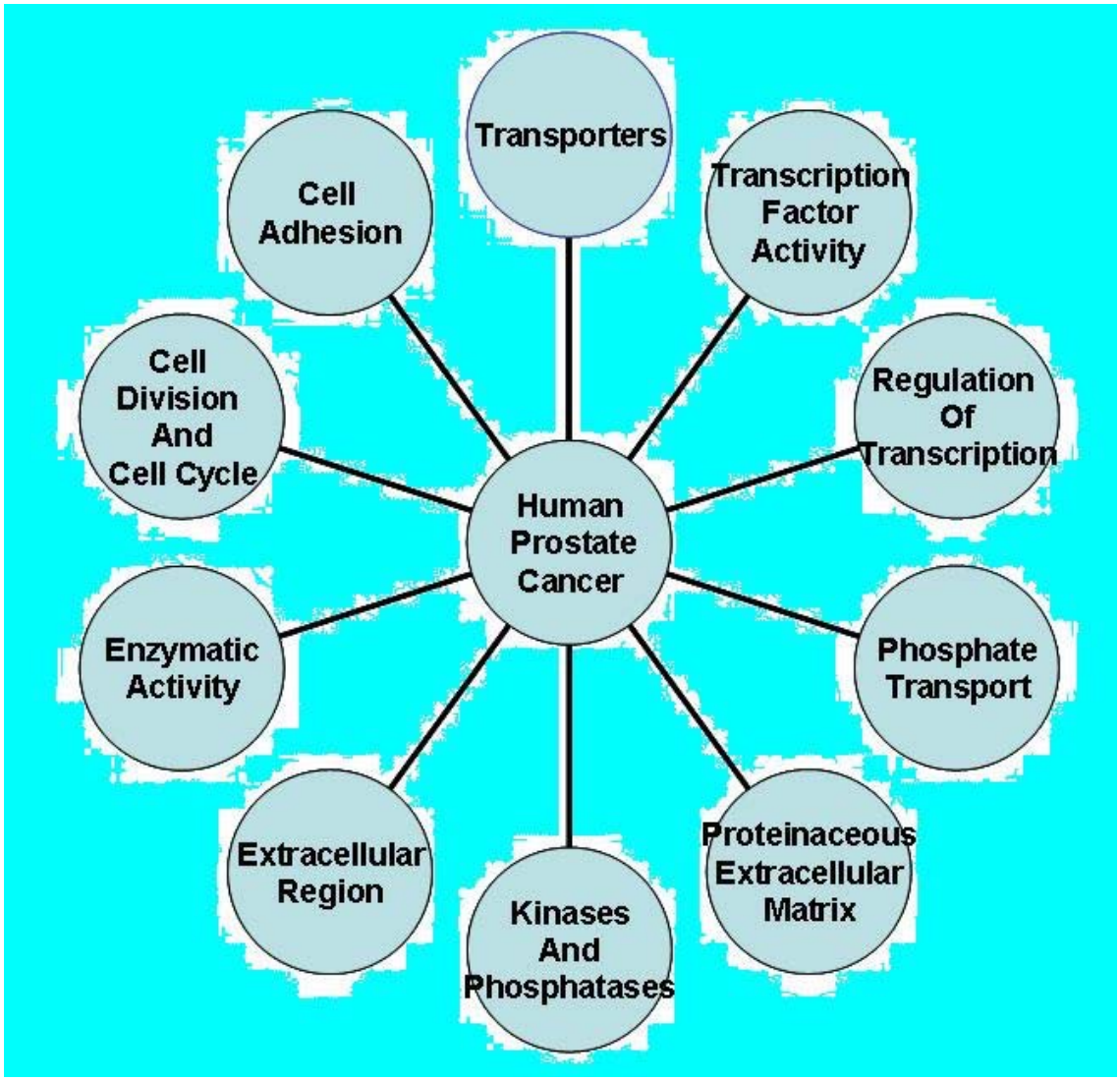

Figure 7.1. Major gene clusters modulated in human prostate cancer

Major gene clusters upregulated or downregulated at least five-fold in human prostate cancer as compared to normal prostate were identified by dChip microarray analyses and are shown here.

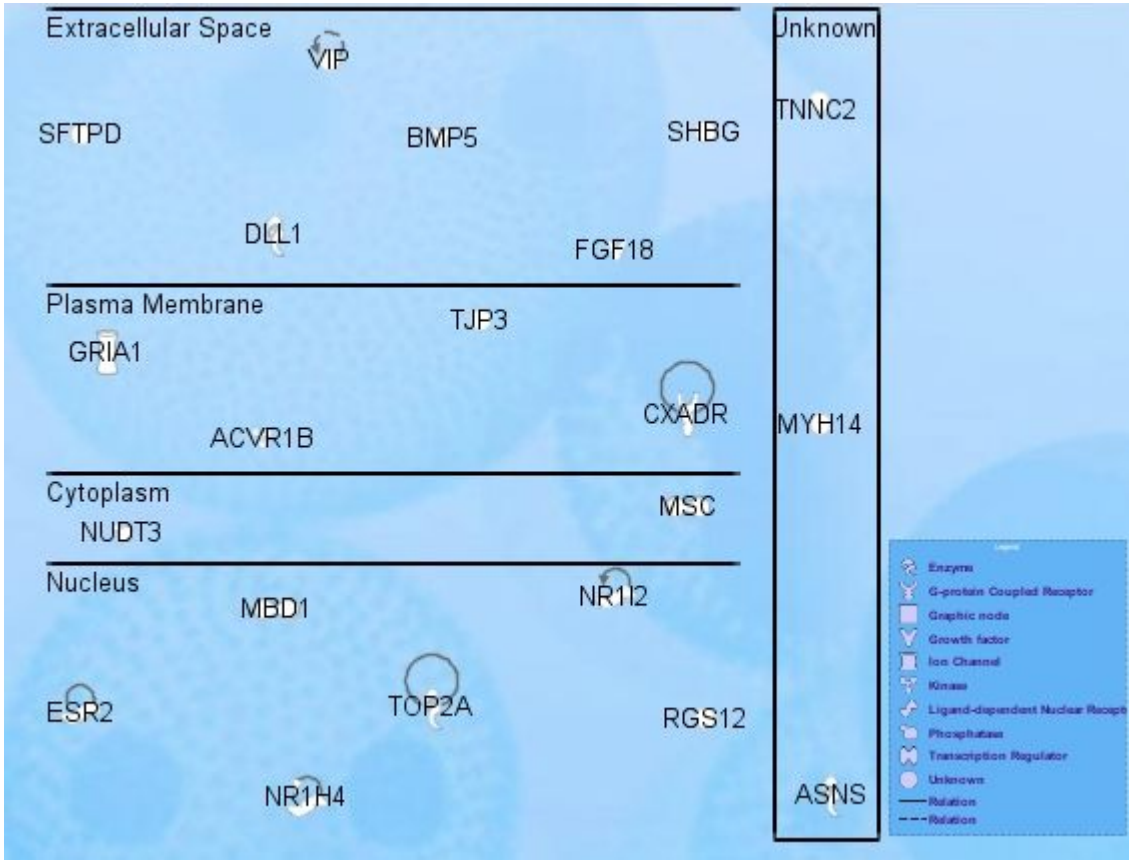
Extracellular Space
VIP
SFTPD
BMP5
SHBG
DLL1
FGF18
Plasma Membrane
TJP3
GRIA1
CXADR
ACVR1B
Cytoplasm
NUDT3
MSC
Nucleus
MBD1
NR1I2
ESR2
TOP2A
RGS12
NR1H4
Unknown
TNNC2
MYH14
ASNS
Enzyme
G-protein Coupled Receptor
Graphic node
Growth factor
Ion Channel
Kinase
Ligand-dependent Nuclear Recept
Phosphatase
Transcription Regulator
Unknown
Relation
Relation

Figure 7.2. A.

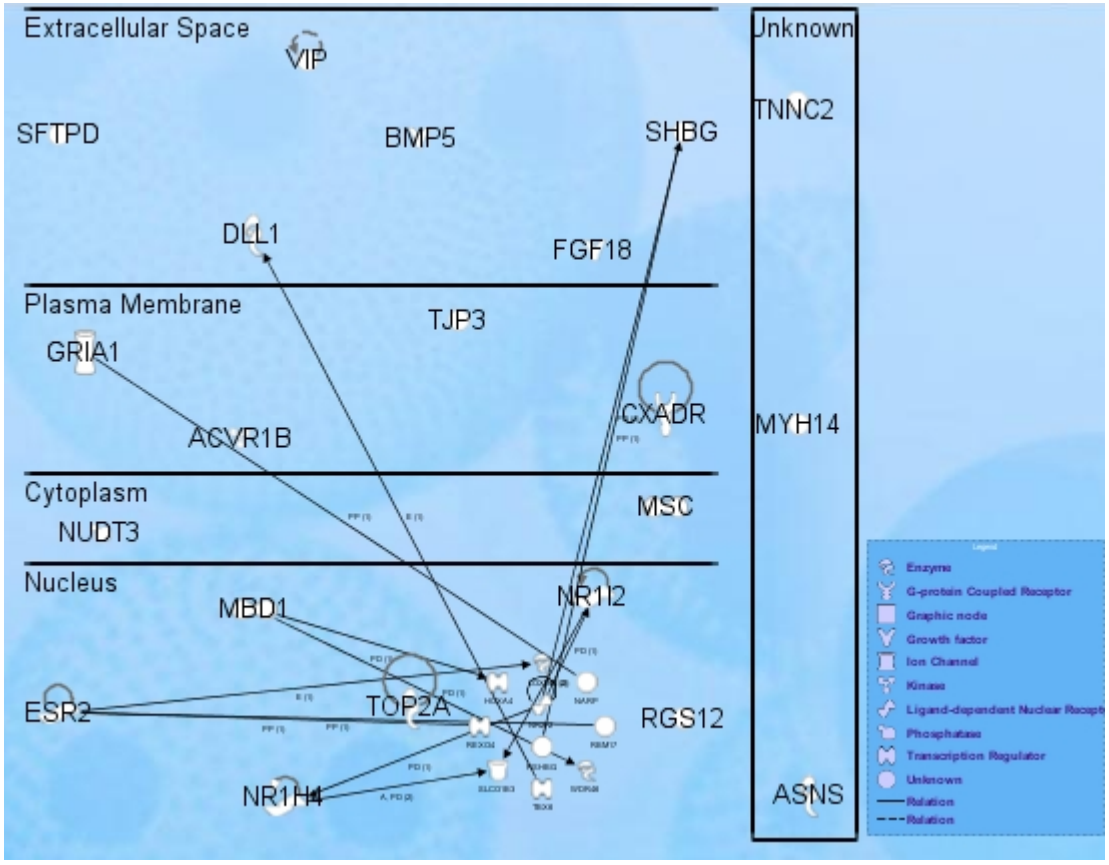

Figure 7.2. B.

Figure 7.2. Candidate biomarkers in human prostate cancer

Genes that passed the Ingenuity® biomarker filter from the genes modulated at least five-fold in the microarray analyses of human prostate cancer were toggled to their subcellular localization and are shown here**. 7.2. A.** Candidate biomarkers; **7.2. B.** Candidate biomarkers and putative crosstalk between them.

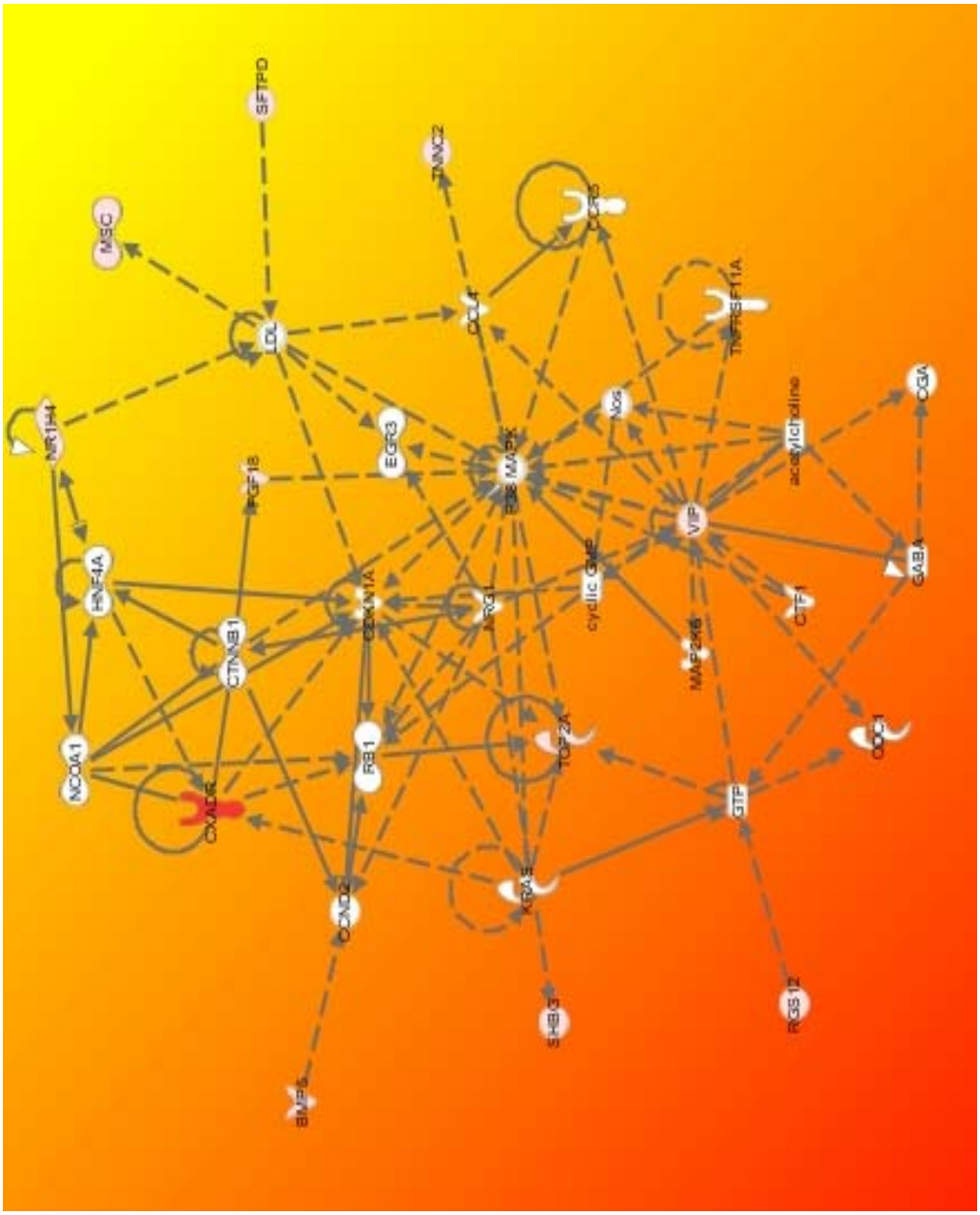
SFTPD
MSC
TNNC2
CCR5
CCL4
TNFRSF11A
LDL
NR1H4
Nos
EGR3
IGF18
ERK/MAPK
acetylcholine
OGA
VIP
HNF4A
GABA
CDKN1A
ARG1
cyclic GMP
CTF1
CTNNB1
MAP2K6
CCR1
TGF2A
NCOA1
RB1
GTP
CXADR
KRAS
CCND2
SHB3
RGS12
BMP5

Figure 7.3. A.

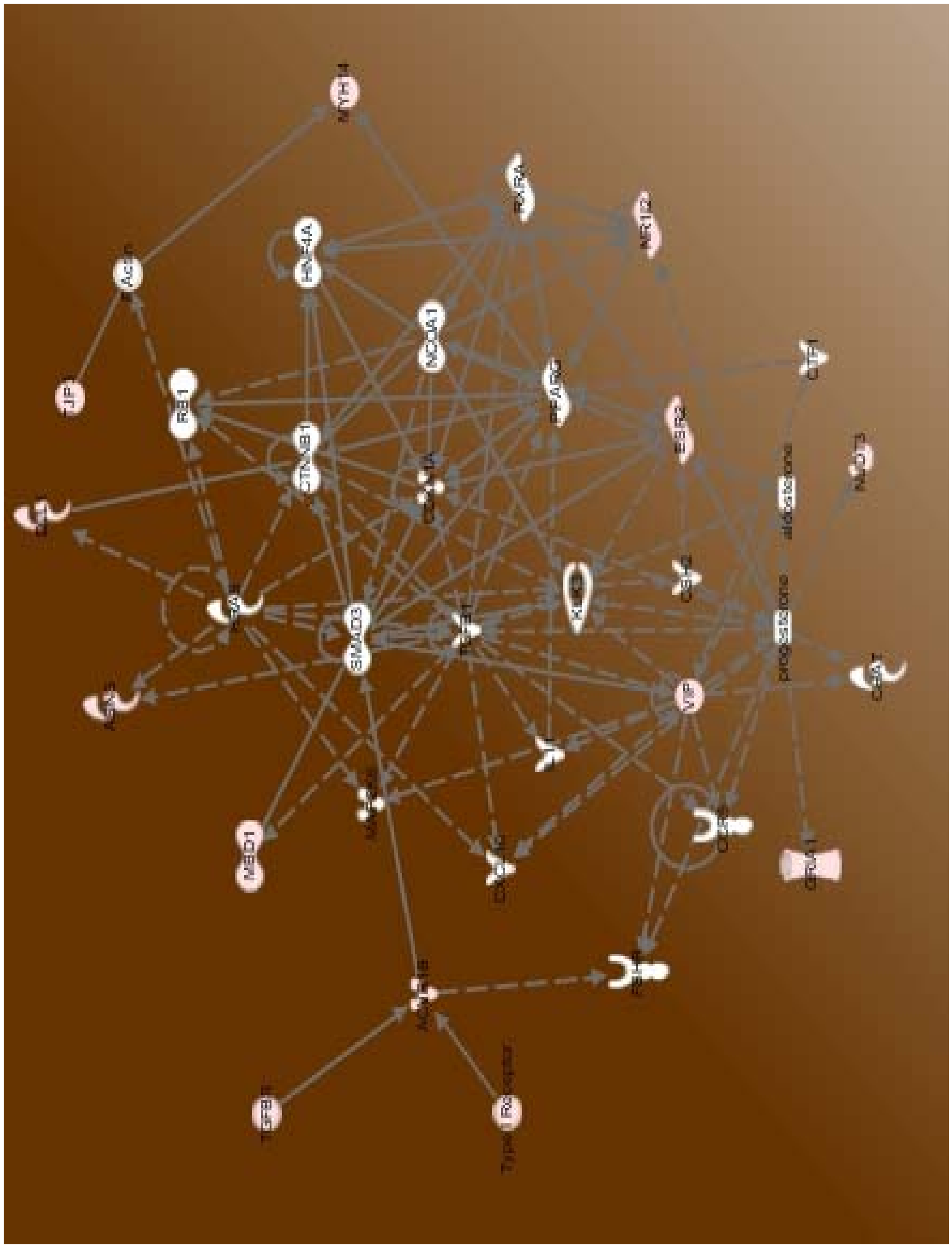
MYH14
RXRA
HNF4A
NCOA1
PPARG
RB1
CTNNB1
SMAD3
CTF1
aldosterone
progesterone
MED1

Figure 7.3. B.

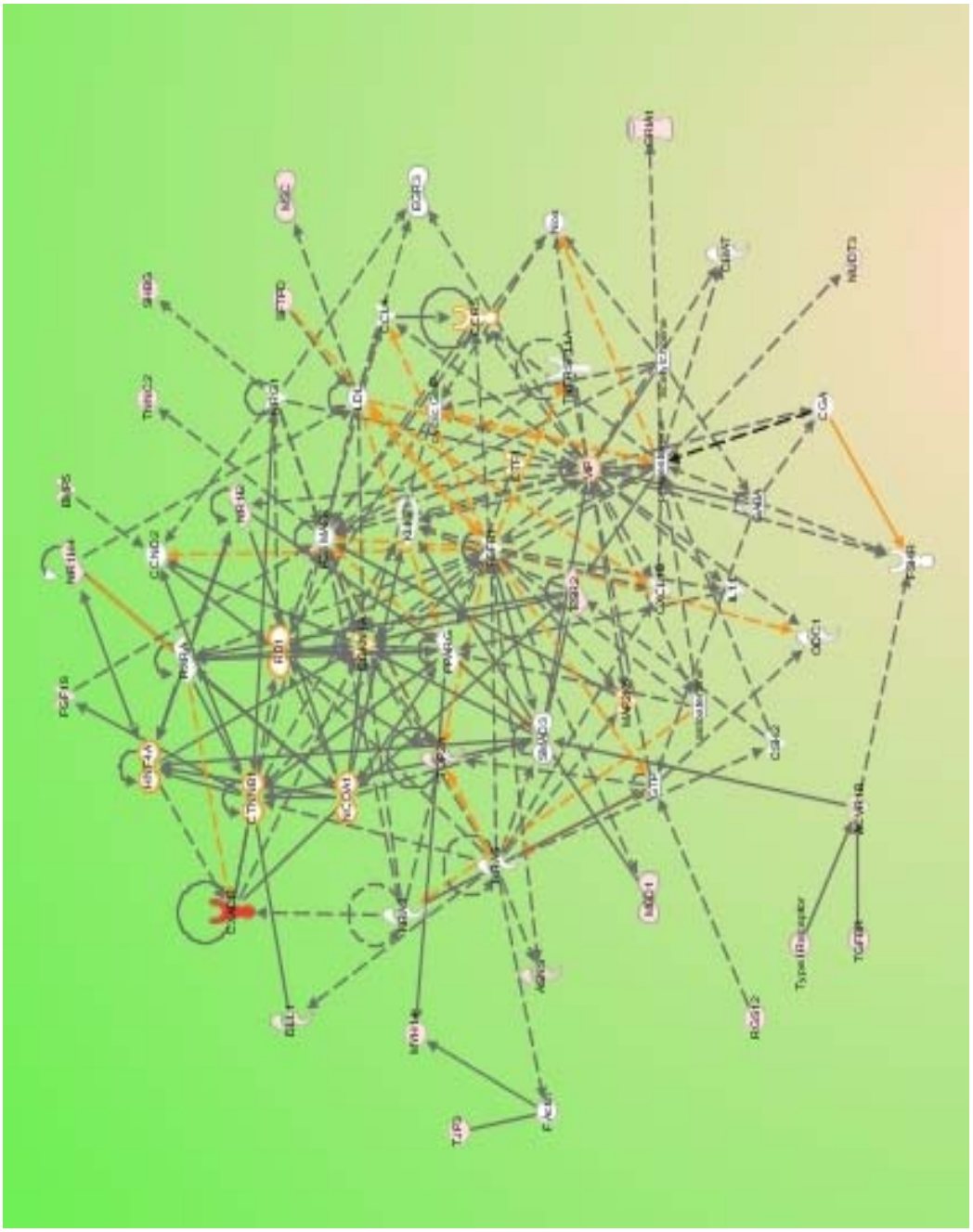

Figure 7.3. C.

Figure 7.3. Functional biological networks in human prostate cancer

Functional biological networks in human prostate cancer were identified through Ingenuity® metabolomics analyses of candidate biomarkers identified from the biomarker filter, and connections with relevant signaling molecules were deciphered as described in Materials and Methods. **7.3. A.** Cell Death, Cellular Growth and Differentiation, Cellular Development Network; **7.3. B.** Gene Expression, Cancer, Cellular Growth and Proliferation Network; **7.3. C.** Merged Network.

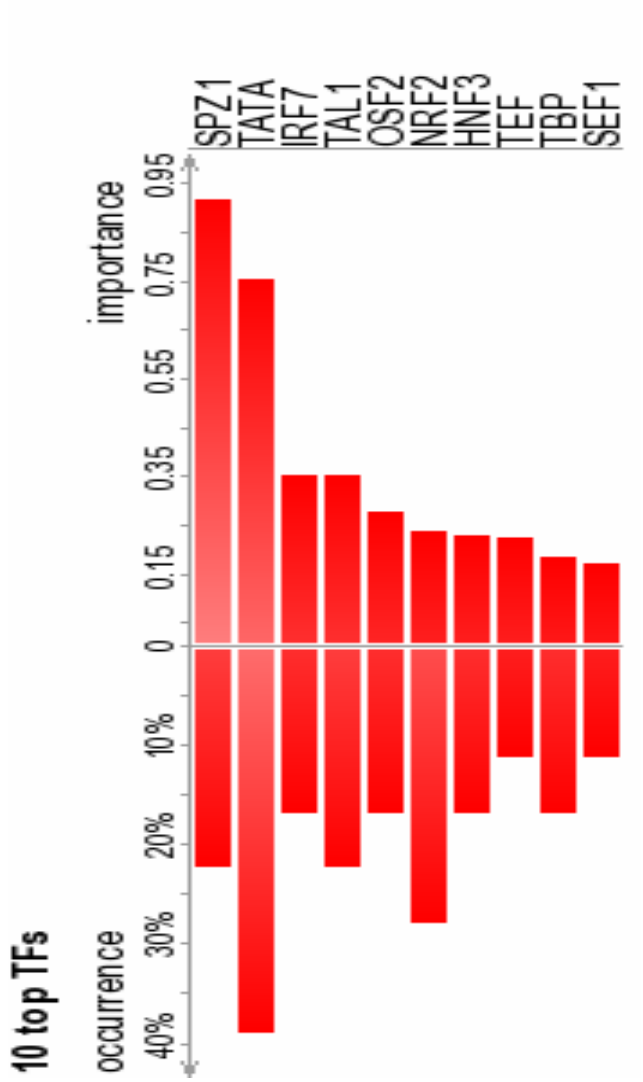

Figure 7. 4. Identification of TFBS-association signatures

TFBS-association signatures in the regulatory regions of the candidate biomarkers were identified by DiRE analyses. The top ten transcription factors based on occurrence and importance are shown here.

CHAPTER 8

Differential regulatory networks elicited in androgen-dependent, androgen- and estrogen-dependent, and androgen-independent human prostate cancer cell lines [22,23,24]

8.1. Abstract

To understand the organization of the transcriptional networks that govern the etiopathogenesis of prostate cancer, we investigated the transcriptional circuitry controlling human prostate cancer in androgen-dependent 22Rv1 and MDA PCa 2b cells, androgen- and estrogen-dependent LNCaP cells and androgen-independent DU 145 and PC-3 prostate cancer cell lines. We performed microarray analyses and used pathway prediction to identify biologically relevant regulatory networks that manifest differentially in the representative prostate cancer cell lines. We present graphical representations of global topology and local network motifs describing network structures as well as sub-network structures for these conditional parameters (hormone dependence) that might be important in carcinogenesis in the prostate gland. The large number of target hubs identified in the current study including AP-1, NF-κB, EGFR, ERK1/2, JNK, p38 MAPK, TGF beta, VEGF, PDGF, CD44, Akt, PI3K, NOTCH1,

---

[22]Work described in this chapter is under consideration for publication as **Nair, S**., Cai, L., Kong, AN.

[23]**Keywords :** Target hub, regulatory network, prostate cancer, biomarker

[24]**Abbreviations :** HRPC, Hormone Refractory Prostate Cancer; MAPK, Mitogen-activated Protein Kinase; AR, Androgen Receptor; TFBS, Transcription Factor Binding Sites.

CASP1, MMP2, and androgen receptor underscore the complexity of cellular events including autoregulation, feedback loops and cross-talk that might govern progression from early lesion to clinical diagnosis of prostate cancer, or metastatic potential of pre-existent high-grade prostate intraepithelial neoplasia (HG-PIN) and advancement to hormone refractory prostate cancer (HRPC). The identification of TFBS-association signatures for TCF/LEF, SOX9 and ELK1 in the regulatory elements of the critical biomarkers identified in this study provide additional prognostic biomarkers for development of novel chemopreventive and therapeutic strategies in prostate cancer. Taken together, the elucidation in this study of several target hubs in the latent structure of biological networks generated in hormone-dependent and hormone-independent cell lines, and the delineation of key TFBS-association signatures, would enhance our understanding of regulatory nodes that might be central to identifying key players in cellular signal transduction cascades that are important in the pathogenesis of prostate cancer.

8.2. Introduction

Prostate cancer is an ideal candidate disease for chemoprevention because it is typically diagnosed in the elderly population with a relatively slower rate of growth and progression, and therefore, even a modest delay in the development of cancer, achieved through pharmacologic or nutritional intervention, could result in substantial reduction in the incidence of clinically detectable disease [249]. The development of rational chemopreventive strategies requires knowledge of the mechanisms of prostate carcinogenesis and identification of agents that interfere with these mechanisms.

Because of the long time period for prostate carcinogenesis and the large size of the cohort required for an evaluable study, identification and characterization of early intermediate biomarkers and their validation as surrogate endpoints for cancer incidence are essential for chemopreventive agent development [250]. One in six men in the United States are at a lifetime risk of developing prostate cancer according to NCI's SEER statistics [173]. Although hormone-based therapies generally result in rapid responses, virtually all patients ultimately develop androgen-independent progressive disease, and it is among these men with hormone-refractory prostate cancer (HRPC) that the role of chemotherapy continues to be investigated with three drugs (estramustine, mitoxantrone, and docetaxel) being approved by the US Food and Drug Administration (FDA) for first-line chemotherapy [247]. The identification of new targets would greatly aid the progress in chemoprevention efforts and delay the clinical diagnosis of cancer, translating into better survival and quality of life for patients.

Advances in diagnostic imaging have resulted in the development of fully automated computer-aided detection systems for detecting prostatic lesions from 4 Tesla ex vivo magnetic resonance imagery of the prostate [260]. Biochemical attempts to detect prostate cancer have recently [261] included cytokine profiling of prostatic fluid from cancerous prostate glands and correlation of cytokines with extent of tumor and inflammation. Despite these technological and biochemical advances, therapeutic options remain limited in patients with cancer that advances during hormone manipulation and chemotherapy. Targeted therapies against receptor tyrosine kinases of the ErbB family [262] have shown some promise in the treatment of HRPC; while targeted inhibition of downstream pathways, namely mammalian target of rapamycin

(mTOR) may prove to be important in the treatment of HRPC because of the prevalence of phosphatase and tensin homolog deleted on chromosome 10 (PTEN) loss, in the light of clinical evidence that mTOR inhibition reverses the phenotype of PTEN loss [262].

Cellular proliferation, differentiation, and environmental interactions each requires the production, assembly, operation, and regulation of many thousands of components, and they do so with remarkable fidelity in the face of many environmental cues and challenges [263]. With the completion of the sequence for many organisms and the potential for near-comprehensive catalogs of genes and regulatory regions for most genes of the genome, new technologies have emerged that allow for global approaches to dissecting signaling pathways and the more precise understanding of how signaling components function within pathways [264]. Understanding how cellular and developmental events occur at a molecular level with such precision has become a major focus for modern molecular biology, and considerable effort has been devoted to determining the regulatory networks that control and mediate complex biological processes [263,264].

In the current study, we characterized and compared gene expression signatures in five human prostate cancer cell lines (22Rv1, LNCaP, MDA PCa 2b, PC-3, and DU 145) and a normal prostate epithelial cell line (PZ-HPV-7). Pathway prediction analyses enabled us to generate functional biological networks for each cancerous cell line versus the normal cell line, as well as networks for genes that were common to all cancerous cell lines. Regulatory element analyses enabled the identification of Transcription Factor Binding Sites (TFBS)-association signatures for the critical biomarkers identified in prostate cancer. Overall, the differential expression of biological networks in prostate

cancer cell lines point to a perturbation of network homeostasis that may be mediated by androgen-dependence or –independence in prostate cancer.

8.3. Materials and Methods

Cell culture : Five human prostate cancer cell lines (22Rv1, LNCaP, MDA PCa 2b, PC-3, and DU 145) and a normal prostate epithelial cell line (PZ-HPV-7) were obtained from ATCC. The 22Rv1, LNCaP and MDA PCa 2b cells were cultured in RPMI-1640 medium containing 10% Fetal Bovine Serum (FBS), whereas PC-3 and DU 145 cells were cultured in Minimum Essential Medium (MEM) containing 10% FBS. The PZ-HPV-7 cells were cultured in Keratinocyte Serum Free Medium (K-SFM, Gibco) containing 0.05mg/ml bovine pituitary extract and 5ng/ml epidermal growth factor.

RNA extraction and Assessment of RNA Integrity : RNA was harvested using the RNeasy Mini Kit (Qiagen) according to the manufacturer's instructions. RNA integrity was assessed using formaldehyde gels in 1X MOPS buffer and RNA concentration was determined by the 260/280 ratio on a DU 530 UV/Visible spectrophotometer (Beckman).

Microarray Sample Preparation and Hybridization : Affymetrix (Affymetrix, Santa Clara, CA) human genome U133 Plus 2.0 array was used to probe the global gene expression profiles in RNA from the five cancerous and one non-cancerous prostate cell lines. The cDNA synthesis and biotin-labeling of cRNA, hybridization and scanning of the arrays, were performed at CINJ Core Expression Array Facility of Robert Wood

Johnson Medical School (New Brunswick, NJ). Each chip was hybridized with cRNA derived from a single prostate cell line. Briefly, double-stranded cDNA was synthesized from 5 μg of total RNA and labeled using the ENZO BioArray RNA transcript labeling kit (Enzo Life Sciences, Inc.,Farmingdale, NY, USA) to generate biotinylated cRNA. Biotin-labeled cRNA was purified and fragmented randomly according to Affymetrix's protocol. Two hundred microliters of sample cocktail containing 15 μg of fragmented and biotin-labeled cRNA was loaded onto each chip. Chips were hybridized at 45°C for 16 h and washed with fluidics protocol EukGE-WS2v5 according to Affymetrix's recommendation. At the completion of the fluidics protocol, the chips were placed into the Affymetrix GeneChip Scanner where the intensity of the fluorescence for each feature was measured.

Affymetrix Data Analyses : The CEL files created from each sample (chip) were first imported into dChip software [197,198] for further data characterization. Briefly, a gene information file with current annotations and functional gene ontology was generated and the Affymetrix Chip Description File (CDF) was specified. The data were then normalized in dChip and the expression value for each gene was determined by calculating the average of differences in intensity (perfect match intensity minus mismatch intensity) between its probe pairs. Lists of genes that were modulated at least five-fold in each cancerous prostate cell line as compared to non-cancerous prostate cell line was generated. Thereafter, Clustering and Enrichment Analysis was performed to obtain hierarchical tree clustering diagrams that provided functional classification of Affymetrix Probe Set IDs and gene descriptions.

Pathway Prediction Analyses : Functional analyses, biomarker filtration, and metabolomics analyses were performed through the use of Ingenuity Pathways Analysis (Ingenuity® Systems, www.ingenuity.com). Starting with the list of genes that were regulated at least five-fold in the dChip analyses described earlier, we performed functional analyses by associating them with biological functions in the Ingenuity Pathways Knowledge Base. Using Ingenuity's Biomarker Filter, we identified representative biomarkers that were greatly modulated (at least five-fold) in cancerous prostate cell lines as compared to normal. The criteria used for the filter were disease state (cancer), tissue type (specific prostate cell line as applicable) and species (human). The candidate biomarkers were toggled to their subcellular localization. Further, we subjected these candidate biomarkers to Ingenuity's Metabolomics analysis and identified biologically relevant signaling networks in prostate cancer. Briefly, a data set containing gene identifiers (GenBank Accession IDs) and corresponding expression values (obtained earlier from our dChip analyses) was uploaded into in the application. Each gene identifier was mapped to its corresponding gene object in the Ingenuity Pathways Knowledge Base. An expression value cut-off of 1.0 was set to identify all genes whose expression was significantly differentially regulated. These genes, called focus genes, were overlaid onto a global molecular network developed from information contained in the Ingenuity Pathways Knowledge Base. Networks of these focus genes were then algorithmically generated based on their connectivity.

Regulatory element analyses : The co-regulated potential biomarkers were now additionally investigated for Transcription Factor Binding Site (TFBS)-association

signatures using NCBI's DiRE (Distant Regulatory Elements of co-regulated genes) at the DiRE server for the identification of distant regulatory elements of coregulated genes (http://dire.dcode.org) and the top ten transcription factors were identified. DiRE's unique feature is the detection of regulatory elements outside of proximal promoter regions, as it takes advantage of the full gene locus to conduct the search. Function-specific regulatory elements consisting of clusters of specifically-associated TFBSs were predicted, and the association of individual transcription factors with the biological function shared by the group of input genes were scored.

8.4. Results

8.4.1. Microarray analyses for cancerous and non-cancerous prostate cell lines

To investigate the global gene expression profiles in prostate cancer, we used androgen-independent DU 145 and PC-3 cells, androgen-dependent 22Rv1 and MDA PCa 2b cells, and androgen- and estrogen-dependent LNCaP cells as shown in Table 8.1. We performed Affymetrix microarray analyses using Human Genome U133 Plus 2.0 array, and analyzed the data using dChip application as discussed in Materials and Methods. We compared them with normal prostate epithelial cell line PZ-HPV-7 and generated lists of genes that were modulated at least five-fold in each of these cancerous cell lines as compared to normal PZ-HPV-7 cells. Further, to restrict the study to genes that are especially relevant in prostate cancer, we subjected these gene lists to biomarker filtration and metabolomics analyses using pathway prediction that we will discuss further. We also clustered the cell lines based on their global gene expression profiles as shown in Figure 8.1. Moreover, we generated a list of genes that are common to all the

five cancerous cell lines irrespective of their fold change values, the major members being listed in Table 8.2. We used this list for further analyses as will be discussed later.

8.4.2. Biological Networks in different prostate cancer cell lines

To investigate the nature of the biological networks, and to detect perturbations in them across different prostate cancer cell lines, we used the gene lists generated as discussed above that were specific to each cancerous cell line versus the normal cell line, and proceeded to perform pathway prediction analyses using Ingenuity Pathways Analysis (Ingenuity® Systems, www.ingenuity.com). Figure 8.2.A shows the complexity of the network in androgen-dependent 22Rv1 cells with 261 members and multiple connections that constitute the network. The major members in this network are seen in the expanded Figure 8.2.B. Similarly, Figures 8.3.A and 8.4.A show the 260 members in the androgen- and estrogen-dependent LNCaP network and the 237 members in the androgen-dependent MDA PCa 2b network respectively. For clarity of presentation, sub-network structures of the LNCaP and MDA PCa 2b networks are shown in Figures 8.3.B and 8.4.B respectively. In addition, Figure 8.5 depicts the major members of the androgen-independent DU 145 network, whereas Figure 8.6 illustrates the major members of the androgen-independent PC-3 network.

The major target hubs in 22Rv1 cells were STAT3, EGFR, TGF beta, CD44, Fos and androgen receptor AR (Figure 8.2. B,C). In LNCaP cells, the major target hubs were EGFR, Fos, AR, and TGF beta (Figure 8.3.B). The prominent target hubs in MDA PCa 2b cells were EGFR, CTNNB1 and AR (Figure 8.4.B). In DU 145 cells, the major target hubs were IL6, EGFR, CD44 and CDKN1A (Figure 8.5), whereas, in PC-3 cells,

the major target hubs were FOS, EGFR, FN1, FRAP1, CD44, CDH1 and SMARCA4. The identification of these target hubs emphasizes their importance as critical regulatory nodes that might govern events responsible for progression of prostate cancer at various stages of carcinogenesis, rendering them as potential biomarkers for chemopreventive or therapeutic intervention.

8.4.3. Metabolomics analyses

To investigate the different biological networks that operate in prostate cancer independent of hormone status, we first subjected the list of genes that were common to all cancerous cell lines, as shown in Table 8.2, to biomarker filtration and identified 57 candidate biomarkers using Ingenuity's application as discussed in Materials and Methods. Further, we subjected these 57 biomarkers to Ingenuity's metabolomics analyses and deciphered four regulatory networks from the crosstalk between these 57 candidate biomarkers based on known interactions accessed from the Ingenuity Knowledge Base. These four networks included (i) Cell Death, Cancer, Cellular Development (Figure 8.7), (ii) Cancer, Endocrine System Development and Function, Organ Development (Figure 8.8), (iii) Cancer, Cell Death, Cellular Movement (Figure 8.9), and (iv) Gene Expression, Cell Cycle, Cancer (Figure 8.10). Further, to obtain a comprehensive overview of regulation amongst all these networks, we merged them as shown in Figure 8.11. A, with expanded versions being shown in Figures 8.11.B and 8.11.C for clarity of presentation.

Perusal of the metabolomics networks (Figures 8.7 through 8.11) enabled the identification of a large number of critical signaling molecules as target hubs, including

AP-1, EGFR, p38 MAPK, TGF beta, NF-κB, Histone H3, VEGF, CD44, Akt, PI3K, AR, CCND1, SMARCA4, CASP1, KLK3, MMP2, JNK, ERK1/2, PDGF, TP53, and NOTCH1. The elucidation of feedback loops and cross-talk between these many members reiterates the complexity of developing suitable agents for therapeutic or preventive intervention strategies.

8.4.4. Regulatory element analyses

To investigate the TFBS-association signatures in the regulatory regions of the 57 candidate biomarkers we had identified earlier, we subjected them to DiRE analyses as discussed in Materials and Methods. Interestingly, we found key transcription factor signatures amongst the top ten hits that are depicted in Figure 8.12. Of note, LEF1, NERF, HEB, ELK1 and MYOD were identified in the regulatory regions of these genes that were expressed in prostate cancers.

8.5. Discussion

Prostate cancer displays considerable clinical, morphological, and biological heterogeneity [265]. To understand the organization of the transcriptional networks that govern the etiopathogenesis of prostate cancer, we investigated the transcriptional circuitry controlling human prostate cancer in androgen-dependent, androgen- and estrogen-dependent and androgen-independent prostate cancer cell lines. We present graphical representations of global topology and local network motifs describing network structures as well as sub-network structures for these conditional parameters (hormone dependence) that might be important in carcinogenesis in the prostate gland.

The targets identified in the current study on differential regulation in prostate cancer based on hormonal status are observed to form complex networks, manifesting distinct patterns characteristic of autoregulation, feedback and feed-forward loops [266], and cross-talk between themselves, thus, underscoring the complexity of cellular events that govern progression from early lesion to clinical diagnosis of prostate cancer, or metastatic potential of pre-existent high-grade PIN. Interestingly, the defining feature of transient hubs is their capacity to change interactions between conditions [267]. In this study, we observed key transient hubs such as CD44, EGFR and FOS that changed interactions based on hormonal status of the cell line. This can have important implications in progression of androgen-dependent prostate cancer to one that is hormone refractory (HRPC), and, therefore, less amenable to successful outcomes in clinical therapy.

Using a yeast developmental model, Borneman et al [266] reported excellent evidence that target hubs can serve as master regulators whose activity is sufficient for the induction of complex developmental responses, and, therefore, represent important regulatory nodes in biological networks. Our results show that a large number of critical signaling molecules revealed themselves as target hubs in the latent network structures, including AP-1, EGFR, p38 MAPK, TGF beta, NF-κB, Histone H3, VEGF, CD44, Akt, PI3K, AR, CCND1, SMARCA4, CASP1, KLK3, MMP2, JNK, ERK1/2, PDGF, TP53, and NOTCH1. The biological role(s) of activator protein 1 (AP-1), epidermal growth factor receptor (EGFR), nuclear factor kappa B (NF-κB) and mitogen-activated protein kinases (ERK1/2, JNK, p38 MAPK) have been the subject of previous studies [18,19,41,184,204,268] from our laboratory and several others [269-272] that elucidate

important roles for these proteins in prostate cancer. CD44 is known to be important for prostate branching morphogenesis and metastasis to the bone microenvironment [273] that has also been previously identified as a prognostic biomarker for biochemical recurrence [274] among prostate cancer patients with clinically localized disease. Vascular endothelial growth factor (VEGF) produced by tumor cells plays a central role in stimulating angiogenesis required for solid tumor growth with a humanized monoclonal anti-VEGF antibody (bevacizumab, i.e., Avastin) approved as a treatment for metastatic cancer [275]. Human bone marrow activates the Akt pathway in metastatic prostate cells through transactivation of the alpha-platelet-derived growth factor (PDGF) receptor [276]. In addition, p53-mediated upregulation of Notch1 expression [277] in human prostate cancer cell lines is known to contribute to cell fate determination after genotoxic stress. Thus, several master regulators of prostate cancer were successfully identified in the current study.

We have shown [184] previously that ERK and JNK signaling pathways are involved in the regulation of activator protein 1 and cell death elicited by chemopreventive isothiocyanates in human prostate cancer. We have also reported [80] the suppression of NF-κB by sulforaphane and phenethyl isothiocyanate in human prostate cancer. From our current results on the metabolomics networks (Figure 8.11. A, B, C), we see that major MAP kinases including ERK1/2, JNK and p38, as well as AP-1 and NF-κB transcription factors are major target hubs, thus validating the relevance of our results from a biological perpective. Further, we have observed [19] inhibition of EGFR signaling in human prostate cancer PC-3 cells by combination treatment with phenylethyl isothiocyanate and curcumin. Our results validated these observations with

EGFR appearing as a major target hub across all prostate cancer cell lines in this study (Figures 8.2 through 8.6) as well as the merged comprehensive network (Figure 8.11 and its substructures).

The conceptual connections associated with progression confirm that prostate cancer biology is largely driven by pathways related to androgen signaling and epithelial cell biology; however, further analysis of concepts associated with progression suggests stromal factors are highly associated with progression of prostate cancer [278]. Tomlins [279] noted that although protein biosynthesis, E26 transformation-specific (ETS) family transcriptional targets, androgen signaling and cell proliferation demarcate critical transitions in progression, it was specifically high-grade cancer (Gleason pattern 4) that showed an attenuated androgen signaling signature, similar to metastatic prostate cancer, which may reflect dedifferentiation and explain the clinical association of grade with prognosis. In agreement with this, our results (Table 8.2) show attenuated androgen receptor in both DU 145 and PC-3 androgen-independent cells that may be indicative of a heightened possibility of progression to HRPC.

Cetuximab (Erbitux), Pertuzumab (Omnitarg) and Trastuzumab (Herceptin) are anti-cancer drugs targeted to EGF family ligands, while Gefitinib (Iressa), Erlotinib (Tarceva) and Lapatinib (GW572016) are anti-cancer drugs targeted to ERBB family receptors [280]. TCF/LEF binding sites which exist within the promoter region of human EGF family members were the topmost hits in our regulatory element analyses for TFBS-association signatures (Figure 8.12) which reiterates the importance of the valid network motifs that were identified in this study. Importantly, transcription factor SOX9 which regulates androgen receptor expression in prostate cancer cells [281] was

elicited in our regulatory study (Figure 8.12). Malignant transformation with acquired androgen-independence of human prostate epithelial cells has been shown [282] to be correlated with increased expression of ELK1 and MEK1/2, thus the identification of ELK1 in Figure 8.12 is significant. Thus, important prognostic biomarkers for development of novel chemopreventive and therapeutic strategies in prostate cancer were potentially identified from our TFBS-association studies.

Rhodes and Chinnaiyan [89] noted that although microarray profiling can to some extent decipher the molecular heterogeneity of cancer, integrative analyses that evaluate cancer transcriptome data in the context of other data sources are more capable of extracting deeper biological insight from the data. Indeed, our integrative computational and analytical approaches, including TFBS-association signature analyses and transcriptional network analyses are a step in this direction with the ultimate aim of enhancing our understanding of prognostic biomarkers and key signaling pathways that are important in prostate cancer progression, thus delineating functionally relevant targets for chemopreventive or therapeutic intervention. Taken together, the elucidation in this study of several target hubs in the latent structure of biological networks generated in hormone-dependent and hormone-independent cell lines, and the delineation of key TFBS-association signatures, would enhance our understanding of regulatory nodes that might be central to identifying key players in cellular signal transduction cascades that are important in the pathogenesis of prostate cancer.

8.6. Acknowledgements

Sujit Nair is extremely thankful to Dr. Li Cai for his expertise and patient training on the bioinformatic approaches used in this study. This work was supported in part by RO1 CA 118947 to Ah-Ng Tony Kong from the National Institutes of Health (NIH).

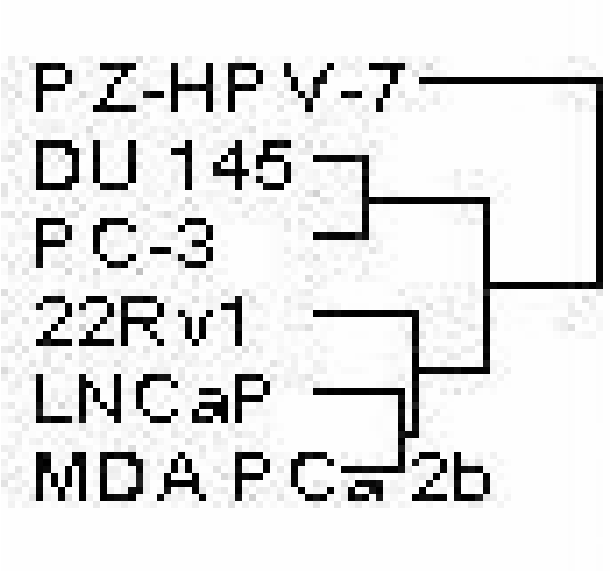

Figure 8.1. Clustering of human prostate cell lines used in the study

Human prostate cell lines used in this study were clustered on the basis of global gene expression using dChip analyses.

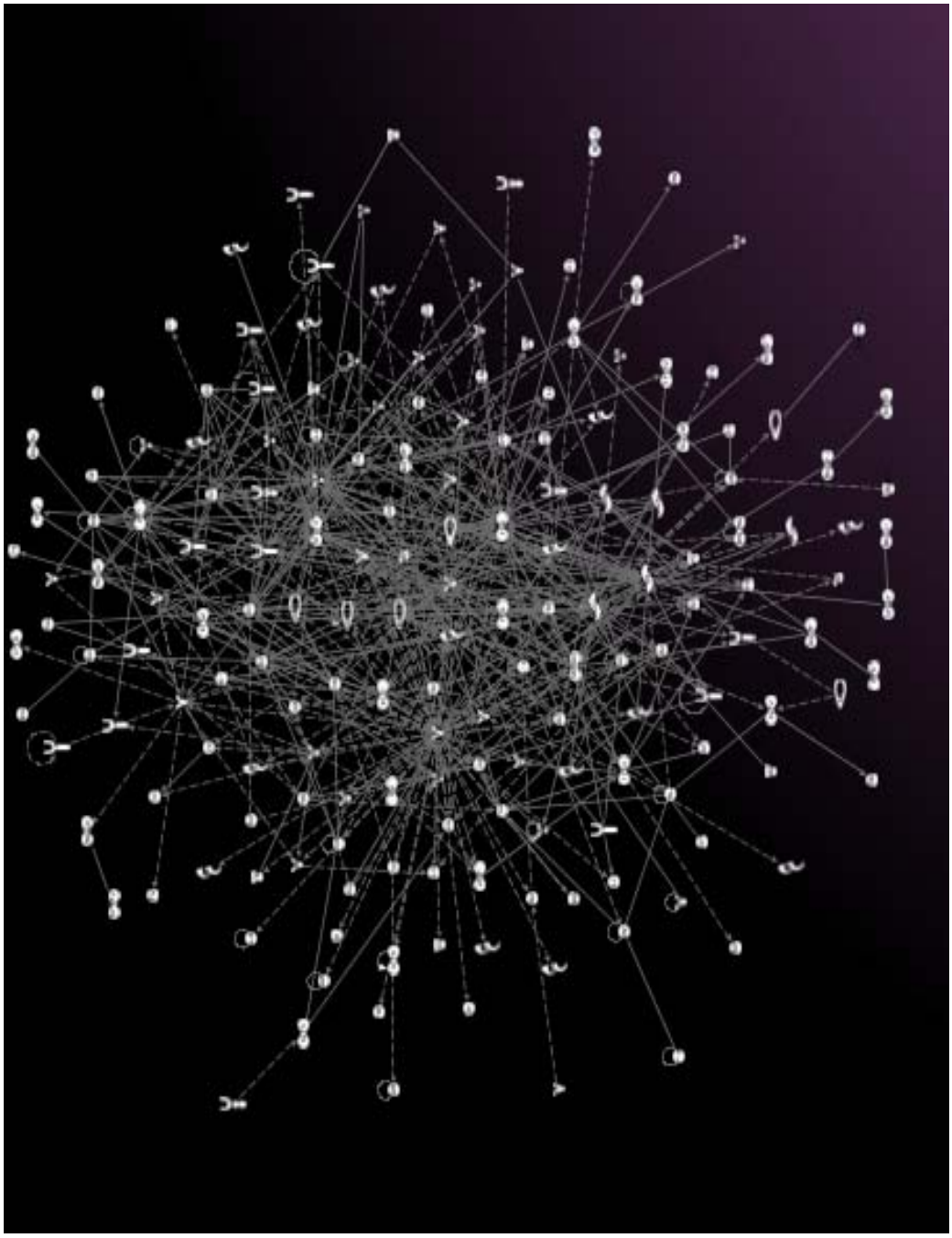

Figure 8.2. A.

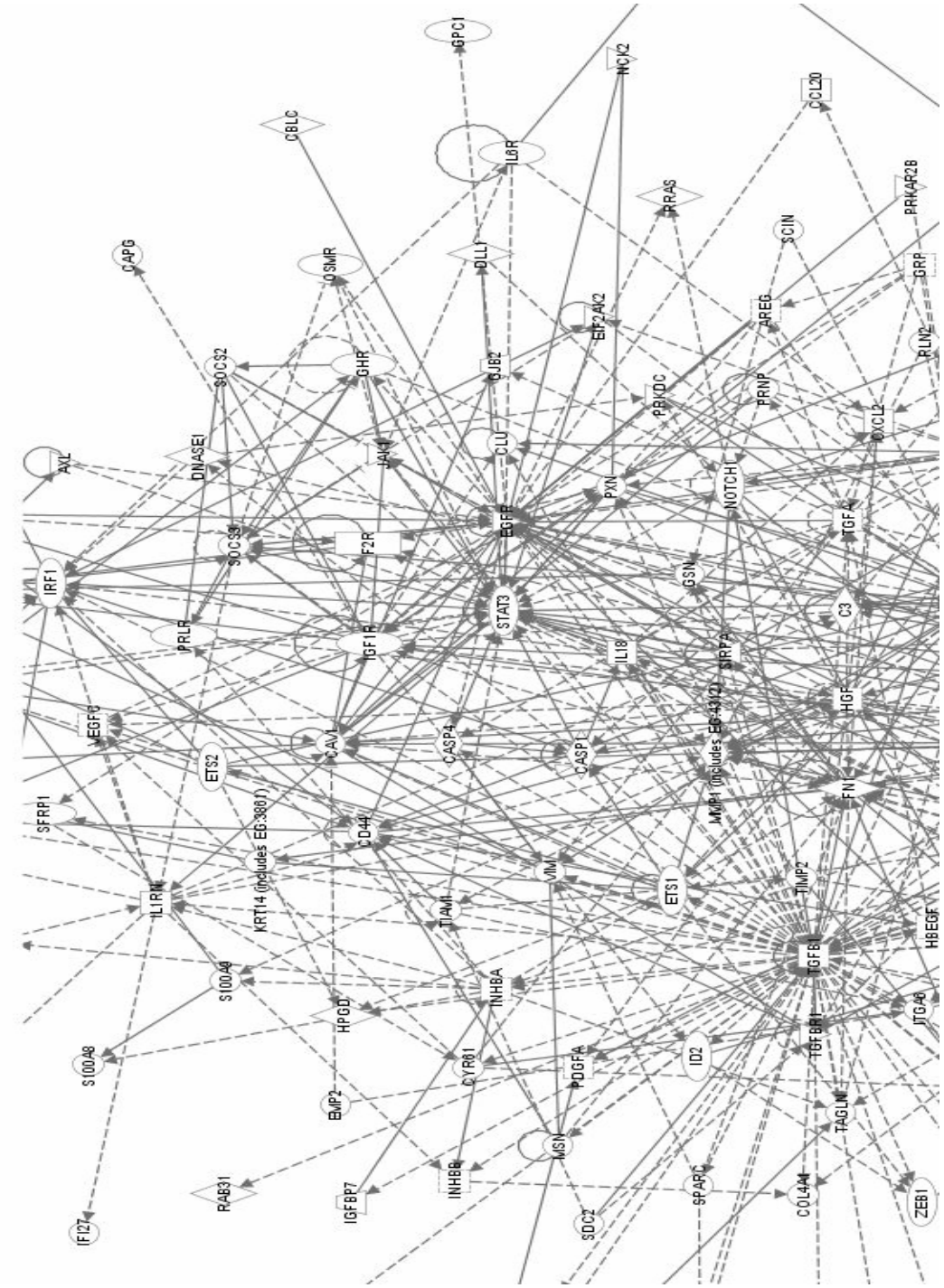
GPC1
NCK2
CBLC
IL6R
CCL20
PRKAR2B
PRRAS
SCIN
CAPG
OSMR
DLL1
AREG
EIF2AK2
GRP
RLN2
SOCS2
GHR
CJB2
PRKDC
PRNP
CXCL2
AXL
DNASE1
JAK1
CLU
PXN
NOTCH1
TGFA
SOCS3
F2R
EGFR
GSN
IRF1
STAT3
C3
PRLR
IGF1R
IL18
SERPINA1
HGF
EGFR
CAV1
CASP4
CASP1
ETS2
MMP1 (includes EG:4312)
FN1
SFRP1
CD44
KRT14 (includes EG:3861)
VIM
ETS1
TIMP2
IL1RN
TIAM1
TGFB1
HBEGF
S100A9
TNHBA
ITGA6
HPGD
TGFBR1
S100A8
CYR61
ID2
PDGFA
BMP2
TAGLN
MSN
RAB31
IGFBP7
INHBB
SPARC
COL4A4
ZEB1
IFI27
SDC2

Figure 8.2. B.

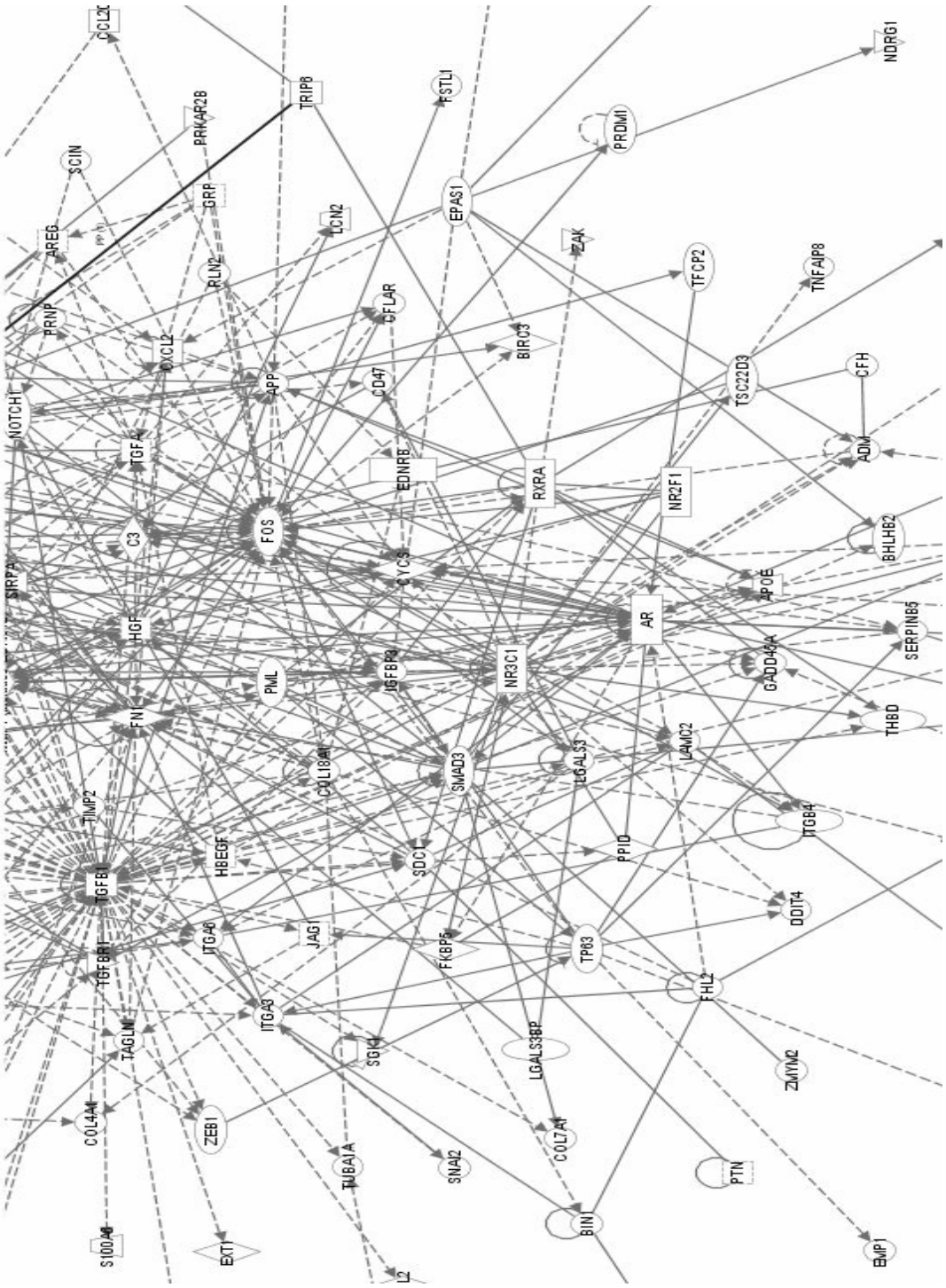
CCL20
TRIP8
PRKAR2B
FSTL1
NDRG1
SCIN
PRDM1
AREG
GRP
EPAS1
LCN2
ZAK
RLN2
TFCP2
TNFAIP8
PRNP
CFLAR
CXCL2
BIRC3
APP
CD47
TSC22D3
CFH
NOTCH1
TGFA
EDNRB
RXRA
NR2F1
ADM
C3
FOS
CYCS
BHLH62
SIRPA
APOE
IHGF
AR
SERPINB5
PML
IGFBP3
NR3C1
GADD45A
FN1
THBD
COL18A1
SMAD3
LGALS3
LAMC2
TIMP2
TGFB1
HBEGF
SDC1
PPID
TGFBR1
ITGA6
JAG1
FKBP5
TP63
DDIT4
FHL2
ITGA3
TAGLN
SGK1
LGALS3BP
ZMYM2
COL4A1
ZEB1
TUBA1A
SNAI2
COL7A1
PTN
S100A6
EXT1
L2
BIN1
BMP1

Figure 8.2. C.

Figure 8.2. Biological network in androgen-dependent human prostate cancer 22Rv1 cells

8.2.A. 261 network motifs comprising the biological network for genes that are modulated at least five-fold in 22Rv1 cells as compared to normal prostate epithelial PZ-HPV-7 cells ; **8.2.B**. Sub-network structure in 22Rv1 network, upper panel ; **8.2.C.** Sub-network structure in 22Rv1 network, lower panel.

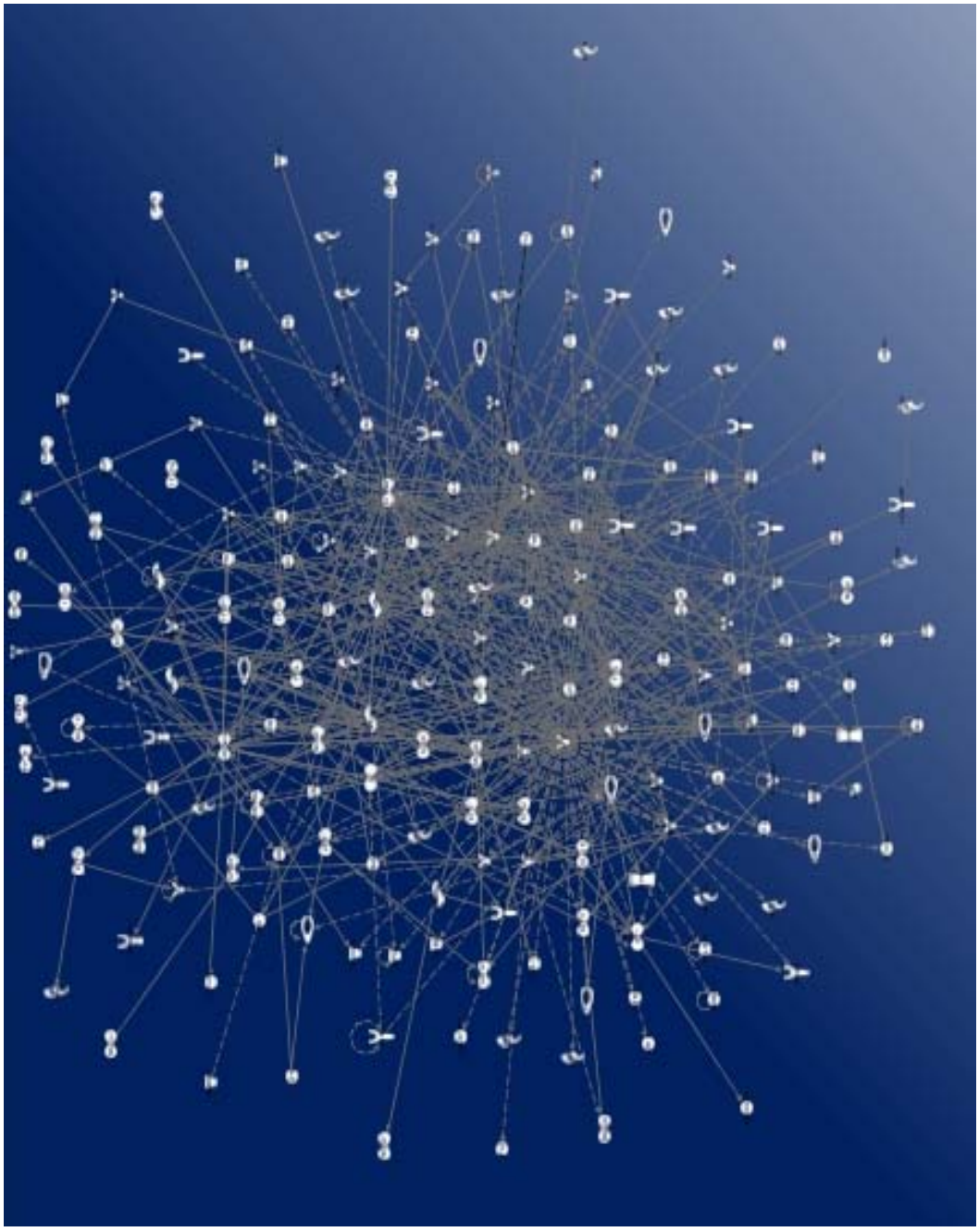

Figure 8.3. A.

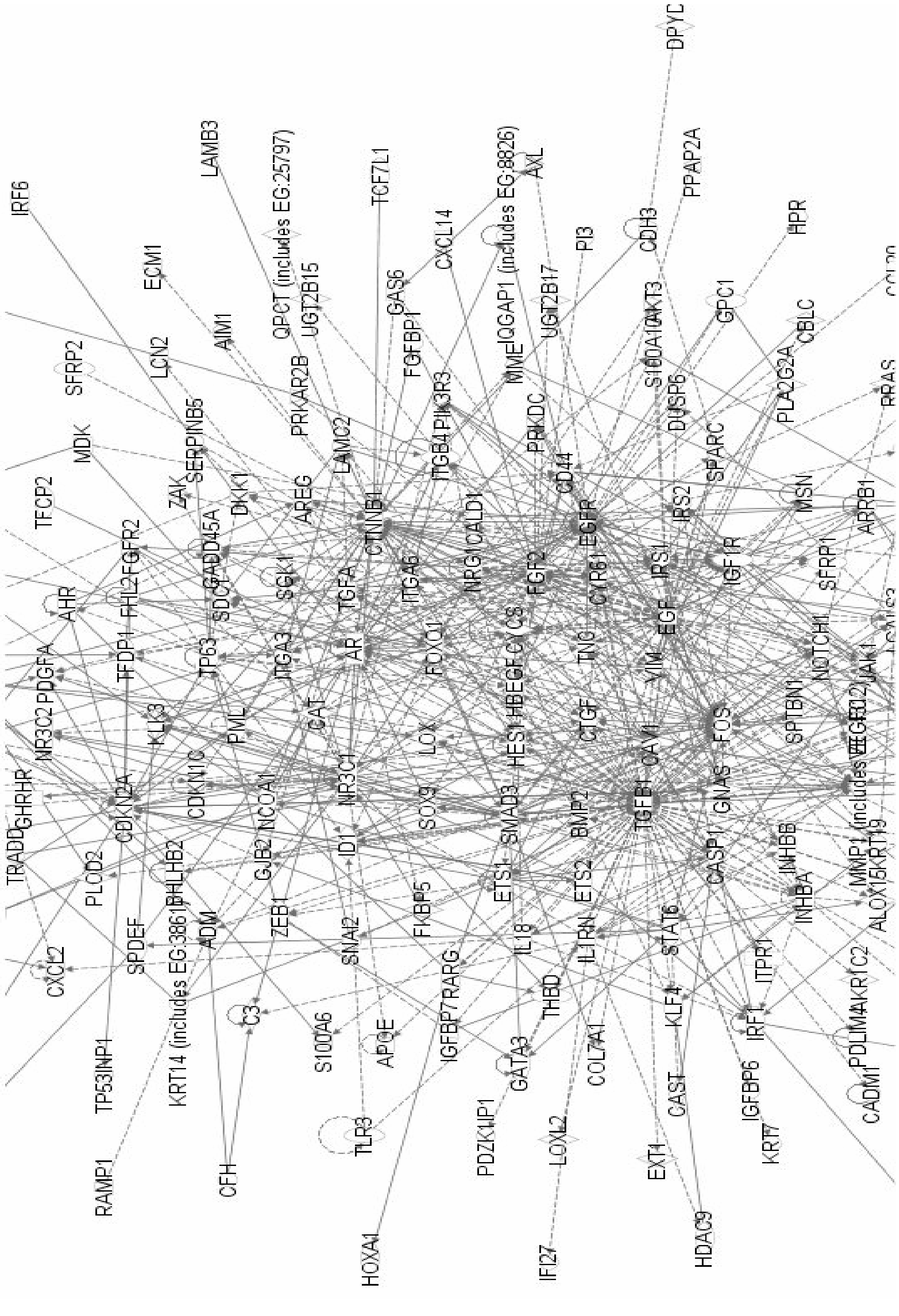
IRF6
LAMB3
TCF7L1
AXL
DPYC
PPAP2A
CDH3
PI3
CXCL14
GAS6
ECM1
AIM1
SFRP2
LCN2
MDK
TFCP2
ZAK
SERPINB5
PRIKAR2B
LAMC2
FGFBP1
MME
PRKDC
S100A10
DUSP6
GPC1
HPR
CBLC
PLA2G2A
SPARC
MSN
ARRB1
IRS2
IRS1
IGF1R
SFRP1
EGFR
CD44
EGF
FGF2
CYR61
NOTCH1
JAK1
VIM
FOS
SPTBN1
TGFB1
GNAS
CTNNB1
ITGA6
NRG1
TGFA
AR
SGK1
AREG
DKK1
AHR
FGFR2
TP63
ITGA3
FOXO1
TNC
CTGF
HES1
LOX
CAT
PML
KLK3
PDGFA
NR3C2
TFDP1
GHRHR
TRADD
CDKN2A
CDKN1C
NCOA1
NR3C1
SOX9
SMAD3
BMP2
CASP1
INHBB
INHBA
MMP1
ALOX15
KRT19
PLOD2
BHLHB2
GJB2
ID1
ETS1
ETS2
IL18
IL1RN
STAT6
ITPR1
AKR1C2
PDLIM4
CADM1
IRF1
IGFBP6
KRT7
KLF4
CAST
COL7A1
EXT1
HDAC9
THBD
GATA3
LOXL2
IFI27
PDZK1IP1
IGFBP7
RARG
FKBP5
SNAI2
ZEB1
ADM
SPDEF
CXCL2
TP53INP1
RAMP1
KRT14
C3
CFH
S100A6
APOE
TLR3
HOXA1

Figure 8.3. B.

Figure 8.3. Biological network in androgen- and estrogen-dependent human prostate cancer LNCaP cells

8.3.A. 260 network motifs comprising the biological network for genes that are modulated at least five-fold in LNCaP cells as compared to normal prostate epithelial PZ-HPV-7 cells ; **8.3.B**. Sub-network structure in LNCaP network.

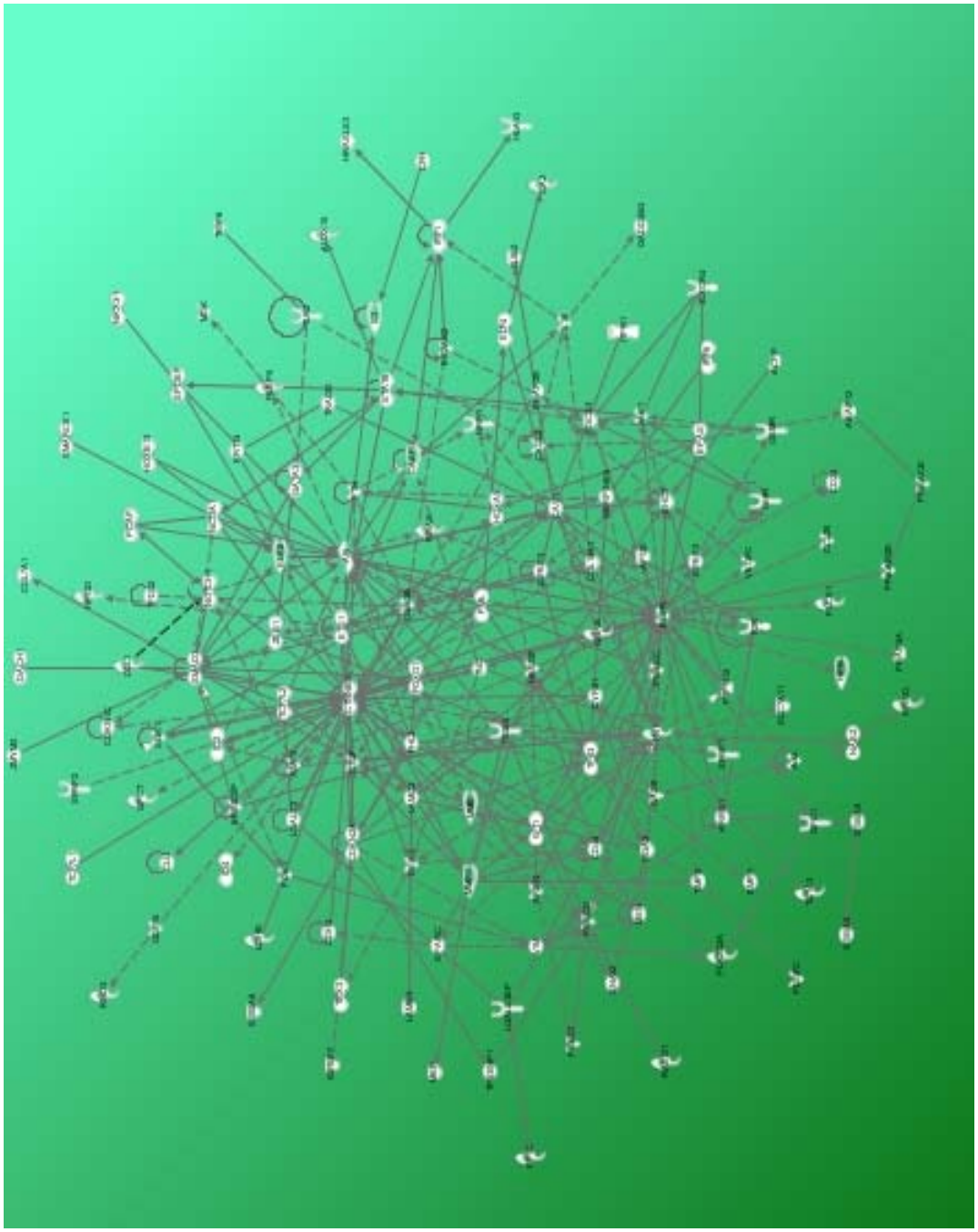

Figure 8.4. A.

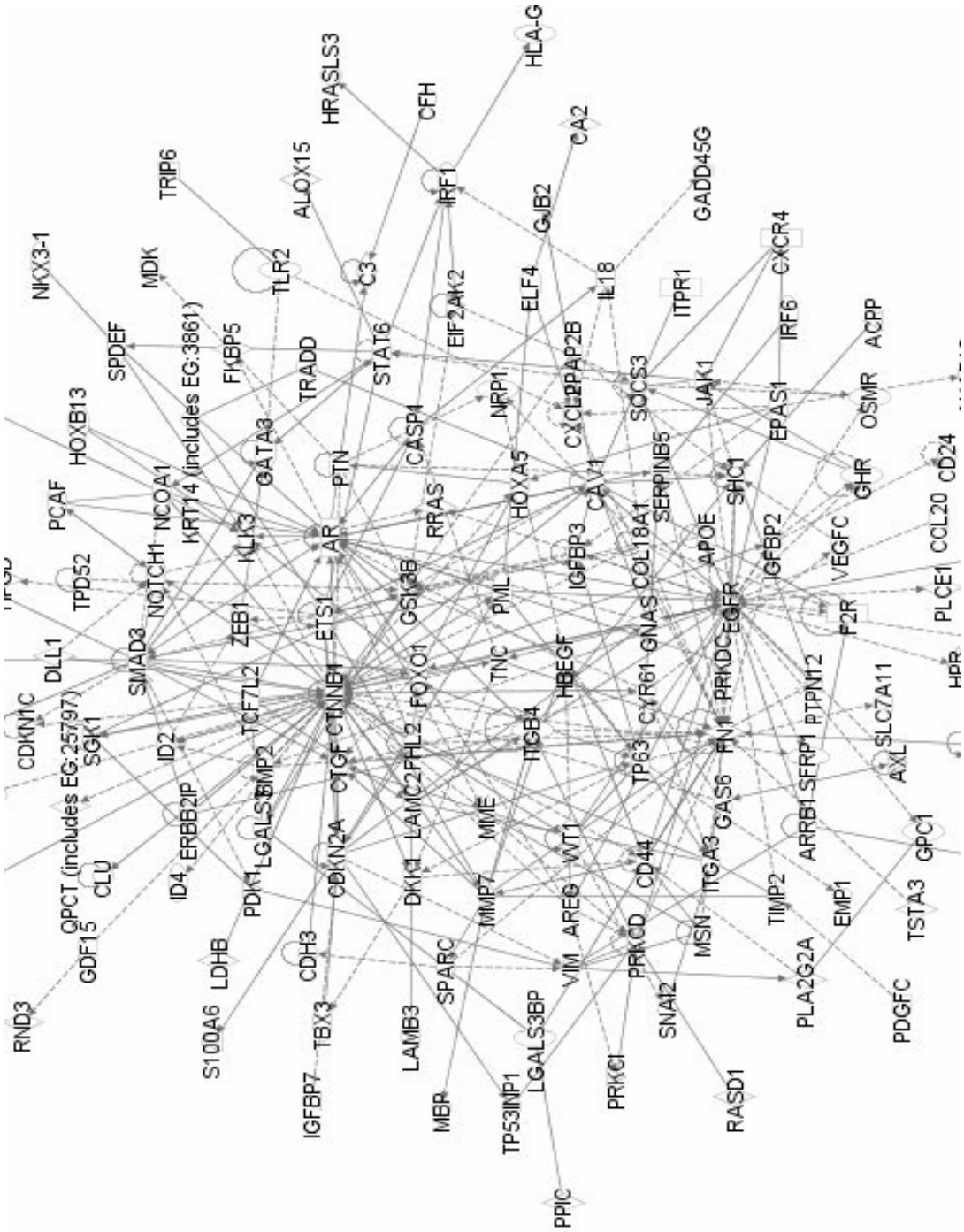
HLA-G
HRASLS3
CFH
CA2
ALOX15
IRF1
GJB2
GADD45G
TRIP6
NKX3-1
MDK
TLR2
C3
IL18
ITPR1
CXCR4
SPDEF
FKBP5
TRADD
STAT6
EIF2AK2
ELF4
IRF6
ACPP
HOXB13
GATA3
PTN
CASP4
NRP1
JAK1
OSMR
PCAF
NCOA1
KRT14 (includes EG:3861)
RRAS
HOXA5
CAV1
SERPINB5
SHC1
EPAS1
GHR
CD24
TPD52
NOTCH1
KLK3
AR
IGFBP3
COL18A1
APOE
IGFBP2
VEGFC
CCL20
DLL1
SMAD3
ZEB1
ETS1
GSK3B
PML
GNAS
EGFR
P2R
PLCE1
CDKN1C
SGK1
ID2
TCF7L2
CTNNB1
FOXO1
TNC
HBEGF
CXCR6
PRKDC
PTPN12
HPR
QPCT (includes EG:25797)
CLU
ERBB2IP
BMP2
CTGF
ITGB4
TP63
FN1
SLC7A11
AXL
GDF15
ID4
LGALS1
CDKN2A
LAMC2
FHL2
MME
GAS6
SFRP1
RND3
PDK1
DKK1
VIT1
CD44
ITGA3
ARRB1
GPC1
S100A6
LDHB
CDH3
MMP7
AREG
TIMP2
EMP1
TBX3
SPARC
VIM
MSN
TSTA3
IGFBP7
LAMB3
PRKCD
PLA2G2A
PDGFC
MBP
SNAI2
TP53INP1
LGALS3BP
PRKCI
RASD1
PPIC

Figure 8.4. B.

Figure 8.4. Biological network in androgen-dependent human prostate cancer MDA PCa 2b cells

8.4.A. 237 network motifs comprising the biological network for genes that are modulated at least five-fold in MDA PCa 2b cells as compared to normal prostate epithelial PZ-HPV-7 cells ; **8.4.B**. Sub-network structure in MDA PCa 2b network.

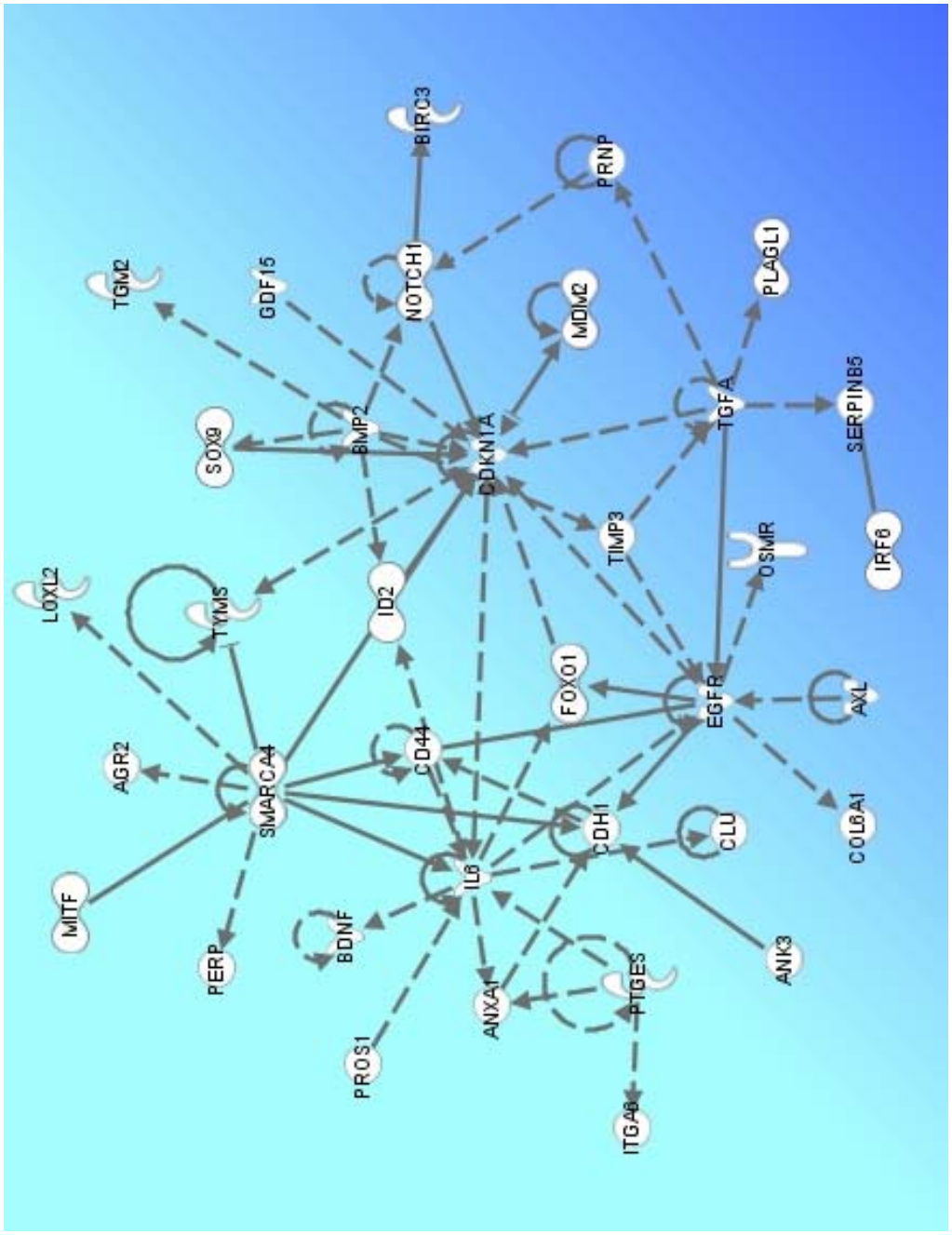

Figure 8.5. Biological network in androgen-independent human prostate cancer DU 145 cells

Major motifs comprising the DU 145 network for genes that are modulated at least five-fold in DU 145 cells as compared to normal prostate epithelial PZ-HPV-7 cells are shown.

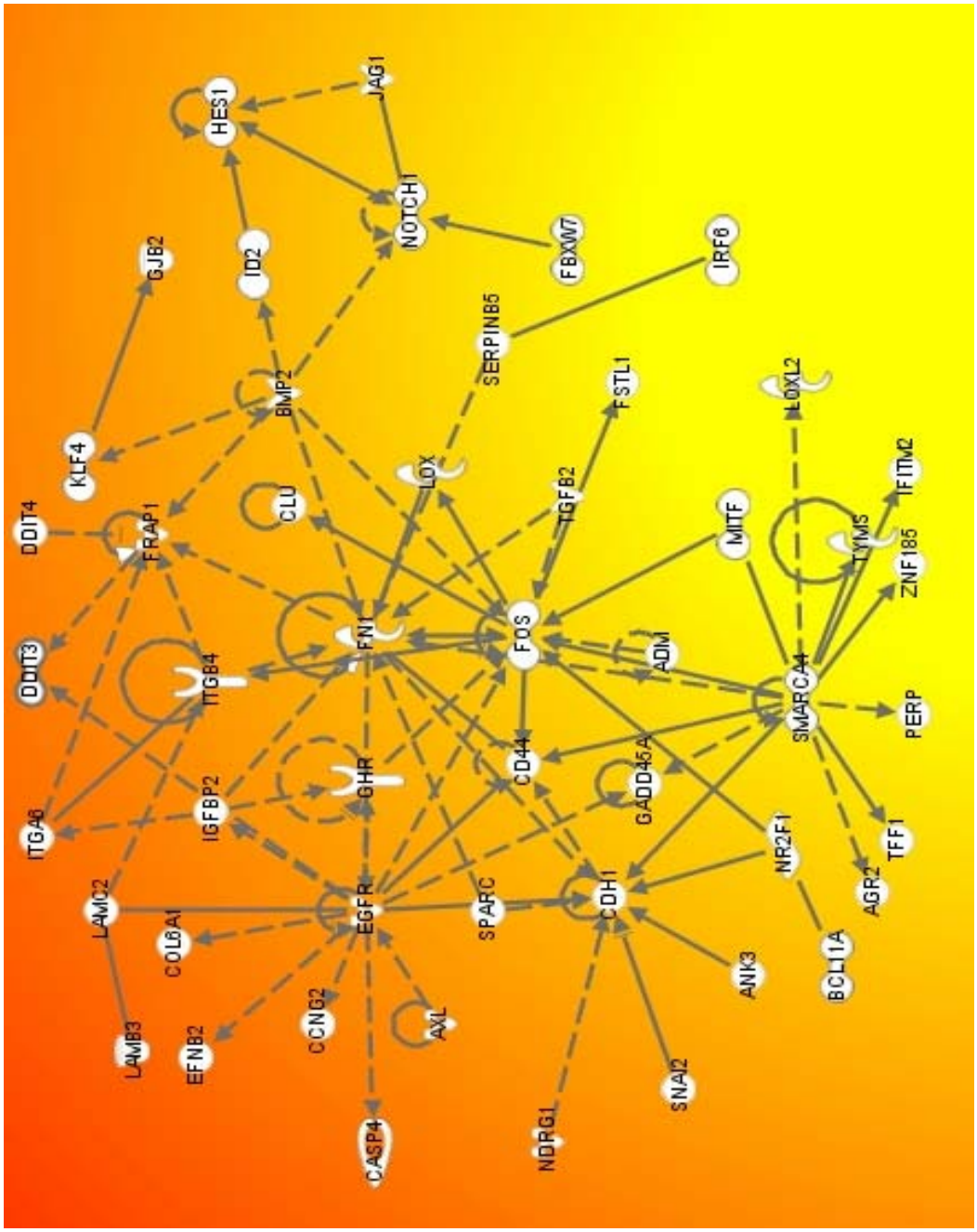

Figure 8.6. Biological network in androgen-independent human prostate cancer PC-3 cells

Major motifs comprising the PC-3 network for genes that are modulated at least five-fold in PC-3 cells as compared to normal prostate epithelial PZ-HPV-7 cells are shown.

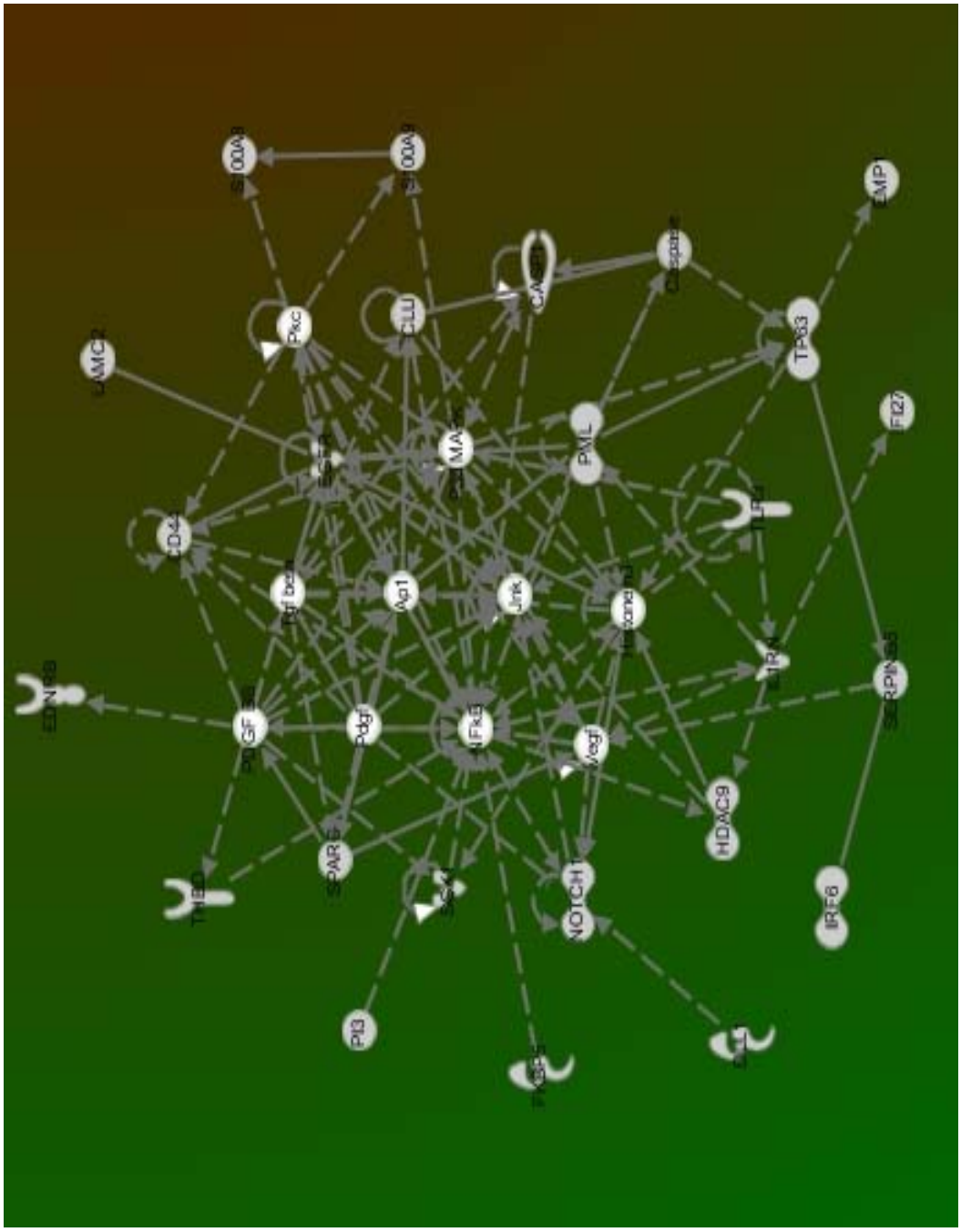

Figure 8.7. Cell Death, Cancer, Cellular Development Network

Network motifs for the Cell Death, Cancer, Cellular Development Network elicited by metabolomics analyses of genes modulated in all prostate cancer cell lines used in this study.

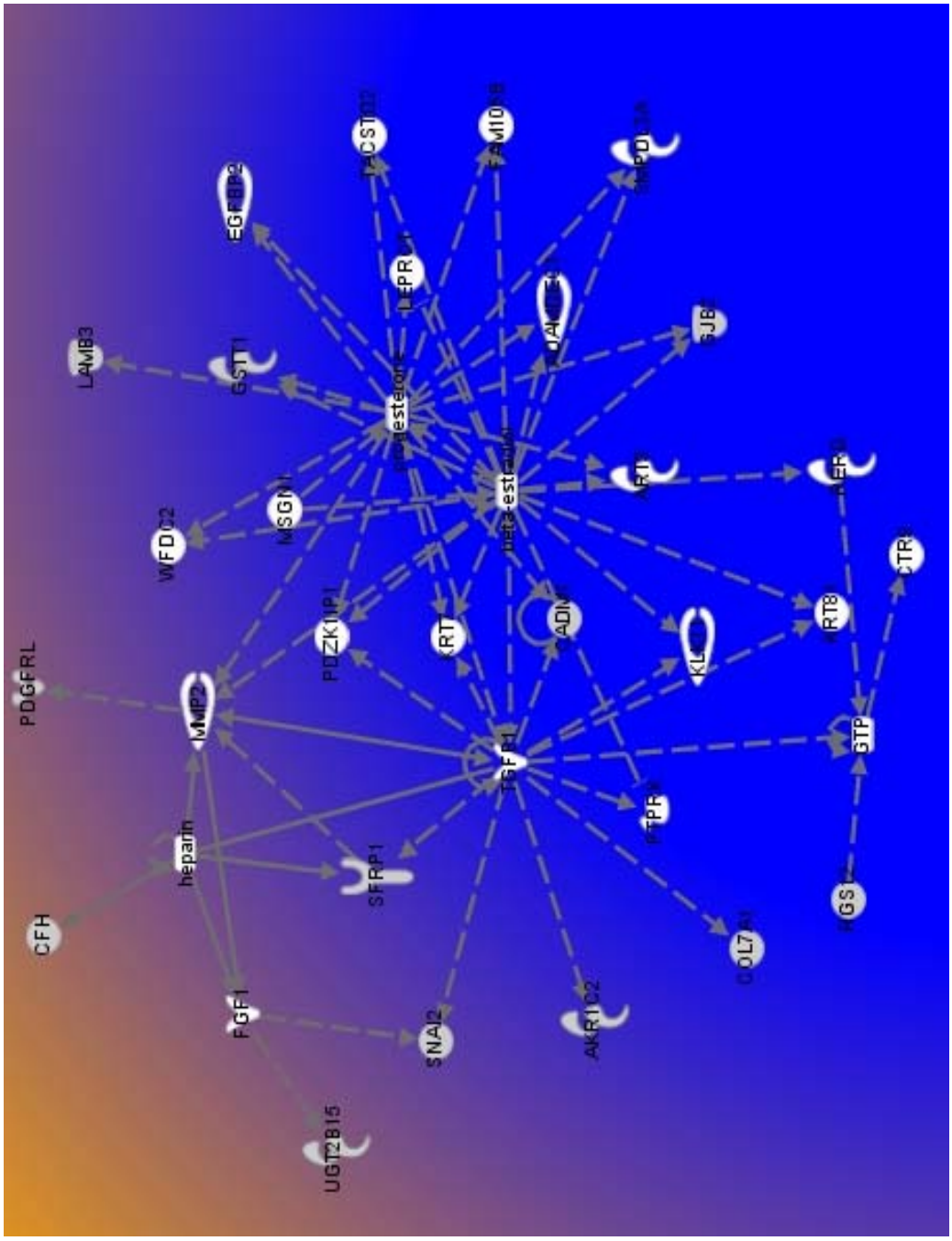

Figure 8.8. Cancer, Endocrine System Development and Function, Organ Development Network

Network motifs for the Cancer, Endocrine System Development and Function, Organ Development Network elicited by metabolomics analyses of genes modulated in all prostate cancer cell lines used in this study.

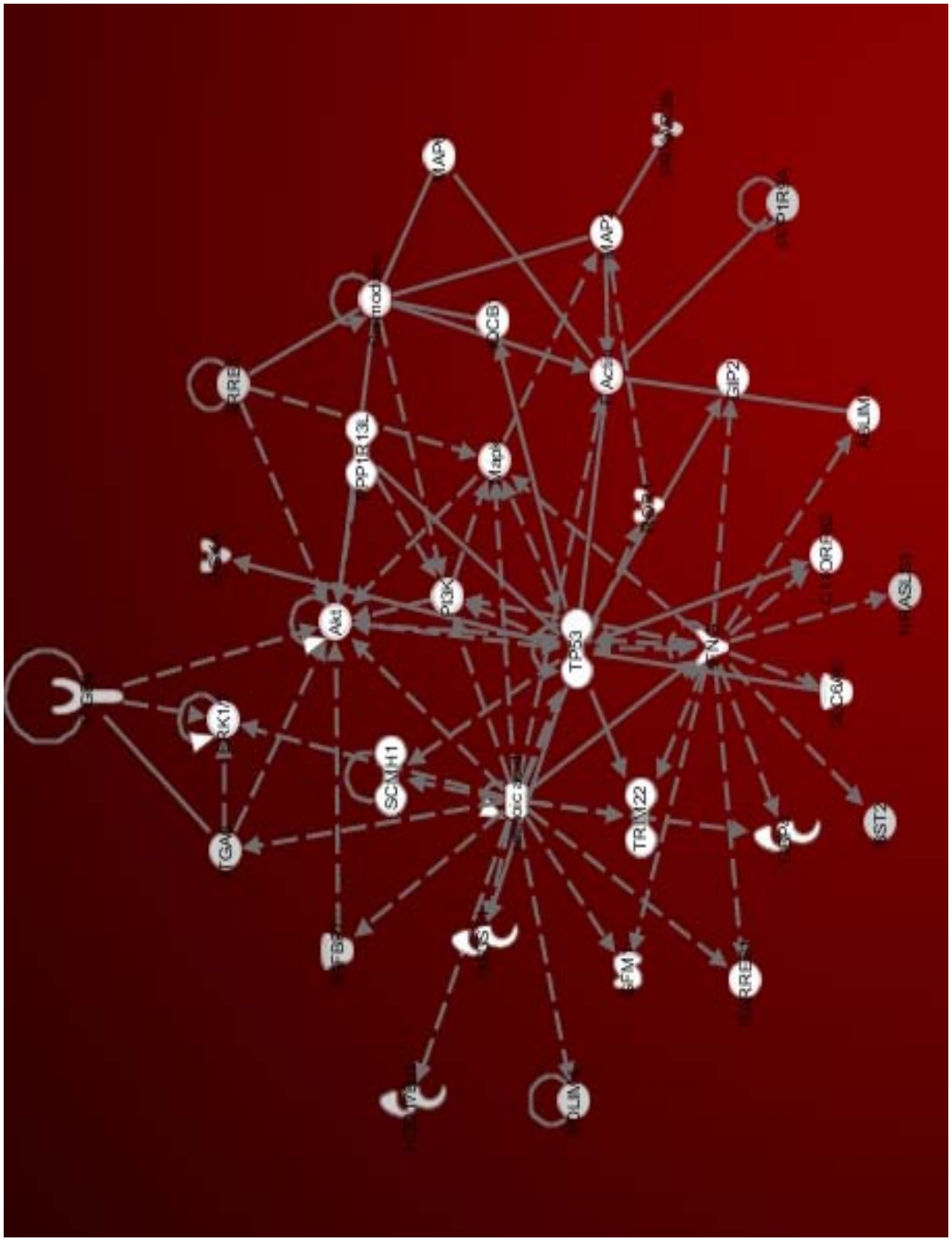

Figure 8.9. Cancer, Cell Death, Cellular Movement Network

Network motifs for the Cancer, Cell Death, Cellular Movement Network elicited by metabolomics analyses of genes modulated in all prostate cancer cell lines used in this study.

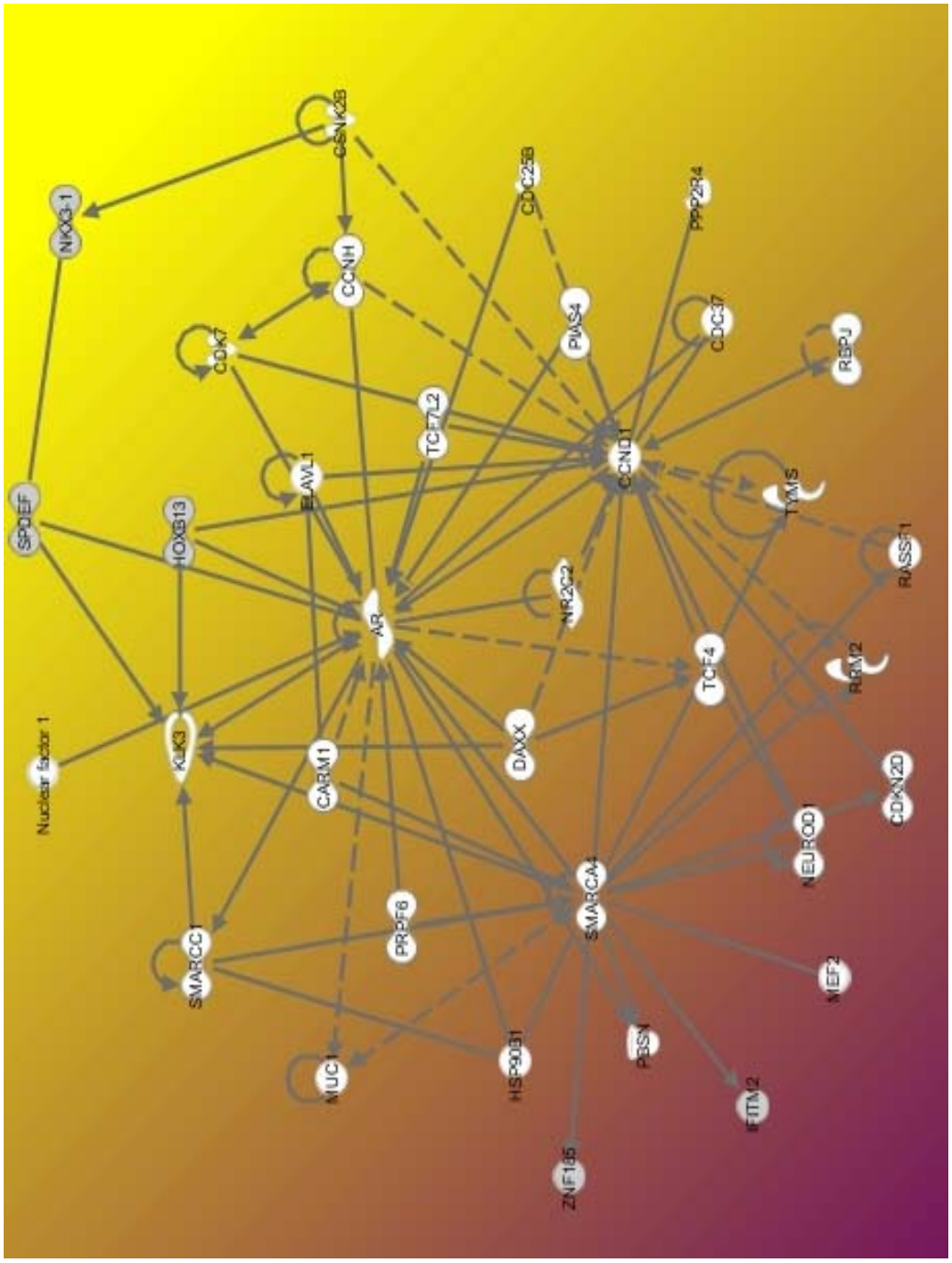

Figure 8.10. Gene Expression, Cell Cycle, Cancer Network

Network motifs for the Gene Expression, Cell Cycle, Cancer Network elicited by metabolomics analyses of genes modulated in all prostate cancer cell lines used in this study.

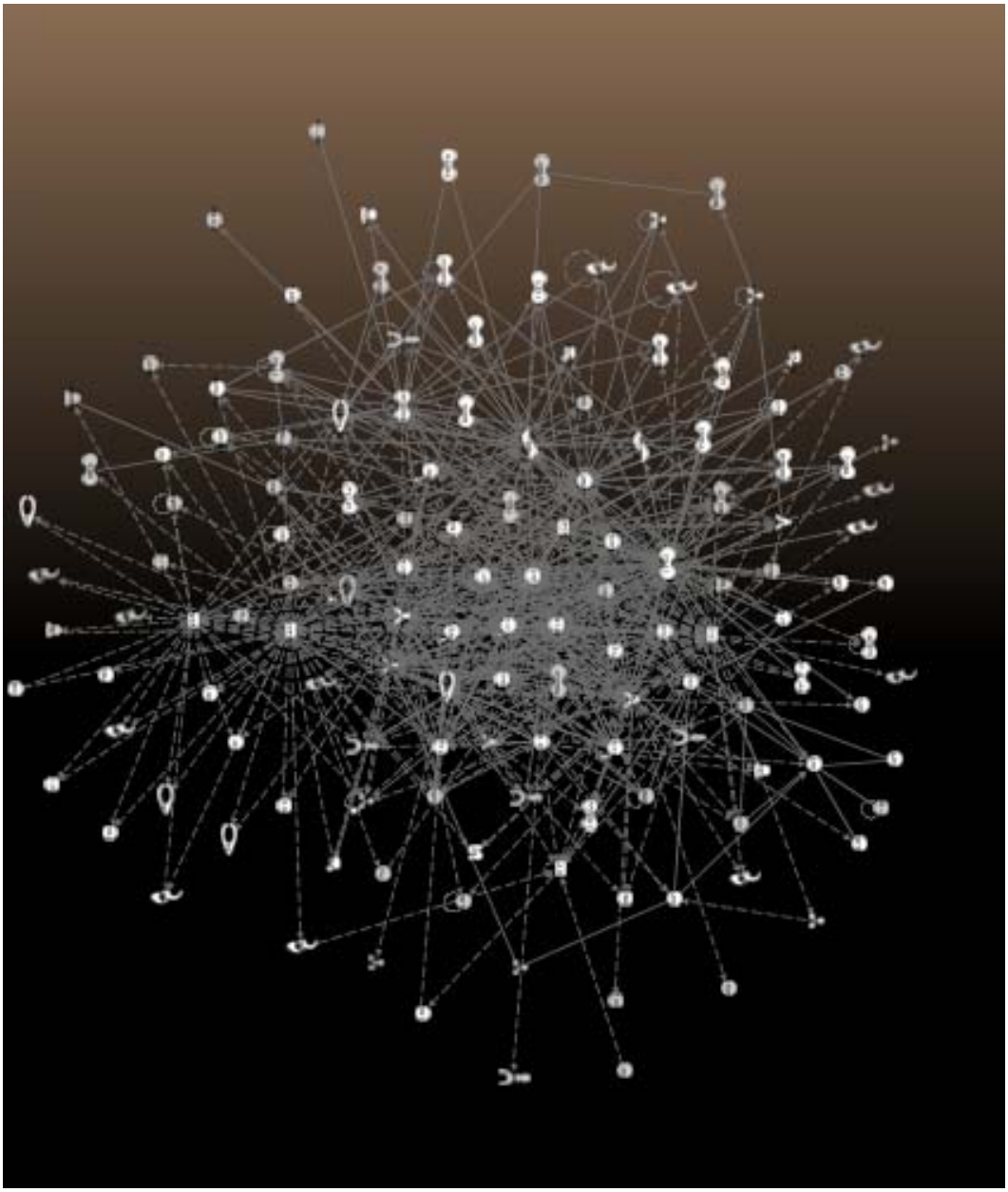

Figure 8.11. A.

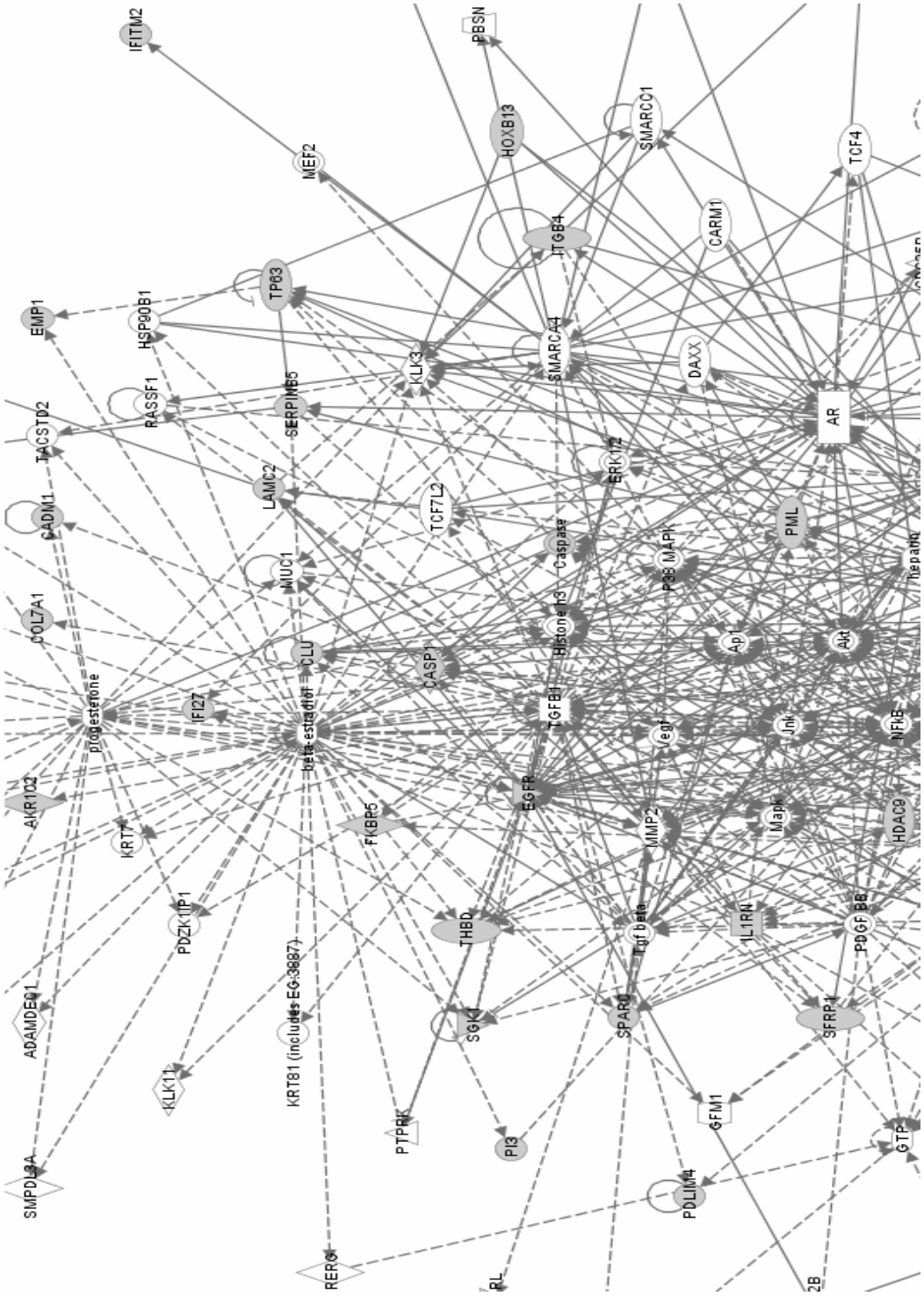
IFITM2
PBSN
MEF2
HOXB13
SMARCC1
TCF4
CARM1
ITGB4
TP63
EMP1
HSPB0B1
SMARCA4
KLK3
DAXX
RASSF1
SERPINB5
AR
TACSTD2
ERK1/2
LAMC2
TCF7L2
CADM1
PML
Caspase
MUC1
P38 MAPK
COL7A1
Histone h3
Ap1
Akt
CLU
CASP1
progesterone
IFI27
TGFB1
Vegf
Jnk
NFkB
beta estradiol
AKR1C2
EGFR
KRT7
FKBP5
MMP2
Mapk
HDAC9
PDZK1IP1
THBD
IL1RN
PDGF BB
Tgf beta
ADAMDEC1
KRT81 (includes EG:3887)
SGK1
SPARC
SFRP4
KLK11
GFM1
PTPRK
PI3
GTP
SMPDL3A
PDLIM4
RERG
RL
2B

Figure 8.11. B.

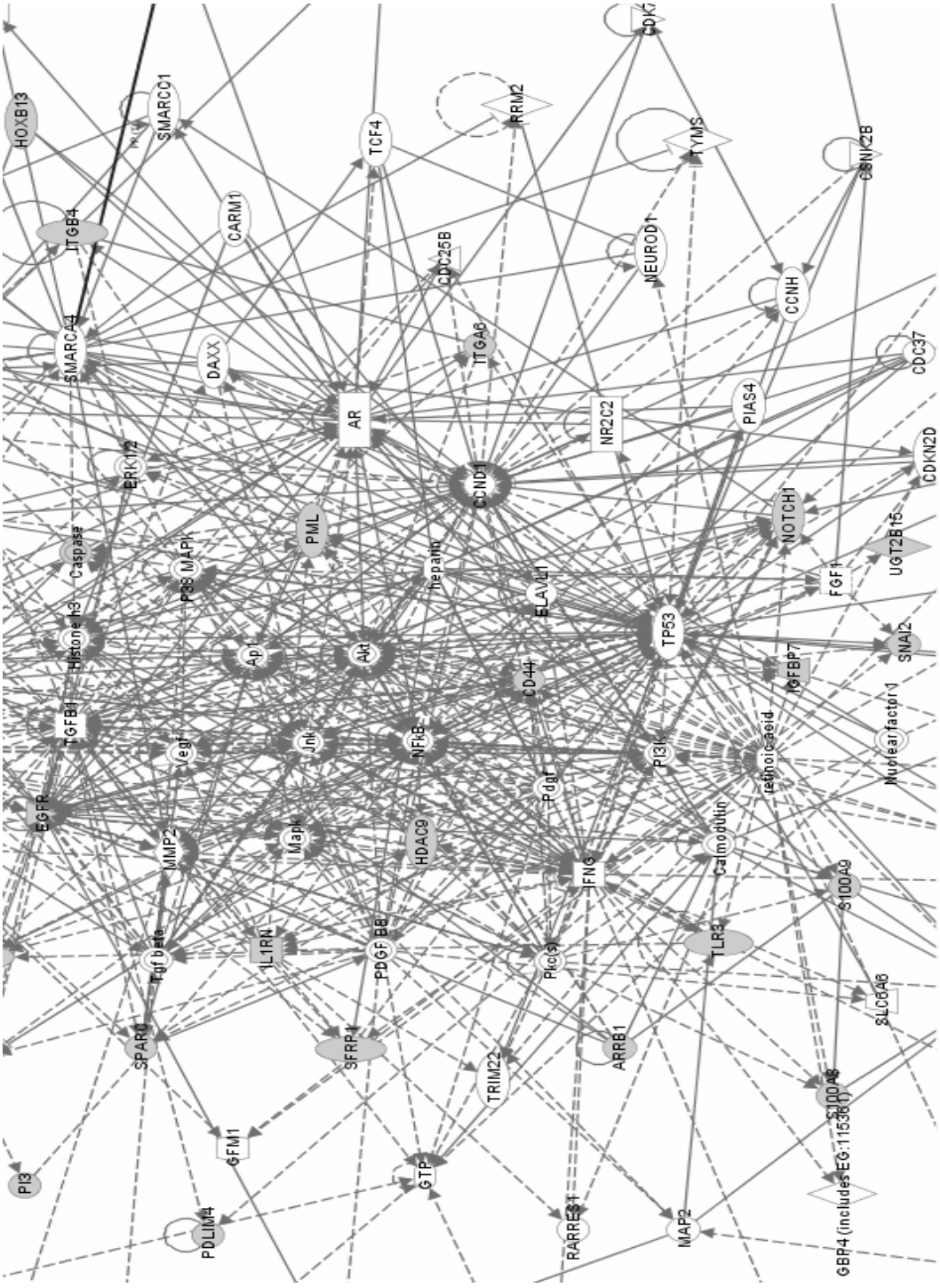
HOXB13
SMARCC1
ITGB4
CARM1
TCF4
RRM2
TYMS
CDK2B
CDC25B
NEUROD1
CCNH
SMARCA4
DAXX
ITGA6
CDC37
AR
NR2C2
PIAS4
ERK1/2
CCND1
CDKN2D
PML
Caspase
P38 MAPK
NOTCH1
UGT2B15
Histone h3
Ap1
Akt
ELAVL1
TP53
FGF1
SNAI2
TGFB1
CD44
IGFBP7
Jnk
NFkB
PI3K
Mutearfactor1
Vegf
Pdgf
EGFR
MMP2
Map3
HDAC9
IFNG
Calmodulin
S100A9
Tgf beta
IL1RN
PDGFBB
Pkc(s)
TLR3
SLC6A6
SPARC
SFRP4
TRIM22
ARRB1
GFM1
GTP
PI3
PDLIM4
RARRES1
MAP2
GBR4 (includes EG:11538)

Figure 8.11. C.

Figure 8.11. Comprehensive overview of all Metabolomics Networks in prostate cancer cell lines

8.11.A. All biological networks elicited by metabolomics analyses (Figures 8.7 through 8.10) were merged to obtain a comprehensive overview of all associations, feedback and feed-forward loops, cross-talk and major target hubs that may be important in prostate cancer. **8.11.B.** Sub-network structure in comprehensive metabolomics network, upper panel ; **8.11.C.** Sub-network structure in comprehensive metabolomics network, lower panel.

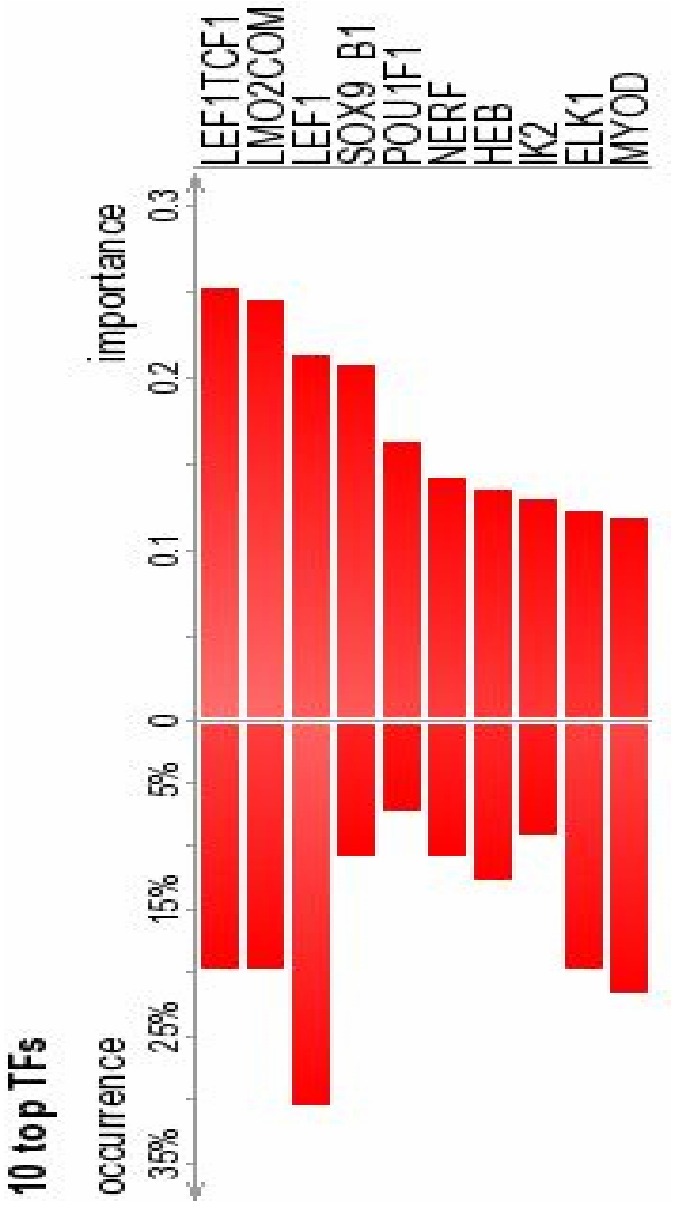

Figure 8.12. Regulatory element analyses for identification of TFBS-association signatures

TFBS-association signatures in the regulatory regions of the candidate biomarkers were identified by DiRE analyses. The top ten transcription factors based on occurrence and importance are shown here.

APPENDIX

Gene Name	Symbol	GenBank Accession	BHA	EGCG	CUR	SFN	PEITC	TM
Glutamate cysteine ligase, catalytic subunit	Gclc	NM_01029	Y	Y	Y	N	N	N
Glutamate cysteine ligase, modifier subunit	Gclm	NM_00812	N	N	N	N	N	Y
Glutathione S-transferase 1, microsomal	Mgst1	NM_01994	N	N	N	N	N	Y
Glutathione S-transferase 3, microsomal	Mgst3	NM_02556	N	N	N	N	N	Y
Glutathione S-transferase, alpha 2 (Yc2)	Gsta2	NM_00818	N	N	Y	Y	Y	N
Glutathione S-transferase, alpha3	Gsta3	AI172943	N	N	Y	N	N	N
Glutathione S-transferase, alpha4	Gsta4	NM_01035	N	N	Y	Y	N	Y
Glutathione S-transferase, kappa1	Gstk1	NM_02965	N	N	N	N	N	Y
Glutathione S-transferase, mu1	Gstm1	NM_01035	Y	N	Y	Y	Y	N
Glutathione S-transferase, mu3	Gstm3	NM_01035	Y	N	Y	Y	Y	Y
Glutathione S-transferase, mu5	Gstm5	NM_01036	N	N	N	Y	N	N
Glutathione S-transferase, mu7	Gstm7	XM_35930	N	N	N	N	N	Y
Glutathione S-transferase, theta1	Gstt1	NM_00818	N	N	N	N	N	Y
Glutathione S-transferase, theta3	Gstt3	BC003903	N	N	N	N	Y	N
Heme oxygenase (decycling) 1	Hmox1	NM_01044	Y	Y	Y	Y	N	N

Table 1.1. Major Phase II detoxifying/antioxidant genes upregulated by select dietary chemopreventive agents and downregulated by a toxicant via the redox-sensitive transcription factor Nrf2.

***BHA*, Butylated Hydroxyanisole; *EGCG*, epigallocatechin-3-gallate; *CUR*, Curcumin; *SFN*, Sulforaphane; *PEITC*, Phenethyl isothiocyanate; *TM*, Tunicamycin (a toxicant); *Y* denotes Yes and *N* denotes No (genes modulated or not modulated respectively by the chemopreventive agents/toxicant).**

Gene Name	GenBank Accession No.	Forward Primer (5'-3')	Reverse Primer (3'-5')
ATP-binding cassette, sub-family B (MDR/TAP),1A (Abcb1a)	NM_011076	5'-TTCAGGGCTTCACATTTGGC-3'	5'-GGAGTCGCTTGGTGAGGATCT-3'
ATP-binding cassette, sub-family C (CFTR/MRP), 1(Abcc1)	NM_008576	5'-CTCACGATTGCTCATCGGCT-3'	5'-AATCACCCGCGTGTAGTCCA-3'
CASP8 and FADD-like apoptosis regulator (Cflar)	NM_207653	5' - CCAGCTTTTCTTGTTTCCCAAG -3'	5'-CGGCGAACAATCTGGGTTAT-3'
Cytochrome c oxidase, subunit VIIa 1(Cox7a1)	NM_009944	5'-CACTTAGAAAACCGTGTGGCAG-3'	5'-ATTGTCGGCCTGGAAGAGCT-3'
Glutathione-S-transferase mu(Gstmu)	NM_010358	5'-GAAGCCAGTGGCTGAATGAGA-3'	5'-GATGGCATTGCTCTGGGTG-3'
Glycogen synthase kinase 3 beta (Gsk3b)	NM_019827	5'-TTTGAGCTGGTACCCTAGGATGA-3'	5'-AGCTGCCCCCTTAACACCAT-3'
Heme oxygenase (decycling) 1(Hmox1)	NM_010442	5'-CCCACCAAGTTCAAACAGCTC-3'	5'-AGGAAGGCGGTCTTAGCCTC-3'
Inhibitor of kappaB kinase gamma (Ikbkg)	NM_010547	5'-CTGAAAGTTGGCTGCCATGAG-3'	5'-GAGTGGTGAGCTGGAGCAGG-3'
Nuclear receptor coactivator 3 (Ncoa3)	NM_013827	5'-GAGGTGTCAGAGACGCCCAG-3'	5'-TTTCTTGTGGCCTTTGCTTTC-3'
Nuclear receptor co-repressor 1 (Ncor1)	NM_011308	5'-GCAGCCTTCTACTTCTACATTCCAA-3'	5'-GTGGATGACAAAGCAGATGGTG-3'
Nuclear receptor interacting protein 1 (Nrip1)	NM_173440	5'-AACAGTGAGCTGCCAACCCT-3'	5'-CTTCGGGACCATGCAGATGT-3'
Protein kinase C, epsilon (Prkce)	NM_011104	5'-ACGCTCCTATCGGCTACGAC-3'	5'-CGAACTGGATGGTGCAGTTG-3'
v-Maf musculoaponeurotic fibrosarcoma oncogene family, protein G (avian) (MafG)	NM_010756	5'-AGAATGGCACCAGCTTGACC-3'	5'-CTCGCACCGACATGGTTACC-3'
Glyceraldehyde-3-phosphate dehydrogenase (GAPDH)	NM_008084	5'-CACCAACTGCTTAGCCCCC-3'	5'-TCTTCTGGGTGGCAGTGATG-3'

Table 2.1.Oligonucleotide primers used in quantitative real-time PCR (qRT-PCR)

Gene Description	Symbol	GenBank Accession No	SIT a	Liver b
Cell Adhesion				
activated leukocyte cell adhesion molecule	Alcam	NM_009655	2.39	
CD47 antigen (Rh-related antigen, integrin-associated signal transducer)	Cd47	NM_010581	2.02	
Apoptosis and cell cycle control				
anaphase promoting complex subunit 1	Anapc1	NM_008569	28.6	
BCL2-like 11 (apoptosis facilitator)	Bcl2l11	NM_207680	2.1	
CASP8 and FADD-like apoptosis regulator	Cflar	NM_207653	3.94	
caspase recruitment domain family, member 6	Card6	XM_139295	2.44	
cyclin G1	Ccng1	NM_009831	2.61	
cyclin T2	Ccnt2	NM_028399	2.37	
G1 to S phase transition 1	Gspt1	NM_146066	2.9	
growth arrest and DNA-damage-inducible 45 alpha	Gadd45a	NM_007836	2.65	
growth arrest and DNA-damage-inducible 45 alpha	Gadd45a	NM_007836		3.02
growth arrest and DNA-damage-inducible 45 beta	Gadd45b	NM_008655	3.19	
growth arrest specific 1	Gas1	NM_008086	2.17	
growth arrest-specific 2 like 3	Gas2l3	XM_137276	2.23	
insulin-like growth factor binding protein 3	Igfbp3	NM_008343	2.26	
Nuclear mitotic apparatus protein 1 (Numa1), mRNA	Numa1	NM_133947	2	
retinoblastoma binding protein 8	Rbbp8	XM_484703		2.38
synaptonemal complex protein 1	Sycp1	NM_011516		2.21
Tnf receptor-associated factor 1	Traf1	NM_009421		5.57
Proliferating cell nuclear antigen	Pcna	NM_011045	4.76	9.76
Biosynthesis and Metabolism				
aldehyde dehydrogenase family 1, subfamily A3	Aldh1a3	NM_053080	2.99	
acyl-CoA synthetase long-chain family member 1	Acsl1	NM_007981	2.05	
acyl-Coenzyme A binding domain containing 3	Acbd3	NM_133225	2.01	
Adenylate kinase 3 (Ak3), mRNA	Ak3l1	NM_021299		2.38
aldehyde dehydrogenase 2, mitochondrial	Aldh2	NM_009656		2.93
arginine decarboxylase	Adc	NM_172875		2.86
creatine kinase, mitochondrial 2	Ckmt2	NM_198415		10.07
creatine kinase, muscle	Ckm	NM_007710	5.17	
creatine kinase, muscle	Ckm	NM_007710		3.88
dopamine beta hydroxylase	Dbh	NM_138942		2.45
ectonucleoside triphosphate diphosphohydrolase 3	Entpd3	NM_178676		5.54
eukaryotic translation initiation factor 3, subunit 10 (theta)	Eif3s10	NM_010123	2.02	
galactose-4-epimerase, UDP	Gale	NM_178389		2
Glyoxalase 1	Glo1	NM_025374	2.05	
GTP binding protein 2	Gtpbp2	NM_019581	2.08	
GTP binding protein 2	Gtpbp2	NM_019581		2.68
guanine nucleotide binding protein-like 2 (nucleolar)	Gnl2	NM_145552	2.25	
guanine nucleotide binding protein-like 2 (nucleolar)	Gnl2	NM_145552		2.16
guanosine monophosphate reductase	Gmpr	NM_145465	3.79	
hydroxysteroid (17-beta) dehydrogenase 7	Hsd17b7	NM_010476	2.19	
nitric oxide synthase 3 antisense	Nos3as	NM_0010028	3.14	
phosphatidylinositol glycan, classC	Pigc	NM_026078	7.44	
phosphoglucomutase 2-like 1	Pgm2l1	NM_027629	14.39	
phospholipase A2, group IIF	Pla2g2f	NM_012045	2.06	
prostaglandin-endoperoxide synthase 2	Ptgs2	NM_011198		4.9

Table 2.2. BHA-induced Nrf2-dependent genes in mouse small intestine and liver…..continued…

Gene Description	Symbol	GenBank Accession No	SIT a	Liver b
stearoyl-Coenzyme A desaturase 1	Scd1	NM_009127	3.39	
tryptophan hydroxylase 1	Tph1	NM_009414		8.64
very low density lipoprotein receptor	Vldlr	NM_013703		2.24
Cell Growth and Differentiation				
cysteine rich transmembrane BMP regulator 1 (chordin like)	Crim1	NM_015800	3.44	
FK506 binding protein 12-rapamycin associated protein 1	Frap1	NM_020009	5.35	
motile sperm domain containing 3	Mospd3	NM_030037	2.21	
neurotrophin 5	Ntf5	NM_198190		5.42
tropomodulin 1	Tmod1	NM_021883	2.25	
tissue inhibitor of metalloproteinase 2	Timp2	NM_011594	3.02	
Detoxification enzymes				
carbohydrate sulfotransferase 10	Chst10	NM_145142	2.44	
esterase D/formylglutathione hydrolase	Esd	NM_016903	4.65	
Esterase D/formylglutathione hydrolase (Esd), mRNA	Esd	NM_016903	2.53	
fucosyltransferase 4	Fut4	NM_010242	2.02	
glutamate-cysteine ligase, catalytic subunit	Gclc	NM_010295	2.69	
glutamate-cysteine ligase, catalytic subunit	Gclc	NM_010295		2.14
glutathione S-transferase, mu 1	Gstm1	NM_010358	3.67	
glutathione S-transferase, mu 3	Gstm3	NM_010359		3.39
heme oxygenase (decycling) 1	Hmox1	NM_010442		3.12
heparan sulfate 6-O-sulfotransferase 2	Hs6st2	NM_015819	6.54	
ST3 beta-galactoside alpha-2,3-sialyltransferase 2	St3gal2	NM_009179	2.9	
thioesterase superfamily member 5	Them5	NM_025416	5.53	
UDP glucuronosylltransferase 8A	**Ugt8a**	NM_011674	5.65	
UDP glucuronosyltransferase 2 family, polypeptide B35	Ugt2b35	NM_172881		2.3
Uronyl-2-sulfotransferase	Ust	NM_177387	2.32	
DNA Replication				
topoisomerase (DNA) I	Top1	NM_009408	2.08	
origin recognition complex, subunit 2-like (S. cerevisiae)	Orc2l	NM_008765	2.15	
Electron Transport				
flavin containing monooxygenase 2	Fmo2	NM_018881	8.72	
monoamine oxidase B	Maob	NM_172778	2.16	
thioredoxin domain containing 10	Txndc10	NM_198295	3.85	
G-protein coupled receptors				
angiotensin receptor 1	Agtr1	NM_177322	4.29	
Calmodulin III (Calm3) mRNA, 3' untranslated region	Calm3	NM_007590		5.59
chemokine (C-X-C motif) receptor 4	Cxcr4	NM_009911	2.3	
coagulation factor II (thrombin) receptor-like 2	F2rl2	NM_010170		2.05
G protein-coupled receptor 133	Gpr133	XM_485685		16.59
G protein-coupled receptor 20	Gpr20	NM_173365	2.1	
guanine nucleotide binding protein (G protein), gamma 3 subunit	Gng3	NM_010316		2.64
guanine nucleotide binding protein (G protein), gamma 7 subunit	Gng7	NM_010319	2.1	
guanine nucleotide binding protein, alpha inhibiting 1	Gnai1	NM_010305	2.11	
regulator of G-protein signaling 9	Rgs9	NM_011268	7.73	
regulator of G-protein signaling 9	Rgs9	AK085443		13.73
Kinases and Phosphatases				
protein tyrosine phosphatase, receptor type, T	Ptprt	NM_021464	2.27	
Serine/threonine kinase 24 (STE20 homolog, yeast)	Stk24	NM_145465	3.84	
diacylglycerol kinase kappa	Dagkk	NM_177914		2.26

Table 2.2…..continued…

Gene Description	Symbol	GenBank Accession No	SIT a	Liver b
ethanolamine kinase 1	Etnk1	XM_284250	3.46	
FMS-like tyrosine kinase 4	Flt4	NM_008029	2.95	
inhibitor of kappaB kinase gamma	Ikbkg	NM_010547		3.92
Janus kinase 2	Jak2	NM_008413	3.09	
microtubule associated serine/threonine kinase-like	Mastl	NM_025979	14.5	
mitogen activated protein kinase 8	Mapk8	NM_016700	10.39	
mitogen-activated protein kinase 6	Mapk6	NM_015806	2.11	
mitogen-activated protein kinase kinase kinase 9	Map3k9	NM_177395	3.06	
mitogen-activated protein kinase kinase kinase kinase 4	Map4k4	NM_008696	2.46	
mitogen-activated protein kinase kinase kinase kinase 5	Map4k5	NM_201519	3.94	
neurotrophic tyrosine kinase, receptor, type 1	Ntrk1	XM_283871	3.88	
neurotrophic tyrosine kinase, receptor, type 2	Ntrk2	NM_0010250	3.3	
protein kinase C, epsilon	Prkce	NM_011104	5.69	
protein kinase C, eta	Prkch	NM_008856	2.87	
protein kinase, cAMP dependent regulatory, type I, alpha	Prkar1a	AK049832		11.6
protein kinase, cAMP dependent regulatory, type II alpha	Prkar2a	NM_008924	2.18	
protein phosphatase 1 (formerly 2C)-like	Ppm1l	NM_178726	2.48	
protein phosphatase 1, regulatory (inhibitor) subunit 14A	Ppp1r14a	NM_026731	2.1	
protein phosphatase 2, regulatory subunit B (B56), epsilon isoform	Ppp2r5e	NM_012024	2.12	
protein phosphatase 3, catalytic subunit, beta isoform	Ppp3cb	NM_008914	2.02	
protein tyrosine phosphatase 4a1	Ptp4a1	NM_011200	3.79	
protein tyrosine phosphatase, receptor type Z, polypeptide 1	Ptprz1	XM_620293	2.34	
Putative membrane-associated guanylate kinase 1 (Magi-1), alternatively spliced c form	Baiap1	NM_010367		2.45
TANK-binding kinase 1	Tbk1	NM_019786	2.06	
Ttk protein kinase	Ttk	NM_009445	2.23	
tyrosine kinase, non-receptor, 1	Tnk1	NM_031880	2.34	
RNA/Protein processing and Nuclear assembly				
Heterogeneous nuclear ribonucleoprotein A1	Hnrpa1	NM_010447	3.45	
histone 1, H4f	Hist1h4f	NM_175655..	7.1	
hypoxia up-regulated 1	Hyou1	NM_021395		3.02
Methionine sulfoxide reductase A	Msra	NM_026322		2.9
methionine sulfoxide reductase B3	Msrb3	NM_177092	3.41	
mitochondrial ribosomal protein L52	Mrpl52	NM_026851		5.18
neuronal pentraxin receptor	Nptxr	NM_030689		3.29
nucleosome assembly protein 1-like 1	Nap1l1	NM_015781	2.21	
peptidyl arginine deiminase, type II	Padi2	NM_008812		3.28
RNA polymerase 1-2	Rpo1-2	NM_009086	2.99	
RNA polymerase 1-4	Rpo1-4	NM_009088	35.71	
sarcolemma associated protein	Slmap	NM_032008	2.17	
tubulin tyrosine ligase-like family, member 4	Ttll4	NM_001014974		2.22
importin 7	Ipo7	NM_181517	2.51	
karyopherin (importin) alpha 1	Kpna1	NM_008465	29.9	
Transcription factors and interacting partners				
heat shock protein, alpha-crystallin-related, B6	Hspb6	NM_0010124	3.72	
bone morphogenetic protein receptor, type 1A	Bmpr1a	NM_009758	2.02	
metallothionein 1	Mt1	NM_013602	6.24	
insulin-like growth factor 2	Igf2	NM_010514	2.59	
Activating signal cointegrator 1 complex subunit 2	Ascc2	NM_029291		3.32

Table 2.2…..continued…

Gene Description	Symbol	GenBank Accession No	SIT a	Liver b
calsequestrin 1	Casq1	NM_009813		2
CBFA2T1 identified gene homolog (human)	Cbfa2t1h	NM_009822	2.42	
CCCTC-binding factor	Ctcf	NM_007794		2.35
C-erbA alpha1 mRNA for thyroid hormone receptor	Thra	NM_178060	2.74	
checkpoint supressor 1	Ches1	NM_183186	2.26	
circadian locomoter output cycles kaput	Clock	NM_007715	2.81	
Eph receptor A3	Epha3	NM_010140		2.23
Eph receptor B1	Ephb1	NM_173447		2.34
fos-like antigen 2	Fosl2	NM_008037		2.36
Hedgehog-interacting protein	Hhip	NM_020259	6.11	
hepatoma-derived growth factor, related protein 2	Hdgfrp2	NM_008233	2.22	
hypermethylated in cancer 2	Hic2	NM_178922		2.82
Insulin-like growth factor 2 receptor	Igf2r	NM_010515		2
Jun oncogene	Jun	NM_010591	2.75	
Kruppel-like factor 7 (ubiquitous)	Klf7	NM_033563	2.21	
lymphoblastomic leukemia	Lyl1	NM_008535		7.36
MAX dimerization protein 1	Mxd1	NM_010751	2.05	
NADH dehydrogenase (ubiquinone) 1 beta subcomplex, 2	Ndufb2	NM_026612	3.43	
Notch gene homolog 4 (Drosophila)	Notch4	NM_010929	2.35	
nuclear factor, interleukin 3, regulated	Nfil3	NM_017373	17.13	
nuclear receptor co-repressor 1	Ncor1	NM_011308	3.39	
nuclear receptor interacting protein 1	Nrip1	NM_173440	2.61	2.63
nuclear receptor subfamily 2, group C, member 2	Nr2c2	NM_011630	2.32	
nuclear receptor subfamily 6, group A, member 1	Nr6a1	NM_010264	2.49	
Phosphodiesterase 8A	Pde8a	NM_008803	2.58	
phosphoprotein associated with glycosphingolipid microdomains 1	Pag1	NM_053182		2.23
Polycystic kidney disease 1 like 3	Pkd1l3	NM_181544	8.44	
polymerase (RNA) I associated factor 1	Praf1	NM_022811		2.28
Pre B-cell leukemia transcription factor 3	Pbx3	NM_016768	2.05	
Purine rich element binding protein B	Purb	NM_011221	2.04	
RAB4A, member RAS oncogene family	Rab4a	BG080696		16.85
Ras and Rab interactor 1	Rin1	NM_145495		3.11
Ras association (RalGDS/AF-6) domain family 2	Rassf2	NM_175445	8.21	
ras homolog gene family, member T1	Rhot1	NM_021536	2.28	
reticuloendotheliosis oncogene	Rel	NM_009044		2.13
retinol binding protein 1, cellular	Rbp1	NM_011254	2.33	
serum response factor binding protein 1	Srfbp1	NM_026040	4.47	
Spred-1	Spred1	NM_033524	43.87	
suppressor of cytokine signaling 5	Socs5	NM_019654	19.3	
T-box brain gene 1	Tbr1	NM_009322	28.35	
thyroid hormone receptor beta	Thrb	NM_009380	2.43	
transcription factor AP-2 beta	Tcfap2b	NM_009334		3.79
transducer of ERBB2, 2	Tob2	NM_020507	2.23	
transforming growth factor beta 1 induced transcript 1	Tgfb1i1	NM_009365	3.36	
transforming growth factor, beta receptor I	Tgfbr1	NM_009370	14.27	
tumor necrosis factor receptor superfamily, member 19	Tnfrsf19	NM_013869	3.49	
tumor necrosis factor receptor superfamily, member 23	Tnfrsf23	NM_024290	2.6	
tumor necrosis factor, alpha-induced protein 2	Tnfaip2	NM_009396	2.13	
V-abl Abelson murine leukemia viral oncogene 2	Abl2	NM_009595	7.44	

Table 2.2…..continued…

Gene Description	Symbol	GenBank Accession No	SIT a	Liver b
v-maf musculoaponeurotic fibrosarcoma oncogene family, protein G (avian)	MafG	NM_010756	2.45	
wingless-type MMTV integration site 9B	Wnt9b	NM_011719	3.35	
Yamaguchi sarcoma viral (v-yes) oncogene homolog 1	Yes1	NM_009535	4.21	
Zinc finger homeobox 1b (Zfhx1b), mRNA	Zfhx1b	NM_015753	2.6	
zinc finger protein 37	Zfp37	NM_009554	3.42	
RAN, member RAS oncogene family	Ran	NM_009391	2	
Transport				
aquaporin 1	Aqp1	NM_007472	2.37	
ATP-binding cassette, sub-family B (MDR/TAP), member 1A	Abcb1a	NM_011076	2.08	
ATP-binding cassette, sub-family C (CFTR/MRP), member 1	Abcc1	NM_008576	2.23	
ATP-binding cassette, sub-family D (ALD), member 3	Abcd3	NM_008991		2.21
basic leucine zipper nuclear factor 1	Blzf1	NM_025505	6.45	
chloride channel calcium activated 4	Clca4	NM_139148	2.64	
cholinergic receptor, nicotinic, alpha polypeptide 3	Chrna3	NM_145129	2.01	
glutamate receptor, ionotropic, AMPA4 (alpha 4)	Gria4	NM_019691	6.76	
Multidrug resistance-associated protein 3 (Abcc3)	Abcc3	NM_029600		2.44
potassium large conductance calcium-activated channel, subfamily M, beta member 2	Kcnmb2	NM_028231	3.63	
Proton/amino acid transporter 4 (PAT4)	Slc36a4	NM_172289	3.04	
sideroflexin 2	Sfxn2	NM_053196	2.05	
signal transducing adaptor molecule (SH3 domain and ITAM motif) 2	Stam2	NM_019667	2.21	
sodium channel, voltage-gated, type VII, alpha	Scn7a	NM_009135	2.19	
solute carrier family 16 (monocarboxylic acid transporters), member 10	Slc16a10	NM_028247		2.38
solute carrier family 35, member A5	Slc35a5	NM_028756		3.32
solute carrier family 39 (zinc transporter), member 10	Slc39a10	NM_172653	8.55	
solute carrier family 5 (sodium/glucose cotransporter), member 12	Slc5a12	NM_0010039	3.69	
solute carrier organic anion transporter family, member 2a1	Slco2a1	NM_033314	2.3	
Type III sodium-dependent phosphate transporter (Slc20a2)	Slc20a2	NM_011394	2.71	
Ubiquitination and Proteolysis				
a disintegrin and metallopeptidase domain 10	Adam10	NM_007399	3.45	
cathepsin B	Ctsb	NM_007798	2.06	
Constitutive photomorphogenic protein (Cop1)	Rfwd2	NM_011931		2.05
HECT domain containing 2	Hectd2	NM_172637		2
serine carboxypeptidase 1	Scpep1	NM_029023	2.05	
SUMO/sentrin specific peptidase 2	Senp2	NM_029457	4.15	
SUMO1/sentrin specific peptidase 1	Senp1	NM_144851	2.62	
ubiquitin-activating enzyme E1, Chr Y 1	Ube1y1	NM_011667	2.39	
Others				
U1 small nuclear ribonucleoprotein 1C	Snrp1c	NM_011432		3.21
melanoma antigen, family H, 1	Mageh1	NM_023788	5.84	
HIV TAT specific factor 1	Htatsf1	NM_028242	2.1	
chemokine (C-X-C motif) ligand 2	Cxcl2	NM_009140		2.1
DEAD (Asp-Glu-Ala-Asp) box polypeptide 10	Ddx10	XM_284494	3.42	
DEAD (Asp-Glu-Ala-Asp) box polypeptide 5	Ddx5	NM_007840		3.05
golgi phosphoprotein 4	Golph4	NM_175193	2.37	
kelch-like 7 (Drosophila)	Klhl7	NM_026448	2.95	
leucine rich repeat containing 48	Lrrc48	NM_029044		9.96
leucine-rich repeats and immunoglobulin-like domains 3	Lrig3	NM_177152	8.43	
protein disulfide isomerase associated 3	Pdia3	NM_007952		2
serine (or cysteine) peptidase inhibitor, clade I, member 1	Serpini1	NM_009250	2.47	

Table 2.2…..continued…

Gene Description	Symbol	GenBank Accession No	SIT a	Liver b
six transmembrane epithelial antigen of prostate 2	Steap2	XM_284053	2.96	
TCDD-inducible poly(ADP-ribose) polymerase	Tiparp	NM_178892	2.5	
tyrosine 3-monooxygenase/tryptophan 5-monooxygenase, activation protein, zeta polypeptide	Ywhaz	NM_011740	2.17	3.46
keratin associated protein 6-1	Krtap6-1	NM_010672		5.04
keratin complex 2, basic, gene 18	Krt2-18	NM_016879		5.85
seminal vesicle secretion 3	Svs3	NM_021363	8.7	
antigen p97 (melanoma associated)	Mfi2	NM_013900		6.73

[a]Genes that were induced >2-fold by BHA only in small intestine of Nrf2 wild-type mice but not in small intestine of Nrf2 knockout mice compared with vehicle treatment at 3h. The relative mRNA expression levels of each gene in treatment group over vehicle group (fold changes) are listed.

[b]Genes that were induced >2-fold by BHA only in liver of Nrf2 wild-type mice but not in liver of Nrf2 knockout mice compared with vehicle treatment at 3h. The relative mRNA expression levels of each gene in treatment group over vehicle group (fold changes) are listed.

Table 2.2.

Gene Description	GenBank Accession No.	Symbol	SIT a	Liver b
Cell Adhesion				
camello-like 2	NM_053096	Cml2	0.03	
catenin (cadherin associated protein), delta 2	NM_008729	Ctnnd2		0.36
intercellular adhesion molecule	NM_010493	Icam1	0.48	
protocadherin 7	NM_018764	Pcdh7		0.43
Apoptosis and cell cycle control				
B-cell leukemia/lymphoma 2	NM_009741	Bcl2		0.32
breast cancer 1	NM_009764	Brca1		0.49
CASP2 and RIPK1 domain containing adaptor with death domain	NM_009950	Cradd		0.39
Cell division cycle 37 homolog (S. cerevisiae)-like 1	NM_025950	Cdc37l1	0.28	
cell division cycle and apoptosis regulator 1	NM_026201	Ccar1		0.4
centrin 4	NM_145825	Cetn4	0.21	
Cyclin I	NM_017367	Ccni		0.28
G0/G1 switch gene 2	NM_008059	G0s2		0.44
integrin beta 1 (fibronectin receptor beta)	NM_010578	Itgb1	0.18	
nuclear factor of activated T-cells, cytoplasmic, calcineurin-dependent 1	NM_016791	Nfatc1	0.09	
Rho GTPase activating protein 4	NM_138630	Arhgap4	0.38	
WW domain-containing oxidoreductase	NM_019573	Wwox	0.47	
Biosynthesis and Metabolism				
abhydrolase domain containing 9	XM_128553	Abhd9	0.22	
Acetyl-Coenzyme A carboxylase beta	NM_133904	Acacb		0.39
alanine-glyoxylate aminotransferase	NM_016702	Agxt	0.48	
B-cell CLL/lymphoma 9-like	XM_620743	Bcl9l	0.1	
butyrobetaine (gamma), 2-oxoglutarate dioxygenase 1 (gamma-butyrobetaine hydroxylase)	NM_130452	Bbox1	0.42	
methylmalonyl-Coenzyme A mutase	NM_008650	Mut		0.17
mitochondrial ribosomal protein L27	NM_053161	Mrpl27	0.47	
mitochondrial ribosomal protein S14	NM_025474	Mrps14		0.35
mitochondrial ribosomal protein S21	NM_078479	Mrps21	0.49	
nicotinamide nucleotide adenylyltransferase 2	NM_175460	Nmnat2	0.33	
pantothenate kinase 1	NM_023792	Pank1	0.18	
phosphoglucomutase 2-like 1	NM_027629	Pgm2l1		0.4
phosphopantothenoylcysteine decarboxylase	NM_176831	Ppcdc	0.05	
phosphoribosyl pyrophosphate synthetase 2	NM_026662	Prps2		0.47
propionyl-Coenzyme A carboxylase, alpha polypeptide	NM_144844	Pcca	0.47	
UDP-glucose ceramide glucosyltransferase	NM_011673	Ugcg		0.37
ureidopropionase, beta	NM_133995	Upb1	0.45	
uroporphyrinogen III synthase	NM_009479	Uros	0.36	
very low density lipoprotein receptor	NM_013703	Vldlr		0.43
Nitric oxide synthase 1, neuronal	NM_008712	Nos1		0.4
Cell Growth and Differentiation				
helicase, lymphoid specific	NM_008234	Hells	0.33	
male enhanced antigen 1	NM_010787	Mea1	0.48	
myosin, light polypeptide 7, regulatory	NM_022879	Myl7	0.46	
DNA Replication				
origin recognition complex, subunit 4-like (S. cerevisiae)	NM_011958	Orc4l	0.1	
Electron Transport				
cytochrome c oxidase, subunit VIIa 1	NM_009944	Cox7a1	0.42	0.4

Table 2.3. BHA-suppressed Nrf2-dependent genes in mouse small intestine and liver…..continued…

Gene Description	GenBank Accession No.	Symbol	SIT a	Liver b
cytochrome P450, family 21, subfamily a, polypeptide 1	NM_009995	Cyp21a1		0.29
cytochrome P450, family 3, subfamily a, polypeptide 44	NM_177380	Cyp3a44	0.38	
cytochrome P450, family 7, subfamily a, polypeptide 1	NM_007824	Cyp7a1		0.37
dual oxidase 1	XM_130483	Duox1	0.39	
NADH dehydrogenase (ubiquinone) 1 beta subcomplex 4	NM_026610	Ndufb4	0.41	
thioredoxin reductase 2	NM_013711	Txnrd2		0.21
ubiquinol-cytochrome c reductase (6.4kD) subunit	NM_025650	Uqcr	0.4	
G-protein coupled receptors				
adrenergic receptor, beta 1	NM_007419	Adrb1		0.45
bombesin-like receptor 3	NM_009766	Brs3	0.35	
calmodulin 3	NM_007590	Calm3	0.45	
cholecystokinin A receptor	NM_009827	Cckar		0.19
G protein-coupled receptor 1	NM_146250	Gpr1	0.45	
G protein-coupled receptor 37	NM_010338	Gpr37		0.1
GNAS (guanine nucleotide binding protein, alpha stimulating) complex locus	NM_010309	Gnas	0.46	
regulator of G-protein signaling 2	NM_009061	Rgs2	0.37	
vomeronasal 1 receptor, B1	NM_053225	V1rb1	0.5	
Kinases and Phosphatases				
calcium/calmodulin-dependent protein kinase II, delta	NM_001025439	Camk2d		0.38
G protein-coupled receptor kinase 5 (GRK5)	NM_018869	Gprk5	0.46	
glycogen synthase kinase 3 beta	NM_019827	Gsk3b	0.15	
inositol polyphosphate multikinase	NM_027184	Ipmk	0.47	
inositol polyphosphate-1-phosphatase	NM_008384	Inpp1		0.37
MAP kinase-activated protein kinase 5	NM_010765	Mapkapk5	0.42	
microtubule associated serine/threonine kinase family member 4	XM_283179	Mast4	0.12	
microtubule associated serine/threonine kinase family member 4	XM_283179	Mast4		0.48
mitogen activated protein kinase kinase 7	NM_011944	Map2k7		0.37
Mitogen-activated protein kinase associated protein 1	NM_177345	Mapkap1	0.34	
multiple substrate lipid kinase	NM_023538	Mulk	0.48	
p21 (CDKN1A)-activated kinase 3	NM_008778	Pak3	0.42	
phosphoinositide-3-kinase, regulatory subunit 5, p101	NM_177320	Pik3r5		0.46
Protein kinase ATR (Atr)	NM_028533	Prk		0.49
protein kinase, AMP-activated, alpha 1 catalytic subunit	NM_001013367	Prkaa1		0.35
Protein phosphatase 3, catalytic subunit, alpha isoform	NM_008913	Ppp3ca	0.37	
Protein phosphatase 3, catalytic subunit, alpha isoform	NM_008913	Ppp3ca	0.1	
Protein tyrosine phosphatase, non-receptor type 4	NM_019933	Ptpn4	0.5	
receptor tyrosine kinase-like orphan receptor 1	NM_013845	Ror1		0.29
ribosomal protein S6 kinase, polypeptide 4	NM_019924	Rps6ka4	0.45	
Ribosomal protein S6 kinase, polypeptide 5	NM_153587	Rps6ka5		0.3
RNA/Protein processing and Nuclear assembly				
aspartate-beta-hydroxylase	NM_023066	Asph		0.17
ATP synthase mitochondrial F1 complex assembly factor 2	NM_145427	Atpaf2	0.48	
chromatin accessibility complex 1	NM_053068	Chrac1	0.49	
Down syndrome critical region gene 3	NM_007834	Dscr3	0.49	
fucosyltransferase 9	NM_010243	Fut9		0.05
histone 3, H2a	NM_178218	Hist3h2a	0.43	
neuronal pentraxin receptor	NM_030689	Nptxr	0.37	
nucleoporin 133	NM_172288	Nup133		0.34
protein-O-mannosyltransferase 2	NM_153415	Pomt2	0.46	

Table 2.3…..continued…

Gene Description	GenBank Accession No.	Symbol	SIT a	Liver b
Zinc finger, matrin-like	NM_008717	Zfml	0.44	
Transcription factors and interacting partners				
activating transcription factor 7 interacting protein 2	XM_148109	Atf7ip2		0.35
angiotensin II, type I receptor-associated protein	NM_009642	Agtrap		0.49
Bone morphogenetic protein 6	NM_007556	Bmp6		0.12
Breast carcinoma amplified sequence 3	NM_138681	Bcas3		0.4
E2F transcription factor 5	NM_007892	E2f5	0.38	
EGF-like module containing, mucin-like, hormone receptor-like sequence 4	NM_139138	Emr4	0.19	
epidermal growth factor receptor pathway substrate 15	NM_007943	Eps15		0.19
Fc receptor, IgG, high affinity I	NM_010186	Fcgr1	0.48	
FEV (ETS oncogene family)	NM_153111	Fev	0.48	
Growth hormone receptor	NM_010284	Ghr		0.31
GTP binding protein 7 (putative)	NM_199301	Gtpbp7	0.49	
heat shock factor 2	NM_008297	Hsf2		0.08
HRAS-like suppressor	NM_013751	Hrasls	0.23	
Human immunodeficiency virus type I enhancer binding protein 2	NM_010437	Hivep2	0.48	
Hypoxia inducible factor 1, alpha subunit	NM_010431	Hif1a		0.4
insulin-like growth factor 1	NM_010512	Igf1	0.43	
Insulin-like growth factor I receptor	NM_010513	Igf1r		0.49
interleukin 2 receptor, gamma chain	NM_013563	Il2rg		0.44
Kruppel-like factor 1 (erythroid)	NM_010635	Klf1	0.43	
lysosomal trafficking regulator	NM_010748	Lyst		0.43
metal response element binding transcription factor 2	NM_013827	Mtf2	0.12	
myc target 1	NM_026793	Myct1		0.43
Nuclear receptor coactivator 3	NM_013827	Ncoa3	0.12	
nuclear receptor subfamily 2, group F, member 1	NM_010151	Nr2f1		0.4
peroxisome biogenesis factor 7	NM_008822	Pex7	0.5	
protein inhibitor of activated STAT 4	NM_021501	Pias4	0.45	
RAB28, member RAS oncogene family	NM_027295	Rab28	0.46	
Rho GTPase activating protein 29	NM_172525	Arhgap29		0.26
SH2 domain containing 4A	XM_134197	Sh2d4a		0.23
Sp2 transcription factor	NM_030220	Sp2		0.45
sphingosine kinase 2	NM_203280	Sphk2	0.45	
src family associated phosphoprotein 1	NM_001033186	Scap1	0.41	
Suppressor of cytokine signaling 2	NM_007706	Socs2		0.27
Tax1 (human T-cell leukemia virus type I) binding protein 3	NM_029564	Tax1bp3		0.39
thrombopoietin	NM_009379	Thpo	0.19	
thyroid hormone receptor associated protein 1	XM_109726	Thrap1		0.37
topoisomerase I binding, arginine/serine-rich	NM_134097	Topors		0.49
v-raf murine sarcoma 3611 viral oncogene homolog	NM_009703	Araf		0.41
Transport				
aquaporin 3	NM_016689	Aqp3		0.35
aquaporin 8	NM_007474	Aqp8	0.33	
ATPase, Ca++ transporting, plasma membrane 4	NM_213616	Atp2b4	0.1	
ATPase, Na+/K+ transporting, alpha 1 polypeptide	NM_144900	Atp1a1		0.39
calcium channel, voltage-dependent, gamma subunit 6	NM_133183	Cacng6		0.41
Chloride intracellular channel 5	NM_172621	Clic5		0.16
fatty acid binding protein 6, ileal (gastrotropin)	NM_008375	Fabp6	0.31	
sodium channel, voltage-gated, type III, beta	NM_153522	Scn3b		0.31

Table 2.3…..continued…

Gene Description	GenBank Accession No.	Symbol	SIT a	Liver b
Ubiquitination and Proteolysis				
F-box and leucine-rich repeat protein 8	NM_015821	Fbxl8	0.43	
granzyme B	NM_013542	Gzmb	0.41	
matrix metalloproteinase 24	NM_010808	Mmp24	0.38	
protease, serine, 19 (neuropsin)	NM_008940	Prss19	0.48	
ubiquitin specific peptidase 16	NM_024258	Usp16	0.26	
Others				
melanoma antigen, family A, 5	NM_020018	Magea5	0.23	
hornerin	NM_133698	Hrnr	0.39	
cystatin E/M	NM_028623	Cst6	0.43	

[a]Genes that were suppressed >2-fold by BHA only in small intestine of Nrf2 wild-type mice but not in small intestine of Nrf2 knockout mice compared with vehicle treatment at 3h. The relative mRNA expression levels of each gene in treatment group over vehicle group (fold changes) are listed.

[b]Genes that were suppressed >2-fold by BHA only in liver of Nrf2 wild-type mice but not in liver of Nrf2 knockout mice compared with vehicle treatment at 3h. The relative mRNA expression levels of each gene in treatment group over vehicle group (fold changes) are listed.

Table 2.3.

Gene Name	GenBank Accession N	Forward Primer	Reverse Primer
ATP-binding cassette, sub-family B (MDR/TAP),1A (Abcb1b)	NM_011075	5'-GAATGTCCAGTGGCTCCGA-3'	5'-CGGCTGTTGTCTCCATAGGC-3'
ATP-binding cassette, sub-family C (CFTR/MRP), 1(Abcc1)	NM_008376	5'-CTCACGATTGCTCATCGGCT-3'	5'-AATCACCCGCGTGTAGTCCA-3'
CASP8 and FADD-like apoptosis regulator (Clar)	NM_207653	5'-CCAGCTTTTCTTGTTTCCCAAG-3'	5'-CGGCGAACAATCTGGGTTAT-3'
Glutamate cysteine ligase, modifier subunit (Gclm)	NM_008129	5'-CGAGGAGCTTCGGGACTGTA-3'	5'-TGGTGCATTCCAAAACATCTG-3'
Glutathione S-transferase, alpha 4	NM_010357	5'-AGGAGTCATGGCAGCCAAAC-3'	5'-CCTCAAACTCCACTCCAGCC-3'
Glutathione S-transferase, mu3	NM_010359	5'-ATCCGCTTGCTCCTGGAATA-3'	5'-TTCTCACTCAGCCACTGGCTT-3'
Inhibitor of kappaB kinase gamma (Ikbkg)	NM_010547	5'-CTGAAAGTTGGCTGCCATGAG-3'	5'-GAGTGGTGAGCTGGAGCAGG-3'
Nuclear receptor coactivator 3 (Ncoa3)	NM-144892	5'-GAGGTGTCAGAGACGCCCAG-3'	5'-TTTCTTGTGGCCTTTGCTTTC-3'
Nuclear receptor interacting protein 1 (Nrip1)	NM_173440	5'-AACAGTGAGCTGCCAACCCT-3'	5'-CTTCGGGACCATGCAGATGT-3'
P300/CBP-associated factor (Pcaf)	NM_020005	5'-AGAGAGGCAGACAACGATCGA-3'	5'-TTGATGCGGTTCAGAAACATCT-3'
Protein kinase C, epsilon (Prkce)	NM_011104	5'-ACGCTCCTATCGGCTACGAC-3'	5'-CGAACTGGATGGTGCAGTTG-3'
Src family associated phosphoprotein 2 (Scap2)	NM_018773	5'- GCTGGCTACCTGGAAAAACG -3'	5'-TTCAAACCCCAGAAAGCTGTG-3'
Glyceraldehyde-3-phosphate dehydrogenase (GAPDH)	NM_008084	5'-CACCAACTGCTTAGCCCCC-3'	5'-TCTTCTGGGTGGCAGTGATG-3'

Table 3.1. Oligonucleotide primers used in quantitative real-time PCR (qRT-PCR)

GenBank Accession	Gene Symbol	Gene Title	SIT*	Liver**
Cell Adhesion				
NM_009864	Cdh1	Cadherin 1	6.77	
XM_283264	Cdh10	cadherin 10		7.01
NM_007664	Cdh2	cadherin 2	9.72	
XM_488510	Cspg2	chondroitin sulfate proteoglycan 2	2.72	2.82
NM_009903	Cldn4	claudin 4	4.86	
NM_018777	Cldn6	claudin 6		2.32
NM_031174	Dscam	Down syndrome cell adhesion molecule (Dscam)	2.25	
NM_010103	Edil3	EGF-like repeats and discoidin I-like domains 3	9.2	
NM_008401	Itgam	integrin alpha M	2.42	
NM_008405	Itgb2l	integrin beta 2-like		9.64
	Jam3	Junction adhesion molecule 3	2.2	
NM_007736	Col4a5	procollagen, type IV, alpha 5	2.54	
XM_139187	Pcdh9	protocadherin 9		2.33
Apoptosis and Cell cycle control				
XM_194020	Acvr1c	activin A receptor, type IC	26.49	
NM_178655	Ank2	ankyrin 2, brain	17.4	
NM_153287	Axud1	AXIN1 up-regulated 1	2.71	
	Bcl2	B-cell leukemia/lymphoma 2 (Bcl2), transcript variant 1	2.68	
NM_009744	Bcl6	B-cell leukemia/lymphoma 6	2.02	
NM_207653	Cflar	CASP8 and FADD-like apoptosis regulator	2.12	
NM_026373	Cdk2ap2	CDK2-associated protein 2		2.35
XM_484088	Cdc27	cell division cycle 27 homolog (S. cerevisiae)	2.36	
NM_009862	Cdc45l	cell division cycle 45 homolog (S. cerevisiae)-like		3.38
NM_026201	Ccar1	cell division cycle and apoptosis regulator 1	9.84	
NM_013538	Cdca3	cell division cycle associated 3	2.18	
NM_011806	Dmtf1	cyclin D binding myb-like transcription factor 1	2.88	
NM_028399	Ccnt2	cyclin T2	9.26	
NM_009874	Cdk7	cyclin-dependent kinase 7 (homolog of Xenopus MO15 cdk-activating kinase)	15.94	
NM_007837	Ddit3	DNA-damage inducible transcript 3	13.72	9
NM_007950	Ereg	epiregulin	5.85	
NM_008087	Gas2	Growth arrest specific 2	2.01	
XM_137276	Gas2l3	growth arrest-specific 2 like 3	4.26	
NM_146071	Muc20	mucin 20		2.96
NM_009044	Rel	reticuloendotheliosis oncogene		2.35
NM_133810	Stk17b	serine/threonine kinase 17b (apoptosis-inducing)	2.27	
NM_028769	Syvn1	synovial apoptosis inhibitor 1, synoviolin		4.77
NM_021897	Trp53inp1	transformation related protein 53 inducible nuclear protein 1	2.49	
Biosynthesis and Metabolism				
	---	Acyl-CoA synthetase long-chain family member 5	17.14	
NM_029901	Akr1c21	aldo-keto reductase family 1, member C21		2.14
NM_023179	Atp6v1g2	ATPase, H+ transporting, V1 subunit G isoform 2		2.23
1451144_at	Bxdc2	brix domain containing 2	2.19	
NM_023525	Cad	carbamoyl-phosphate synthetase 2, aspartate transcarbamylase, and dihydroorotase		2.4
NM_198415	Ckmt2	creatine kinase, mitochondrial 2		29.85
NM_007710	Ckm	creatine kinase, muscle		21.08
NM_030225	Dlst	dihydrolipoamide S-succinyltransferase (E2 component of 2-oxo-glutarate complex)	3.28	
NM_021896	Gucy1a3	guanylate cyclase 1, soluble, alpha 3	5.6	
NM_011846	Mmp17	matrix metallopeptidase 17	24.22	
NM_138656	Mvd	mevalonate (diphospho) decarboxylase		3.46
NM_009127	Scd1	stearoyl-Coenzyme A desaturase 1	2.26	

Table 3.2. TM-induced Nrf2-dependent genes in mouse small intestine and liver…..continued…

GenBank Accession	Gene Symbol	Gene Title	SIT*	Liver**
Calcium homeostasis				
NM_013471	Anxa4	Annexin A4	5.2	
NM_009722	Atp2a2	ATPase, Ca++ transporting, cardiac muscle, slow twitch 2		2.65
NM_023116	Cacnb2	Calcium channel, voltage-dependent, beta 2 subunit	14.13	
NM_009781	Cacna1c	Calcium channel, voltage-dependent, L type, alpha 1C subunit	7.94	
NM_028231	Kcnmb2	potassium large conductance calcium-activated channel, subfamily M, beta member 2	4.62	
Cell Growth and Differentiation				
NM_010111	Efnb2	ephrin B2	2.67	
NM_177390	Myo1d	Myosin ID	2.68	
NM_145610	Ppan	peter pan homolog (Drosophila)		2.04
NM_021883	Tmod1	tropomodulin 1	2.7	
NM_009394	Tnnc2	troponin C2, fast		16.76
ER/Golgi transport and ER/Golgi biosynthesis/metabolism				
NM_025445	Arfgap3	ADP-ribosylation factor GTPase activating protein 3		2.58
NM_025505	Blzf1	basic leucine zipper nuclear factor 1	7.72	
NM_009938	Copa	coatomer protein complex subunit alpha		2.4
NM_025673	Golph3	Golgi phosphoprotein 3	2.57	
NM_146133	Golph3l	golgi phosphoprotein 3-like		2.41
NM_008408	Itm1	intergral membrane protein 1	6.62	2.56
NM_027400	Lman1	Lectin, mannose-binding		2.79
NM_025408	Phca	phytoceramidase, alkaline	3.04	
NM_009178	Siat4c	ST3 beta-galactoside alpha-2,3-sialyltransferase 4	2.4	
NM_020283	B3galt1	UDP-Gal:betaGlcNAc beta 1,3-galactosyltransferase, polypeptide 1		2.54
NM_011716	Wfs1	Wolfram syndrome 1 homolog (human)		2.02
Electron Transport				
NM_015751	Abce1	ATP-binding cassette, sub-family E (OABP), member 1		2.48
NM_010001	Cyp2c37	cytochrome P450, family 2. subfamily c, polypeptide 37	5.58	
NM_023913	Ern1	Endoplasmic reticulum (ER) to nucleus signalling 1		2.12
XM_129326	Gucy2g	guanylate cyclase 2g	2.39	
NM_007952	Pdia3	protein disulfide isomerase associated 3		3.11
NM_009787	Pdia4	protein disulfide isomerase associated 4		3.19
XM_907880	Pdia6	protein disulfide isomerase associated 6		2.9
XM_284053	Steap2	six transmembrane epithelial antigen of prostate 2	3.23	
NM_198295	A730024F05Rik	Thioredoxin domain containing 10	2.91	
NM_029572	Txndc4	thioredoxin domain containing 4 (endoplasmic reticulum)		2.47
NM_023140	Txnl2	Thioredoxin-like 2	8.25	
G-protein coupled receptors				
NM_008158	Gpr27	G protein-coupled receptor 27	2.72	
NM_145066	Gpr85	G protein-coupled receptor 85		3.78
AK015353	Grm2	G protein-coupled receptor, family C, group 1, member B	2.18	
NM_008177	Grpr	gastrin releasing peptide receptor		2.18
NM_010314	Gngt1	guanine nucleotide binding protein (G protein), gamma transducing activity polypeptide 1		2.02
NM_139270	Pthr2	parathyroid hormone receptor 2		2.12
NM_011056	Pde4d	phosphodiesterase 4D, cAMP specific	2.78	
NM_022881	Rgs18	regulator of G-protein signaling 18		2.36
Kinases and Phosphatases				
NM_153066	Ak5	adenylate kinase 5	2.33	
NM_144817	Camk1g	calcium/calmodulin-dependent protein kinase I gamma		2.32
NM_139059	Csnk1d	Casein kinase 1, delta (Csnk1d), transcript variant 2	2.08	
NM_177914	MGI:3580254	diacylglycerol kinase kappa	13.2	
NM_130447	Dusp16	dual specificity phosphatase 16	3.17	2.13
NM_019987	Ick	intestinal cell kinase		2.06

Table 3.2…..continued…

GenBank Accession	Gene Symbol	Gene Title	SIT*	Liver**
XM_283179	Mast4	microtubule associated serine/threonine kinase family member 4	3.62	
NM_016700	Mapk8	mitogen activated protein kinase 8	12.43	
	Mapk8	mitogen activated protein kinase 8	7.41	
NM_172688	Map3k7	mitogen activated protein kinase kinase kinase 7	3.29	
NM_011101	Prkca	Protein kinase C, alpha	2.04	
NM_011104	Prkce	protein kinase C, epsilon	3.3	
NM_021880	Prkar1a	protein kinase, cAMP dependent regulatory, type I, alpha		15.23
NM_175638	Prkwnk4	Protein kinase, lysine deficient 4		8.16
NM_016979	Prkx	protein kinase, X-linked	2.27	
NM_133485	Ppp1r14c	Protein phosphatase 1, regulatory (inhibitor) subunit 14c		5.03
NM_012024	Ppp2r5e	protein phosphatase 2, regulatory subunit B (B56), epsilon isoform	2.49	
NM_008913	Ppp3ca	Protein phosphatase 3, catalytic subunit, alpha isoform	14.5	
AK134422	Ptp	Protein tyrosine phosphatase		3.27
NM_028259	Rps6kb1	ribosomal protein S6 kinase, polypeptide 1	2.05	
NM_031880	Tnk1	tyrosine kinase, non-receptor, 1	2.54	
Nuclear Assembly and Processing				
NM_010613	Khsrp	KH-type splicing regulatory protein	2.44	
NM_008671	Nap1l2	nucleosome assembly protein 1-like 2		4.7
NM_026175	Sf3a1	splicing factor 3a, subunit 1		2.77
NM_009408	Top1	Topoisomerase (DNA) I	5.94	
NM_008717	Zfml	Zinc finger, matrin-like		2.19
Glucose biosynthesis/metabolism				
NM_009605	Adipoq	adiponectin, C1Q and collagen domain containing		2.23
NM_018763	Chst2	Carbohydrate sulfotransferase 2		2.02
NM_008079	Galc	galactosylceramidase		2.95
NM_029626	Glt8d1	glycosyltransferase 8 domain containing 1		2.17
NM_013820	Hk2	hexokinase 2	2.46	
NM_010705	Lgals3	Lectin, galactose binding, soluble 3	3.2	
NM_199446	Phkb	phosphorylase kinase beta	2.06	
NM_016752	Slc35b1	solute carrier family 35, member B1		2.13
Signaling molecules and interacting partners				
NM_029291	Ascc2	Activating signal cointegrator 1 complex subunit 2		3.24
NM_007498	Atf3	activating transcription factor 3	8.73	
NM_016707	Bcl11a	B-cell CLL/lymphoma 11A (zinc finger protein)	4.2	
NM_033601	Bcl3	B-cell leukemia/lymphoma 3	2.08	
NM_007553	Bmp2	bone morphogenetic protein 2	2.55	
NM_007558	Bmp8a	bone morphogenetic protein 8a	2.39	
NM_178661	Creb3l2	cAMP responsive element binding protein 3-like 2		2.01
NM_010016	Daf1	decay accelerating factor 1	2.29	
NM_007897	Ebf1	early B-cell factor 1	8.98	
NM_023580	Epha1	Eph receptor A1		2.037
NM_133753	Errfi1	ERBB receptor feedback inhibitor 1	2.53	
NM_0010058(	Erbb2ip	Erbb2 interacting protein	2.11	
NM_0010058(	Erbb2ip	Erbb2 interacting protein	2.04	
NM_007906	Eef1a2	eukaryotic translation elongation factor 1 alpha 2		3.67
NM_007917	Eif4e	eukaryotic translation initiation factor 4E	3.05	
NM_173363	Eif5	eukaryotic translation initiation factor 5	2.13	
NM_010515	Igf2r	Insulin-like growth factor 2 receptor		2.22
NM_010591	Jun	Jun oncogene		2.29
NM_010592	Jund1	Jun proto-oncogene related gene d1		2.43
NM_008416	Junb	Jun-B oncogene	2.36	
NM_013602	Mt1	metallothionein 1		2.15

Table 3.2…..continued…

GenBank Accession	Gene Symbol	Gene Title	SIT*	Liver**
NM_008630	Mt2	metallothionein 2	2.79	
NM_170671	Mycbpap	Mycbp associated protein		3.97
NM_177619	Myst2	MYST histone acetyltransferase 2		2
NM_009123	Nkx1-2	NK1 transcription factor related, locus 2 (Drosophila)	2.45	
NM_030612	Nfkbiz	nuclear factor of kappa light polypeptide gene enhancer in B-cells inhibitor, zeta	2.67	
NM_017373	Nfil3	nuclear factor, interleukin 3, regulated	12.68	3.34
NM_144892	Ncoa5	nuclear receptor coactivator 5	14.65	
NM_173440	Nrip1	nuclear receptor interacting protein 1	2.87	
BC032981	Nfxl1	nuclear transcription factor, X-box binding-like 1		3.13
NM_020005	Pcaf	P300/CBP-associated factor	2.33	
NM_027924	Pdgfd	platelet-derived growth factor, D polypeptide	6.17	
NM_017463	Pbx2	pre B-cell leukemia transcription factor 2		2.84
NM_026383	Pnrc2	proline-rich nuclear receptor coactivator 2		2.08
NM_145495	Rin1	Ras and Rab interactor 1	7.01	2.87
NM_011651	Stk22s1	serine/threonine kinase 22 substrate 1	2.36	
NM_175246	Snip1	Smad nuclear interacting protein 1		2.07
NM_007707	Socs3	suppressor of cytokine signaling 3	2.45	
NM_080843	Socs4	suppressor of cytokine signaling 4	2	
NM_009365	Tgfb1i1	transforming growth factor beta 1 induced transcript 1	2.22	
NM_0010130	Tgfbrap1	transforming growth factor, beta receptor associated protein 1	2.7	
NM_013869	Tnfrsf19	tumor necrosis factor receptor superfamily, member 19	2.4	
NM_010755	Maff	v-maf musculoaponeurotic fibrosarcoma oncogene family, protein F (avian)	2.92	
NM_009524	Wnt5a	wingless-related MMTV integration site 5A		8.25
Transport				
NM_007511	Atp7b	ATPase, Cu++ transporting, beta polypeptide		2.34
NM_011075	Abcb1b	ATP-binding cassette, sub-family B (MDR/TAP), member 1B		4.65
NM_008576	Abcc1	ATP-binding cassette, sub-family C (CFTR/MRP), member 1	2.37	
NM_172621	Clic5	Chloride intracellular channel 5, mRNA		2.39
NM_024406	Fabp4	Fatty acid binding protein 4, adipocyte	3.7	
NM_146188	Kctd15	potassium channel tetramerisation domain containing 15	2.82	
	Kctd7	potassium channel tetramerisation domain containing 7		2.65
NM_148938	Slc1a3	solute carrier family 1 (glial high affinity glutamate transporter), member 3	4.03	
NM_019481	Slc13a1	solute carrier family 13 (sodium/sulphate symporters), member 1	2.09	
NM_0010041	Slc13a5	solute carrier family 13 (sodium-dependent citrate transporter), member 5	6.88	
NM_011395	Slc22a3	solute carrier family 22 (organic cation transporter), member 3		2.07
NM_172980	Slc28a2	solute carrier family 28 (sodium-coupled nucleoside transporter), member 2	2	
NM_078484	Slc35a2	solute carrier family 35 (UDP-galactose transporter), member 2		6.5
NM_011990	Slc7a11	solute carrier family 7 (cationic amino acid transporter, y+ system), member 11	5.93	
NM_080852	Slc7a12	solute carrier family 7 (cationic amino acid transporter, y+ system), member 12		2.95
NM_011406	Slc8a1	Solute carrier family 8 (sodium/calcium exchanger), member 1	2.86	
NM_178892	Tiparp	TCDD-inducible poly(ADP-ribose) polymerase	2.27	
Ubiquitination and Proteolysis				
NM_027926	Cpa4	carboxypeptidase A4	2.29	
NM_011931	Cop1	Constitutive photomorphogenic protein		2.52
NM_013868	Hspb7	heat shock protein family, member 7 (cardiovascular)		2.25
NM_146042	Ibrdc2	IBR domain containing 2	6.77	
NM_009174	Siah2	seven in absentia 2	2.46	
	Siah2	seven in absentia 2		2.12
NM_025692	Ube1dc1	ubiquitin-activating enzyme E1-domain containing 1		2.79
NM_173443	Vcpip1	valosin containing protein (p97)/p47 complex interacting protein 1	2.12	
Molecular chaperones and Heat Shock Proteins				
NM_0010124	Hspb6	heat shock protein, alpha-crystallin-related, B6	2.13	

Table 3.2…..continued…

GenBank Accession	Gene Symbol	Gene Title	SIT*	Liver**
NM_010918	Nktr	natural killer tumor recognition sequence		2.02
NM_030201	Stch	stress 70 protein chaperone, microsome-associated, human homolog		2.47
	Stch	stress 70 protein chaperone, microsome-associated, human homolog	2.37	
Miscellaneous				
NM_008161	Gpx3	glutathione peroxidase 3		5.79
NM_028733	Pacsin3	Protein kinase C and casein kinase II substrate 3 (Pacsin3)		2.12
NM_009409	Top2b	Topoisomerase (DNA) II beta (Top2b), mRNA		3.39
NM_020283	B3galt1	UDP-Gal:betaGlcNAc beta 1,3-galactosyltransferase, polypeptide 1		2.45

*Genes that were induced >2-fold by TM only in small intestine of Nrf2 wild-type mice but not in small intestine of Nrf2 knockout mice compared with vehicle treatment at 3h. The relative mRNA expression levels of each gene in treatment group over vehicle group (fold changes) are listed.

**Genes that were induced >2-fold by TM only in liver of Nrf2 wild-type mice but not in liver of Nrf2 knockout mice compared with vehicle treatment at 3h. The relative mRNA expression levels of each gene in treatment group over vehicle group (fold changes) are listed.

Table 3.2.

GenBank Accession	Gene Symbol	Gene Title	SIT*	Liver**
Cell Adhesion				
NM_174988	Cdh22	cadherin 22	0.47	
NM_053096	Cml2	camello-like 2	0.45	
NM_009818	Catna1	Catenin (cadherin associated protein), alpha 1		0.13
NM_008729	Catnd2	Catenin (cadherin associated protein), delta 2		0.5
XM_488510	Cspg2	chondroitin sulfate proteoglycan 2	0.43	
NM_018764	Pcdh7	protocadherin 7	0.21	
NM_053134	Pcdhb9	protocadherin beta 9	0.28	
NM_033595	Pcdhga12	Protocadherin gamma subfamily A, 10, mRNA		0.4
Apoptosis and Cell cycle control				
NM_007566	Birc6	baculoviral IAP repeat-containing 6	0.49	
NM_009741	Bcl2	B-cell leukemia/lymphoma 2		0.25
NM_009950	Cradd	CASP2 and RIPK1 domain containing adaptor with death domain		0.43
NM_007609	Casp11	caspase 11, apoptosis-related cysteine peptidase	0.45	
NM_009811	Casp6	caspase 6	0.36	
NM_025680	Ctnnbl1	catenin, beta like 1	0.45	
NM_025866	Cdca7	cell division cycle associated 7		0.36
NM_026560	Cdca8	cell division cycle associated 8		0.37
XM_181420	Cgref1	cell growth regulator with EF hand domain 1	0.47	
NM_009131	Clec11a	C-type lectin domain family 11, member a	0.2	
NM_146207	Cul4a	cullin 4A	0.49	
NM_009873	Cdk6	cyclin-dependent kinase 6		0.47
NM_009876	Cdkn1c	cyclin-dependent kinase inhibitor 1C (P57)	0.48	
NM_007892	E2f5	E2F transcription factor 5	0.25	
NM_008655	Gadd45b	growth arrest and DNA-damage-inducible 45 beta		0.18
NM_183358	Gadd45gip1	growth arrest and DNA-damage-inducible, gamma interacting protein 1	0.45	
NM_010578	Itgb1	integrin beta 1 (fibronectin receptor beta)	0.12	
NM_019745	Pdcd10	programmed cell death 10	0.46	
NM_009383	Tial1	Tial1 cytotoxic granule-associated RNA binding protein-like 1	0.07	0.36
NM_009425	Tnfsf10	tumor necrosis factor (ligand) superfamily, member 10	0.33	
NM_009517	Wig1	wild-type p53-induced gene 1		0.5
Biosynthesis and Metabolism				
NM_177470	Acaa2	acetyl-Coenzyme A acyltransferase 2 (mitochondrial 3-oxoacyl-Coenzyme A thiolase)	0.49	
NM_133904	Acacb	Acetyl-Coenzyme A carboxylase beta		0.14
NM_009695	Apoc2	apolipoprotein C-II	0.41	
NM_010174	Fabp3	Fatty acid binding protein 3, muscle and heart	0.23	
NM_008609	Mmp15	matrix metallopeptidase 15	0.46	
NM_023792	Pank1	pantothenate kinase 1	0.29	0.3
NM_144844	Pcca	propionyl-Coenzyme A carboxylase, alpha polypeptide	0.49	
NM_013743	Pdk4	pyruvate dehydrogenase kinase, isoenzyme 4	0.4	
NM_019437	Rfk	riboflavin kinase	0.48	
NM_138758	Tmlhe	trimethyllysine hydroxylase, epsilon		0.37
NM_133995	Upb1	ureidopropionase, beta	0.42	
NM_009471	Umps	uridine monophosphate synthetase		0.36
Calcium homeostasis				
NM_013472	Anxa6	annexin A6		0.43
NM_007590	Calm3	calmodulin 3	0.43	
NM_023051	Clstn1	calsyntenin 1	0.5	
Electron Transport				
XM_485295	Cyb561d1	cytochrome b-561 domain containing 1	0.44	
NM_013809	Cyp2g1	cytochrome P450, family 2, subfamily g, polypeptide 1		0.43

Table 3.3. TM-suppressed Nrf2-dependent genes in mouse small intestine and liver…..continued…

GenBank Accession	Gene Symbol	Gene Title	SIT*	Liver**
NM_177380	Cyp3a44	cytochrome P450, family 3, subfamily a, polypeptide 44	0.39	
NM_018887	Cyp39a1	cytochrome P450, family 39, subfamily a, polypeptide 1	0.41	
NM_010012	Cyp8b1	cytochrome P450, family 8, subfamily b, polypeptide 1		0.5
NM_170778	Dpyd	dihydropyrimidine dehydrogenase	0.49	
NM_010231	Fmo1	flavin containing monooxygenase 1	0.42	
NM_008631	Mt4	metallothionein 4	0.13	
NM_026614	Ndufa5	NADH dehydrogenase (ubiquinone) 1 alpha subcomplex, 5	0.4	
NM_026610	Ndufb4	NADH dehydrogenase (ubiquinone) 1 beta subcomplex 4	0.47	
NM_010887	Ndufs4	NADH dehydrogenase (ubiquinone) Fe-S protein 4	0.47	
NM_178239	Ndor1	NADPH dependent diflavin oxidoreductase 1		0.44
XM_128552	Pdia2	protein disulfide isomerase associated 2	0.43	
NM_025848	Sdhd	succinate dehydrogenase complex, subunit D, integral membrane protein	0.45	
NM_013711	Txnrd2	thioredoxin reductase 2		0.4
NM_011743	Zfp106	zinc finger protein 106	0.1	
Golgi assembly and glycosylation				
NM_007454	Ap1b1	adaptor protein complex AP-1, beta 1 subunit	0.49	
NM_028758	Gga2	Golgi associated, gamma adaptin ear containing, ARF binding protein 2		0.44
NM_008315	St3gal2	ST3 beta-galactoside alpha-2,3-sialyltransferase 2	0.5	
G-protein coupled receptors				
NM_008315	Htr7	5-hydroxytryptamine (serotonin) receptor 7 (Htr7), mRNA		0.47
NM_177231	Arrb1	arrestin, beta 1	0.38	
NM_030258	Gpr146	G protein-coupled receptor 146		0.49
NM_010309	Gnas	GNAS (guanine nucleotide binding protein, alpha stimulating) complex locus	0.38	
NM_023121	Gngt2	guanine nucleotide binding protein (G protein), gamma transducing activity polypeptide 2		0.47
NM_008142	Gnb1	guanine nucleotide binding protein, beta 1	0.5	
NM_053235	V1rc5	vomeronasal 1 receptor, C5		0.43
Kinases and Phosphatases				
NM_177343	Camk1d	Calcium/calmodulin-dependent protein kinase 1D		0.18
NM_009793	Camk4	Calcium/calmodulin-dependent protein kinase IV (Camk4)		0.11
NM_013642	Dusp1	dual specificity phosphatase 1		0.44
NM_010765	Mapkapk5	MAP kinase-activated protein kinase 5	0.47	
NM_011951	Mapk14	mitogen activated protein kinase 14	0.46	
NM_011944	Map2k7	mitogen activated protein kinase kinase 7		0.16
NM_023538	Mulk	multiple substrate lipid kinase	0.45	
NM_145962	Pank3	pantothenate kinase 3	0.4	
NM_00102495	Pik3r1	phosphatidylinositol 3-kinase, regulatory subunit, polypeptide 1 (p85 alpha)	0.46	
NM_145401	Prkag2	protein kinase, AMP-activated, gamma 2 non-catalytic subunit	0.49	0.12
NM_017374	Ppp2cb	Protein phosphatase 2a, catalytic subunit, beta isoform	0.44	
NM_008914	Ppp3cb	protein phosphatase 3, catalytic subunit, beta isoform		0.44
NM_019651	Ptpn9	Protein tyrosine phosphatase, non-receptor type 9		0.23
NM_011213	Ptprf	protein tyrosine phosphatase, receptor type, F	0.4	
NM_009184	Ptk6	PTK6 protein tyrosine kinase 6	0.37	
NM_013845	Ror1	Receptor tyrosine kinase-like orphan receptor 1		0.43
NM_019924	Rps6ka4	ribosomal protein S6 kinase, polypeptide 4	0.43	
Nuclear assembly and processing				
NM_148948	Dicer1	Dicer1, Dcr-1 homolog (Drosophila)	0.43	
XM_131040	Hist2h2bb	Histone 2, H2bb	0.37	
NM_019786	Tbk1	TANK-binding kinase 1	0.4	
Glucose biosynthesis/metabolism				
NM_019395	Fbp1	fructose bisphosphatase 1	0.47	
NM_025799	Fuca2	fucosidase, alpha-L- 2, plasma	0.44	

Table 3.3…..continued…

GenBank Accession	Gene Symbol	Gene Title	SIT*	Liver**
NM_008155	Gpi1	glucose phosphate isomerase 1		0.49
NM_008061	G6pc	glucose-6-phosphatase, catalytic	0.26	
NM_00101337	Lman2l	lectin, mannose-binding 2-like		0.49
NM_008548	Man1a	mannosidase 1, alpha	0.45	
NM_010956	Ogdh	Oxoglutarate dehydrogenase (lipoamide)	0.25	
NM_00101336	Prkaa1	protein kinase, AMP-activated, alpha 1 catalytic subunit		0.49
Signaling molecules and interacting partners				
NM_009755	Bmp1	bone morphogenetic protein 1	0.42	
NM_00101336	E2f8	E2F transcription factor 8		0.41
NM_010141	Epha7	Eph receptor A7		0.49
NM_020273	Gmeb1	glucocorticoid modulatory element binding protein 1	0.48	
NM_010323	Gnrhr	Gonadotropin releasing hormone receptor	0.28	
NM_176958	Hif1an	hypoxia-inducible factor 1, alpha subunit inhibitor	0.49	
NM_010547	Ikbkg	inhibitor of kappaB kinase gamma		0.45
NM_010515	Igf2r	insulin-like growth factor 2 receptor	0.44	
NM_010513	Igf1r	insulin-like growth factor I receptor	0.35	0.5
NM_009697	Nr2f2	Nuclear receptor subfamily 2, group F, member 2		0.45
	Pdap1	PDGFA associated protein 1		0.47
NM_013634	Pparbp	peroxisome proliferator activated receptor binding protein	0.44	
NM_027230	Prkcbp1	protein kinase C binding protein 1	0.48	
NM_026880	Pink1	PTEN induced putative kinase 1	0.48	
NM_018773	Scap2	src family associated phosphoprotein 2	0.49	
NM_007706	Socs2	Suppressor of cytokine signaling 2		0.44
NM_178111	Trp53inp2	tumor protein p53 inducible nuclear protein 2		0.47
NM_011703	Vipr1	vasoactive intestinal peptide receptor 1		0.4
NM_010153	Erbb3	v-erb-b2 erythroblastic leukemia viral oncogene homolog 3 (avian)	0.46	
Transport				
NM_009727	Atp8a1	ATPase, aminophospholipid transporter (APLT), class I, type 8A, member 1		0.44
NM_024173	Atp6v1g1	ATPase, H+ transporting, V1 subunit G isoform 1	0.46	
NM_029600	Abcc3	Multidrug resistance-associated protein 3 (Abcc3)		0.46
NM_010604	Kcnj16	potassium inwardly-rectifying channel, subfamily J, member 16	0.15	
NM_018824	Slc23a2	Sodium-dependent vitamin C transporter type 2 (Slc23a1)		0.45
NM_011397	Slc23a1	solute carrier family 23 (nucleobase transporters), member 1		0.3
NM_008063	Slc37a4	solute carrier family 37 (glycerol-6-phosphate transporter), member 4	0.46	
NM_018760	Slc4a4	solute carrier family 4 (anion exchanger), member 4	0.5	
NM_016917	Slc40a1	Solute carrier family 40 (iron-regulated transporter), member 1		0.45
XM_127434	Slc9a3	solute carrier family 9 (sodium/hydrogen exchanger), member 3	0.41	
Detoxifying enzymes				
NM_008129	Gclm	glutamate-cysteine ligase , modifier subunit	0.45	
NM_029555	Gstk1	glutathione S-transferase kappa 1	0.45	
NM_010357	Gsta4	glutathione S-transferase, alpha 4	0.49	
NM_010359	Gstm3	glutathione S-transferase, mu 3	0.22	
XM_359308	Gstm7	glutathione S-transferase, mu 7	0.46	
NM_008185	Gstt1	glutathione S-transferase, theta 1	0.43	
NM_025304	Lcmt1	leucine carboxyl methyltransferase 1	0.48	
NM_019946	Mgst1	microsomal glutathione S-transferase 1	0.18	
NM_025569	Mgst3	microsomal glutathione S-transferase 3	0.47	
NM_019878	Sult1b1	sulfotransferase family 1B, member 1	0.41	
Ubiquitination and Proteolysis				
NM_011780	Adam23	A disintegrin and metallopeptidase domain 23		0.34
NM_007754	Cpd	carboxypeptidase D	0.45	

Table 3.3…..continued…

GenBank Accession	Gene Symbol	Gene Title	SIT*	Liver**
NM_134015	Fbxw11	F-box and WD-40 domain protein 11	0.27	
NM_177703	Fbxw19	F-box and WD-40 domain protein 19		0.11
NM_028705	Herc3	hect domain and RLD 3		0.35
NM_145486	Mar 2	membrane-associated ring finger (C3HC4) 2	0.5	0.28
NM_020487	Prss21	protease, serine, 21	0.12	
NM_008944	Psma2	proteasome (prosome, macropain) subunit, alpha type 2	0.49	
NM_013640	Psmb10	proteasome (prosome, macropain) subunit, beta type 10	0.5	
XM_483996	Usp34	ubiquitin specific peptidase 34		0.49
NM_013918	Usp25	Ubiquitin-specific processing protease		0.47
Molecular Chaperones and Heat Shock Proteins				
NM_146036	Ahsa1	AHA1, activator of heat shock 90kDa protein ATPase homolog 1 (yeast)		0.4
NM_025384	Dnajc15	DnaJ (Hsp40) homolog, subfamily C, member 15	0.5	
NM_139139	Dnajc17	DnaJ (Hsp40) homolog, subfamily C, member 17		0.43
NM_024219	Hsbp1	heat shock factor binding protein 1	0.46	
	Hspa1b	heat shock protein 1B		0.41
NM_019960	Hspb3	heat shock protein 3	0.3	
Miscellaneous				
NM_008708	Nmt2	N-myristoyltransferase 2	0.14	
NM_007453	Prdx6	peroxiredoxin 6	0.46	
NM_011434	Sod1	Superoxide dismutase 1, soluble	0.25	

*Genes that were suppressed >2-fold by TM only in small intestine of Nrf2 wild-type mice but not in small intestine of Nrf2 knockout mice compared with vehicle treatment at 3h. The relative mRNA expression levels of each gene in treatment group over vehicle group (fold changes) are listed.

**Genes that were suppressed >2-fold by TM only in liver of Nrf2 wild-type mice but not in liver of Nrf2 knockout mice compared with vehicle treatment at 3h. The relative mRNA expression levels of each gene in treatment group over vehicle group (fold changes) are listed.

Table 3.3.

Gene Name	GenBank Accession No.	Forward Primer	Reverse Primer
P.pyralis (firefly) luciferase	M15077	5'-TCATTCTTCGCCAAAAGCACT-3'	5'-GCTTCCCCGACTTCTTTCG-3'
Homo sapiens cyclin D1	NM_053056	5'-CCGCACGATTTCATTGAAC-3'	5'-CACAGAGGGCAACGAAGGTC-3'
Homo sapiens c-myc binding protein (MYCBP)	NM_012333	5'-CTGCTTCGCCTAGAACTGGC-3'	5'-TGAGGTGGTTCATACTGAGCAAG-3'
Homo sapiens activating transcription factor 2 (ATF2)	NM_001880	5'-GGTCATGGTAGCGGATTGGT-3'	5'-GCTGGAGAAGCCGGAGTTTC-3'
Homo sapiens ELK1, member of ETS oncogene family (ELK1)	NM_005229	5'-TGGACCCATCTGTGACGCT-3'	5'-GAATTCACCACCATCCCGTG-3'
Homo sapiens serum response factor (c-fos serum response element-binding transcription factor, SRF)	NM_003131	5'-TCAACTCGCCAGACTCTCCA-3'	5'-CTCCGACACCTGGTAGGTGAG-3'
Homo sapiens cAMP responsive element binding protein 1 (CREB1)	NM_182898	5'-GACGAGGATCCGGACGAGA-3'	5'-TCCAATGACATCACCCAGACC-3'
Homo sapiens solute carrier organic anion transporter family, member 1B3 (SLCO1B3)	NM_019844	5'-GCTTTGCACTGGGATCTCTGT-3'	5'-TCCAACCCAACGAGAGTCCT-3'
Homo sapiens ATP-binding cassette, sub-family C (CFTR/MRP), member 1 (ABCC1)	NM_004996	5'-GCGCTGGCTTCCAACTATTG-3'	5'-AGGGCTCCATAGACGCTCAG-3'
Homo sapiens ATP-binding cassette, sub-family C (CFTR/MRP), member 2 (ABCC2)	NM_000392	5'-GTCATGATCTGCATGGCCAC-3'	5'-TGGCGGGAGGTAGACACATAA-3'
Homo sapiens ATP-binding cassette, sub-family C (CFTR/MRP), member 3 (ABCC3)	NM_003786	5'-GGTCAGCACCCCTGCAGAT-3'	5'-TGGAATCAGCAAGACCATGAAA-3'
Homo sapiens cytoplasmic beta-actin	M10277	5'-CCCAGCCATGTACGTTGCTA-3'	5'-CAGTGTGGGTGACCCCGT-3'

Table 4.1.Oligonucleotide primers used for quantitative real-time PCR (qRT-PCR)

	Luc	Luc	CyD1	CyD1	cMyc	cMyc	ATF-2	ATF-2	Elk-1	Elk-1	SRF	SRF	CREB5	CREB5	SLCO	SLCO	MRP1	MRP1	MRP2	MRP2	MRP3	MRP3
	6hr	10hr	6hr	10hr	6hr	10hr	6hr	10hr	6hr	10hr	6hr	10hr	6hr	10hr	6hr	10hr	6hr	10hr	6hr	10hr	6hr	10hr
Control (DMSO)	1.00	1.00	1.00	1.00	1.00	1.00	1.00	1.00	1.00	1.00	1.00	1.00	1.00	1.00	1.00	1.00	1.00	1.00	1.00	1.00	1.00	1.00
S25	2.78	2.3	1.09	0.89	1.03	1.28	2.64	1.43	2.84	1.32	1.26	0.88	0.32	0.15	0.36	0.40	1.63	0.93	2.71	2.30	2.37	0.84
	±0.16	± 0.10	±0.15	±0.23	±0.31	±0.34	±0.18	±0.22	±0.10	±0.26	±0.35	±0.2	±0.06	±0.04	±0.10	±0.15	±0.19	±0.11	±0.24	±0.28	±0.32	±0.16
E20	1.16	1.78	1.71	1.32	1.08	1.17	1.07	1.10	1.12	1.11	0.49	1.16	0.46	0.10	1.47	1.27	2.11	1.39	1.79	1.85	1.59	1.07
	±0.22	±0.29	±0.31	±0.19	±0.24	±0.17	±0.16	±0.27	±0.13	±0.17	±0.09	±0.11	±0.20	±0.03	±0.22	±0.16	±0.28	±0.21	±0.16	±0.21	±0.25	±0.10
E100	6.74	2.73	3.30	1.22	1.04	0.70	1.36	0.70	1.25	0.78	1.02	0.97	0.48	0.32	1.48	2.02	2.49	1.89	1.26	1.85	0.86	0.65
	±0.54	±0.25	±0.47	±0.16	±0.09	±0.15	±0.25	±0.14	±0.2	±0.14	±0.23	±0.14	±0.18	±0.21	±0.18	±0.31	±0.37	±0.19	±0.15	±0.27	±0.19	±0.23
E20+S25	7.60	3.17	0.94	0.53	1.40	1.40	2.34	1.48	1.43	0.87	0.56	0.44	0.25	0.52	0.64	0.22	1.07	0.81	3.34	4.75	1.34	0.75
	±0.78	±0.37	±0.26	±0.14	±0.23	±0.37	±0.35	±0.23	±0.31	±0.15	±0.12	±0.07	±0.13	±0.19	±0.23	±0.11	±0.17	±0.05	±0.25	±0.68	±0.14	±0.08
E100+S25	16.41	3.43	0.90	0.52	1.23	0.94	1.68	0.81	1.42	0.67	0.71	0.42	0.21	0.17	0.46	0.24	1.22	0.77	2.87	4.56	1.24	0.61
	±0.98	±0.41	±0.32	±0.22	±0.17	±0.22	±0.16	±0.25	±0.15	±0.21	±0.16	±0.13	±0.06	±0.08	±0.16	±0.09	±0.33	±0.12	±0.20	±0.74	±0.06	±0.11

Table 4.2. Temporal gene expression profiles elicited by combinations of SFN and EGCG

HT-29 AP-1 cells were treated for 6 hr or 10 hr with individual dietary factors or combinations of SFN and EGCG as indicated. RNA was extracted, transcribed into

cDNA after ascertaining RNA integrity, and quantitative real-time PCR assays were performed using beta-actin as the housekeeping gene. Values represent mean ± standard deviation for three replicates of each gene, and are representative of two independent experiments.

	Luc	Luc	CyD1	CyD1	cMyc	cMyc	ATF-2	ATF-2	Elk-1	Elk-1	SRF	SRF	CREB5	CREB5	SLCO	SLCO	MRP1	MRP1	MRP2	MRP2	MRP3	MRP3
	6hr	10hr	6hr	10hr	6hr	10hr	6hr	10hr	6hr	10hr	6hr	10hr	6hr	10hr	6hr	10hr	6hr	10hr	6hr	10hr	6hr	10hr
Control (DMSO)	1.00	1.00	1.00	1.00	1.00	1.00	1.00	1.00	1.00	1.00	1.00	1.00	1.00	1.00	1.00	1.00	1.00	1.00	1.00	1.00	1.00	1.00
S25 +SOD	3.18 ±0.24	3.61 ±0.34	0.83 ±0.11	1.10 ±0.20	1.18 ±0.12	0.63 ±0.16	1.91 ±0.26	1.33 ±0.31	0.81 ±0.12	1.26 ±0.34	0.60 ±0.15	1.50 ±0.27	0.25 ±0.12	0.46 ±0.15	0.83 ±0.19	0.63 ±0.10	1.07 ±0.21	2.42 ±0.32	3.17 ±0.26	5.44 ±0.38	0.57 ±0.15	1.31 ±0.22
E20 +SOD	0.66 ±0.14	1.57 ±0.28	1.15 ±0.05	2.10 ±0.26	1.07 ±0.13	1.50 ±0.19	1.20 ±0.15	0.98 ±0.17	1.09 ±0.16	1.05 ±0.13	1.11 ±0.10	1.23 ±0.19	0.20 ±0.09	0.76 ±0.11	1.23 ±0.22	1.25 ±0.27	1.69 ±0.18	1.45 ±0.31	3.39 ±0.34	1.50 ±0.18	1.68 ±0.23	1.67 ±0.31
E100+SOD	3.24 ±0.35	3.97 0.21	0.60 ±0.17	0.87 ±0.11	0.42 ±0.15	0.41 ±0.10	0.62 ±0.16	0.30 ±0.12	0.37 ±0.15	0.41 ±0.17	1.24 ±0.33	1.88 ±0.45	0.07 ±0.03	0.20 ±0.08	0.68 ±0.16	0.45 ±0.12	0.69 ±0.24	0.89 ±0.18	5.35 ±0.29	0.80 ±0.12	0.35 ±0.18	0.74 ±0.24
E20+S25+SOD	2.21 ±0.15	1.58 ±0.13	0.80 ±0.19	2.01 ±0.25	0.86 ±0.22	1.14 ±0.17	1.99 ±0.25	1.43 ±0.18	1.57 ±0.25	1.21 ±0.19	1.12 ±0.24	1.37 ±0.15	0.12 ±0.07	0.54 ±0.16	0.72 ±0.21	0.64 ±0.19	2.26 ±0.26	3.46 ±0.35	6.96 ±0.48	5.38 ±0.35	1.69 ±0.13	1.52 ±0.20
E100+S25+SOD	6.93 ±0.36	1.67 ±0.23	0.32 ±0.14	1.83 ±0.27	0.38 ±0.16	0.86 ±0.09	0.38 ±0.21	0.94 ±0.29	1.08 ±0.15	1.51 ±0.23	0.82 ±0.14	1.65 ±0.25	0.22 ±0.13	0.71 ±0.20	0.49 ±0.18	0.48 ±0.15	1.61 ±0.14	3.20 ±0.20	1.61 ±0.23	7.04 ±0.28	0.60 ±0.15	1.35 ±0.28

Table 4.3. Temporal gene expression profiles elicited by combinations of SFN and EGCG in the presence of SOD

HT-29 AP-1 cells were co-treated for 6 hr or 10 hr with 20U/ml SOD and individual dietary factors or combinations of SFN and EGCG as indicated. RNA was extracted,

transcribed into cDNA after ascertaining RNA integrity, and quantitative real-time PCR assays were performed using beta-actin as the housekeeping gene. Values represent mean ± standard deviation for three replicates of each gene, and are representative of two independent experiments.

Matrix Family Human Nrf2 vs. AP-1	Matrix Family Murine Nrf2 vs. AP-1	Family Information
V$AP4R	V$AP4R	Activator protein 4 and related proteins
V$CDEF	-	Cell cycle regulators: Cell cycle dependent element
V$CHRF	-	Cell cycle regulators: Cell cycle homology element
-	V$CP2F	CP2-erythrocyte Factor related to drosophila Elf1
V$E2FF	-	E2F-myc activator/cell cycle regulator
-	V$E4FF	Ubiquitous GLI - Krueppel like zinc finger involved in cell cycle regulation
V$EBOX	-	E-box binding factors
V$EGRF	V$EGRF	EGR/nerve growth factor induced protein C & related factors
-	V$EKLF	Basic and erythroid krueppel like factors
-	V$ETSF	Human and murine ETS1 factors
V$EVI1	-	EVI1-myleoid transforming protein
-	V$FKHD	Fork head domain factors
V$GATA	-	GATA binding factors
-	V$GLIF	GLI zinc finger family
-	V$GREF	Glucocorticoid responsive and related elements
V$HAND	-	bHLH transcription factor dimer of HAND2 and E12
-	V$HESF	Vertebrate homologues of enhancer of split complex
-	V$HIFF	Hypoxia inducible factor, bHLH/PAS protein family
-	V$HNF6	Onecut homeodomain factor HNF6
-	V$INSM	Insulinoma associated factors
V$MAZF	V$MAZF	Myc associated zinc fingers
-	V$MOKF	Mouse Krueppel like factor
V$MYBL	-	Cellular and viral myb-like transcriptional regulators
V$MYOD	V$MYOD	Myoblast determining factors
V$NEUR	-	NeuroD, Beta2, HLH domain
V$NFKB	-	Nuclear factor kappa B/c-rel
V$NRF1	V$NRF1	Nuclear respiratory factor 1
V$PAX5	-	PAX-5 B-cell-specific activator protein
V$PAX9	-	PAX-9 binding sites
V$PBXC	-	PBX1 - MEIS1 complexes
-	V$PLAG	Pleomorphic adenoma gene
-	V$SF1F	Vertebrate steroidogenic factor
V$SP1F	V$SP1F	GC-Box factors SP1/GC
-	V$SRFF	Serum response element binding factor
V$STAF	-	Selenocysteine tRNA activating factor
V$STAT	-	Signal transducer and activator of transcription
-	V$XBBF	X-box binding factors
V$ZBPF	V$ZBPF	Zinc binding protein factors
-	V$ZF35	Zinc finger protein ZNF35

Table 5.1. A. Human and Murine Matrix Families conserved between Nrf2 and AP-1

Matrix Family Human ATF2 vs. ELK1	Matrix Family Murine Atf2 vs. Elk1	Family Information
V$AP1F	-	AP1, Activator protein 1
-	V$BARB	Barbiturate-inducible element box from pro+eukaryotic genes
-	V$BNCF	Basonuclein rDNA transcription factor (PolI)
-	V$BRNF	Brn POU domain factors
V$CAAT	-	CCAAT binding factors
-	V$CLOX	CLOX and CLOX homology (CDP) factors
V$COMP	-	Factors which cooperate with myogenic proteins
-	V$CP2F	CP2-erythrocyte Factor related to drosophila Elf1
V$CREB	-	Camp-responsive element binding proteins
-	V$E2FF	E2F-myc activator/cell cycle regulator
V$EBOX	-	E-box binding factors
V$EGRF	-	EGR/nerve growth factor induced protein C & related factors
V$EKLF	-	Basic and erythroid krueppel like factors
V$EREF	-	Estrogen response elements
V$ETSF	V$ETSF	Human and murine ETS1 factors
-	V$EVI1	EVI1-myleoid transforming protein
V$FKHD	V$FKHD	Fork head domain factors
-	V$FXRE	Farnesoid X - activated receptor response elements
-	V$GATA	GATA binding factors
-	V$GCMF	Chorion-specific transcription factors with a GCM DNA binding domain
V$GFI1	-	Growth factor independence transcriptional repressor
V$GKLF	V$GKLF	Gut-enriched Krueppel like binding factor
V$GLIF	-	GLI zinc finger family
-	V$HAML	Human acute myelogenous leukemia factors
-	V$HOXC	HOX - PBX complexes
-	V$HOXF	Factors with moderate activity to homeo domain consensus sequence
-	V$IKRS	Ikaros zinc finger family
V$IRFF	V$IRFF	Interferon regulatory factors
V$LEFF	V$LEFF	LEF1/TCF, involved in the Wnt signal transduction pathway
V$MAZF	-	Myc associated zinc fingers
-	V$MEF2	MEF2, myocyte-specific enhancer binding factor
V$MYBL	-	Cellular and viral myb-like transcriptional regulators
-	V$MYT1	MYT1 C2HC zinc finger protein
V$MZF1	-	Myeloid zinc finger 1 factors
V$NBRE	-	NGFI-B response elements, nur subfamily of nuclear receptors
-	V$NFAT	Nuclear factor of activated T-cells
V$NFKB	-	Nuclear factor kappa B/c-rel
V$NKXH	V$NKXH	NKX homeodomain factors
V$NR2F	V$NR2F	Nuclear receptor subfamily 2 factors
-	V$OCT1	Octamer binding protein
V$PARF	V$PARF	PAR/bZIP family
V$PAX5	-	PAX-5 B-cell-specific activator protein
V$PAX6	-	PAX-4/PAX-6 paired domain binding sites
V$PBXC	-	PBX1 - MEIS1 complexes
V$PERO	-	Peroxisome proliferator-activated receptor
-	V$PLZF	C2H2 zinc finger protein PLZF
V$RREB	-	Ras-responsive element binding protein
V$RXRF	-	RXR heterodimer binding sites
V$SNAP	-	snRNA-activating protein complex
V$SP1F	-	GC-Box factors SP1/GC
-	V$SRFF	Serum response element binding factor
V$STAF	-	Selenocysteine tRNA activating factor
-	V$STAT	Signal transducer and activator of transcription
V$TALE	-	TALE homeodomain class recognizing TG motifs
-	V$TBPF	Tata-binding protein factor
-	V$TEAF	TEA/ATTS DNA binding domain factors
-	V$XBBF	X-box binding factors
V$ZBPF	-	Zinc binding protein factors

Table 5.1. B. Human and Murine Matrix Families conserved between ATF-2 and ELK1

Family/Matrix	Sequence Name	Optimized Threshold	Start Position	End Position	Strand	Matrix Similarity	Core Similarity	Sequence (Core Sequence in Upper Case)
Activator protein 1, AP-1								
V$AP1F/V$AP1.02	Nrf2-mouse	0.87	237	247	-	0.88	1	gcgGAGTcagg
Nuclear factor (erythroid-derived 2)-like 2, NRF2								
V$AP1R/V$NFE2L2.01	Ap1-human	0.7	265	289	+	0.718	0.826	accagacaATGAatcagctcccttg
Activator protein 4								
V$AP4R/V$AP4.01	Ap1-human	0.85	236	252	-	0.887	1	gggccCAGCtggcggcc
V$AP4R/V$AP4.01	Ap1-human	0.85	554	570	-	0.926	1	agaacCAGCtcctggcc
V$AP4R/V$AP4.01	Nrf2-human	0.85	279	295	-	0.942	1	actgcCAGCtggggtcc
Activator protein 4								
V$AP4R/V$AP4.02	Nrf2-mouse	0.92	133	149	-	0.925	1	attagcAGCTgtttgcc
V$AP4R/V$AP4.02	Ap1-mouse	0.92	183	199	-	0.944	1	ctttacAGCTgtttccc
V$AP4R/V$AP4.02	Nrf2-mouse	0.92	134	150	+	0.943	1	gcaaacAGCTgctaatc
V$AP4R/V$AP4.02	Ap1-mouse	0.92	469	485	+	0.975	1	gctgacAGCTgctggcg
BTB/POZ-bZIP transcription factor BACH1, forms heterodimers with the small Maf protein family								
V$AP1R/V$BACH1.01	Ap1-human	0.82	40	64	-	0.866	1	cagcactgaTGAGtgatcagctctc
Bach2 bound TRE								
V$AP1R/V$BACH2.01	Nrf2-human	0.89	316	340	+	0.918	0.868	cgagcttctTGCGtcagccccggcg
Paraxis (TCF15), member of the Twist subfamily of Class B bHLH factors, forms heterodimers with E12								
V$AP4R/V$PARAXIS.01	Ap1-mouse	0.86	55	71	+	0.904	0.882	ccgACCAcatgagtagg
V$AP4R/V$PARAXIS.01	Nrf2-mouse	0.86	770	786	-	0.891	0.882	ggcAGCAcctgctggga
V$AP4R/V$PARAXIS.01	Ap1-mouse	0.86	18	34	-	0.888	0.882	gtgAGCAcatgctgaac
Cell cycle-dependent element, CDF-1 binding site (CDE/CHR tandem elements regulate cell cycle dependent repression)								
V$CDEF/V$CDE.01	Ap1-human	0.87	185	197	-	0.898	1	tgatCGCGgttag
V$CDEF/V$CDE.01	Nrf2-human	0.87	364	376	-	0.92	1	gccgCGCGggctg
V$CDEF/V$CDE.01	Nrf2-human	0.87	540	552	-	0.875	1	gcggCGCGgacag
Cell cycle gene homology region (CDE/CHR tandem elements regulate cell cycle dependent repression)								
V$CHRF/V$CHR.01	Ap1-human	0.92	199	211	-	0.943	1	ccgtTTGAaaacc
V$CHRF/V$CHR.01	Nrf2-human	0.92	131	143	-	0.929	1	cgctTTGAaacag
CP2								
V$CP2F/V$CP2.01	Nrf2-mouse	0.9	800	818	+	0.9	1	ccCTGGgctgtgccaagaa
V$CP2F/V$CP2.01	Ap1-mouse	0.9	518	536	-	0.912	1	cgCTGGctccggctcccgg
V$CP2F/V$CP2.01	Ap1-mouse	0.9	427	445	+	0.949	0.909	gaCTTGgtgggggcggtgtc
E2F, involved in cell cycle regulation, interacts with Rb p107 protein								
V$E2FF/V$E2F.03	Ap1-human	0.85	368	384	-	0.874	1	gcgtgGCGCgcccacgg
V$E2FF/V$E2F.03	Ap1-human	0.85	369	385	+	0.928	1	cgtggGCGCgcccacgcc
V$E2FF/V$E2F.03	Nrf2-human	0.85	538	554	-	0.898	1	gcgcgGCGCggacaggg
GLI-Krueppel-related transcription factor, regulator of adenovirus E4 promoter								
V$E4FF/V$E4F.01	Ap1-mouse	0.82	384	396	+	0.887	0.789	atgAAGTcacgtg
V$E4FF/V$E4F.01	Nrf2-mouse	0.82	220	232	-	0.831	0.789	ctgAAGTcgcacg
MYC-MAX binding sites								
V$EBOX/V$MYCMAX.03	Ap1-human	0.91	411	423	-	0.925	1	gggcctCGCGccc
V$EBOX/V$MYCMAX.03	Nrf2-human	0.91	366	378	-	0.925	1	cggccgCGCGggc

Table 5.2. Matrices with conserved regulatory sequences in promoter regions of human, or murine, NRF2 and AP-1…..continued…

Family/Matrix	Sequence Name	Optimized Threshold	Start Position	End Position	Strand	Matrix Similarity	Core Similarity	Sequence (Core Sequence in Upper Case)
EGR1, early growth response 1 - in human								
V$EGRF/V$EGR1.02	Ap1-human	0.86	302	318	-	0.894	1	ggctggtgGGGCggtcg
V$EGRF/V$EGR1.02	Ap1-human	0.86	420	436	-	0.879	1	gggcgatgGGGCggggc
V$EGRF/V$EGR1.02	Ap1-human	0.86	506	522	+	0.866	0.789	ggtggcggCGGCgaagg
V$EGRF/V$EGR1.02	Ap1-human	0.86	568	584	+	0.862	0.789	tctggtggCGGCggggc
V$EGRF/V$EGR1.02	Nrf2-human	0.86	299	315	-	0.904	1	cggtccggGGGCcggaa
V$EGRF/V$EGR1.02	Nrf2-human	0.86	412	428	+	0.875	1	cccttgtgGGGCgggag
V$EGRF/V$EGR1.02	Nrf2-human	0.86	502	518	-	0.906	0.789	ggcggcggTGGCggctg
V$EGRF/V$EGR1.02	Nrf2-human	0.86	508	524	-	0.914	0.789	ggcggcggCGGCggtgg
V$EGRF/V$EGR1.02	Nrf2-human	0.86	511	527	-	0.911	0.789	ggcggcggCGGCggcgg
V$EGRF/V$EGR1.02	Nrf2-human	0.86	514	530	-	0.872	0.789	ggtggcggCGGCggcgg
V$EGRF/V$EGR1.02	Nrf2-human	0.86	694	710	+	0.915	1	cgggacggGGGCgggggg
EGR1, early growth response 1 - in mouse								
V$EGRF/V$EGR1.02	Ap1-mouse	0.86	428	444	+	0.863	1	acttggtgGGGCggtgt
V$EGRF/V$EGR1.02	Nrf2-mouse	0.86	663	679	-	0.865	0.789	aggtgaggCGGCggcaa
V$EGRF/V$EGR1.02	Nrf2-mouse	0.86	572	588	+	0.905	1	cccccaggGGGCgggag
V$EGRF/V$EGR1.02	Nrf2-mouse	0.86	566	582	-	0.903	1	ccccctggGGGCggaac
V$EGRF/V$EGR1.02	Ap1-mouse	0.86	405	421	-	0.874	1	cgacgacgGGGCggggc
V$EGRF/V$EGR1.02	Nrf2-mouse	0.86	209	225	-	0.902	1	cgcacgggGGGCggagc
V$EGRF/V$EGR1.02	Ap1-mouse	0.86	538	554	+	0.978	1	cgcggcggGGGCgggcg
V$EGRF/V$EGR1.02	Nrf2-mouse	0.86	583	599	+	0.896	1	cgggggcgGGGCggact
V$EGRF/V$EGR1.02	Nrf2-mouse	0.86	179	195	+	0.893	1	gactggggGGGCcgaag
V$EGRF/V$EGR1.02	Ap1-mouse	0.86	584	600	+	0.891	1	ggcgggcGGGCggagt
V$EGRF/V$EGR1.02	Nrf2-mouse	0.86	460	476	-	0.875	1	ggggtaagGGGCggggc
Wilms Tumor Suppressor								
V$EGRF/V$WT1.01	Nrf2-mouse	0.92	372	388	-	0.945	0.837	agggaAGGGgggacaa
V$EGRF/V$WT1.01	Ap1-mouse	0.92	544	560	+	0.928	0.953	ggggCGGGcgcgggc
V$EGRF/V$WT1.01	Nrf2-mouse	0.92	578	594	+	0.98	0.953	ggggCGGGggcgggc
Kidney-enriched kruppel-like factor, KLF15								
V$EKLF/V$KKLF.01	Nrf2-mouse	0.91	372	388	-	0.949	1	aggggaGGGGgggacaa
V$EKLF/V$KKLF.01	Ap1-mouse	0.91	429	445	+	0.931	1	cttggtGGGGcggtgtc
V$EKLF/V$KKLF.01	Nrf2-mouse	0.91	579	595	+	0.94	1	ggggcgGGGGcgggggcg
V$EKLF/V$KKLF.01	Nrf2-mouse	0.91	584	600	+	0.948	1	ggggcgGGGGcggacta
V$EKLF/V$KKLF.01	Ap1-mouse	0.91	581	597	+	0.921	1	gtcggcGGGGcgggcgg
Elk-1 - in human								
V$ETSF/V$ELK1.02	Nrf2-human	0.91	84	104	-	0.958	1	ggagccccGGAAaggcgttgg
V$ETSF/V$ELK1.02	Nrf2-human	0.91	557	577	+	0.951	1	cggcagccGGAAcagggccgc
Elk-1 - in mouse								
V$ETSF/V$ELK1.02	Nrf2-mouse	0.91	305	325	+	0.987	1	ctccggccGGAAgcactcagg
V$ETSF/V$ELK1.02	Ap1-mouse	0.91	444	464	+	0.977	1	tctgccccGGAAgtgcctgtc

Table 5.2…..continued…

Family/Matrix	Sequence Name	Optimized Threshold	Start Position	End Position	Strand	Matrix Similarity	Core Similarity	Sequence (Core Sequence in Upper Case)
MEL1 (MDS1/EVI1-like gene 1) DNA-binding domain 2								
V$EVI1/V$MEL1.02	Ap1-human	0.99	48	64	-	1	1	cagcactGATGagtgat
V$EVI1/V$MEL1.02	Nrf2-human	0.99	604	620	-	0.995	1	ccatcatGATGagctgt
Fork head related activator-4 (FOXD1)								
V$FKHD/V$FREAC4.01	Ap1-mouse	0.78	179	195	+	0.811	1	ccaagggaAACAgctgt
V$FKHD/V$FREAC4.01	Nrf2-mouse	0.78	129	145	+	0.784	1	cttcggcaAACAgctgc
GATA-binding factor 1								
V$GATA/V$GATA1.03	Ap1-human	0.95	88	100	-	0.972	1	aacaGATAggtcc
V$GATA/V$GATA1.03	Nrf2-human	0.95	172	184	-	0.963	1	gcgaGATAaagag
Zinc finger transcription factor, Zic family member 2 (odd-paired homolog, Drosophila)								
V$GLIF/V$ZIC2.01	Ap1-mouse	0.89	431	445	-	0.938	1	gacaccgCCCCacca
V$GLIF/V$ZIC2.01	Nrf2-mouse	0.89	156	170	-	0.914	1	gacagcaCCCCcttg
Glucocorticoid receptor, C2C2 zinc finger protein binds glucocorticoid dependent to GREs, IR3 sites								
V$GREF/V$GRE.01	Nrf2-mouse	0.85	66	84	+	0.886	0.833	ggggctcccggtGTGCttg
V$GREF/V$GRE.01	Ap1-mouse	0.85	15	33	+	0.898	0.833	taggttcagcatGTGCtca
Heterodimers of the bHLH transcription factors HAND2 (Thing2) and E12								
V$HAND/V$HAND2_E12.01	Ap1-human	0.75	234	248	+	0.779	1	tgggccGCCAgctgg
V$HAND/V$HAND2_E12.01	Ap1-human	0.75	241	255	-	0.806	0.759	gcagggCCCAgctgg
V$HAND/V$HAND2_E12.01	Ap1-human	0.75	540	554	-	0.773	1	cgcagcGCCAtcttg
V$HAND/V$HAND2_E12.01	Nrf2-human	0.75	284	298	-	0.755	1	gggactGCCAgctgg
Hey-like bHLH-transcriptional repressor								
V$HESF/V$HELT.01	Nrf2-mouse	0.91	54	68	+	0.949	1	agcgCACGggccggg
V$HESF/V$HELT.01	Ap1-mouse	0.91	363	377	-	0.949	1	cgggCACGagcggcg
V$HESF/V$HELT.01	Nrf2-mouse	0.91	213	227	-	0.917	1	gtcgCACGgggggcg
Hypoxia inducible factor, bHLH / PAS protein family								
V$HIFF/V$HIF1.02	Nrf2-mouse	0.93	213	225	+	0.934	1	cgcccccCGTGcg
V$HIFF/V$HIF1.02	Ap1-mouse	0.93	389	401	-	0.964	1	gcgcccaCGTGac
Liver enriched Cut - Homeodomain transcription factor HNF6 (ONECUT)								
V$HNF6/V$HNF6.01	Nrf2-mouse	0.82	733	749	-	0.873	0.833	actccaagTCCAtcatg
V$HNF6/V$HNF6.01	Ap1-mouse	0.82	119	135	-	0.935	1	tacttaagTCAAtctag
Zinc finger protein insulinoma-associated 1 (IA-1) functions as a transcriptional repressor								
V$INSM/V$INSM1.01	Ap1-mouse	0.9	372	384	+	0.952	1	tgcccGGGGgcca
V$INSM/V$INSM1.01	Ap1-mouse	0.9	491	503	-	0.915	1	tgctcGGGGccgc
V$INSM/V$INSM1.01	Nrf2-mouse	0.9	248	260	-	0.934	1	tgtccGGGGcatg
MYC-associated zinc finger protein related transcription factor - in human								
V$MAZF/V$MAZR.01	Ap1-human	0.88	418	430	-	0.929	1	tggggcGGGGcct
V$MAZF/V$MAZR.01	Ap1-human	0.88	446	458	+	0.895	1	cgaggtGGGGcct
V$MAZF/V$MAZR.01	Ap1-human	0.88	574	586	+	0.889	1	ggcggcGGGGccg
V$MAZF/V$MAZR.01	Nrf2-human	0.88	340	352	+	0.889	1	gcgggtGGGGgat
V$MAZF/V$MAZR.01	Nrf2-human	0.88	404	416	-	0.905	1	aagggcGGGGcaa
V$MAZF/V$MAZR.01	Nrf2-human	0.88	700	712	+	0.893	1	gggggcGGGGgag

Table 5.2…..continued…

Family/Matrix	Sequence Name	Optimized Threshold	Start Position	End Position	Strand	Matrix Similarity	Core Similarity	Sequence (Core Sequence in Upper Case)
MYC-associated zinc finger protein related transcription factor - in mouse								
V$MAZF/V$MAZR.01	Nrf2-mouse	0.88	180	192	+	0.93	1	actgggGGGGccg
V$MAZF/V$MAZR.01	Nrf2-mouse	0.88	458	470	-	0.929	1	agggggcGGGGGcaa
V$MAZF/V$MAZR.01	Ap1-mouse	0.88	403	415	-	0.913	1	cgggggcGGGGctg
V$MAZF/V$MAZR.01	Nrf2-mouse	0.88	329	341	-	0.896	1	gagggcGGGGGcat
V$MAZF/V$MAZR.01	Nrf2-mouse	0.88	373	385	-	0.95	1	ggagggGGGGGaca
V$MAZF/V$MAZR.01	Nrf2-mouse	0.88	584	596	+	0.917	1	gggggcGGGGGcgg
V$MAZF/V$MAZR.01	Nrf2-mouse	0.88	578	590	+	0.904	1	gggggcGGGGGgcg
V$MAZF/V$MAZR.01	Nrf2-mouse	0.88	388	400	-	0.904	1	tagggcGGGGcaa
Ribonucleoprotein associated zinc finger protein MOK-2 (human)								
V$MOKF/V$MOK2.02	Ap1-mouse	0.98	62	82	+	0.983	1	catgagtagggcaCCTTggag
V$MOKF/V$MOK2.02	Ap1-mouse	0.98	549	569	+	0.981	1	cccgtccctaggtCCTTgttc
V$MOKF/V$MOK2.02	Ap1-mouse	0.98	133	153	-	0.984	1	gacactgacagtaCCTTttac
V$MOKF/V$MOK2.02	Ap1-mouse	0.98	193	213	-	1	1	ggatcctagagggCCTTtaca
V$MOKF/V$MOK2.02	Nrf2-mouse	0.98	412	432	+	0.981	1	ggggccctcgggtCCTTgccc
V$MOKF/V$MOK2.02	Nrf2-mouse	0.98	7	27	-	0.983	1	tggacctgcagaaCCTTgccc
c-Myb, important in hematopoesis, cellular equivalent to avian myoblastosis virus oncogene v-myb								
V$MYBL/V$CMYB.02	Ap1-human	0.96	184	196	+	0.971	1	acTAACcgcgatc
V$MYBL/V$CMYB.02	Nrf2-human	0.96	117	129	+	0.961	0.99	tcCAACtgtttaa
v-Myb								
V$MYBL/V$VMYB.02	Ap1-human	0.9	215	227	+	0.978	1	accAACGgcgctt
V$MYBL/V$VMYB.02	Nrf2-human	0.9	243	255	+	0.991	1	gctAACGgagacc
Myf5 myogenic bHLH protein - in human								
V$MYOD/V$MYF5.01	Ap1-human	0.9	488	504	+	0.932	1	gctgaCAGCtgctgata
V$MYOD/V$MYF5.01	Ap1-human	0.9	490	506	-	0.905	1	cttatCAGCagctgtca
V$MYOD/V$MYF5.01	Ap1-human	0.9	518	534	+	0.91	1	gaaggCAGCggcaggtc
V$MYOD/V$MYF5.01	Nrf2-human	0.9	650	666	-	0.953	0.836	ggcagCACCtgctggga
Myf5 myogenic bHLH protein - in mouse								
V$MYOD/V$MYF5.01	Ap1-mouse	0.9	471	487	-	0.936	1	cgcgcCAGCagctgtca
V$MYOD/V$MYF5.01	Ap1-mouse	0.9	469	485	+	0.932	1	gctgaCAGCtgctggcg
V$MYOD/V$MYF5.01	Nrf2-mouse	0.9	770	786	-	0.953	0.836	ggcagCACCtgctggga
Complex of Lmo2 bound to Tal-1, E2A proteins, and GATA-1, half-site 1								
V$MYOD/V$TAL1_E2A.01	Nrf2-mouse	0.98	771	787	+	0.99	1	cccagCAGGtgctgccc
V$MYOD/V$TAL1_E2A.01	Ap1-mouse	0.98	237	253	-	0.98	1	gaacaCAGGtgctttttc
Neurogenin 1 and 3 (ngn1/3) binding sites								
V$NEUR/V$NEUROG.01	Ap1-human	0.92	239	251	-	0.94	0.875	ggcCCAGctggcg
V$NEUR/V$NEUROG.01	Nrf2-human	0.92	281	293	+	0.935	0.875	accCCAGctggca
NF-kappaB (p50)								
V$NFKB/V$NFKAPPAB50.01	Ap1-human	0.83	397	409	+	0.832	1	cggGGGAgtcacg
V$NFKB/V$NFKAPPAB50.01	Nrf2-human	0.83	580	592	+	0.944	1	tcgGGGAgcccca
V$NFKB/V$NFKAPPAB50.01	Nrf2-human	0.83	581	593	-	0.877	0.75	ttgGGGCtccccg
V$NFKB/V$NFKAPPAB50.01	Nrf2-human	0.83	637	649	+	0.846	1	gccGGGActcccg
V$NFKB/V$NFKAPPAB50.01	Nrf2-human	0.83	639	651	-	0.855	1	gacGGGAgtcccg

Table 5.2…..continued…

Family/Matrix	Sequence Name	Optimized Threshold	Start Position	End Position	Strand	Matrix Similarity	Core Similarity	Sequence (Core Sequence in Upper Case)
Nuclear respiratory factor 1 (NRF1), bZIP transcription factor that acts on nuclear genes encoding mitochondrial proteins- in human								
V$NRF1/V$NRF1.01	Ap1-human	0.78	291	307	-	0.788	0.75	cggTCGCgggcgcctct
V$NRF1/V$NRF1.01	Ap1-human	0.78	292	308	+	0.783	1	gagGCGCccgcgaccgc
V$NRF1/V$NRF1.01	Nrf2-human	0.78	183	199	-	0.781	1	gcaGCGCtctcgcccgc
V$NRF1/V$NRF1.01	Nrf2-human	0.78	328	344	-	0.826	1	cccGCGCcggggctgac
Nuclear respiratory factor 1 (NRF1), bZIP transcription factor that acts on nuclear genes encoding mitochondrial proteins-in mouse								
V$NRF1/V$NRF1.01	Ap1-mouse	0.78	542	558	-	0.835	1	cccGCGCcccgccccccgc
V$NRF1/V$NRF1.01	Nrf2-mouse	0.78	51	67	-	0.794	0.75	ccgGCCCgtgcgctgct
V$NRF1/V$NRF1.01	Ap1-mouse	0.78	543	559	+	0.788	0.75	cggGGGCgggcgcgggg
V$NRF1/V$NRF1.01	Nrf2-mouse	0.78	52	68	+	0.823	1	gcaGCGCacgggccggg
V$NRF1/V$NRF1.01	Ap1-mouse	0.78	397	413	+	0.784	1	ggcGCGCagcccccgccc
Tumor suppressor p53 (3' half site)								
V$P53F/V$P53.03	Ap1-human	0.92	514	536	+	0.921	0.828	cggcgaaggcagcggCAGGtcgg
V$P53F/V$P53.05	Nrf2-human	0.78	399	421	-	0.799	1	cccaCAAGggcgggggcaagagtc
B-cell-specific activator protein - in human								
V$PAX5/V$PAX5.01	Ap1-human	0.79	41	69	-	0.796	0.905	tctcgcAGCActgatgagtgatcagctct
V$PAX5/V$PAX5.01	Nrf2-human	0.79	55	83	+	0.798	0.81	ctccaaATCAgggaggcgcagctcctaca
B-cell-specific activator protein - in mouse								
V$PAX5/V$PAX5.02	Ap1-human	0.73	413	441	-	0.731	0.842	ggacccgggcgatggGGCGgggcctcgcgc
V$PAX5/V$PAX5.02	Nrf2-human	0.73	419	447	+	0.734	1	ggggcgggagggcggAGCGgggcaggggcc
Zebrafish PAX9 binding sites								
V$PAX9/V$PAX9.01	Ap1-human	0.78	43	63	-	0.833	0.824	agCACTgatgagtgatcagct
V$PAX9/V$PAX9.01	Nrf2-human	0.78	232	252	+	0.825	1	ggCACCggggagctaacggag
Binding site for a Pbx1/Meis1 heterodimer								
V$PBXC/V$PBX1_MEIS1.02	Ap1-human	0.77	457	473	+	0.772	0.75	ctggTGTTtgacccgga
V$PBXC/V$PBX1_MEIS1.02	Nrf2-human	0.77	611	627	+	0.779	1	atcaTGATggacttgga
Pleomorphic adenoma gene (PLAG) 1, a developmentally regulated C2H2 zinc finger protein								
V$PLAG/V$PLAG1.01	Nrf2-mouse	0.88	268	288	+	0.893	1	GAGGatcaacagtgggggtc
V$PLAG/V$PLAG1.01	Nrf2-mouse	0.88	655	675	-	0.886	1	GAGGcggcggcaatggctagt
V$PLAG/V$PLAG1.01	Nrf2-mouse	0.88	461	481	-	0.932	1	GAGGcgggtaagggcgggg
V$PLAG/V$PLAG1.01	Nrf2-mouse	0.88	374	394	-	0.939	0.958	GGGGcaagggagggggggac
V$PLAG/V$PLAG1.01	Ap1-mouse	0.88	586	586	+	0.889	0.958	GGGGcaggcaggtgggtcggc
V$PLAG/V$PLAG1.01	Nrf2-mouse	0.88	782	802	-	0.881	0.958	GGGGcccgaaggttgggcag
V$PLAG/V$PLAG1.01	Ap1-mouse	0.88	406	426	-	0.912	0.958	GGGGccgacgacgggggcgggg
V$PLAG/V$PLAG1.01	Nrf2-mouse	0.88	360	380	-	0.926	0.958	GGGGgacaagacgggggccag
V$PLAG/V$PLAG1.01	Nrf2-mouse	0.88	578	598	+	0.892	0.958	GGGGgcgggggcggggcggac
Alpha (1)-fetoprotein transcription factor (FTF), liver receptor homologue-1 (LRH-1)								
V$SF1F/V$FTF.01	Ap1-mouse	0.94	71	83	-	0.974	1	cctcCAAGgtgcc
V$SF1F/V$FTF.01	Nrf2-mouse	0.94	6	18	+	0.945	1	cgggCAAGgttct

Table 5.2…..continued…

Family/Matrix	Sequence Name	Optimized Threshold	Start Position	End Position	Strand	Matrix Similarity	Core Similarity	Sequence (Core Sequence in Upper Case)
GC box elements								
V$SP1F/V$GC.01	Ap1-human	0.88	418	432	-	0.981	1	gatggGGCGgggcct
V$SP1F/V$GC.01	Ap1-human	0.88	572	586	+	0.9	1	gtggcGGCGgggccg
V$SP1F/V$GC.01	Nrf2-human	0.88	423	437	+	0.89	1	cgggaGGCGgagcgg
Stimulating protein 1, ubiquitous zinc finger transcription factor								
V$SP1F/V$SP1.01	Nrf2-mouse	0.88	427	441	-	0.904	1	acagGGGCagggcaa
V$SP1F/V$SP1.01	Nrf2-mouse	0.88	470	484	-	0.884	0.772	atggAGGCgggtaa
V$SP1F/V$SP1.01	Nrf2-mouse	0.88	576	590	+	0.997	1	caggGGGCgggggcg
V$SP1F/V$SP1.01	Nrf2-mouse	0.88	564	578	-	0.912	1	ctggGGGCggaacaa
V$SP1F/V$SP1.01	Ap1-mouse	0.88	403	417	-	1	1	gacgGGGCgggggctg
V$SP1F/V$SP1.01	Ap1-mouse	0.88	542	556	+	0.977	1	gcggGGGCgggcgcg
V$SP1F/V$SP1.01	Nrf2-mouse	0.88	582	596	+	1	1	gcggGGGCgggcggg
V$SP1F/V$SP1.01	Ap1-mouse	0.88	563	577	+	0.891	1	ggcgGGGCaggcagg
V$SP1F/V$SP1.01	Nrf2-mouse	0.88	587	601	+	0.913	1	ggcgGGGCggactaa
V$SP1F/V$SP1.01	Ap1-mouse	0.88	584	598	+	0.977	1	ggcgGGGCgggcgga
V$SP1F/V$SP1.01	Nrf2-mouse	0.88	458	472	-	0.989	1	taagGGGCggggcaa
V$SP1F/V$SP1.02	Nrf2-mouse	0.85	58	72	+	0.852	0.75	cacgGGCCggggctc
V$SP1F/V$SP1.02	Nrf2-mouse	0.85	207	221	-	0.959	1	cgggGGGCggagcgc
V$SP1F/V$SP1.02	Ap1-mouse	0.85	432	446	+	0.916	1	ggtgGGGCggtgtct
Serum response factor								
V$SRFF/V$SRF.02	Nrf2-mouse	0.84	21	39	+	0.857	0.889	aggtcCAAAtcagggagtg
V$SRFF/V$SRF.02	Ap1-mouse	0.84	103	121	-	0.851	1	tagagCATAcatggaccca
ZNF143 (the human ortholog of Xenopus Staf, and a DNA binding protein related to ZNF143 and Staf)								
V$STAF/V$ZNF76_143.01	Ap1-human	0.76	305	327	+	0.793	1	ccgcCCCAccagcccgagagcta
V$STAF/V$ZNF76_143.01	Nrf2-human	0.76	366	388	-	0.825	0.81	cttcCCCCgccggccgcgcgggc
V$STAF/V$ZNF76_143.01	Nrf2-human	0.76	667	689	+	0.796	0.81	tcggCCCTctgggccctgcggtg
Signal transducers and activators of transcription								
V$STAT/V$STAT.01	Ap1-human	0.87	174	192	-	0.908	1	gcggttagtGGAAagagta
V$STAT/V$STAT.01	Nrf2-human	0.87	348	366	+	0.887	1	gggattttcGGAAgctcag
Core promoter-binding protein (CPBP) with 3 Krueppel-type zinc fingers - in human								
V$ZBPF/V$ZF9.01	Ap1-human	0.87	298	320	+	0.882	1	cccgcgaCCGCccccaccagcccg
V$ZBPF/V$ZF9.01	Ap1-human	0.87	414	436	+	0.879	0.821	cgcgaggCCCCgccccatcgccc
V$ZBPF/V$ZF9.01	Ap1-human	0.87	416	438	+	0.942	1	cgaggccCCGCccccatcgcccgg
V$ZBPF/V$ZF9.01	Nrf2-human	0.87	542	564	+	0.884	1	gtccgcgCCGCgcctcggcagcc
Core promoter-binding protein (CPBP) with 3 Krueppel-type zinc fingers - in mouse								
V$ZBPF/V$ZF9.01	Ap1-mouse	0.87	578	600	-	0.885	1	actccgcCCGCcccgccgaccca
V$ZBPF/V$ZF9.01	Ap1-mouse	0.87	536	558	-	0.957	1	cccgcgcCCGCccccgccgcgcc
V$ZBPF/V$ZF9.01	Ap1-mouse	0.87	542	564	-	0.937	1	ccgggcCCGCgccccgcccccgc
V$ZBPF/V$ZF9.01	Ap1-mouse	0.87	401	423	+	0.915	1	cgcagccCCGCccccgtcgtcggc
V$ZBPF/V$ZF9.01	Ap1-mouse	0.87	479	501	-	0.87	1	ctcggggCCGCcgccgcgccagc
V$ZBPF/V$ZF9.01	Ap1-mouse	0.87	426	448	-	0.903	1	gcagacaCCGCccccaccaagtcg
V$ZBPF/V$ZF9.01	Ap1-mouse	0.87	473	495	-	0.879	1	gccgccgCCGCgccagcagctgt
V$ZBPF/V$ZF9.01	Nrf2-mouse	0.87	456	478	+	0.917	1	tcttgccCCGCccctttaccccgc

Table 5.2…..continued…

Family/Matrix	Sequence Name	Optimized Threshold	Start Position	End Position	Strand	Matrix Similarity	Core Similarity	Sequence (Core Sequence in Upper Case)
Kruppel-like zinc finger protein 219 - in human								
V$ZBPF/V$ZNF219.01	Ap1-human	0.91	387	409	-	0.988	1	cgtgactCCCCcggccctcgggg
V$ZBPF/V$ZNF219.01	Nrf2-human	0.91	298	320	+	0.95	1	cttcccgCCCCcggaccgcgagc
V$ZBPF/V$ZNF219.01	Nrf2-human	0.91	689	711	-	0.987	1	tcccccgCCCCcgtcccggcacc
Kruppel-like zinc finger protein 219 - in mouse								
V$ZBPF/V$ZNF219.01	Nrf2-mouse	0.91	573	595	-	0.996	1	cgccccgCCCCcgcccccctgggg
V$ZBPF/V$ZNF219.01	Nrf2-mouse	0.91	208	230	+	0.918	1	cgctccgCCCCcccgtgcgacttc
V$ZBPF/V$ZNF219.01	Nrf2-mouse	0.91	371	393	+	0.993	1	cttgtccCCCCctcccccttgccc
V$ZBPF/V$ZNF219.01	Ap1-mouse	0.91	533	555	-	0.973	1	gcgcccgCCCCcgccgcgccgct
V$ZBPF/V$ZNF219.01	Nrf2-mouse	0.91	172	194	-	0.943	1	ttcggccCCCCcagtcctctgta
Human zinc finger protein ZNF35								
V$ZF35/V$ZNF35.01	Ap1-mouse	0.96	497	509	+	0.967	1	ccgagcAAGAtgg
V$ZF35/V$ZNF35.01	Nrf2-mouse	0.96	453	465	-	0.964	1	cggggcAAGAgct

Table 5.2.

GenBank Accession No.	Gene Symbol	Gene Title	Prostate 3hr*	Prostate 12hr**
Apoptosis and cell cycle				
NM_019816	Aatf	apoptosis antagonizing transcription factor	-	3.09
NM_007466	Api5	apoptosis inhibitor 5	-	7.26
NM_007609	Casp4	caspase 4, apoptosis-related cysteine peptidase	-	4.24
NM_011997	Casp8ap2	caspase 8 associated protein 2	-	4.67
NM_026201	Ccar1	cell division cycle and apoptosis regulator 1	-	3.31
NM_027545	Cwf19l2	CWF19-like 2, cell cycle control (S. pombe)	-	3.48
NM_001037134	Ccne2	cyclin E2	-	4.04
NM_009831	Ccng1	cyclin G1	-	3.82
NM_028399	Ccnt2	cyclin T2	-	3.16
NM_145991	Cdc73	Vcell division cycle 73, Paf1/RNA polymerase II complex component, homolog (S. cerevisiae)	-	6.13
Calcium ion binding				
NM_009722	Atp2a2	ATPase, Ca++ transporting, cardiac muscle, slow twitch 2	-	3.14
NM_009784	Cacna2d1	calcium channel, voltage-dependent, alpha2/delta subunit 1	-	4.81
NM_007977	F8	coagulation factor VIII	-	4.18
NM_007868	Dmd	dystrophin, muscular dystrophy	-	3.21
NM_007943	Eps15	epidermal growth factor receptor pathway substrate 15	-	5.26
NM_001039644	Edem3	ER degradation enhancer, mannosidase alpha-like 3	-	4.54
NM_010427	Hgf	hepatocyte growth factor	-	4.49
XM_001472723	Macf1	microtubule-actin crosslinking factor 1	-	3.96
NM_011110	Pla2g5	phospholipase A2, group V	-	3.89
NM_013829	Plcb4	phospholipase C, beta 4	-	3.94
NM_009048	Reps1	RalBP1 associated Eps domain containing protein	-	6.19
NM_021450	Trpm7	transient receptor potential cation channel, subfamily M, member 7	-	4.46
Digestion				
NM_025583	Ctrb1	chymotrypsinogen B1	-	4.43
NM_025469	Clps	colipase, pancreatic	-	3.85
NM_009430	Prss2	protease, serine, 2	-	28.91
Extracellular space				
NM_009692	Apoa1	apolipoprotein A-I	-	9.72
NM_018782	Calcrl	calcitonin receptor-like	-	5.1
NM_001042611	Cp	ceruloplasmin	-	3.77
NM_019919	Ltbp1	latent transforming growth factor beta binding protein 1	-	3.46
NM_001039094	Negr1	neuronal growth regulator 1	-	3.15
NM_011964	Psg19	pregnancy specific glycoprotein 19	-	8.93
NM_009936	Col9a3	procollagen, type IX, alpha 3	-	3.48
NM_001081385	Pcdh11x	protocadherin 11 X-linked	-	8.52
NM_053141	Pcdhb16	protocadherin beta 16	-	3.17
NM_021289	Smr2	submaxillary gland androgen regulated protein 2	-	29.55
Integral to Plasma Membrane				
NM_008309	Htr1d	5-hydroxytryptamine (serotonin) receptor 1D	10.02	-
NM_008427	Kcnj4	potassium inwardly-rectifying channel, subfamily J, member 4	3.49	-
NM_008422	Kcnc3	potassium voltage gated channel, Shaw-related subfamily, member 3	11.48	-
NM_008434	Kcnq1	potassium voltage-gated channel, subfamily Q, member 1	3.34	-
NM_001098170	Pcdh10	protocadherin 10	4.1	-
BC098457	Pcdhgc3	protocadherin gamma subfamily C, 3	3.5	-
AK041751	Tcrb-J	T-cell receptor beta, joining region	11.66	-
NM_029975	Ulbp1	UL16 binding protein 1	3.57	-
Intracellular				
NM_007478	Arf3	ADP-ribosylation factor 3	-	4.82
NM_134037	Acly	ATP citrate lyase	-	4.49
NM_015802	Dlc1	deleted in liver cancer 1	3.23	-
NM_178118	Dixdc1	DIX domain containing 1	8.24	3.65
NM_007961	Etv6	ets variant gene 6 (TEL oncogene)	4.57	-
NM_080433	Fezf2	Fez family zinc finger 2	-	3.44
NM_053202	Foxp1	forkhead box P1	-	3.09
NM_175143	Qrich1	glutamine-rich 1	4.75	-
NM_178888	Garnl3	GTPase activating RANGAP domain-like 3	3.02	-
NM_001025597	Ikzf1	IKAROS family zinc finger 1	13.8	-
NM_011771	Ikzf3	IKAROS family zinc finger 3	-	5.44

Table 5.3. Temporal microarray analyses of genes suppressed by SFN+EGCG combination in the prostate of NRF2-deficient mice…..continued…

GenBank Accession No.	Gene Symbol	Gene Title	Prostate 3hr*	Prostate 12hr**
NM_016889	Insm1	insulinoma-associated 1	4.07	-
NM_029416	Klf17	Kruppel-like factor 17	3.25	-
NM_053158	Mrpl1	mitochondrial ribosomal protein L1	-	7.61
NM_031260	Mov10l1	Moloney leukemia virus 10-like 1	4.83	-
NM_010823	Mpl	myeloproliferative leukemia virus oncogene	4.77	-
NM_031881	Nedd4l	neural precursor cell expressed, developmentally down-regulated gene 4-like	3.76	-
NM_139144	Ogt	O-linked N-acetylglucosamine (GlcNAc) transferase (UDP-N-acetylglucosamine:polypeptide-N-acetylglucosaminyl transferase)	3.02	-
AY033991	Plcd4	phospholipase C, delta 4	4.55	-
NM_008884	Pml	promyelocytic leukemia	4.5	-
NM_009391	Ran	RAN, member RAS oncogene family	-	3.96
NM_011246	Rasgrp1	RAS guanyl releasing protein 1	3.43	-
NM_001081105	Rhoh	ras homolog gene family, member H	5.73	-
NM_145452	Rasa1	RAS p21 protein activator 1	-	3.31
NM_172525	Arhgap29	Rho GTPase activating protein 29	-	5.05
NM_015830	Solh	small optic lobes homolog (Drosophila)	4.86	-
NM_028004	Ttn	titin	4.77	-
NM_011529	Tank	TRAF family member-associated Nf-kappa B activator	-	6.11
NM_009541	Zbtb17	zinc finger and BTB domain containing 17	5.46	-
NM_008717	Zfml	zinc finger, matrin-like	3.36	-
Kinases				
NM_134079	Adk	Adenosine kinase	-	4.07
NM_007561	Bmpr2	bone morphogenic protein receptor, type II (serine/threonine kinase)	-	6.14
NM_001025439	Camk2d	calcium/calmodulin-dependent protein kinase II, delta	-	4.6
NM_001042634	Clk1	CDC-like kinase 1	-	3.61
NM_007714	Clk4	CDC like kinase 4	-	3.33
NM_001109626	Crkrs	Cdc2-related kinase, arginine/serine-rich	-	7.33
NM_009974	Csnk2a2	Casein kinase 2, alpha prime polypeptide	6.07	-
XM_979562	Etnk1	ethanolamine kinase 1	-	3.19
NM_019827	Gsk3b	Glycogen synthase kinase 3 beta	-	4.47
NM_010367	Magi1	Membrane associated guanylate kinase, WW and PDZ domain containing 1	3.12	-
NM_015823	Magi2	Membrane associated guanylate kinase, WW and PDZ domain containing 2		6.15
NM_009157	Map2k4	Mitogen activated protein kinase kinase 4	-	3.31
NM_011946	Map3k2	Mitogen activated protein kinase kinase kinase 2	-	5.02
NM_025609	Map3k7ip1	mitogen-activated protein kinase kinase kinase 7 interacting protein 1	3.04	3.93
NM_008696	Map4k4	mitogen-activated protein kinase kinase kinase kinase 4	3.54	-
NM_201519	Map4k5	Mitogen-activated protein kinase kinase kinase kinase 5	-	3.28
NM_011161	Mapk11	mitogen-activated protein kinase 11	-	10.9
NM_172632	Mapk4	mitogen-activated protein kinase 4	3.51	-
NM_015806	Mapk6	mitogen-activated protein kinase 6	3.53	-
NM_010878	Nck1	Non-catalytic region of tyrosine kinase adaptor protein 1	-	4.24
NM_010879	Nck2	Non-catalytic region of tyrosine kinase adaptor protein 2	3.38	-
NM_021605	Nek7	NIMA (never in mitosis gene a)-related expressed kinase 7	-	3.13
NM_008702	Nlk	Nemo like kinase	-	3.99
NM_172783	Phka2	Phosphorylase kinase alpha 2	3.07	-
NM_011083	Pik3c2a	phosphatidylinositol 3-kinase, C2 domain containing, alpha polypeptide	-	5.18
NM_008839	Pik3ca	phosphatidylinositol 3-kinase, catalytic, alpha polypeptide	-	3.92
NM_008862	Pkia	protein kinase inhibitor, alpha	-	3.28
NM_008855	Prkcb1	protein kinase C, beta 1	-	3.34
NM_029239	Prkcn	protein kinase C, nu	3.93	-
NM_001013833	Prkg1	Protein kinase, cGMP-dependent, type I	3.31	-
NM_007982	Ptk2	PTK2 protein tyrosine kinase 2	3.47	-
NM_009184	Ptk6	PTK6 protein tyrosine kinase 6	4.66	-
NM_009071	Rock1	Rho-associated coiled-coil containing protein kinase 1	-	4.71
NM_009072	Rock2	Rho-associated coiled-coil containing protein kinase 2	-	4.42
NM_148945	Rps6ka3	Ribosomal protein S6 kinase polypeptide 3	-	8.82
NM_028259	Rps6kb1	ribosomal protein S6 kinase, polypeptide 1	-	3.36
NM_019635	Stk3	serine/threonine kinase 3 (Ste20, yeast homolog)	-	3.03
NM_144825	Taok1	TAO kinase 1	-	3.93
XM_001474897	Tnik	TRAF2 and NCK interacting kinase	4.01	8.1
NM_010633	Uhmk1	U2AF homology motif (UHM) kinase 1	3.19	-
NM_030724	Uck2	Uridine-cytidine kinase 2	4.1	-
NM_198703	Wnk1	WNK lysine deficient protein kinase 1	-	6.45

Table 5.3…..continued…

GenBank Accession No.	Gene Symbol	Gene Title	Prostate 3hr*	Prostate 12hr**
Metal ion binding				
NM_009530	Atrx	alpha thalassemia/mental retardation syndrome X-linked homolog (human)	-	4.12
NM_013476	Ar	androgen receptor	3.23	-
NM_133738	Antxr2	anthrax toxin receptor 2	-	3.15
AB088408	Atp6v0d1	ATPase, H+ transporting, lysosomal V0 subunit D1	6.95	-
NM_139294	Braf	Braf transforming gene	-	3.67
NM_153788	Centb1	centaurin, beta 1	-	6.1
NM_007805	Cyb561	cytochrome b-561	5.53	-
NM_010006	Cyp2d9	cytochrome P450, family 2, subfamily d, polypeptide 9	3.28	-
NM_027816	Cyp2u1	cytochrome P450, family 2, subfamily u, polypeptide 1	5.7	-
NM_011935	Esrrg	estrogen-related receptor gamma	3.85	-
NM_025923	Fancl	Fanconi anemia, complementation group L	-	3.38
NM_053242	Foxp2	forkhead box P2	-	4.42
NM_026148	Lims1	LIM and senescent cell antigen-like domains 1	-	4.31
NM_008636	Mtf1	metal response element binding transcription factor 1	15.93	-
NM_028757	Nebl	nebulette	4.66	-
NM_152229	Nr2e1	nuclear receptor subfamily 2, group E, member 1	11.85	-
NM_030676	Nr5a2	nuclear receptor subfamily 5, group A, member 2	4.12	-
NM_010264	Nr6a1	nuclear receptor subfamily 6, group A, member 1	10.31	-
NM_026000	Psmd9	proteasome (prosome, macropain) 26S subunit, non-ATPase, 9	3.96	-
NM_177167	Ppm1e	protein phosphatase 1E (PP2C domain containing)	3.56	-
NM_009088	Rpo1-4	RNA polymerase 1-4	4.87	4.31
NM_001103157	Steap2	six transmembrane epithelial antigen of prostate 2	-	3.76
NM_009380	Thrb	thyroid hormone receptor beta	-	4.67
NM_009371	Tgfbr2	transforming growth factor, beta receptor II	4.54	-
Phosphatases				
NM_008960	Pten	phosphatase and tensin homolog	-	3.05
NM_027892	Ppp1r12a	protein phosphatase 1, regulatory (inhibitor) subunit 12A	-	3.77
NM_008913	Ppp3ca	Protein phosphatase 3, catalytic subunit, alpha isoform	-	9.33
NM_182939	Ppp4r2	protein phosphatase 4, regulatory subunit 2	-	3.39
NM_011200	Ptp4a1	protein tyrosine phosphatase 4a1	-	3.11
NM_008979	Ptpn22	Protein tyrosine phosphatase, non-receptor type 22 (lymphoid)	-	3.65
NM_001014288	Ptprd	Protein tyrosine phosphatase, receptor type, D	-	6.2
NM_025760	Ptplad2	Protein tyrosine phosphatase-like A domain containing 2	-	4.42
NM_130447	Dusp16	dual specificity phosphatase 16	-	5.97
NM_177730	Impad1	inositol monophosphatase domain containing 1	-	3.72
NM_011210	Ptprc	protein tyrosine phosphatase, receptor type, C	4.33	-
Transcription factors and interacting partners				
AY902311	Atf2	Activating transcription factor 2	-	8.21
AY903215	Atf7ip2	activating transcription factor 7 interacting protein 2	-	9.83
NM_001025392	Bclaf1	BCL2-associated transcription factor 1	-	3.78
NM_015826	Dmrt1	doublesex and mab-3 related transcription factor 1	-	6.96
NM_009210	Hltf	helicase-like transcription factor	-	3.93
NM_033322	Lztfl1	leucine zipper transcription factor-like 1	-	4.08
NM_172153	Lcorl	ligand dependent nuclear receptor corepressor-like	-	3.68
NM_183355	Pbx1	pre B-cell leukemia transcription factor 1	-	5.26
NM_001018042	Sp3	trans-acting transcription factor 3	-	3.65
AM295492	Sp6	trans-acting transcription factor 6	-	32.91
NM_013685	Tcf4	Transcription factor 4	-	3.84
NM_178254	Tcfl5	transcription factor-like 5 (basic helix-loop-helix)	-	4.6
NM_016767	Batf	basic leucine zipper transcription factor, ATF-like	-	3.89
NM_001109661	Bach2	BTB and CNC homology 2	-	4.89
NM_133828	Creb1	cAMP responsive element binding protein 1	-	5.33
NM_001005868	Erbb2ip	Erbb2 interacting protein	-	3.66
NM_008031	Fmr1	fragile X mental retardation syndrome 1 homolog	-	3.96
NM_010431	Hif1a	hypoxia inducible factor 1, alpha subunit	-	8.62
NM_009951	Igf2bp1	insulin-like growth factor 2 mRNA binding protein 1	5.27	-
NM_027910	Klhdc3	kelch domain containing 3	3.33	-
NM_172154	Lcor	ligand dependent nuclear receptor corepressor	-	3.25
NM_001005863	Mtus1	mitochondrial tumor suppressor 1	3.29	-
NM_001081445	Ncam1	neural cell adhesion molecule 1	3.08	-
AY050663	Nfat5	nuclear factor of activated T-cells 5	-	4.4
NM_010903	Nfe2l3	nuclear factor, erythroid derived 2, like 3 (Nrf3)	-	3.03
NM_001024205	Nufip2	nuclear fragile X mental retardation protein interacting protein 2	-	4.4
NM_010881	Ncoa1	nuclear receptor coactivator 1	3.55	3.36
NM_172495	Ncoa7	nuclear receptor coactivator 7	-	4.46
NM_011308	Ncor1	nuclear receptor co-repressor 1	-	5.37
NM_011544	Tcf12	Transcription factor 12	-	6.06

Table 5.3…..continued…

GenBank Accession No.	Gene Symbol	Gene Title	Prostate 3hr*	Prostate 12hr**
Transferases				
NM_144807	Chpt1	choline phosphotransferase 1	-	4.13
NM_133869	Cept1	Choline/ethanolaminephosphotransferase 1	-	5.65
NM_030225	Dlst	dihydrolipoamide S-succinyltransferase (E2 component of 2-oxo-glutarate complex)	-	4.04
NM_028087	Gcnt3	glucosaminyl (N-acetyl) transferase 3, mucin type	-	7.23
NM_028108	Nat13	N-acetyltransferase 13	-	4.05
NM_008708	Nmt2	N-myristoyltransferase 2	-	4.07
NM_027869	Pnpt1	polyribonucleotide nucleotidyltransferase 1	-	3.04
NM_172627	Pggt1b	protein geranylgeranyltransferase type I, beta subunit	-	5.61
NM_183028	Pcmtd1	protein-L-isoaspartate (D-aspartate) O-methyltransferase domain containing	-	7.36
NM_028604	Trmt11	tRNA methyltransferase 11 homolog (S. cerevisiae)	-	3.67
NM_144731	Galnt7	UDP-N-acetyl-alpha-D-galactosamine: polypeptide N-acetylgalactosaminyltransferase 7	-	3.06
NM_172829	St6gal2	beta galactoside alpha 2,6 sialyltransferase 2	-	3.22
NM_009178	St3gal4	ST3 beta-galactoside alpha-2,3-sialyltransferase 4	-	8.11
NM_011674	Ugt8a	UDP galactosyltransferase 8A	-	13.64
Ubiquitination				
XM_001478436	Fbxl17	F-box and leucine-rich repeat protein 17	-	3.86
NM_016736	Nub1	negative regulator of ubiquitin-like proteins 1	3.57	-
NM_146003	Senp6	SUMO/sentrin specific peptidase 6	-	4.5
NM_016723	Uchl3	ubiquitin carboxyl-terminal esterase L3 (ubiquitin thiolesterase)	-	6.71
NM_173010	Ube3a	ubiquitin protein ligase E3A	-	3.12
NM_009481	Usp9x	ubiquitin specific peptidase 9, X chromosome	-	3.47
NM_152825	Usp45	ubiquitin specific petidase 45	-	3.09
NM_023585	Ube2v2	ubiquitin-conjugating enzyme E2 variant 2	-	5.5
NM_172300	Ube2z	ubiquitin-conjugating enzyme E2Z (putative)	3.41	-
NM_177327	Wwp1	WW domain containing E3 ubiquitin protein ligase 1	-	3.9
Others				
NM_007462	Apc	adenomatosis polyposis coli	-	5.42
NM_021456	Ces1	carboxylesterase 1	4.09	-
NM_021369	Chrna6	cholinergic receptor, nicotinic, alpha polypeptide 6	4.25	-
NM_028870	Cltb	clathrin, light polypeptide (Lcb)	22.37	-
NM_016716	Cul3	cullin 3	-	3.2
NM_010076	Drd1a	dopamine receptor D1A	12.13	-
NM_001033360	Gpr101	G protein-coupled receptor 101	4.26	-
NM_008211	H3f3b	H3 histone, family 3B	3.47	-
NM_008285	Hrh1	histamine receptor H 1	10.24	-
NM_133892	Lao1	L-amino acid oxidase 1	3.39	-
NM_020280	Magea4	melanoma antigen, family A, 4	22.06	-
NM_175632	Oscar	osteoclast associated receptor	3.36	-
NM_009419	Tpst2	protein-tyrosine sulfotransferase 2	7.76	-
NM_146255	Slc1a7	solute carrier family 1 (glutamate transporter), member 7	9.36	-
NM_009206	Slc4a1ap	solute carrier family 4 (anion exchanger), member 1, adaptor protein	-	3.27
NM_022025	Slc5a7	solute carrier family 5 (choline transporter), member 7	9.51	-
NM_177909	Slc9a9	solute carrier family 9 (sodium/hydrogen exchanger), isoform 9	4.23	-
NM_011506	Sucla2	succinate-Coenzyme A ligase, ADP-forming, beta subunit	5.02	-
NM_009409	Top2b	topoisomerase (DNA) II beta		3.3

* Relative mRNA expression levels of genes that were suppressed >3-fold by SFN+EGCG combination in prostate of Nrf2 wild-type mice but not in prostate of Nrf2 knockout mice compared with vehicle treatment at 3 hr.

** Relative mRNA expression levels of genes that were suppressed >3-fold by SFN+EGCG combination in prostate of Nrf2 wild-type mice but not in prostate of Nrf2 knockout mice compared with vehicle treatment at 12 hr.

Table 5.3.

Species	Tissue	Study	Data Source	Descriptor	Affymetrix Platform
Human	Prostate	Lapointe	ONCOMINE	Prostate cancer	Non-Affymetrix
Human	Prostate	Luo	ONCOMINE	Prostate cancer and Benign prostatic hyperplasia	Non-Affymetrix
Mouse	Lung	Kleeberger	GEO	Hyperoxic lung injury	MG U74Av2
Mouse	Lung	Papaiahgari	GEO	Lung injury and inflammatory response	MG 430A 2.0
Mouse	Spleen and Liver	Li	GEO	Autoimmune disease and Nrf2	MG U74Av2
Mouse	Type II Cells	Marchireddy	GEO	Nrf2 wild-type and knockout cells	MG 430 2.0
Mouse	Prostate	Nair 1	Kong Laboratory	EGCG+SFN combination treatment	MG 430 2.0
Mouse	Small intestine and Liver	Nair 2	Kong Laboratory	BHA treatment	MG 430 2.0
Mouse	Small intestine and Liver	Nair 3	Kong Laboratory	Induction of ER stress with Tunicamycin	MG 430 2.0
Rat	Spinal cord	Faden 1	PEPR	Supraspinal tracts	RG_U34A
Rat	Spinal cord	Faden 2	PEPR	Trauma above T9	RG_U34A
Rat	Spinal cord	Faden 3	PEPR	Trauma below T9	RG_U34A
Rat	Spinal cord	Faden 4	PEPR	Trauma T9	RG_U34A

Table 6.1. Microarray datasets bearing inflammation/injury or cancer signatures

All ‘Nair’ datasets are from the Kong Laboratory; all ‘Faden’ datasets are as defined by descriptors detailed above at the PEPR resource; all other datasets are as defined by descriptors detailed above at the ONCOMINE or GEO resources; EGCG,

epigallocatechin-3-gallate; SFN, sulforaphane; BHA; butylated hydroxyanisole; ER, endoplasmic reticulum; TM, tunicamycin.

Matrix Family Human NRF2 vs. NFKB1	Matrix Family Murine Nrf2 vs. Nfkb1	Matrix Family Conserved After Multiple Species Alignment NRF2 vs. NFKB1	Family Information
-	**V$AHRR**	-	AHR-arnt heterodimers and AHR-related factors
-	-	**V$AIRE**	Autoimmune regulatory element binding factor
-	-	**V$AP1R**	MAF and AP1 related factors
-	**V$AP2F**	-	Activator protein 2
V$AP4R	**V$AP4R**	-	Activator protein 4 and related proteins
-	-	**V$ATBF**	AT-binding transcription factor
-	**V$BCL6**	**V$BCL6**	POZ domain zinc finger expressed in B-Cells
-	-	**V$BRAC**	Brachyury gene, mesoderm developmental factor
-	-	**V$BRNF**	Brn POU domain factors
-	-	**V$CAAT**	CCAAT binding factors
-	-	**V$CART**	Cart-1 (cartilage homeoprotein 1)
-	-	**V$CDXF**	Vertebrate caudal related homeodomain protein
V$CEBP	-	-	Ccaat/Enhancer Binding Protein
V$CHRF	-	**V$CHRF**	Cell cycle regulators: Cell cycle homology element
-	-	**V$CIZF**	CAS interating zinc finger protein
-	-	**V$CLOX**	CLOX and CLOX homology (CDP) factors
-	-	**V$COMP**	Factors which cooperate with myogenic proteins
V$CREB	-	**V$CREB**	Camp-responsive element binding proteins
-	**V$CTCF**	-	CTCF and BORIS gene family, transcriptional regulators with 11 highly conserved zinc finger domains
V$E2FF	**V$E2FF**	-	E2F-myc activator/cell cycle regulator
-	**V$E4FF**	-	Ubiquitous GLI - Krueppel like zinc finger involved in cell cycle regulation
V$EBOX	**V$EBOX**	-	E-box binding factors
-	**V$EGRF**	-	EGR/nerve growth factor induced protein C & related factors
V$EKLF	**V$EKLF**	**V$EKLF**	Basic and erythroid krueppel like factors
-	**V$EREF**	-	Estrogen response elements
V$ETSF	**V$ETSF**	-	Human and murine ETS1 factors
-	-	**V$EVI1**	EVI1-myleoid transforming protein
V$FKHD	-	**V$FKHD**	Fork head domain factors
-	**V$FXRE**	-	Farnesoid X - activated receptor response elements
V$GATA	**V$GATA**	**V$GATA**	GATA binding factors
V$GFI1	-	**V$GFI1**	Growth factor independence transcriptional repressor
-	-	**V$GREF**	Glucocorticoid responsive and related elements
-	-	**V$GRHL**	Grainyhead-like transcription factors
V$HAND	-	-	bHLH transcription factor dimer of HAND2 and E12
-	**V$HEAT**	**V$HEAT**	Heat shock factors
-	**V$HESF**	-	Vertebrate homologues of enhancer of split complex
-	-	**V$HNF1**	Hepatic Nuclear Factor 1
-	-	**V$HNF6**	Onecut homeodomain factor HNF6
-	-	**V$HOMF**	Homeodomain transcription factors
-	-	**V$HOXC**	HOX - PBX complexes
V$HOXF	**V$HOXF**	**V$HOXF**	Factors with moderate activity to homeo domain consensus sequence
-	**V$IKRS**	-	Ikaros zinc finger family
-	-	**V$IRFF**	Interferon regulatory factors
V$LEFF	-	**V$LEFF**	LEF1/TCF, involved in the Wnt signal transduction pathway
-	-	**V$LHXF**	Lim homeodomain factors
V$MAZF	**V$MAZF**	-	Myc associated zinc fingers
-	-	**V$MEF2**	MEF2, myocyte-specific enhancer binding factor
V$MYBL	-	-	Cellular and viral myb-like transcriptional regulators
V$MYOD	**V$MYOD**	-	Myoblast determining factors
-	-	**V$MYT1**	MYT1 C2HC zinc finger protein
-	**V$MZF1**	-	Myeloid zinc finger 1 factors
V$NEUR	-	**V$NEUR**	NeuroD, Beta2, HLH domain
-	-	**V$NF1F**	Nuclear factor 1
-	-	**V$NFAT**	Nuclear factor of activated T-cells
-	**V$NFKB**	-	Nuclear factor kappa B/c-rel
-	-	**V$NKX6**	NK6 homeobox transcription factors
-	-	**V$NKXH**	NKX homeodomain factors
V$NR2F	**V$NR2F**	**V$NR2F**	Nuclear receptor subfamily 2 factors
-	**V$NRF1**	-	Nuclear respiratory factor 1
-	-	**V$OCT1**	Octamer binding protein
-	-	**V$OCTP**	OCT1 binding factor (POU-specific domain)
V$P53F	**V$P53F**	-	p53 tumor suppressor
-	-	**V$PARF**	PAR/bZIP family
V$PAX5	-	-	PAX-5 B-cell-specific activator protein
-	**V$PAX6**	**V$PAX6**	PAX-4/PAX-6 paired domain binding sites
-	-	**V$PBXC**	PBX1 - MEIS1 complexes
-	-	**V$PDX1**	Pancreatic and intestinal homeodomain transcr. factor
-	-	**V$PERO**	Peroxisome proliferator-activated receptor
-	-	**V$PIT1**	GHF-1 pituitary specific pou domain transcription factor
-	**V$PLAG**	-	Pleomorphic adenoma gene
V$PLZF	-	**V$PLZF**	C2H2 zinc finger protein PLZF
-	-	**V$PRDF**	Positive regulatory domain I binding factor
-	-	**V$PTF1**	Pancreas transcription factor 1, heterotrimeric transcription factor
-	-	**V$RBIT**	Regulator of B-Cell IgH transcription
-	-	**V$RUSH**	SWI/SNF related nucleophosphoproteins with a RING finger DNA binding motif
V$RXRF	**V$RXRF**	**V$RXRF**	RXR heterodimer binding sites
-	-	**V$SATB**	Special AT-rich sequence binding protein
V$SF1F	-	**V$SF1F**	Vertebrate steroidogenic factor
-	**V$SMAD**	-	Vertebrate SMAD family of transcription factors
-	-	**V$SNAP**	snRNA-activating protein complex
V$SORY	**V$SORY**	**V$SORY**	SOX/SRY-sex/testis determining and related HMG box factors
V$SP1F	**V$SP1F**	**V$SP1F**	GC-Box factors SP1/GC
-	**V$SRFF**	**V$SRFF**	Serum response element binding factor
V$STAT	-	**V$STAT**	Signal transducer and activator of transcription
-	-	**V$TALE**	TALE homeodomain class recognizing TG motifs
-	**V$TBPF**	**V$TBPF**	Tata-binding protein factor
-	**V$WHNF**	-	Winged helix binding sites
V$XBBF	-	-	X-box binding factors
V$ZBPF	**V$ZBPF**	-	Zinc binding protein factors
V$ZF35	-	-	Zinc finger protein ZNF35
V$ZFHX	-	**V$ZFHX**	Two-handed zinc finger homeodomain transcription factors

Table 6.2. Human and Murine Matrix Families conserved between Nrf2 and Nfkb1

Nfe2l2	CNS Start	CNS End	%id	location	Length	Score	Chr	Strand	Start	End
1			84.2		200.5	**87.57**				
human	4424	4568	-	intergenic	144		2	-	177796698	177796842
chimp	1559	12467	98.4	intergenic			2b	-	182248910	182259818
dog	4037	4426	78.9	intergenic	389		36	-	24010936	24011325
mouse	3993	4131	79.6	intergenic	138		2	-	75470119	75470257
rat	4002	4133	80	intergenic	131		3	-	58360804	58360935
2			79.9		801.25	**93.25**				
human	46618	47576	-	intronic	958		2	-	177838892	177839850
chimp	16433	72741	98	intronic			2b	-	182263784	182320092
dog	44082	45048	76.3	intronic	966		36	-	24050981	24051947
mouse	49275	49911	73	intronic	636		2	-	75515401	75516037
rat	48247	48892	72.3	intronic	645		3	-	58405049	58405694
3			81.6		746.5	**94.04**				
human	63951	64978	-	intronic	1027		2	-	177856225	177857252
chimp	16433	72741	98	intronic			2b	-	182263784	182320092
dog	63914	64953	78	intronic	1039		36	-	24070813	24071852
mouse	69040	69553	74.9	intronic	513		2	-	75535166	75535679
rat	68447	68854	75.5	intronic	407		3	-	58425249	58425656
4			82.8		962.25	**98.86**				
human	95699	97201	-	intronic	1502		2	-	177887973	177889475
chimp	93603	105622	98.3	intronic			2b	-	182340954	182352973
dog	94052	95563	80.9	intronic	1511		36	-	24100951	24102462
mouse	99967	100384	76.4	intronic	417		2	-	75566093	75566510
rat	103210	103629	75.7	intronic	419		3	-	58460012	58460431
5			82.8		418.75	**89.74**				
human	112361	112533	-	intronic	172		2	-	177904635	177904807
chimp	113121	117879	98.1	intronic			2b	-	182360472	182365230
dog	105905	106887	82.1	intronic	517		36	-	24112804	24113786
mouse	115077	115617	74.8	intronic	540		2	-	75581203	75581743
rat	119448	119894	76.1	intronic	446		3	-	58476250	58476696

Table 6.3. A. Multiple species alignment for Nfe2l2

CNS, Conserved Non-Coding Sequences; Chr, chromosome.

Nfkb1	CNS start	CNS end	%id	location	length	score	chr	strand	start	end
1			78		491	**86.58**				
human	75272	75516	-	intergenic	244		4	+	103675774	103675545
rat	190119	189890	77	intergenic	229		2	-	233663290	233663525
mouse	585736	585501	80	intergenic	235		3	-	135287512	135286504
dog	52140	53148	78	intergenic	1008		32	+	26791395	26841008
chimp	67709	117322	98	intergenic	49613		4	+	105654198	105654198
2			80		319	**84.82**				
human	93740	94016	-	intergenic	276		4	+	103659473	103659195
rat	173818	173540	79	intergenic	278		2	-	233651850	233652129
mouse	574340	574061	78	intergenic	279		3	-	135307030	135306630
dog	72266	72666	81	intergenic	400		32	+	26791395	26841008
chimp	67709	117322	98	intergenic	49613		4	+	105654198	105654198
3			74		469	**81.92**				
human	148427	148852	-	intergenic	425		4	+	103626900	103626486
rat	141245	140831	73	intergenic	414		2	-	233620618	233620924
mouse	543135	542829	73	intergenic	306		3	-	135342413	135341726
dog	107362	108049	76	intergenic	687		32	+	26841253	26877988
chimp	117567	154302	99	intergenic	36735		4	+	105654198	105654198

Table 6.3. B. Multiple species alignment for Nfkb1

CNS, Conserved Non-Coding Sequences; chr, chromosome.

Sr. No.	GenBank Accession No.	Gene Name	Gene Symbol	Papaiahgari Lung injury and inflammation	SFN+EGCG Nrf2-dependent genes	BHA Nrf2-dependent genes	Tunicamycin Nrf2-dependent genes	Faden Supraspinal Tracts
1	NM_172154	ligand dependent nuclear receptor corepressor	Lcor	-	-3.25	-	-	-
2	NM_010756	v-maf musculoaponeurotic fibrosarcoma oncogene family, protein G (avian)	Mafg	-	-	2.45	-	-
3	NM_008927	mitogen-activated protein kinase kinase 1	Map2k1	-2.7	-4.12	2.28	-	1.59
4	NM_023138	mitogen-activated protein kinase kinase 2	Map2k2	-	-	2.75	1.15	1.1
5	NM_009157	mitogen-activated protein kinase kinase 4	Map2k4	-1.55	-3.31	-	-1.68	-
6	NM_011840	mitogen-activated protein kinase kinase 5	Map2k5	-1.56	-	-1.45	-	1.59
7	NM_011943	mitogen-activated protein kinase kinase 6	Map2k6	-	-3.98	-	-	1.19
8	NM_011944	mitogen-activated protein kinase kinase 7	Map2k7	-1.32	-	-0.37	-0.16	-
9	NM_011945	mitogen-activated protein kinase kinase kinase 1	Map3k1	-	-	-0.28	-0.18	1.11
10	NM_011946	mitogen-activated protein kinase kinase kinase 2	Map3k2	-	-5.02	-	2.25	-
11	NM_011947	mitogen-activated protein kinase kinase kinase 3	Map3k3	-2.08	-	-	-	-
12	NM_011948	mitogen-activated protein kinase kinase kinase 4	Map3k4	-1.87	-3.52	-1.98	1.51	-
13	NM_008580	mitogen-activated protein kinase kinase kinase 5	Map3k5	-1.71		-	-	-
14	NM_016693	mitogen-activated protein kinase kinase kinase 6	Map3k6	1.58	-5.25	3.25	-	-
15	NM_172688	mitogen-activated protein kinase kinase kinase 7	Map3k7	1.51	-3.07	2.52	3.29	-
16	NM_025609	mitogen-activated protein kinase kinase kinase 7 interacting protein 1	Map3k7ip1	-	-3.93	-	-1.91	-
17	NM_138667	mitogen-activated protein kinase kinase kinase 7 interacting protein 2	Map3k7ip2	-1.56	-	-	-	-
18	NM_007746	mitogen-activated protein kinase kinase kinase 8	Map3k8	-2.04	-	-0.58	2.76	1.55
19	NM_177395	mitogen-activated protein kinase kinase kinase 9	Map3k9	-	-6.48	3.06	4.77	-
20	NM_009582	mitogen-activated protein kinase kinase kinase 12	Map3k12	-7.07	-3.51	-	-	-
21	NM_016896	mitogen-activated protein kinase kinase kinase 14	Map3k14	1.38	-	2.12	1.51	-
22	NM_008279	mitogen-activated protein kinase kinase kinase kinase 1	Map4k1	-	-3.35	-	-	1.4
23	NM_009006	mitogen-activated protein kinase kinase kinase kinase 2	Map4k2	-6.72		2.35	-1.35	-
24	NM_001081357	mitogen-activated protein kinase kinase kinase kinase 3	Map4k3	-1.73		-	-	-
25	NM_008696	mitogen-activated protein kinase kinase kinase kinase 4	Map4k4	-1.58	-3.54	2.46	-	-0.74
26	NM_201519	mitogen-activated protein kinase kinase kinase kinase 5	Map4k5	-2.45	-3.28	3.94	-2.52	-
27	NM_031248	mitogen-activated protein binding protein interacting protein	Mapbpip	2.29		-	-	-
28	NM_001038663	mitogen-activated protein kinase 1	Mapk1	-	-	-	1.08	1.51
29	NM_011952	mitogen-activated protein kinase 3	Mapk3 (ERK1)	-1.4	-7.48	-	-	1.09
30	NM_172632	mitogen-activated protein kinase 4	Mapk4	-	-3.51	-	-	1.11
31	NM_015806	mitogen-activated protein kinase 6	Mapk6	-	-3.53	2.11	1.76	1.07
32	NM_011841	mitogen-activated protein kinase 7	Mapk7	-16.44	-	-	-	-0.99
33	NM_016700	mitogen-activated protein kinase 8	Mapk8	-	-	10.39	12.43	1.21
34	NM_011162	mitogen-activated protein kinase 8 interacting protein 1	Mapk8ip1	2.22	-10.62	-	-	-0.84
35	NM_016961	mitogen-activated protein kinase 9	Mapk9	-1.88	-4.77	1.68	2.33	1.4
36	NM_009158	mitogen-activated protein kinase 10	Mapk10	1.47	-	2.25	-	1.29
37	NM_011161	mitogen-activated protein kinase 11	Mapk11	-	-10.9	1.78	2.32	-
38	NM_013871	mitogen-activated protein kinase 12	Mapk12	-	-	-0.24	-	-0.88
39	NM_011950	mitogen-activated protein kinase 13	Mapk13	1.44	-	-	-0.21	-
40	NM_011951	mitogen-activated protein kinase 14	Mapk14	-1.62	-	1.14	-0.46	1.38
41	NM_145527	mitogen-activated protein kinase activating death domain	Mapkadd(Madd)	-	-	-	-	1.03
42	NM_177345	mitogen-activated protein kinase associated protein 1	Mapkap1	-1.62	-6.56	-0.34	-	-
43	NM_008551	mitogen-activated protein kinase-activated protein kinase 2	Mapkapk2	-	-	-	4.31	1.34
44	NM_178907	mitogen-activated protein kinase-activated protein kinase 3	Mapkapk3	-	-3.39	-	2.38	1.19
45	NM_010765	mitogen-activated protein kinase-activated protein kinase 5	Mapkapk5	-	-4.58	-0.42	-0.47	-
46	NM_011941	mitogen-activated protein kinase binding protein 1	Mapkbp1	1.42	-	-	-	-
47	NM_010881	nuclear receptor coactivator 1	Ncoa1	-	-3.55	-	-	-
48	NM_008679	nuclear receptor coactivator 3	Ncoa3	-	-	-0.12	-	-
49	NM_144892	nuclear receptor coactivator 5	Ncoa5	-	-	-	14.65	-
50	NM_172495	nuclear receptor coactivator 7	Ncoa7	-	-4.46	-	-	-
51	NM_011308	nuclear receptor corepressor 1	Ncor1	-	-5.37	3.39	-	-
52	NM_008689	nuclear factor of kappa light chain gene enhancer in B-cells 1, p105	Nfkb1	-1.52	-	-	-	1.21
53	NM_019408	nuclear factor of kappa light polypeptide gene enhancer in B-cells 2, p49/p100	Nfkb2	-2.56	-	-	-	-
54	NM_010907	nuclear factor of kappa light chain gene enhancer in B-cells inhibitor, alpha	Nfkbia	-	-	-	-	-0.77
55	NM_030612	nuclear factor of kappa light polypeptide gene enhancer in B-cells inhibitor, zeta	Nfkbiz	-	-	-	2.67	-
56	NM_028024	NFKB inhibitor interacting Ras-like protein 2	Nkiras2	-1.33	-	-	-	-0.94
57	NM_010902	nuclear factor, erythroid derived 2, like 2	Nrf2	1.54	-	-	-	1.26
58	NM_173440	nuclear receptor interacting protein 1	Nrip1	-	-	2.63	2.87	-
59	NM_020005	P300/CBP-associated factor	P/caf	-	-	-	2.33	-

Table 6.4. Canonical first-generation regulatory network members representing putative crosstalk between Nrf2 (Nfe2l2) and Nfkb1 in inflammation-associated carcinogenesis*

*Fold change values are listed.

Accession No.	Gene Symbol	Gene Name	Fold Change
Cell Adhesion			
H16245	ACTN2	actinin, alpha 2	7.02
NM_018836	AJAP1	adherens junction associated protein 1	-12.26
NM_004932	CDH6	cadherin 6, type 2, K-cadherin (fetal kidney)	-11.09
AL021786	ITM2A	integral membrane protein 2A	6.51
AI753143	ITGBL1	Integrin, beta-like 1 (with EGF-like repeat domains)	-6.35
NM_000425	L1CAM	L1 cell adhesion molecule	10.84
AL834134	PCDH15	protocadherin 15	9.61
AF152481	PCDHA3	protocadherin alpha 3	-12.64
NM_014428	TJP3	tight junction protein 3 (zona occludens 3)	-11.64
Cell Division and Cell Cycle			
NM_018123	ASPM	asp (abnormal spindle) homolog, microcephaly associated (Drosophila)	9.45
AL832227	BCL8	B-cell CLL/lymphoma 8	12.08
AF043294	BUB1	BUB1 budding uninhibited by benzimidazoles 1 homolog (yeast)	8.09
AL524035	CDC2	cell division cycle 2, G1 to S and G2 to M	35.49
NM_031299	CDCA3	cell division cycle associated 3	20.34
NM_022112	P53AIP1	p53-regulated apoptosis-inducing protein 1	-9.86
AL031680	PARD6B	par-6 partitioning defective 6 homolog beta (C. elegans)	7.68
Enzymatic activity			
AL031848	ACOT7	acyl-CoA thioesterase 7	8.37
BF224349	ASNS	Asparagine synthetase	7.49
BC033179	ATP8B3	ATPase, Class I, type 8B, member 3	-8.73
AW294145	CMBL	carboxymethylenebutenolidase homolog (Pseudomonas)	9.97
AW184014	CPA5	carboxypeptidase A5	-8.09
AW292273	CARS	cysteinyl-tRNA synthetase	-13.22
BE855963	CARS2	cysteinyl-tRNA synthetase 2, mitochondrial (putative)	17.36
AF110329	GLS2	glutaminase 2 (liver, mitochondrial)	-11.36
AI990469	HEXDC	Hexosaminidase (glycosyl hydrolase family 20, catalytic domain) containing	8.71
AF149304	HYALP1	hyaluronoglucosaminidase pseudogene 1	12.06
AI985835	PCCB	Propionyl Coenzyme A carboxylase, beta polypeptide	5.82
NM_003122	SPINK1	serine peptidase inhibitor, Kazal type 1	48.45
NM_001041	SI	sucrase-isomaltase (alpha-glucosidase)	6.67
AV691323	UGT1A1	UDP glucuronosyltransferase 1 family, polypeptide A1	11.62
NM_021139	UGT2B4	UDP glucuronosyltransferase 2 family, polypeptide B4	42.39
BF346193	GALNT13	UDP-N-acetyl-alpha-D-galactosamine:polypeptide N-acetylgalactosaminyltransferase 13 (	7.76
Extracellular Region			
NM_000490	AVP	arginine vasopressin (neurophysin II, antidiuretic hormone, diabetes insipidus, neurohyp	8.83
NM_006419	CXCL13	chemokine (C-X-C motif) ligand 13 (B-cell chemoattractant)	27.14
NM_000130	F5	coagulation factor V (proaccelerin, labile factor)	5.91
NM_001131	CRISP1	cysteine-rich secretory protein 1	-15.29
AW131561	DLL1	delta-like 1 (Drosophila)	-7.42
NM_001971	ELA2A	elastase 2A	-7.53
NM_003665	FCN3	ficolin (collagen/fibrinogen domain containing) 3 (Hakata antigen)	-10.02
NM_000583	GC	group-specific component (vitamin D binding protein)	15.06
AF105378	HS3ST4	heparan sulfate (glucosamine) 3-O-sulfotransferase 4	8.4
NM_024013	IFNA1	interferon, alpha 1	14.27
AF152099	IL17C	interleukin 17C	-17.3
AF147790	MUC12	mucin 12, cell surface associated	-6.15
AL022718	ODZ1	odz, odd Oz/ten-m homolog 1(Drosophila)	9.1
NM_000312	PROC	protein C (inactivator of coagulation factors Va and VIIIa)	79.94
BC005956	RLN1	relaxin 1	9.33
NM_006846	SPINK5	serine peptidase inhibitor, Kazal type 5	-10.12
AI056852	SHBG	sex hormone-binding globulin	16.9
NM_003381	VIP	vasoactive intestinal peptide	24.3
Kinases and Phosphatases			
AA400121	AKAP14	A kinase (PRKA) anchor protein 14	13.38
BC022297	DGKE	diacylglycerol kinase, epsilon 64kDa	36.07
AA971768	KSR1	kinase suppressor of ras 1	-15.18
NM_000431	MVK	mevalonate kinase (mevalonic aciduria)	-9.6
BC040177	PPM1H	Protein phosphatase 1H (PP2C domain containing)	-8.44
AV649337	PTPN2	Protein tyrosine phosphatase, non-receptor type 2	9.31
AK023365	PPFIA4	protein tyrosine phosphatase, receptor type, f polypeptide (PTPRF), interacting protein (li	10.7
NM_003215	TEC	tec protein tyrosine kinase	-8.04

Table 7.1. Major gene clusters modulated in human prostate cancer…..continued…

Accession No.	Gene Symbol	Gene Name	Fold Change
Proteinaceous extracellular matrix			
X16468	COL2A1	collagen, type II, alpha 1 (primary osteoarthritis, spondyloepiphyseal dysplasia, congenita	-9.15
NM_015719	COL5A3	collagen, type V, alpha 3	-11.97
J04177	COL11A1	collagen, type XI, alpha 1	6.98
NM_024302	MMP28	matrix metallopeptidase 28	-7.06
NM_003019	SFTPD	surfactant, pulmonary-associated protein D	-9.13
Phosphate transport			
AK022765	AMACR	alpha-methylacyl-CoA racemase	6.12
AF061191	EDA	ectodysplasin A	-8.04
NM_002445	MSR1	macrophage scavenger receptor 1	12.54
Regulation of transcription			
NM_020328	ACVR1B	activin A receptor, type IB	10.45
AF060154	MSC	musculin (activated B-cell factor-1)	-14.48
AU159942	TOP2A	topoisomerase (DNA) II alpha 170kDa	19.24
BE542323	VGLL1	vestigial like 1 (Drosophila)	-16.81
Transcription factor activity			
AK055536	ASB10	ankyrin repeat and SOCS box-containing 10	-9.17
NM_021073	BMP5	bone morphogenetic protein 5	12.55
NM_000623	BDKRB2	bradykinin receptor B2	-9.89
AF054818	CD84	CD84 molecule	-17.74
AY072911	CXADR	coxsackie virus and adenovirus receptor	24.8
BC011877	DOCK5	dedicator of cytokinesis 5	-23.33
NM_004405	DLX2	distal-less homeobox 2	14.36
AF115403	ELF5	E74-like factor 5 (ets domain transcription factor)	7.35
NM_173503	EFCAB3	EF-hand calcium binding domain 3	-8.68
AW196403	EMX1	empty spiracles homeobox 1	15.27
AF060555	ESR2	estrogen receptor 2 (ER beta)	9.12
BC017869	FBXO36	F-box protein 36	17.88
AF204674	FBXO40	F-box protein 40	-9.08
AL119322	FGF12	fibroblast growth factor 12	-6.08
AA022949	FGF18	Fibroblast growth factor 18	-20.06
AI867445	FOXD3	Forkhead box D3	8.1
NM_153839	GPR111	G protein-coupled receptor 111	12.05
AF317652	GPR61	G protein-coupled receptor 61	16.8
AL567302	GRIA1	glutamate receptor, ionotropic, AMPA 1	7.06
AJ301610	GRIK2	glutamate receptor, ionotropic, kainate 2	7.09
AF332227	HSFY1	heat shock transcription factor, Y-linked 1	12.07
AL157773	KLHL31	kelch-like 31 (Drosophila)	8.44
AI089312	LASS5	LAG1 homolog, ceramide synthase 5	12.79
NM_006840	LILRB5	leukocyte immunoglobulin-like receptor, subfamily B (with TM and ITIM domains), memb	23.12
AF211968	LENG3	leukocyte receptor cluster (LRC) member 3	-6.38
X55503	MT4	metallothionein 4	7.6
BG252318	MBD1	methyl-CpG binding domain protein 1	-7.48
M96980	MYT1	myelin transcription factor 1	18.89
AF192523	NPC1L1	NPC1 (Niemann-Pick disease, type C1, gene)-like 1	12.57
AI051958	NR1H4	nuclear receptor subfamily 1, group H, member 4	9.94
AF061056	NR1I2	nuclear receptor subfamily 1, group I, member 2	8.62
BE674245	NUDT3	Nudix (nucleoside diphosphate linked moiety X)-type motif 3	9.42
X89666	OR2M4	olfactory receptor, family 2, subfamily M, member 4	7.56
AU145336	ONECUT2	one cut homeobox 2	13.71
NM_002699	POU3F1	POU class 3 homeobox 1	8.47
AF072826	RREB1	ras responsive element binding protein 1	10.35
AF464736	RGS12	regulator of G-protein signaling 12	7.19
NM_002924	RGS7	regulator of G-protein signaling 7	6.19
NM_173560	RFXDC1	regulatory factor X domain containing 1	6.09
AW469546	RUNX2	runt-related transcription factor 2	19.57
AY027526	SPATA9	spermatogenesis associated 9	-11.24
BF058505	SHB	Src homology 2 domain containing adaptor protein B	-8.31
BF527050	SOX8	SRY (sex determining region Y)-box 8	-13.33
NM_138780	SYTL5	synaptotagmin-like 5	-9.03
NM_016170	TLX2	T-cell leukemia homeobox 2	9.07
AF519569	TCTE3	t-complex-associated-testis-expressed 3	6.93
AI436409	THAP11	THAP domain containing 11	-19.37
AI769310	TLL1	tolloid-like 1	10.13
NM_003279	TNNC2	troponin C type 2 (fast)	-22.55
AW873556	WNT10A	Wingless-type MMTV integration site family, member 10A	-11.55
AY009402	WNT8A	wingless-type MMTV integration site family, member 8A	7.05

Table 7.1…..continued…

Accession No.	Gene Symbol	Gene Name	Fold Change
Transporters			
U15688	ATP2B2	ATPase, Ca++ transporting, plasma membrane 2	-10.72
AA877910	ATP2A3	ATPase, Ca++ transporting, ubiquitous	-9.95
NM_005177	ATP6V0A1	ATPase, H+ transporting, lysosomal V0 subunit a1	-9.01
AI928218	ATP1B3	ATPase, Na+/K+ transporting, beta 3 polypeptide	9.64
R44603	KCNJ9	potassium inwardly-rectifying channel, subfamily J, member 9	-9.51
NM_000341	SLC3A1	solute carrier family 3 (cystine, dibasic and neutral amino acid transporters, activator of cy	8.38
AB022847	SLC6A2	solute carrier family 6 (neurotransmitter transporter, noradrenalin), member 2	-14.89
U16120	SLC6A6	solute carrier family 6 (neurotransmitter transporter, taurine), member 6	9.17
AA708152	TMED6	transmembrane emp24 protein transport domain containing 6	23.2
Miscellaneous			
N93313	ATXN7L2	ataxin 7-like 2	-12.22
NM_152336	AGBL1	ATP/GTP binding protein-like 1	-7.99
BE551319	BTNL9	Butyrophilin-like 9	14.24
AV746580	COG1	component of oligomeric golgi complex 1	8.53
NM_005210	CRYGB	crystallin, gamma B	12.65
AI365263	DPPA5	developmental pluripotency associated 5	14.01
NM_014419	DKKL1	dickkopf-like 1 (soggy)	9.9
BM681417	DGCR10	DiGeorge syndrome critical region gene 10	-8.33
BC020878	DNMBP	dynamin binding protein	10.04
AI927458	ESPN	espin	-8.02
BF792773	FIBCD1	fibrinogen C domain containing 1	-17.19
AA129444	FSTL5	follistatin-like 5	-9.33
AF039196	HR	hairless homolog (mouse)	-8.94
BQ025558	HEMK1	HemK methyltransferase family member 1	-19.63
NM_003545	HIST1H4E	histone cluster 1, H4e	6.25
NM_002196	INSM1	insulinoma-associated 1	39.14
AL022575	ITIH5L	inter-alpha (globulin) inhibitor H5-like	17.92
AL512748	KATNAL2	katanin p60 subunit A-like 2	-10.09
AL022068	KRT18P38	keratin 18 pseudogene 38	-9.7
AJ406929	KRTAP2-2	keratin associated protein 2-2	9.04
BC001291	LY6K	lymphocyte antigen 6 complex, locus K	8.18
NM_004997	MYBPH	myosin binding protein H	-14.37
AI709055	MYH14	myosin, heavy chain 14	7.49
NM_000257	MYH6	myosin, heavy chain 6, cardiac muscle, alpha (cardiomyopathy, hypertrophic 1)	12.85
AI160292	MYH7B	myosin, heavy chain 7B, cardiac muscle, beta	-10.96
R78299	NEB	Nebulin	-12.71
AW085558	HNT	neurotrimin	7.66
AK091796	NUDT22	Nudix (nucleoside diphosphate linked moiety X)-type motif 22	10.13
AI925361	KCTD15	potassium channel tetramerisation domain containing 15	-14.39
AI867408	Rgr	Ral-GDS related protein Rgr	12.1
BC014155	RHEBL1	Ras homolog enriched in brain like 1	-8.92
NM_022448	RGNEF	Rho-guanine nucleotide exchange factor	-6.67
NM_018957	SH3BP1	SH3-domain binding protein 1	9.39
AI263819	SRGAP2	SLIT-ROBO Rho GTPase activating protein 2	-6.39
BF062187	SNIP	SNAP25-interacting protein	11.06
BF435122	SYNJ1	Synaptojanin 1	-19.42
AE000659	TRAalpha	T cell receptor alpha locus	-7.06
NM_018393	TCP11L1	t-complex 11 (mouse)-like 1	-9.26
NM_012457	TIMM13	translocase of inner mitochondrial membrane 13 homolog (yeast)	-7.39
AW969675	TRDN	triadin	-7.58
AA868267	TRIM54	tripartite motif-containing 54	-6.8
NM_003322	TULP1	tubby like protein 1	-10.32
BM726860	TUBA1B	tubulin, alpha 1b	7.16
NM_018943	TUBA8	tubulin, alpha 8	-14.75
AI122699	VASH1	Vasohibin 1	-17.66
NM_080827	WFDC6	WAP four-disulfide core domain 6	14.53
BF355863	ZBTB40	zinc finger and BTB domain containing 40	8.97
AW469591	ZSCAN5	zinc finger and SCAN domain containing 5	-7.29

Genes upregulated or downregulated at least five-fold in human prostate cancer as compared to normal prostate were identified by microarray analyses and are listed.

Table 7.1.

Cell lines	ATCC#	Receptors	Antigen expression	Origin
22Rv1	CRL-2505	androgen receptor +	PSA	Xenograft from Mice
LNCaP	CRL-1740	androgen and estrogen receptor +	-	50yr old Caucasian male
MDA PCa 2b	CRL-2422	androgen receptor +	PSA	63yr old Black male
PC-3	CRL-1435	androgen-independent	HLA A1, A9	62yr old Caucasian male
DU 145	HTB-81	androgen-independent	-	69yr old Caucasian male
PZ-HPV-7	CRL-2221	-	PSA negative	70yr old Caucasian male
PSA, prostate specific antigen;HLA, human leucocyte antigen				

Table 8.1. Human prostate cell lines used in this study and their descriptors

Accession	Gene	Gene	22Rv1	DU 145	LNCaP	MDA PCa 2b	PC-3
	Symbol		Fold	Fold	Fold	Fold	Fold
NM_016816	OAS1	2',5'-oligoadenylate synthetase 1, 40/46kDa	-25.54	-9.04	-36.07	-22.53	-15.79
NM_016817	OAS2	2'-5'-oligoadenylate synthetase 2, 69/71kDa	-101.85	-104.88	-71.59	-50.03	-78.66
NM_006187	OAS3	2'-5'-oligoadenylate synthetase 3, 100kDa	-13.91	-3.67	-19.38	-25.69	-15.74
NM_003733	OASL	2'-5'-oligoadenylate synthetase-like	-32.59	-4.25	-20.61	-43.51	-14.35
NM_148914	ABHD11	abhydrolase domain containing 11	27.14	4.06	15.43	17.64	10.59
NM_017977	AIM1L	absent in melanoma 1-like	-14.01	-13.87	-13.58	-5.52	-11.55
NM_005622	ACSM3	acyl-CoA synthetase medium-chain family member 3	25.78	2.75	21.68	16.21	3.49
BE897866	ACADSB	acyl-Coenzyme A dehydrogenase, short/branched chain	21.95	7.64	51.14	55.38	15.86
BG435404	ARL4C	ADP-ribosylation factor-like 4C	-47.22	-5.16	-29.81	-14.13	-7.97
U05598	AKR1C2	aldo-keto reductase family 1, member C2	-3.36	-8.06	-81.48	-113.30	-29.33
AL137586	ANAPC7	anaphase promoting complex subunit 7	6.47	8.21	12.21	8.46	11.03
AW173504	AR	androgen receptor (dihydrotestosterone receptor)	24.69	-1.92	47.95	52.57	-1.03
NM_001630	ANXA8	annexin A8	-51.06	-24.51	-53.40	-28.74	-36.75
NM_004041	ARRB1	arrestin, beta 1	16.08	1.04	31.22	39.14	9.79
AF120274	ARTN	artemin	-5.20	-17.43	-7.13	-47.47	-32.12
AI928342	ASRGL1	asparaginase like 1	103.44	68.07	24.99	338.55	70.89
NM_017935	BANK1	B-cell scaffold protein with ankyrin repeats 1	20.06	7.77	59.44	34.82	9.93
NM_004335	BST2	bone marrow stromal cell antigen 2	-25.23	-61.23	-49.59	-126.36	-112.44
NM_000055	BCHE	butyrylcholinesterase	2.46	121.32	50.06	-1.39	118.99
NM_001257	CDH13	cadherin 13, H-cadherin (heart)	-50.69	-36.80	-96.19	-21.71	-40.70
AA743820	CAPN14	calpain 14	-20.92	-10.74	-12.27	-15.30	-13.54
AF038567	CTAG1A	cancer/testis antigen 1A	209.64	1.00	6.43	36.71	1.00
BC042510	CEL	carboxyl ester lipase (bile salt-stimulated lipase)	-30.28	-19.22	-3.60	-12.56	-11.17
AI719655	CASP1	caspase 1, apoptosis-related cysteine peptidase	-4.44	-8.35	-6.86	-8.16	-6.57
AI246687	CTSC	cathepsin C	-38.36	-10.05	-91.33	-127.99	-6.91
NM_001766	CD1D	CD1d molecule	-23.46	-16.53	-56.53	-8.94	-56.53
AV700298	CD44	CD44 molecule (Indian blood group)	-8.94	-8.27	-17.19	-12.56	-8.72
AL519710	CADM1	cell adhesion molecule 1	23.55	119.41	32.80	1.57	285.99
NM_024053	CENPM	centromere protein M	14.73	8.21	7.82	5.55	7.23
AF030514	CXCL11	chemokine (C-X-C motif) ligand 11	-77.51	-51.51	-38.88	-22.26	-73.49
NM_006536	CLCA2	chloride channel, calcium activated, family member 2	-26.05	-27.03	-23.89	-14.89	-25.52
AF195624	CHPT1	choline phosphotransferase 1	35.81	8.06	18.62	17.94	9.17
NM_000745	CHRNA5	cholinergic receptor, nicotinic, alpha 5	7.78	12.35	7.63	6.24	14.04
AF059274	CSPG5	chondroitin sulfate proteoglycan 5 (neuroglycan C)	21.64	19.08	36.61	22.46	11.80
BE568660	CHURC1	churchill domain containing 1	5.61	13.71	7.25	7.30	7.46
AW264204	CLDN11	claudin 11 (oligodendrocyte transmembrane protein)	63.69	70.63	-3.04	-2.77	49.88
BE791251	CLDN3	claudin 3	95.11	44.40	105.92	437.99	48.90
M25915	CLU	clusterin	31.42	7.54	1.10	21.72	12.25
AI889941	COL4A6	collagen, type IV, alpha 6	-22.67	-40.14	-48.15	-9.20	-20.12
NM_000094	COL7A1	collagen, type VII, alpha 1	-14.07	-11.68	-18.00	-16.61	-18.62

Table 8.2. Genes modulated in all prostate cancer cell lines…..continued…

Accession	Gene Symbol	Gene	22Rv1 Fold	DU 145 Fold	LNCaP Fold	MDA PCa 2b Fold	PC-3 Fold
X04697	CFH	complement factor H	-39.94	-22.07	-39.94	-39.94	-26.28
NM_015198	COBL	cordon-bleu homolog (mouse)	8.77	18.76	12.68	17.21	14.60
AF007162	CRYAB	crystallin, alpha B	-10.16	-13.13	-10.84	-21.51	-11.84
NM_000496	CRYBB2	crystallin, beta B2	1.00	1.00	1.00	156.83	1.00
BF448201	CUL5	cullin 5	17.90	57.78	70.63	47.53	51.87
NM_001759	CCND2	cyclin D2	-104.35	-61.43	-191.96	-97.63	-54.61
AA922068	CDK6	cyclin-dependent kinase 6	-5.63	-5.39	-14.33	-16.13	-8.13
AW444761	CDKN2B	cyclin-dependent kinase inhibitor 2B (p15, inhibits CDK4)	-18.23	-6.28	-77.00	-96.89	-5.45
NM_001262	CDKN2C	cyclin-dependent kinase inhibitor 2C (p18, inhibits CDK4)	10.52	9.09	5.59	3.16	11.70
NM_005213	CSTA	cystatin A (stefin A)	-144.29	-426.21	-165.89	-148.84	-397.66
NM_000784	CYP27A1	cytochrome P450, family 27, subfamily A, polypeptide 1	10.17	12.74	11.00	8.08	12.66
NM_018665	DDX43	DEAD (Asp-Glu-Ala-Asp) box polypeptide 43	1.44	131.78	37.27	1.45	91.72
NM_014314	DDX58	DEAD (Asp-Glu-Ala-Asp) box polypeptide 58	-54.53	-4.76	-47.44	-22.23	-18.52
AF196571	DLL1	delta-like 1 (Drosophila)	-13.73	-61.59	-3.53	-20.18	-32.94
NM_001941	DSC3	desmocollin 3	-22.46	-15.44	-16.85	-29.42	-19.29
AF064771	DGKA	diacylglycerol kinase, alpha 80kDa	-5.24	-6.90	-26.75	-5.24	-7.68
AU148057	DKK3	dickkopf homolog 3 (Xenopus laevis)	-106.37	-6.60	-165.41	-219.87	-13.04
AI144299	DHFR	dihydrofolate reductase	18.90	8.33	12.04	7.91	6.05
AI620209	DPP7	Dipeptidyl-peptidase 7	14.45	2.66	17.31	12.98	5.21
X93921	DUSP7	dual specificity phosphatase 7	-8.23	-30.38	-8.56	-7.32	-31.28
AC005393	DYRK1B	dual-specificity tyrosine-(Y)-phosphorylation regulated kinase 1B	7.96	14.60	11.71	11.09	12.20
AL096710	DST	dystonin	-68.73	-177.40	-171.32	-120.16	-71.88
AA609053	ENPP5	ectonucleotide pyrophosphatase/phosphodiesterase 5	12.71	20.71	29.35	16.67	7.29
M74921	EDNRB	endothelin receptor type B	13.44	14.11	11.76	9.14	14.95
BC000686	EPDR1	ependymin related protein 1 (zebrafish)	17.01	33.67	1.56	12.04	43.54
NM_005228	EGFR	epidermal growth factor receptor	-23.87	-6.65	-21.54	-7.05	-12.06
NM_001423	EMP1	epithelial membrane protein 1	-16.42	-7.47	-29.44	-17.67	-29.30
AA633203	EPSTI1	epithelial stromal interaction 1 (breast)	-13.53	-17.01	-22.07	-13.54	-15.37
AL120674	ESCO2	establishment of cohesion 1 homolog 2 (S. cerevisiae)	20.15	7.25	11.18	2.22	9.56
NM_005103	FEZ1	fasciculation and elongation protein zeta 1 (zygin I)	-20.54	-10.19	-77.20	-76.99	-13.38
AL832251	FBXO18	F-box protein, helicase, 18	-0.05	25.44	15.12	20.55	32.69
AU152635	FECH:	ferrochelatase (protoporphyria)	21.74	5.25	29.63	22.17	6.81
AB016517	FGF5	fibroblast growth factor 5	-34.83	-34.83	-34.83	-34.83	-34.83
NM_013281	FLRT3	fibronectin leucine rich transmembrane protein 3	-5.20	-10.07	-43.97	-34.42	-17.31
NM_004476	FOLH1	folate hydrolase (prostate-specific membrane antigen) 1	138.34	1.32	390.46	448.93	1.83
BF438173	FST	follistatin	-60.98	-163.08	-208.34	-57.88	-189.16
NM_004496	FOXA1	forkhead box A1	12.87	3.81	13.06	15.50	3.89
AI676059	FOXQ1	forkhead box Q1	-15.54	-9.98	-11.41	-5.74	-20.95
NM_006018	GPR109B	G protein-coupled receptor 109B	-23.95	-99.38	-56.79	-99.38	-12.94
W67511	GPR115	G protein-coupled receptor 115	-32.62	-32.84	-42.53	-8.19	-45.57

Table 8.2…..continued…

Accession	Gene Symbol	Gene	22Rv1 Fold	DU 145 Fold	LNCaP Fold	MDA PCa 2b Fold	PC-3 Fold
BC000181	GPR160	G protein-coupled receptor 160	14.04	12.48	22.35	37.86	13.62
NM_023915	GPR87	G protein-coupled receptor 87	-60.52	-24.61	-145.06	-60.95	-90.17
AW183080	GPR92	G protein-coupled receptor 92	-35.76	-21.12	-34.92	-14.65	-35.55
NM_004961	GABRE	gamma-aminobutyric acid (GABA) A receptor, epsilon	-6.41	-9.31	-10.71	-23.63	-9.19
N46350	GDAP1	ganglioside-induced differentiation-associated protein 1	10.19	3.72	7.18	16.00	6.83
M86849	GJB2	gap junction protein, beta 2, 26kDa	-133.01	-145.24	-249.89	-177.13	-110.03
AI694073	GJB6	gap junction protein, beta 6	-485.64	-264.73	-213.17	-291.00	-572.90
BC002557	GATA2	GATA binding protein 2	20.94	4.45	28.96	49.23	5.35
BE675337	GSN	gelsolin (amyloidosis, Finnish type)	-104.87	-68.10	-68.10	-104.87	-81.93
NM_012413	QPCT	glutaminyl-peptide cyclotransferase (glutaminyl cyclase)	-7.27	-3.30	-192.43	-40.25	-11.82
AL527430	GSTM3	glutathione S-transferase M3 (brain)	9.86	7.10	19.40	21.41	7.05
NM_000852	GSTP1	glutathione S-transferase pi	-66.56	-6.24	-73.26	-69.50	-6.17
NM_000853	GSTT1	glutathione S-transferase theta 1	6.43	12.27	5.69	10.23	9.72
BF432254	GLYATL1	glycine-N-acyltransferase-like 1	97.60	1.70	65.04	78.44	-1.48
NM_002510	GPNMB	glycoprotein (transmembrane) nmb	-8.52	-20.83	-6.76	-4.07	-11.92
X61094	GM2A	GM2 ganglioside activator	-13.12	-11.48	-4.33	-4.97	-10.16
NM_016548	GOLM1	golgi membrane protein 1	1.95	23.30	10.38	14.35	14.34
AL137763	GRHL3	grainyhead-like 3 (Drosophila)	-36.55	-14.23	-9.34	-16.44	-13.75
AF261715	PSMAL	growth-inhibiting protein 26	60.46	1.23	193.75	229.75	2.49
BM666010	GNG4	guanine nucleotide binding protein (G protein), gamma 4	47.30	38.18	1.65	1.11	32.68
AW014593	GBP1	guanylate binding protein 1, interferon-inducible, 67kDa	-60.08	-8.70	-36.06	-55.12	-40.02
AL136680	GBP3	guanylate binding protein 3	-58.72	-18.78	-60.61	-13.02	-57.85
AW392952	GBP4	guanylate binding protein 4	-22.16	-14.39	-11.54	-4.35	-22.16
AK023754	HES2	hairy and enhancer of split 2 (Drosophila)	-14.92	-16.40	-16.54	-16.27	-17.51
NM_016323	HERC5	hect domain and RLD 5	-22.73	-4.25	-15.57	-17.41	-6.18
NM_003483	HMGA2	high mobility group AT-hook 2	-12.05	-23.50	-49.50	-27.00	-12.63
NM_014707	HDAC9	histone deacetylase 9	-19.74	-17.43	-40.60	-25.50	-17.93
AI246769	HOXA9	homeobox A9	-8.92	-14.06	-68.17	-54.63	-17.78
BF062550	HOXB13	homeobox B13	48.31	-4.61	55.12	64.52	-3.23
NM_017409	HOXC10	homeobox C10	28.51	33.51	2.54	1.12	38.16
NM_004503	HOXC6	homeobox C6	13.54	10.04	25.48	12.86	9.18
AW299531	HOXD10	homeobox D10	-31.02	-35.35	-58.49	-24.46	-25.37
BC001387	HRASLS3	HRAS-like suppressor 3	62.70	78.17	47.51	238.97	44.60
NM_016245	HSD17B11	hydroxysteroid (17-beta) dehydrogenase 11	15.08	11.33	1.76	16.14	10.69
NM_001553	IGFBP7	insulin-like growth factor binding protein 7	-242.44	-347.59	-250.06	-341.20	-523.01
AV733308	ITGA6	integrin, alpha 6	-62.11	-6.88	-23.30	-5.50	-8.26
NM_000213	ITGB4	integrin, beta 4	-45.44	-4.77	-24.84	-13.75	-16.02
NM_000888	ITGB6	integrin, beta 6	-29.49	-30.01	-26.69	-5.19	-37.46
BF513121	ITGB8	integrin, beta 8	-7.22	-27.15	-107.12	-25.65	-52.75
AA749101	IFITM1	interferon induced transmembrane protein 1 (9-27)	-83.96	-55.65	-104.15	-125.96	-121.95

Table 8.2…..continued…

Accession	Gene	Gene	22Rv1	DU 145	LNCaP	MDA PCa 2b	PC-3
	Symbol		Fold	Fold	Fold	Fold	Fold
NM_006435	IFITM2	interferon induced transmembrane protein 2 (1-8D)	-17.47	-3.69	-8.49	-11.15	-52.59
NM_022168	IFIH1	interferon induced with helicase C domain 1	-26.99	-10.09	-15.42	-7.74	-30.42
NM_004030	IRF7	interferon regulatory factor	-19.81	-4.17	-6.50	-10.24	-12.11
AU144284	IRF6	interferon regulatory factor 6	-25.52	-34.57	-8.23	-3.83	-53.14
NM_005532	IFI27	interferon, alpha-inducible protein 27	-244.57	-34.89	-214.29	-168.40	-224.19
NM_022873	IFI6	interferon, alpha-inducible protein 6	-250.97	-8.75	-24.39	-53.71	-19.60
AF208043	IFI16	interferon, gamma-inducible protein 16	-109.01	-18.51	-84.87	-201.47	-257.39
NM_001548	IFIT1	interferon-induced protein with tetratricopeptide repeats 1	-779.95	-4.30	-61.25	-2119.70	-14.87
BE888744	IFIT2	interferon-induced protein with tetratricopeptide repeats 2	-14.32	-7.66	-17.86	-18.19	-10.94
NM_001549	IFIT3	interferon-induced protein with tetratricopeptide repeats 3	-22.60	-4.99	-17.57	-19.36	-17.58
N47725	IFIT5	interferon-induced protein with tetratricopeptide repeats 5	-9.90	-4.60	-7.17	-9.07	-5.30
NM_012420	IFIT5	interferon-induced protein with tetratricopeptide repeats 5	-8.53	-4.99	-6.39	-7.03	-7.26
NM_006084	ISGF3G	interferon-stimulated transcription factor 3, gamma 48kDa	-22.39	-7.37	-29.25	-26.90	-12.74
BE563442	IL1RN	interleukin 1 receptor antagonist	-28.91	-22.30	-5.98	-4.67	-21.63
M15329	IL1A	interleukin 1, alpha	-121.86	-91.83	-163.18	-173.36	-105.82
NM_000576	IL1B	interleukin 1, beta	-45.61	-23.18	-51.53	-30.37	-23.73
AL578102	IL20RB	interleukin 20 receptor beta	-64.83	-5.52	-74.74	-29.44	-45.70
NM_005547	IVL	involucrin	-7.88	-8.38	-8.63	-8.67	-8.62
NM_006633	IQGAP2	IQ motif containing GTPase activating protein 2	2.98	17.97	13.89	42.01	16.92
AI928035	IRX2	iroquois homeobox 2	-108.53	-121.68	-9.34	-218.53	-77.04
BC002710	KLK10	kallikrein-related peptidase 10	-74.89	-61.21	-92.99	-350.24	-194.51
AF243527	KLK5	kallikrein-related peptidase 5	-17.38	-22.13	-14.10	-16.53	-14.72
AU155415	KLK7	kallikrein-related peptidase 7	-15.39	-7.53	-12.18	-10.65	-8.73
NM_007196	KLK8	kallikrein-related peptidase 8	-457.43	-66.10	-223.14	-457.43	-59.95
BC002690	KRT14	keratin 14	-452.88	-1664.70	-173.10	-47.19	-357.82
NM_002275	KRT15	keratin 15	-115.43	-98.12	-772.21	-18.31	-33.79
NM_000422	KRT17	keratin 17	-76.07	-57.10	-57.94	-96.62	-71.05
NM_000424	KRT5	keratin 5	-165.28	-863.87	-568.05	-136.84	-225.51
AL569511	KRT6A	keratin 6A	-426.03	-503.08	-347.95	-522.30	-273.23
L42612	KRT6B	keratin 6B	-38.75	-80.78	-46.41	-36.54	-43.11
AI668605	KLB	klotho beta	18.75	41.35	9.08	19.44	8.96
BC012919	KLF7	Kruppel-like factor 7 (ubiquitous)	-6.06	-23.76	-65.01	-6.34	-24.11
NM_000227	LAMA3	laminin, alpha 3	-125.88	-5.33	-13.28	-17.77	-15.37
L25541	LAMB3	laminin, beta 3	-134.23	-3.31	-105.47	-79.92	-5.64
NM_005562	LAMC2	laminin, gamma 2	-209.40	-9.45	-340.91	-34.52	-26.86
NM_024679	LPHN1	latrophilin 1	14.24	17.43	23.29	10.15	12.33
U50748	LEPR	leptin receptor	-16.88	-6.39	-38.45	-20.56	-9.51
AK027231	LIMCH1	LIM and calponin homology domains 1	5.75	10.11	28.95	31.13	5.58
AV709727	LONRF2	LON peptidase N-terminal domain and ring finger 2	34.18	9.03	23.84	54.39	31.56
NM_014400	LY6PLAUR	LY6/PLAUR domain containing 3	-293.91	-4.71	-134.69	-15.76	-10.26

Table 8.2…..continued…

Accession	Gene	Gene	22Rv1	DU 145	LNCaP	MDA PCa 2b	PC-3
	Symbol		Fold	Fold	Fold	Fold	Fold
NM_014398	LAMP3	lysosomal-associated membrane protein 3	-36.11	-12.04	-39.33	-19.83	-12.03
AU149305	MMP14	matrix metallopeptidase 14 (membrane-inserted)	-18.97	-8.04	-17.16	-16.30	-7.09
NM_024302	MMP28	matrix metallopeptidase 28	-16.71	-15.41	-13.37	-35.25	-33.64
BC003408	MAGEA12	melanoma antigen family A, 12	239.35	-1.00	255.91	201.46	1.48
NM_005361	MAGEA2	melanoma antigen family A, 2	172.01	4.48	216.63	114.79	1.77
BC000340	MAGEA3	melanoma antigen family A, 3	95.16	-1.54	89.87	74.61	1.02
U10691	MAGEA6	melanoma antigen family A, 6	284.97	1.03	269.67	228.42	1.03
AF216650	MTAP	methylthioadenosine phosphorylase	20.36	14.79	9.99	7.02	11.07
NM_014033	METTL7A	methyltransferase like 7A	127.17	-2.33	46.97	42.28	-2.19
AI674759	MAPKBP1	mitogen activated protein kinase binding protein 1	-9.69	-4.25	-5.59	-12.33	-7.00
BE967311	MCC	mutated in colorectal cancers	-68.62	-6.26	-84.26	-48.81	-18.27
AI318120	MAZ	MYC-associated zinc finger protein	14.30	13.93	17.49	4.64	7.58
NM_005368	MB	myoglobin	42.58	7.21	46.01	111.61	4.49
NM_002462	MX1	myxovirus (influenza virus) resistance 1	-157.24	-15.89	-91.15	-92.74	-44.16
AF119848	NDUFA2	NADH dehydrogenase (ubiquinone) 1 alpha subcomplex, 2	9.33	24.24	19.00	21.33	29.11
NM_015678	NBEA	neurobeachin	14.01	6.88	6.20	22.11	10.19
BC001606	NCF2	neutrophil cytosolic factor 2 (65kDa)	-31.05	-27.92	-38.94	-32.75	-72.04
AF247704	NKX3-1	NK3 homeobox 1	68.90	5.72	54.01	76.77	2.98
NM_017617	NOTCH1	Notch homolog 1, translocation-associated	-6.47	-9.60	-7.29	-8.91	-16.07
NM_021963	NAP1L2	nucleosome assembly protein 1-like 2	72.01	13.29	144.02	32.94	1.92
AI381524	NAP1L4	Nucleosome assembly protein 1-like 4	-12.40	-12.40	-12.40	-12.40	-12.40
AL833418	PNLIPRP3	pancreatic lipase-related protein 3	-69.04	-202.43	-93.69	-88.87	-51.00
NM_002820	PTHLH	parathyroid hormone-like hormone	-20.09	-123.00	-37.74	-38.34	-24.05
BC003096	PDLIM4	PDZ and LIM domain 4	-14.57	-64.24	-21.71	-8.35	-14.19
L10343	PI3	peptidase inhibitor 3, skin-derived (SKALP)	-19.12	-12.57	-15.05	-13.85	-26.81
NM_002705	PPL	periplakin	-78.62	-6.40	-15.27	-20.76	-7.89
AB028127	PIGM	phosphatidylinositol glycan anchor biosynthesis, class M	14.93	5.85	11.67	6.02	5.74
AA888858	PDE3B	Phosphodiesterase 3B, cGMP-inhibited	13.04	10.45	9.57	18.26	17.82
NM_021105	PLSCR1	phospholipid scramblase 1	-9.84	-3.60	-224.26	-192.22	-5.78
AI378979	PKP1	plakophilin 1 (ectodermal dysplasia/skin fragility syndrome)	-139.13	-720.45	-187.75	-3.34	-209.79
NM_006207	PDGFRL	platelet-derived growth factor receptor-like	24.60	58.50	19.60	11.00	30.42
AI718937	KCTD12	potassium channel tetramerisation domain containing 12	-6.60	-5.50	-76.09	-57.88	-42.43
U73191	KCNJ15	potassium inwardly-rectifying channel, subfamily J, member 15	-74.08	-61.76	-19.57	-219.41	-108.16
D82346	KCNQ2	potassium voltage-gated channel, KQT-like subfamily, member 2	28.58	14.10	23.91	1.68	18.34
NM_006115	PRAME	preferentially expressed antigen in melanoma	5.37	13.27	26.11	26.68	7.32
NM_002675	PML	promyelocytic leukemia	-122.23	-3.27	-23.15	-23.69	-7.42
NM_002736	PRKAR2B	protein kinase, cAMP-dependent, regulatory, type II, beta	-0.01	58.54	89.56	188.69	62.68
AI888150	PPP1R9A	protein phosphatase 1, regulatory (inhibitor) subunit 9A	40.96	21.80	10.64	15.44	36.41
AB032983	PPM1H	protein phosphatase 1H (PP2C domain containing)	15.87	16.92	13.58	28.54	10.09
AI631833	PTPRJ	protein tyrosine phosphatase, receptor type, J	9.82	21.04	6.51	42.31	11.53

Table 8.2…..continued…

Accession	Gene	Gene	22Rv1	DU 145	LNCaP	MDA PCa 2b	PC-3
	Symbol		Fold	Fold	Fold	Fold	Fold
NM_022337	RAB38	RAB38, member RAS oncogene family	-144.22	-7.37	-98.64	-156.05	-4.82
AI805050	RAB6B	RAB6B, member RAS oncogene family	4.85	23.40	49.25	44.82	19.80
BC005153	RPH3AL	rabphilin 3A-like (without C2 domains)	-1.06	19.01	12.49	26.11	12.23
AW189843	RSAD2	radical S-adenosyl methionine domain containing 2	-18.15	-16.13	-27.89	-37.68	-19.57
AL096776	RHOU	ras homolog gene family, member U	40.44	5.77	12.94	37.51	7.66
AK000776	ROR1	receptor tyrosine kinase-like orphan receptor 1	-1.46	25.59	4.89	22.77	37.97
AI824113	RGS12	regulator of G-protein signaling 12	-6.04	-4.98	-5.80	-7.87	-4.97
NM_014882	ARHGAP25	Rho GTPase activating protein 25	-31.17	-31.17	-31.17	-31.17	-31.17
AJ131212	RNASE7	ribonuclease, RNase A family, 7	-89.11	-55.35	-89.11	-31.16	-28.20
NM_024539	RNF128	ring finger protein 128	-10.84	-6.26	-11.49	-263.10	-199.65
BF056204	RNF157	ring finger protein 157	145.67	233.27	136.43	24.37	185.86
AI677701	RBM24	RNA binding motif protein 24	1.19	41.83	17.61	19.35	44.01
AF312386	RUNX1	runt-related transcription factor 1	15.24	9.51	18.46	12.51	12.40
NM_005978	S100A2	S100 calcium binding protein A2	-448.88	-27.01	-332.20	-361.20	-67.90
NM_002961	S100A4	S100 calcium binding protein A4	-202.92	-3.03	-110.20	-56.99	-9.78
NM_002964	S100A8	S100 calcium binding protein A8	-2670.91	-128.39	-4059.78	-2218.46	-4059.78
NM_002965	S100A9	S100 calcium binding protein A9	-153.41	-10.57	-310.86	-157.64	-147.79
AI745526	SPDEF	SAM pointed domain containing ets transcription factor	46.66	1.65	21.12	69.42	1.49
AW470178	SCEL	sciellin	-17.11	-5.01	-29.53	-17.66	-6.91
AI332407	SFRP1	secreted frizzled-related protein 1	-55.23	-4.18	-22.67	-56.73	-4.28
NM_003118	SPARC	secreted protein, acidic, cysteine-rich (osteonectin)	-64.77	-53.23	-34.49	-130.50	-251.64
NM_005410	SEPP1	selenoprotein P, plasma, 1	48.22	7.67	41.51	91.28	2.41
M23699	SAA1	serum amyloid A1	-507.23	-14.10	-182.46	-507.23	-207.88
NM_005627	SGK	serum/glucocorticoid regulated kinase	-29.73	-5.74	-15.43	-38.10	-7.92
AF022654	SHOX2	short stature homeobox 2	38.16	12.44	22.92	6.55	47.29
BC002704	STAT1	signal transducer and activator of transcription 1, 91kDa	-92.22	-7.22	-31.34	-58.45	-9.32
BF680588	STEAP2	six transmembrane epithelial antigen of the prostate 2	20.56	2.05	31.70	16.44	1.95
AV730849	SLAIN1	SLAIN motif family, member 1	171.53	60.87	102.88	83.72	16.02
NM_033438	SLAMF9	SLAM family member 9	-18.31	-23.25	-8.71	-23.25	-23.25
NM_005585	SMAD6	SMAD family member 6	101.25	173.03	66.79	105.02	90.49
NM_005987	SPRR1A	small proline-rich protein 1A	-21.94	-43.04	-18.62	-16.36	-27.34
NM_006945	SPRR2B	small proline-rich protein 2B	-9.43	-14.01	-16.71	-9.45	-13.00
BF575466	SPRR3	small proline-rich protein 3	-35.84	-29.38	-83.03	-36.35	-29.19
AI572079	SNAI2	snail homolog 2 (Drosophila)	-17.97	-19.19	-39.40	-12.80	-13.99
NM_004696	SLC16A4	solute carrier family 16, member 4 (monocarboxylic acid transporter 5)	-4.06	-91.47	-45.66	-86.64	-63.26
NM_020041	SLC2A9	solute carrier family 2 (facilitated glucose transporter), member 9	-7.56	-7.07	-7.63	-6.76	-5.96
AI279062	SLC22A15	solute carrier family 22 (organic cation transporter), member 15	-13.17	-19.32	-25.29	-4.02	-29.00
NM_030631	SLC25A21	solute carrier family 25 (mitochondrial oxodicarboxylate carrier), member 21	8.54	251.44	8.58	10.53	278.27
NM_022154	SLC39A8	solute carrier family 39 (zinc transporter), member 8	13.49	8.05	5.38	10.35	8.36
NM_003759	SLC4A4	solute carrier family 4, sodium bicarbonate cotransporter, member 4	2.07	14.95	50.38	41.23	13.41

Table 8.2…..continued…

Accession	Gene Symbol	Gene	22Rv1 Fold	DU 145 Fold	LNCaP Fold	MDA PCa 2b Fold	PC-3 Fold
AA631143	SLC45A3	solute carrier family 45, member 3	35.60	3.83	44.33	66.87	3.35
AA876372	SLC7A2	solute carrier family 7 (cationic amino acid transporter, y+ system), member 2	42.26	-0.85	15.81	17.63	8.35
NM_013272	SLCO3A1	solute carrier organic anion transporter family, member 3A1	-12.58	-10.40	-15.81	-17.49	-16.04
NM_003113	SP100	SP100 nuclear antigen	-131.33	-5.50	-11.73	-6.46	-6.78
NM_014474	SMPDL3B	sphingomyelin phosphodiesterase, acid-like 3B	12.55	19.65	28.88	25.93	23.89
AI989530	SGEF	Src homology 3 domain-containing guanine nucleotide exchange factor	4.82	9.27	29.50	19.94	11.90
AI808807	SOX7	SRY (sex determining region Y)-box 7	-19.95	-18.16	-34.09	-15.30	-15.52
AW328672	STARD10	StAR-related lipid transfer (START) domain containing 10	6.52	5.98	29.60	19.58	16.61
AA741307	SAMD9	sterile alpha motif domain containing 9	-124.65	-3.99	-33.85	-54.31	-228.87
AI122754	STS	steroid sulfatase (microsomal), isozyme S	9.10	8.87	18.81	18.27	5.37
BE379761	STON2	Stonin 2	-5.02	-9.42	-10.12	-5.87	-9.47
AL034418	SULF2	sulfatase 2	-20.42	-22.35	-21.10	-17.11	-34.88
AW663885	SUHW2	suppressor of hairy wing homolog 2 (Drosophila)	10.31	6.56	10.69	12.17	14.44
BC000731	SYNGR1	synaptogyrin 1	10.57	17.08	15.73	1.77	15.37
NM_016524	SYT17	synaptotagmin XVII	6.36	26.90	-1.54	46.47	21.01
AA158731	TNS4	tensin 4	-45.50	-45.50	-45.50	-45.50	-45.50
NM_000361	THBD	thrombomodulin	-11.89	-7.06	-18.07	-17.25	-8.15
AF021834	TFPI	tissue factor pathway inhibitor	8.19	38.71	75.58	-1.09	62.78
NM_003265	TLR3	toll-like receptor 3	-9.67	-6.60	-7.49	-5.56	-7.22
AK025084	TOX3	TOX high mobility group box family member 3	219.85	1.25	40.74	327.87	1.29
AL008730	TRAF3IP2	TRAF3 interacting protein 2	-7.69	-5.44	-6.06	-5.10	-5.83
BC001830	TGFB1I1	transforming growth factor beta 1 induced transcript 1	-8.29	-4.51	-66.24	-36.92	-14.12
AA806283	TMEM154	transmembrane protein 154	-65.76	-89.80	-29.22	-11.83	-521.75
AI087937	TMEM40	transmembrane protein 40	-43.62	-21.71	-41.21	-43.96	-57.99
AA054642	TMEM56	transmembrane protein 56	11.09	18.38	8.44	22.19	26.17
AF162690	TTR	transthyretin (prealbumin, amyloidosis type I)	33.70	15.44	40.67	16.77	20.82
AA083478	TRIM22	tripartite motif-containing 22	-68.85	-590.91	-112.16	-40.68	-90.86
NM_012101	TRIM29	tripartite motif-containing 29	-51.63	-35.11	-59.67	-25.81	-78.05
NM_003810	TNFSF10	tumor necrosis factor (ligand) superfamily, member 10	-26.42	-19.14	-50.00	-10.41	-30.82
AF026071	PLEKHG5	pleckstrin homology domain containing, family G, member 5	-11.30	-3.88	-5.82	-11.30	-11.30
AF091627	TP63	tumor protein p63	-38.64	-34.77	-22.67	-32.41	-18.75
BE551138	ARTS-1	type 1 tumor necrosis factor receptor shedding aminopeptidase regulator	-40.93	-14.14	-9.23	-37.02	-41.02
AK022859	UNC5B	unc-5 homolog B (C. elegans)	-28.89	-78.91	-31.41	-6.10	-70.72
AI754423	VGLL3	vestigial like 3 (Drosophila)	-44.90	-38.45	-47.05	-28.81	-63.04
BC036233	WDR66	WD repeat domain 66	-14.28	-10.90	-7.31	-12.46	-6.03
BC005056	WBSCR18	Williams Beuren syndrome chromosome region 18	8.51	4.54	11.28	10.62	5.94
NM_030761	WNT4	wingless-type MMTV integration site family, member 4	-6.16	-5.46	-7.36	-10.03	-6.58
AA167449	XIST	X (inactive)-specific transcript	-15.57	-31.30	-16.58	-4.60	-24.55
AF193855	ZIC2	Zic family member 2 (odd-paired homolog, Drosophila)	163.82	9.16	255.13	218.58	73.08
NM_007150	ZNF185	zinc finger protein 185 (LIM domain)	-18.96	-4.20	-29.85	-15.03	-7.98
NM_024702	ZNF750	zinc finger protein 750	-158.61	-112.12	-96.79	-101.47	-112.12
AK097019	ZNF781	zinc finger protein 781	7.81	19.72	12.62	20.80	20.79

Genes modulated in specific prostate cancer cell lines as indicated. Fold change values as compared to expression in normal prostate epithelial cells are listed.

Table 8.2.

REFERENCES

1. Chen, C. and Kong, A.N. (2004) Dietary chemopreventive compounds and ARE/EpRE signaling. *Free Radic Biol Med*, **36**, 1505-16.
2. Chen, C. and Kong, A.N. (2005) Dietary cancer-chemopreventive compounds: from signaling and gene expression to pharmacological effects. *Trends Pharmacol Sci*, **26**, 318-26.
3. Hu, R., Khor, T.O., Shen, G., Jeong, W.S., Hebbar, V., Chen, C., Xu, C., Reddy, B., Chada, K. and Kong, A.N. (2006) Cancer chemoprevention of intestinal polyposis in ApcMin/+ mice by sulforaphane, a natural product derived from cruciferous vegetable. *Carcinogenesis*, **27**, 2038-46.
4. Xu C, Huang MT, Shen G, Yuan X, Lin W, Khor TO, Conney AH and Kong AN . (2006) Inhibition of 7,12-Dimethylbenz(a)anthracene-Induced Skin Tumorigenesis in C57BL/6 Mice by Sulforaphane is Mediated by Nuclear Factor E2-Related Factor 2. *Cancer Res*, **66**, 8293-8296.
5. Forman, H.J., Torres, M. and Fukuto, J. (2002) Redox signaling. *Mol Cell Biochem*, **234-235**, 49-62.
6. Hansen, J.M., Go, Y.M. and Jones, D.P. (2006) Nuclear and mitochondrial compartmentation of oxidative stress and redox signaling. *Annu Rev Pharmacol Toxicol*, **46**, 215-34.
7. Hansen, J.M., Watson, W.H. and Jones, D.P. (2004) Compartmentation of Nrf-2 redox control: regulation of cytoplasmic activation by glutathione and DNA binding by thioredoxin-1. *Toxicol Sci*, **82**, 308-17.
8. Barford, D. (2004) The role of cysteine residues as redox-sensitive regulatory switches. *Curr Opin Struct Biol*, **14**, 679-86.
9. Sporn, M.B. and Liby, K.T. (2005) Cancer chemoprevention: scientific promise, clinical uncertainty. *Nat Clin Pract Oncol*, **2**, 518-25.
10. Lotem, J., Netanely, D., Domany, E. and Sachs, L. (2005) Human cancers overexpress genes that are specific to a variety of normal human tissues. *Proc Natl Acad Sci U S A*, **102**, 18556-61.
11. Surh, Y.J. (2003) Cancer chemoprevention with dietary phytochemicals. *Nat Rev Cancer*, **3**, 768-80.
12. Conney, A.H. (2004) Tailoring cancer chemoprevention regimens to the individual. *J Cell Biochem*, **91**, 277-86.
13. Itoh, K., Wakabayashi, N., Katoh, Y., Ishii, T., Igarashi, K., Engel, J.D. and Yamamoto, M. (1999) Keap1 represses nuclear activation of antioxidant responsive elements by Nrf2 through binding to the amino-terminal Neh2 domain. *Genes Dev*, **13**, 76-86.
14. Chen, C., Shen, G., Hebbar, V., Hu, R., Owuor, E.D. and Kong, A.N. (2003) Epigallocatechin-3-gallate-induced stress signals in HT-29 human colon adenocarcinoma cells. *Carcinogenesis*, **24**, 1369-78.
15. Hu, R., Kim, B.R., Chen, C., Hebbar, V. and Kong, A.N. (2003) The roles of JNK and apoptotic signaling pathways in PEITC-mediated responses in human HT-29 colon adenocarcinoma cells. *Carcinogenesis*, **24**, 1361-7.

16. Jeong, W.S., Kim, I.W., Hu, R. and Kong, A.N. (2004) Modulatory properties of various natural chemopreventive agents on the activation of NF-kappaB signaling pathway. *Pharm Res*, **21**, 661-70.
17. Keum, Y.S., Yu, S., Chang, P.P., Yuan, X., Kim, J.H., Xu, C., Han, J., Agarwal, A. and Kong, A.N. (2006) Mechanism of Action of Sulforaphane: Inhibition of p38 Mitogen-Activated Protein Kinase Isoforms Contributing to the Induction of Antioxidant Response Element-Mediated Heme Oxygenase-1 in Human Hepatoma HepG2 Cells. *Cancer Res*, **66**, 8804-13.
18. Xu, C., Yuan, X., Pan, Z., Shen, G., Kim, J.H., Yu, S., Khor, T.O., Li, W., Ma, J. and Kong, A.N. (2006) Mechanism of action of isothiocyanates: the induction of ARE-regulated genes is associated with activation of ERK and JNK and the phosphorylation and nuclear translocation of Nrf2. *Mol Cancer Ther*, **5**, 1918-26.
19. Kim, J.H., Xu, C., Keum, Y.S., Reddy, B., Conney, A. and Kong, A.N. (2006) Inhibition of EGFR signaling in human prostate cancer PC-3 cells by combination treatment with beta-phenylethyl isothiocyanate and curcumin. *Carcinogenesis*, **27**, 475-82.
20. Khor, T.O., Keum, Y.S., Lin, W., Kim, J.H., Hu, R., Shen, G., Xu, C., Gopalakrishnan, A., Reddy, B., Zheng, X., Conney, A.H. and Kong, A.N. (2006) Combined inhibitory effects of curcumin and phenethyl isothiocyanate on the growth of human PC-3 prostate xenografts in immunodeficient mice. *Cancer Res*, **66**, 613-21.
21. Myzak, M.C., Dashwood, W.M., Orner, G.A., Ho, E. and Dashwood, R.H. (2006) Sulforaphane inhibits histone deacetylase in vivo and suppresses tumorigenesis in Apc-minus mice. *Faseb J*, **20**, 506-8.
22. Kim, B.R., Hu, R., Keum, Y.S., Hebbar, V., Shen, G., Nair, S.S. and Kong, A.N. (2003) Effects of glutathione on antioxidant response element-mediated gene expression and apoptosis elicited by sulforaphane. *Cancer Res*, **63**, 7520-5.
23. Khor TO, Huang MT, Kwon KH, Reddy BS and Kong AN (2006) Nrf2-deficient mice have an increased susceptibility to dextran sulfate sodium-induced colitis. *Cancer Res*, Accepted for Publication.
24. Dinkova-Kostova, A.T., Liby, K.T., Stephenson, K.K., Holtzclaw, W.D., Gao, X., Suh, N., Williams, C., Risingsong, R., Honda, T., Gribble, G.W., Sporn, M.B. and Talalay, P. (2005) Extremely potent triterpenoid inducers of the phase 2 response: correlations of protection against oxidant and inflammatory stress. *Proc Natl Acad Sci U S A*, **102**, 4584-9.
25. Moriarty-Craige, S.E. and Jones, D.P. (2004) Extracellular thiols and thiol/disulfide redox in metabolism. *Annu Rev Nutr*, **24**, 481-509.
26. Georgiou, G. (2002) How to flip the (redox) switch. *Cell*, **111**, 607-10.
27. Jacob, C., Lancaster, J.R. and Giles, G.I. (2004) Reactive sulphur species in oxidative signal transduction. *Biochem Soc Trans*, **32**, 1015-7.
28. Karin, M. (1995) The regulation of AP-1 activity by mitogen-activated protein kinases. *J Biol Chem*, **270**, 16483-6.
29. Smeal, T., Binetruy, B., Mercola, D., Grover-Bardwick, A., Heidecker, G., Rapp, U.R. and Karin, M. (1992) Oncoprotein-mediated signalling cascade

stimulates c-Jun activity by phosphorylation of serines 63 and 73. *Mol Cell Biol*, **12**, 3507-13.
30. Abate, C., Patel, L., Rauscher, F.J., 3rd and Curran, T. (1990) Redox regulation of fos and jun DNA-binding activity in vitro. *Science*, **249**, 1157-61.
31. Xanthoudakis, S. and Curran, T. (1996) Redox regulation of AP-1: a link between transcription factor signaling and DNA repair. *Adv Exp Med Biol*, **387**, 69-75.
32. Hirota, K., Matsui, M., Iwata, S., Nishiyama, A., Mori, K. and Yodoi, J. (1997) AP-1 transcriptional activity is regulated by a direct association between thioredoxin and Ref-1. *Proc Natl Acad Sci U S A*, **94**, 3633-8.
33. Matthews, J.R., Kaszubska, W., Turcatti, G., Wells, T.N. and Hay, R.T. (1993) Role of cysteine62 in DNA recognition by the P50 subunit of NF-kappa B. *Nucleic Acids Res*, **21**, 1727-34.
34. Galter, D., Mihm, S. and Droge, W. (1994) Distinct effects of glutathione disulphide on the nuclear transcription factor kappa B and the activator protein-1. *Eur J Biochem*, **221**, 639-48.
35. Hirota, K., Murata, M., Sachi, Y., Nakamura, H., Takeuchi, J., Mori, K. and Yodoi, J. (1999) Distinct roles of thioredoxin in the cytoplasm and in the nucleus. A two-step mechanism of redox regulation of transcription factor NF-kappaB. *J Biol Chem*, **274**, 27891-7.
36. Alam, J., Stewart, D., Touchard, C., Boinapally, S., Choi, A.M. and Cook, J.L. (1999) Nrf2, a Cap'n'Collar transcription factor, regulates induction of the heme oxygenase-1 gene. *J Biol Chem*, **274**, 26071-8.
37. McMahon, M., Itoh, K., Yamamoto, M., Chanas, S.A., Henderson, C.J., McLellan, L.I., Wolf, C.R., Cavin, C. and Hayes, J.D. (2001) The Cap'n'Collar basic leucine zipper transcription factor Nrf2 (NF-E2 p45-related factor 2) controls both constitutive and inducible expression of intestinal detoxification and glutathione biosynthetic enzymes. *Cancer Res*, **61**, 3299-307.
38. Thimmulappa, R.K., Mai, K.H., Srisuma, S., Kensler, T.W., Yamamoto, M. and Biswal, S. (2002) Identification of Nrf2-regulated genes induced by the chemopreventive agent sulforaphane by oligonucleotide microarray. *Cancer Res*, **62**, 5196-203.
39. Prochaska, H.J., De Long, M.J. and Talalay, P. (1985) On the mechanisms of induction of cancer-protective enzymes: a unifying proposal. *Proc Natl Acad Sci U S A*, **82**, 8232-6.
40. Li, W., Jain, M.R., Chen, C., Yue, X., Hebbar, V., Zhou, R. and Kong, A.N. (2005) Nrf2 Possesses a redox-insensitive nuclear export signal overlapping with the leucine zipper motif. *J Biol Chem*, **280**, 28430-8.
41. Shen, G., Hebbar, V., Nair, S., Xu, C., Li, W., Lin, W., Keum, Y.S., Han, J., Gallo, M.A. and Kong, A.N. (2004) Regulation of Nrf2 transactivation domain activity. The differential effects of mitogen-activated protein kinase cascades and synergistic stimulatory effect of Raf and CREB-binding protein. *J Biol Chem*, **279**, 23052-60.
42. Keum, Y.S., Owuor, E.D., Kim, B.R., Hu, R. and Kong, A.N. (2003) Involvement of Nrf2 and JNK1 in the activation of antioxidant responsive

element (ARE) by chemopreventive agent phenethyl isothiocyanate (PEITC). *Pharm Res*, **20**, 1351-6.
43. Yu, X. and Kensler, T. (2005) Nrf2 as a target for cancer chemoprevention. *Mutat Res*, **591**, 93-102.
44. Burton, N.C., Kensler, T.W. and Guilarte, T.R. (2006) In vivo modulation of the Parkinsonian phenotype by Nrf2. *Neurotoxicology*, Aug Epub.
45. Dhakshinamoorthy, S. and Jaiswal, A.K. (2001) Functional characterization and role of INrf2 in antioxidant response element-mediated expression and antioxidant induction of NAD(P)H:quinone oxidoreductase1 gene. *Oncogene*, **20**, 3906-17.
46. Zhang, D.D. and Hannink, M. (2003) Distinct cysteine residues in Keap1 are required for Keap1-dependent ubiquitination of Nrf2 and for stabilization of Nrf2 by chemopreventive agents and oxidative stress. *Mol Cell Biol*, **23**, 8137-51.
47. Zhang, D.D., Lo, S.C., Cross, J.V., Templeton, D.J. and Hannink, M. (2004) Keap1 is a redox-regulated substrate adaptor protein for a Cul3-dependent ubiquitin ligase complex. *Mol Cell Biol*, **24**, 10941-53.
48. Velichkova, M. and Hasson, T. (2005) Keap1 regulates the oxidation-sensitive shuttling of Nrf2 into and out of the nucleus via a Crm1-dependent nuclear export mechanism. *Mol Cell Biol*, **25**, 4501-13.
49. Wakabayashi, N., Dinkova-Kostova, A.T., Holtzclaw, W.D., Kang, M.I., Kobayashi, A., Yamamoto, M., Kensler, T.W. and Talalay, P. (2004) Protection against electrophile and oxidant stress by induction of the phase 2 response: fate of cysteines of the Keap1 sensor modified by inducers. *Proc Natl Acad Sci U S A*, **101**, 2040-5.
50. Li, W., Yu, S.W. and Kong, A.N. (2006) Nrf2 possesses a redox-sensitive nuclear exporting signal in the Neh5 transactivation domain. *J Biol Chem*, **281**, 27251-63.
51. Dhakshinamoorthy, S. and Jaiswal, A.K. (2000) Small maf (MafG and MafK) proteins negatively regulate antioxidant response element-mediated expression and antioxidant induction of the NAD(P)H:Quinone oxidoreductase1 gene. *J Biol Chem*, **275**, 40134-41.
52. Nair, S., Xu, C., Shen, G., Hebbar, V., Gopalakrishnan, A., Hu, R., Jain, M.R., Lin, W., Keum, Y.S., Liew, C., Chan, J.Y. and Kong, A.N. (2006) Pharmacogenomics of Phenolic Antioxidant Butylated Hydroxyanisole (BHA) in the Small Intestine and Liver of Nrf2 Knockout and C57BL/6J Mice. *Pharm Res*, **23**, 2621-37.
53. Jain, A.K., Bloom, D.A. and Jaiswal, A.K. (2005) Nuclear import and export signals in control of Nrf2. *J Biol Chem*, **280**, 29158-68.
54. Bloom, D., Dhakshinamoorthy, S. and Jaiswal, A.K. (2002) Site-directed mutagenesis of cysteine to serine in the DNA binding region of Nrf2 decreases its capacity to upregulate antioxidant response element-mediated expression and antioxidant induction of NAD(P)H:quinone oxidoreductase1 gene. *Oncogene*, **21**, 2191-200.
55. Shen, G., Xu, C., Hu, R., Jain, M.R., Nair, S., Lin, W., Yang, C.S., Chan, J.Y. and Kong, A.N. (2005) Comparison of (-)-epigallocatechin-3-gallate elicited

liver and small intestine gene expression profiles between C57BL/6J mice and C57BL/6J/Nrf2 (-/-) mice. *Pharm Res*, **22**, 1805-20.

56. Shen, G., Xu, C., Hu, R., Jain, M.R., Gopalkrishnan, A., Nair, S., Huang, M.T., Chan, J.Y. and Kong, A.N. (2006) Modulation of nuclear factor E2-related factor 2-mediated gene expression in mice liver and small intestine by cancer chemopreventive agent curcumin. *Mol Cancer Ther*, **5**, 39-51.
57. Hu, P., Han, Z., Couvillon, A.D., Kaufman, R.J. and Exton, J.H. (2006) Autocrine tumor necrosis factor alpha links endoplasmic reticulum stress to the membrane death receptor pathway through IRE1alpha-mediated NF-kappaB activation and down-regulation of TRAF2 expression. *Mol Cell Biol*, **26**, 3071-84.
58. Hu, R., Xu, C., Shen, G., Jain, M.R., Khor, T.O., Gopalkrishnan, A., Lin, W., Reddy, B., Chan, J.Y. and Kong, A.N. (2006) Identification of Nrf2-regulated genes induced by chemopreventive isothiocyanate PEITC by oligonucleotide microarray. *Life Sci*, **79**, 1944-55.
59. Nair S, Xu C, Shen G, Hebbar V, Gopalakrishnan A, Hu R, Jain MR, Liew C, Chan JY and Kong A.-N T (2006) Toxicogenomics of Endoplasmic Reticulum stress inducer Tunicamycin in the Small Intestine and Liver of Nrf2 Knockout and C57BL/6J Mice. *Toxicology Letters*, Accepted for Publication.
60. Katoh, Y., Itoh, K., Yoshida, E., Miyagishi, M., Fukamizu, A. and Yamamoto, M. (2001) Two domains of Nrf2 cooperatively bind CBP, a CREB binding protein, and synergistically activate transcription. *Genes Cells*, **6**, 857-68.
61. Lin, W., Shen, G., Yuan, X., Jain, M.R., Yu, S., Zhang, A., Chen, J.D. and Kong, A.N. (2006) Regulation of Nrf2 transactivation domain activity by p160 RAC3/SRC3 and other nuclear co-regulators. *J Biochem Mol Biol*, **39**, 304-10.
62. Chen, H., Tini, M. and Evans, R.M. (2001) HATs on and beyond chromatin. *Curr Opin Cell Biol*, **13**, 218-24.
63. Ceribelli, M., Alcalay, M., Vigano, M.A. and Mantovani, R. (2006) Repression of new p53 targets revealed by ChIP on chip experiments. *Cell Cycle*, **5**, 1102-10.
64. Talalay, P. (2000) Chemoprotection against cancer by induction of phase 2 enzymes. *Biofactors*, **12**, 5-11.
65. Zhang, J., Ohta, T., Maruyama, A., Hosoya, T., Nishikawa, K., Maher, J.M., Shibahara, S., Itoh, K. and Yamamoto, M. (2006) BRG1 interacts with Nrf2 to selectively mediate HO-1 induction in response to oxidative stress. *Mol Cell Biol*, **26**, 7942-52.
66. Wang, W. and Chan, J.Y. (2006) Nrf1 is targeted to the endoplasmic reticulum membrane by an N-terminal transmembrane domain. Inhibition of nuclear translocation and transacting function. *J Biol Chem*, **281**, 19676-87.
67. Zhang, K. and Kaufman, R.J. (2006) Protein folding in the endoplasmic reticulum and the unfolded protein response. *Handb Exp Pharmacol*, 69-91.
68. Hetz, C., Bernasconi, P., Fisher, J., Lee, A.H., Bassik, M.C., Antonsson, B., Brandt, G.S., Iwakoshi, N.N., Schinzel, A., Glimcher, L.H. and Korsmeyer, S.J. (2006) Proapoptotic BAX and BAK modulate the unfolded protein response by a direct interaction with IRE1alpha. *Science*, **312**, 572-6.

69. Srivastava, R.K., Sollott, S.J., Khan, L., Hansford, R., Lakatta, E.G. and Longo, D.L. (1999) Bcl-2 and Bcl-X(L) block thapsigargin-induced nitric oxide generation, c-Jun NH(2)-terminal kinase activity, and apoptosis. *Mol Cell Biol*, **19**, 5659-74.
70. Kyriakis, J.M., Banerjee, P., Nikolakaki, E., Dai, T., Rubie, E.A., Ahmad, M.F., Avruch, J. and Woodgett, J.R. (1994) The stress-activated protein kinase subfamily of c-Jun kinases. *Nature*, **369**, 156-60.
71. Urano, F., Wang, X., Bertolotti, A., Zhang, Y., Chung, P., Harding, H.P. and Ron, D. (2000) Coupling of stress in the ER to activation of JNK protein kinases by transmembrane protein kinase IRE1. *Science*, **287**, 664-6.
72. Yu, R., Jiao, J.J., Duh, J.L., Tan, T.H. and Kong, A.N. (1996) Phenethyl isothiocyanate, a natural chemopreventive agent, activates c-Jun N-terminal kinase 1. *Cancer Res*, **56**, 2954-9.
73. Garber, K. (2006) Researchers target unfolded protein response in cancerous tumor growth. *J Natl Cancer Inst*, **98**, 512-4.
74. Jones, D.P. (2006) Extracellular redox state: refining the definition of oxidative stress in aging. *Rejuvenation Res*, **9**, 169-81.
75. Catarzi, S., Biagioni, C., Giannoni, E., Favilli, F., Marcucci, T., Iantomasi, T. and Vincenzini, M.T. (2005) Redox regulation of platelet-derived-growth-factor-receptor: role of NADPH-oxidase and c-Src tyrosine kinase. *Biochim Biophys Acta*, **1745**, 166-75.
76. Cheng, Y.J. and Liu, M.Y. (2005) Modulation of tumor necrosis factor-alpha and oxidative stress through protein kinase C and P42/44 mitogen-activated protein kinase in lead increases lipopolysaccharide-induced liver damage in rats. *Shock*, **24**, 188-93.
77. Engers, R., Springer, E., Kehren, V., Simic, T., Young, D.A., Beier, J., Klotz, L.O., Clark, I.M., Sies, H. and Gabbert, H.E. (2006) Rac upregulates tissue inhibitor of metalloproteinase-1 expression by redox-dependent activation of extracellular signal-regulated kinase signaling. *Febs J*, **273**, 4754-69.
78. Erker, L., Schubert, R., Yakushiji, H., Barlow, C., Larson, D., Mitchell, J.B. and Wynshaw-Boris, A. (2005) Cancer chemoprevention by the antioxidant tempol acts partially via the p53 tumor suppressor. *Hum Mol Genet*, **14**, 1699-708.
79. Trachootham, D., Zhou, Y., Zhang, H., Demizu, Y., Chen, Z., Pelicano, H., Chiao, P.J., Achanta, G., Arlinghaus, R.B., Liu, J. and Huang, P. (2006) Selective killing of oncogenically transformed cells through a ROS-mediated mechanism by beta-phenylethyl isothiocyanate. *Cancer Cell*, **10**, 241-52.
80. Xu, C., Shen, G., Chen, C., Gelinas, C. and Kong, A.N. (2005) Suppression of NF-kappaB and NF-kappaB-regulated gene expression by sulforaphane and PEITC through IkappaBalpha, IKK pathway in human prostate cancer PC-3 cells. *Oncogene*, **24**, 4486-95.
81. Shen, H.M. and Pervaiz, S. (2006) TNF receptor superfamily-induced cell death: redox-dependent execution. *Faseb J*, **20**, 1589-98.
82. Han, D., Hanawa, N., Saberi, B. and Kaplowitz, N. (2006) Hydrogen peroxide and redox modulation sensitize primary mouse hepatocytes to TNF-induced apoptosis. *Free Radic Biol Med*, **41**, 627-39.

83. Arai, R.J., Masutani, H., Yodoi, J., Debbas, V., Laurindo, F.R., Stern, A. and Monteiro, H.P. (2006) Nitric oxide induces thioredoxin-1 nuclear translocation: possible association with the p21Ras survival pathway. *Biochem Biophys Res Commun*, **348**, 1254-60.
84. Shen, G., Xu, C., Chen, C., Hebbar, V. and Kong, A.N. (2006) p53-independent G1 cell cycle arrest of human colon carcinoma cells HT-29 by sulforaphane is associated with induction of p21CIP1 and inhibition of expression of cyclin D1. *Cancer Chemother Pharmacol*, **57**, 317-27.
85. Luo, T. and Xia, Z. (2006) A small dose of hydrogen peroxide enhances tumor necrosis factor-alpha toxicity in inducing human vascular endothelial cell apoptosis: reversal with propofol. *Anesth Analg*, **103**, 110-6, table of contents.
86. Ge, Y., Montano, I., Rustici, G., Freebern, W.J., Haggerty, C.M., Cui, W., Ponciano-Jackson, D., Chandramouli, G.V., Gardner, E.R., Figg, W.D., Abu-Asab, M., Tsokos, M., Jackson, S.H. and Gardner, K. (2006) Selective leukemic cell killing by a novel functional class of thalidomide analogs. *Blood*.
87. Macho, A., Calzado, M.A., Munoz-Blanco, J., Gomez-Diaz, C., Gajate, C., Mollinedo, F., Navas, P. and Munoz, E. (1999) Selective induction of apoptosis by capsaicin in transformed cells: the role of reactive oxygen species and calcium. *Cell Death Differ*, **6**, 155-65.
88. Reynaert, N.L., Wouters, E.F. and Janssen-Heininger, Y.M. (2006) Modulation of Glutaredoxin-1 Expression in a Mouse Model of Allergic Airway Disease. *Am J Respir Cell Mol Biol*.
89. Rhodes, D.R. and Chinnaiyan, A.M. (2005) Integrative analysis of the cancer transcriptome. *Nat Genet*, **37 Suppl**, S31-7.
90. Yu, R., Tan, T.H. and Kong, A.T. (1997) Butylated hydroxyanisole and its metabolite tert-butylhydroquinone differentially regulate mitogen-activated protein kinases. The role of oxidative stress in the activation of mitogen-activated protein kinases by phenolic antioxidants. *J Biol Chem*, **272**, 28962-70.
91. Saito, M., Sakagami, H. and Fujisawa, S. (2003) Cytotoxicity and apoptosis induction by butylated hydroxyanisole (BHA) and butylated hydroxytoluene (BHT). *Anticancer Res*, **23**, 4693-701.
92. Festjens, N., Kalai, M., Smet, J., Meeus, A., Van Coster, R., Saelens, X. and Vandenabeele, P. (2006) Butylated hydroxyanisole is more than a reactive oxygen species scavenger. *Cell Death Differ*, **13**, 166-9.
93. Kalai, M., Van Loo, G., Vanden Berghe, T., Meeus, A., Burm, W., Saelens, X. and Vandenabeele, P. (2002) Tipping the balance between necrosis and apoptosis in human and murine cells treated with interferon and dsRNA. *Cell Death Differ*, **9**, 981-94.
94. Hayes, J.D., Pulford, D.J., Ellis, E.M., McLeod, R., James, R.F., Seidegard, J., Mosialou, E., Jernstrom, B. and Neal, G.E. (1998) Regulation of rat glutathione S-transferase A5 by cancer chemopreventive agents: mechanisms of inducible resistance to aflatoxin B1. *Chem Biol Interact*, **111-112**, 51-67.
95. McCormick, D.L., Major, N. and Moon, R.C. (1984) Inhibition of 7,12-dimethylbenz(a)anthracene-induced rat mammary carcinogenesis by concomitant or postcarcinogen antioxidant exposure. *Cancer Res*, **44**, 2858-63.

96. Jones, F.E., Komorowski, R.A. and Condon, R.E. (1984) The effects of ascorbic acid and butylated hydroxyanisole in the chemoprevention of 1,2-dimethylhydrazine-induced large bowel neoplasms. *J Surg Oncol*, **25**, 54-60.
97. Williams, G.M., Iatropoulos, M.J. and Jeffrey, A.M. (2002) Anticarcinogenicity of monocyclic phenolic compounds. *Eur J Cancer Prev*, **11 Suppl 2**, S101-7.
98. Yu, R., Mandlekar, S. and Kong, A.T. (2000) Molecular mechanisms of butylated hydroxylanisole-induced toxicity: induction of apoptosis through direct release of cytochrome c. *Mol Pharmacol*, **58**, 431-7.
99. Kong, A.N., Yu, R., Lei, W., Mandlekar, S., Tan, T.H. and Ucker, D.S. (1998) Differential activation of MAPK and ICE/Ced-3 protease in chemical-induced apoptosis. The role of oxidative stress in the regulation of mitogen-activated protein kinases (MAPKs) leading to gene expression and survival or activation of caspases leading to apoptosis. *Restor Neurol Neurosci*, **12**, 63-70.
100. Chan, K., Lu, R., Chang, J.C. and Kan, Y.W. (1996) NRF2, a member of the NFE2 family of transcription factors, is not essential for murine erythropoiesis, growth, and development. *Proc Natl Acad Sci U S A*, **93**, 13943-8.
101. Lin, W., Shen, G., Yuan, X., Jain, M.R., Yu, S., Zhang, A., Chen, J.D. and Kong, A.N. (Accepted for publication) Regulation of Nrf2 Transactivation Domain Activity by p160 RAC3/SRC3 and Other Nuclear Co-Regulators. *Journal of Biochemistry and Molecular Biology*.
102. Borroz, K.I., Buetler, T.M. and Eaton, D.L. (1994) Modulation of gamma-glutamylcysteine synthetase large subunit mRNA expression by butylated hydroxyanisole. *Toxicol Appl Pharmacol*, **126**, 150-5.
103. Buetler, T.M., Gallagher, E.P., Wang, C., Stahl, D.L., Hayes, J.D. and Eaton, D.L. (1995) Induction of phase I and phase II drug-metabolizing enzyme mRNA, protein, and activity by BHA, ethoxyquin, and oltipraz. *Toxicol Appl Pharmacol*, **135**, 45-57.
104. McLellan, L.I., Harrison, D.J. and Hayes, J.D. (1992) Modulation of glutathione S-transferases and glutathione peroxidase by the anticarcinogen butylated hydroxyanisole in murine extrahepatic organs. *Carcinogenesis*, **13**, 2255-61.
105. Chanas, S.A., Jiang, Q., McMahon, M., McWalter, G.K., McLellan, L.I., Elcombe, C.R., Henderson, C.J., Wolf, C.R., Moffat, G.J., Itoh, K., Yamamoto, M. and Hayes, J.D. (2002) Loss of the Nrf2 transcription factor causes a marked reduction in constitutive and inducible expression of the glutathione S-transferase Gsta1, Gsta2, Gstm1, Gstm2, Gstm3 and Gstm4 genes in the livers of male and female mice. *Biochem J*, **365**, 405-16.
106. Tanaka, A.R., Tanabe, K., Morita, M., Kurisu, M., Kasiwayama, Y., Matsuo, M., Kioka, N., Amachi, T., Imanaka, T. and Ueda, K. (2002) ATP binding/hydrolysis by and phosphorylation of peroxisomal ATP-binding cassette proteins PMP70 (ABCD3) and adrenoleukodystrophy protein (ABCD1). *J Biol Chem*, **277**, 40142-7.
107. Verkman, A.S. (2005) More than just water channels: unexpected cellular roles of aquaporins. *J Cell Sci*, **118**, 3225-32.
108. Shi, Y. and Massague, J. (2003) Mechanisms of TGF-beta signaling from cell membrane to the nucleus. *Cell*, **113**, 685-700.

109. Vittal, R., Selvanayagam, Z.E., Sun, Y., Hong, J., Liu, F., Chin, K.V. and Yang, C.S. (2004) Gene expression changes induced by green tea polyphenol (-)-epigallocatechin-3-gallate in human bronchial epithelial 21BES cells analyzed by DNA microarray. *Mol Cancer Ther*, **3**, 1091-9.
110. Beck, G.R., Jr., Zerler, B. and Moran, E. (2001) Gene array analysis of osteoblast differentiation. *Cell Growth Differ*, **12**, 61-83.
111. Yang, L., Yamasaki, K., Shirakata, Y., Dai, X., Tokumaru, S., Yahata, Y., Tohyama, M., Hanakawa, Y., Sayama, K. and Hashimoto, K. (2006) Bone morphogenetic protein-2 modulates Wnt and frizzled expression and enhances the canonical pathway of Wnt signaling in normal keratinocytes. *J Dermatol Sci*.
112. Motohashi, H., Katsuoka, F., Engel, J.D. and Yamamoto, M. (2004) Small Maf proteins serve as transcriptional cofactors for keratinocyte differentiation in the Keap1-Nrf2 regulatory pathway. *Proc Natl Acad Sci U S A*, **101**, 6379-84.
113. Lizcano, J.M., Alrubaie, S., Kieloch, A., Deak, M., Leevers, S.J. and Alessi, D.R. (2003) Insulin-induced Drosophila S6 kinase activation requires phosphoinositide 3-kinase and protein kinase B. *Biochem J*, **374**, 297-306.
114. Dornand, J., Sekkat, C., Mani, J.C. and Gerber, M. (1987) Lipoxygenase inhibitors suppress IL-2 synthesis: relationship with rise of [Ca++]i and the events dependent on protein kinase C activation. *Immunol Lett*, **16**, 101-6.
115. Ruzzene, M., Donella-Deana, A., Alexandre, A., Francesconi, M.A. and Deana, R. (1991) The antioxidant butylated hydroxytoluene stimulates platelet protein kinase C and inhibits subsequent protein phosphorylation induced by thrombin. *Biochim Biophys Acta*, **1094**, 121-9.
116. van Huizen, R., Martindale, J.L., Gorospe, M. and Holbrook, N.J. (2003) P58IPK, a novel endoplasmic reticulum stress-inducible protein and potential negative regulator of eIF2alpha signaling. *J Biol Chem*, **278**, 15558-64.
117. Kaufman, R.J. (1999) Stress signaling from the lumen of the endoplasmic reticulum: coordination of gene transcriptional and translational controls. *Genes Dev*, **13**, 1211-33.
118. Reimertz, C., Kogel, D., Rami, A., Chittenden, T. and Prehn, J.H. (2003) Gene expression during ER stress-induced apoptosis in neurons: induction of the BH3-only protein Bbc3/PUMA and activation of the mitochondrial apoptosis pathway. *J Cell Biol*, **162**, 587-97.
119. Mahoney, W.C. and Duksin, D. (1979) Biological activities of the two major components of tunicamycin. *J Biol Chem*, **254**, 6572-6.
120. Olden, K., Pratt, R.M., Jaworski, C. and Yamada, K.M. (1979) Evidence for role of glycoprotein carbohydrates in membrane transport: specific inhibition by tunicamycin. *Proc Natl Acad Sci U S A*, **76**, 791-5.
121. Li, W., Yu, S.W. and Kong, A.N. (2006) Nrf2 Possesses a Redox-Sensitive NES in the Neh5 transactivation Domain. *J Biol Chem*, *In Press.*
122. Wang, W. and Chan, J.Y. (2006) Nrf1 is targeted to the ER membrane by a N-terminal transmembrane domain: inhibition of nuclear translocation and transacting function. *J Biol Chem*.
123. Steller, H. (1995) Mechanisms and genes of cellular suicide. *Science*, **267**, 1445-9.

124. Tegethoff, S., Behlke, J. and Scheidereit, C. (2003) Tetrameric oligomerization of IkappaB kinase gamma (IKKgamma) is obligatory for IKK complex activity and NF-kappaB activation. *Mol Cell Biol*, **23**, 2029-41.
125. Jiang, H.Y. and Wek, R.C. (2005) Phosphorylation of the alpha-subunit of the eukaryotic initiation factor-2 (eIF2alpha) reduces protein synthesis and enhances apoptosis in response to proteasome inhibition. *J Biol Chem*, **280**, 14189-202.
126. Wang, H., Kouri, G. and Wollheim, C.B. (2005) ER stress and SREBP-1 activation are implicated in beta-cell glucolipotoxicity. *J Cell Sci*, **118**, 3905-15.
127. Nawrocki, S.T., Carew, J.S., Dunner, K., Jr., Boise, L.H., Chiao, P.J., Huang, P., Abbruzzese, J.L. and McConkey, D.J. (2005) Bortezomib inhibits PKR-like endoplasmic reticulum (ER) kinase and induces apoptosis via ER stress in human pancreatic cancer cells. *Cancer Res*, **65**, 11510-9.
128. Carew, J.S., Nawrocki, S.T., Krupnik, Y.V., Dunner, K., Jr., McConkey, D.J., Keating, M.J. and Huang, P. (2006) Targeting endoplasmic reticulum protein transport: a novel strategy to kill malignant B cells and overcome fludarabine resistance in CLL. *Blood*, **107**, 222-31.
129. Kwak, M.K., Wakabayashi, N., Itoh, K., Motohashi, H., Yamamoto, M. and Kensler, T.W. (2003) Modulation of gene expression by cancer chemopreventive dithiolethiones through the Keap1-Nrf2 pathway. Identification of novel gene clusters for cell survival. *J Biol Chem*, **278**, 8135-45.
130. Centers for Disease Control and Prevention (CDC) Department of Health and Human Services. *http://www.cdc.gov/cancer/colorectal/statistics/death_rates.htm*.
131. Surveillance Epidemiology and End Results (SEER) National Cancer Institute (NCI). *http://www.seer.cancer.gov/statfacts/html/colorect.html?statfacts_page=colorect.html&x=14&y=23*.
132. Johnston, M.D., Edwards, C.M., Bodmer, W.F., Maini, P.K. and Chapman, S.J. (2007) Mathematical modeling of cell population dynamics in the colonic crypt and in colorectal cancer. *Proc Natl Acad Sci U S A*, **104**, 4008-13.
133. Tomlinson, I.P. and Bodmer, W.F. (1995) Failure of programmed cell death and differentiation as causes of tumors: some simple mathematical models. *Proc Natl Acad Sci U S A*, **92**, 11130-4.
134. Vogelstein, B. and Kinzler, K.W. (2004) Cancer genes and the pathways they control. *Nat Med*, **10**, 789-99.
135. Castellone, M.D., Teramoto, H. and Gutkind, J.S. (2006) Cyclooxygenase-2 and colorectal cancer chemoprevention: the beta-catenin connection. *Cancer Res*, **66**, 11085-8.
136. Steinmetz, K.A. and Potter, J.D. (1991) Vegetables, fruit, and cancer. I. Epidemiology. *Cancer Causes Control*, **2**, 325-57.
137. Steinmetz, K.A. and Potter, J.D. (1991) Vegetables, fruit, and cancer. II. Mechanisms. *Cancer Causes Control*, **2**, 427-42.
138. Smith-Warner, S.A., Elmer, P.J., Fosdick, L., Randall, B., Bostick, R.M., Grandits, G., Grambsch, P., Louis, T.A., Wood, J.R. and Potter, J.D. (2002)

Fruits, vegetables, and adenomatous polyps: the Minnesota Cancer Prevention Research Unit case-control study. *Am J Epidemiol*, **155**, 1104-13.
139. Leoni, O., Iori, R. and Palmieri, S. (2000) Hydrolysis of glucosinolates using nylon-immobilized myrosinase to produce pure bioactive molecules. *Biotechnol Bioeng*, **68**, 660-4.
140. Getahun, S.M. and Chung, F.L. (1999) Conversion of glucosinolates to isothiocyanates in humans after ingestion of cooked watercress. *Cancer Epidemiol Biomarkers Prev*, **8**, 447-51.
141. Myzak, M.C., Karplus, P.A., Chung, F.L. and Dashwood, R.H. (2004) A novel mechanism of chemoprotection by sulforaphane: inhibition of histone deacetylase. *Cancer Res*, **64**, 5767-74.
142. Higdon, J.V., Delage, B., Williams, D.E. and Dashwood, R.H. (2007) Cruciferous vegetables and human cancer risk: epidemiologic evidence and mechanistic basis. *Pharmacol Res*.
143. Mukhtar, H. and Ahmad, N. (1999) Mechanism of cancer chemopreventive activity of green Tea. *Proc Soc Exp Biol Med*, **220**, 234-8.
144. Yamane, T., Nakatani, H., Kikuoka, N., Matsumoto, H., Iwata, Y., Kitao, Y., Oya, K. and Takahashi, T. (1996) Inhibitory effects and toxicity of green tea polyphenols for gastrointestinal carcinogenesis. *Cancer*, **77**, 1662-7.
145. Jia, X. and Han, C. (2001) Effects of green tea on colonic aberrant crypt foci and proliferative indexes in rats. *Nutr Cancer*, **39**, 239-43.
146. Noonan, D.M., Benelli, R. and Albini, A. (2007) Angiogenesis and cancer prevention: a vision. *Recent Results Cancer Res*, **174**, 219-24.
147. Fang, M.Z., Wang, Y., Ai, N., Hou, Z., Sun, Y., Lu, H., Welsh, W. and Yang, C.S. (2003) Tea polyphenol (-)-epigallocatechin-3-gallate inhibits DNA methyltransferase and reactivates methylation-silenced genes in cancer cell lines. *Cancer Res*, **63**, 7563-70.
148. Fang, M., Chen, D. and Yang, C.S. (2007) Dietary polyphenols may affect DNA methylation. *J Nutr*, **137**, 223S-228S.
149. Nair, S., Li, W. and Kong, A.N. (2007) Natural dietary anti-cancer chemopreventive compounds: redox-mediated differential signaling mechanisms in cytoprotection of normal cells versus cytotoxicity in tumor cells. *Acta Pharmacol Sin*, **28**, 459-72.
150. Zhao, L., Wientjes, M.G. and Au, J.L. (2004) Evaluation of combination chemotherapy: integration of nonlinear regression, curve shift, isobologram, and combination index analyses. *Clin Cancer Res*, **10**, 7994-8004.
151. Seimiya, H., Oh-hara, T., Suzuki, T., Naasani, I., Shimazaki, T., Tsuchiya, K. and Tsuruo, T. (2002) Telomere shortening and growth inhibition of human cancer cells by novel synthetic telomerase inhibitors MST-312, MST-295, and MST-1991. *Mol Cancer Ther*, **1**, 657-65.
152. Arber, N. and Levin, B. (2005) Chemoprevention of colorectal cancer: ready for routine use? *Curr Top Med Chem*, **5**, 517-25.
153. Rennert, G. (2007) Prevention and early detection of colorectal cancer--new horizons. *Recent Results Cancer Res*, **174**, 179-87.
154. Escudier, B., Lassau, N., Angevin, E., Soria, J.C., Chami, L., Lamuraglia, M., Zafarana, E., Landreau, V., Schwartz, B., Brendel, E., Armand, J.P. and Robert,

C. (2007) Phase I Trial of Sorafenib in Combination with IFN {alpha}-2a in Patients with Unresectable and/or Metastatic Renal Cell Carcinoma or Malignant Melanoma. *Clin Cancer Res*, **13**, 1801-9.

155. Kudo-Saito, C., Wansley, E.K., Gruys, M.E., Wiltrout, R., Schlom, J. and Hodge, J.W. (2007) Combination therapy of an orthotopic renal cell carcinoma model using intratumoral vector-mediated costimulation and systemic interleukin-2. *Clin Cancer Res*, **13**, 1936-46.
156. Adhami, V.M., Malik, A., Zaman, N., Sarfaraz, S., Siddiqui, I.A., Syed, D.N., Afaq, F., Pasha, F.S., Saleem, M. and Mukhtar, H. (2007) Combined inhibitory effects of green tea polyphenols and selective cyclooxygenase-2 inhibitors on the growth of human prostate cancer cells both in vitro and in vivo. *Clin Cancer Res*, **13**, 1611-9.
157. Xu, C., Huang, M.T., Shen, G., Yuan, X., Lin, W., Khor, T.O., Conney, A.H. and Tony Kong, A.N. (2006) Inhibition of 7,12-Dimethylbenz(a)anthracene-Induced Skin Tumorigenesis in C57BL/6 Mice by Sulforaphane Is Mediated by Nuclear Factor E2-Related Factor 2. *Cancer Res*, **66**, 8293-8296.
158. Bakiri, L., Matsuo, K., Wisniewska, M., Wagner, E.F. and Yaniv, M. (2002) Promoter specificity and biological activity of tethered AP-1 dimers. *Mol Cell Biol*, **22**, 4952-64.
159. Hess, J., Angel, P. and Schorpp-Kistner, M. (2004) AP-1 subunits: quarrel and harmony among siblings. *J Cell Sci*, **117**, 5965-73.
160. Maurer, G.D., Leupold, J.H., Schewe, D.M., Biller, T., Kates, R.E., Hornung, H.M., Lau-Werner, U., Post, S. and Allgayer, H. (2007) Analysis of specific transcriptional regulators as early predictors of independent prognostic relevance in resected colorectal cancer. *Clin Cancer Res*, **13**, 1123-32.
161. Herdegen, T. and Leah, J.D. (1998) Inducible and constitutive transcription factors in the mammalian nervous system: control of gene expression by Jun, Fos and Krox, and CREB/ATF proteins. *Brain Res Brain Res Rev*, **28**, 370-490.
162. Hill, C.S. and Treisman, R. (1995) Transcriptional regulation by extracellular signals: mechanisms and specificity. *Cell*, **80**, 199-211.
163. Hagenbuch, B. and Meier, P.J. (2004) Organic anion transporting polypeptides of the OATP/ SLC21 family: phylogenetic classification as OATP/ SLCO superfamily, new nomenclature and molecular/functional properties. *Pflugers Arch*, **447**, 653-65.
164. Ballestero, M.R., Monte, M.J., Briz, O., Jimenez, F., Gonzalez-San Martin, F. and Marin, J.J. (2006) Expression of transporters potentially involved in the targeting of cytostatic bile acid derivatives to colon cancer and polyps. *Biochem Pharmacol*, **72**, 729-38.
165. Roninson, I.B. (2003) Tumor cell senescence in cancer treatment. *Cancer Res*, **63**, 2705-15.
166. Yaglom, J.A., Gabai, V.L. and Sherman, M.Y. (2007) High levels of heat shock protein Hsp72 in cancer cells suppress default senescence pathways. *Cancer Res*, **67**, 2373-81.
167. Schmitt, C.A., Fridman, J.S., Yang, M., Lee, S., Baranov, E., Hoffman, R.M. and Lowe, S.W. (2002) A senescence program controlled by p53 and p16INK4a contributes to the outcome of cancer therapy. *Cell*, **109**, 335-46.

168. Khor, T.O., Hu, R., Shen, G., Jeong, W.S., Hebbar, V., Chen, C., Xu, C., Nair, S., Reddy, B., Chada, K. and Kong, A.N. (2006) Pharmacogenomics of cancer chemopreventive isothiocyanate compound sulforaphane in the intestinal polyps of ApcMin/+ mice. *Biopharm Drug Dispos*, **27**, 407-20.
169. Hu, R., Hebbar, V., Kim, B.R., Chen, C., Winnik, B., Buckley, B., Soteropoulos, P., Tolias, P., Hart, R.P. and Kong, A.N. (2004) In vivo pharmacokinetics and regulation of gene expression profiles by isothiocyanate sulforaphane in the rat. *J Pharmacol Exp Ther*, **310**, 263-71.
170. Lambert, J.D., Lee, M.J., Diamond, L., Ju, J., Hong, J., Bose, M., Newmark, H.L. and Yang, C.S. (2006) Dose-dependent levels of epigallocatechin-3-gallate in human colon cancer cells and mouse plasma and tissues. *Drug Metab Dispos*, **34**, 8-11.
171. Lambert, J.D. and Yang, C.S. (2003) Mechanisms of cancer prevention by tea constituents. *J Nutr*, **133**, 3262S-3267S.
172. U.S. Cancer Statistics Working Group. United States Cancer Statistics : 2003 Incidence and Mortality. Atlanta (GA) Department of Health and Human Services, Centers for Disease Control and Prevention, and National Cancer Institute; 2007.
173. National Cancer Institute (NCI) Surveillance Epidemiology and End Results (SEER). *Available at http://seer.cancer.gov/statfacts/html/prost.html*.
174. Scholz, M., Lam, R., Strum, S., Jennrich, R., Johnson, H. and Trilling, T. (2007) Prostate cancer-specific survival and clinical progression-free survival in men with prostate cancer treated intermittently with testosterone inactivating pharmaceuticals. *Urology*, **70**, 506-10.
175. Welch, H.G., Fisher, E.S., Gottlieb, D.J. and Barry, M.J. (2007) Detection of prostate cancer via biopsy in the Medicare-SEER population during the PSA era. *J Natl Cancer Inst*, **99**, 1395-400.
176. Yates, M.S. and Kensler, T.W. (2007) Keap1 eye on the target: chemoprevention of liver cancer. *Acta Pharmacol Sin*, **28**, 1331-42.
177. Khor, T.O., Huang, M.T., Kwon, K.H., Chan, J.Y., Reddy, B.S. and Kong, A.N. (2006) Nrf2-deficient mice have an increased susceptibility to dextran sulfate sodium-induced colitis. *Cancer Res*, **66**, 11580-4.
178. Rushmore, T.H., Morton, M.R. and Pickett, C.B. (1991) The antioxidant responsive element. Activation by oxidative stress and identification of the DNA consensus sequence required for functional activity. *J Biol Chem*, **266**, 11632-9.
179. Wasserman, W.W. and Fahl, W.E. (1997) Functional antioxidant responsive elements. *Proc Natl Acad Sci U S A*, **94**, 5361-6.
180. Nerland, D.E. (2007) The antioxidant/electrophile response element motif. *Drug Metab Rev*, **39**, 235-48.
181. Watai, Y., Kobayashi, A., Nagase, H., Mizukami, M., McEvoy, J., Singer, J.D., Itoh, K. and Yamamoto, M. (2007) Subcellular localization and cytoplasmic complex status of endogenous Keap1. *Genes Cells*, **12**, 1163-78.
182. Shaulian, E. and Karin, M. (2002) AP-1 as a regulator of cell life and death. *Nat Cell Biol*, **4**, E131-6.

183. Hsu, T.C., Young, M.R., Cmarik, J. and Colburn, N.H. (2000) Activator protein 1 (AP-1)- and nuclear factor kappaB (NF-kappaB)-dependent transcriptional events in carcinogenesis. *Free Radic Biol Med*, **28**, 1338-48.
184. Xu, C., Shen, G., Yuan, X., Kim, J.H., Gopalkrishnan, A., Keum, Y.S., Nair, S. and Kong, A.N. (2006) ERK and JNK signaling pathways are involved in the regulation of activator protein 1 and cell death elicited by three isothiocyanates in human prostate cancer PC-3 cells. *Carcinogenesis*, **27**, 437-45.
185. Chinenov, Y. and Kerppola, T.K. (2001) Close encounters of many kinds: Fos-Jun interactions that mediate transcription regulatory specificity. *Oncogene*, **20**, 2438-52.
186. Traka, M., Gasper, A.V., Smith, J.A., Hawkey, C.J., Bao, Y. and Mithen, R.F. (2005) Transcriptome analysis of human colon Caco-2 cells exposed to sulforaphane. *J Nutr*, **135**, 1865-72.
187. Dashwood, R.H. and Ho, E. (2007) Dietary histone deacetylase inhibitors: From cells to mice to man. *Semin Cancer Biol*, **17**, 363-9.
188. Myzak, M.C., Tong, P., Dashwood, W.M., Dashwood, R.H. and Ho, E. (2007) Sulforaphane retards the growth of human PC-3 xenografts and inhibits HDAC activity in human subjects. *Exp Biol Med (Maywood)*, **232**, 227-34.
189. Singh, S.V., Srivastava, S.K., Choi, S., Lew, K.L., Antosiewicz, J., Xiao, D., Zeng, Y., Watkins, S.C., Johnson, C.S., Trump, D.L., Lee, Y.J., Xiao, H. and Herman-Antosiewicz, A. (2005) Sulforaphane-induced cell death in human prostate cancer cells is initiated by reactive oxygen species. *J Biol Chem*, **280**, 19911-24.
190. Herman-Antosiewicz, A., Johnson, D.E. and Singh, S.V. (2006) Sulforaphane causes autophagy to inhibit release of cytochrome C and apoptosis in human prostate cancer cells. *Cancer Res*, **66**, 5828-35.
191. Harper, C.E., Patel, B.B., Wang, J., Eltoum, I.A. and Lamartiniere, C.A. (2007) Epigallocatechin-3-Gallate suppresses early stage, but not late stage prostate cancer in TRAMP mice: Mechanisms of action. *Prostate*, **67**, 1576-1589.
192. Morrissey, C., Brown, M., O'Sullivan, J., Weathered, N., Watson, R.W. and Tenniswood, M. (2007) Epigallocatechin-3-gallate and bicalutamide cause growth arrest and apoptosis in NRP-152 and NRP-154 prostate epithelial cells. *Int J Urol*, **14**, 545-51.
193. Siddiqui, I.A., Adhami, V.M., Afaq, F., Ahmad, N. and Mukhtar, H. (2004) Modulation of phosphatidylinositol-3-kinase/protein kinase B- and mitogen-activated protein kinase-pathways by tea polyphenols in human prostate cancer cells. *J Cell Biochem*, **91**, 232-42.
194. Nair, S., Hebbar, V., Shen, G., Gopalakrishnan, A., Khor, T.O., Yu, S., Xu, C. and Kong, A.N. (2007) Synergistic Effects of a Combination of Dietary Factors Sulforaphane and (-) Epigallocatechin-3-gallate in HT-29 AP-1 Human Colon Carcinoma Cells. *Pharm Res*.
195. Quandt, K., Frech, K., Karas, H., Wingender, E. and Werner, T. (1995) MatInd and MatInspector: new fast and versatile tools for detection of consensus matches in nucleotide sequence data. *Nucleic Acids Res*, **23**, 4878-84.
196. Cartharius, K., Frech, K., Grote, K., Klocke, B., Haltmeier, M., Klingenhoff, A., Frisch, M., Bayerlein, M. and Werner, T. (2005) MatInspector and beyond:

promoter analysis based on transcription factor binding sites. *Bioinformatics*, **21**, 2933-42.
197. Li, C. and Wong, W.H. (2001) Model-based analysis of oligonucleotide arrays: expression index computation and outlier detection. *Proc Natl Acad Sci U S A*, **98**, 31-6.
198. Li, C. and Hung Wong, W. (2001) Model-based analysis of oligonucleotide arrays: model validation, design issues and standard error application. *Genome Biol*, **2**, RESEARCH0032.
199. Masters, J.R. (2007) Clinical applications of expression profiling and proteomics in prostate cancer. *Anticancer Res*, **27**, 1273-6.
200. Sankaranarayanan, K. and Jaiswal, A.K. (2004) Nrf3 negatively regulates antioxidant-response element-mediated expression and antioxidant induction of NAD(P)H:quinone oxidoreductase1 gene. *J Biol Chem*, **279**, 50810-7.
201. Executive Summary of the National Cancer Institute (NCI) Inflammation and Cancer Think Tank in Cancer Biology. *Available at*, http://www.cancer.gov/think-tanks-cancer-biology/page8.
202. Osburn, W.O., Karim, B., Dolan, P.M., Liu, G., Yamamoto, M., Huso, D.L. and Kensler, T.W. (2007) Increased colonic inflammatory injury and formation of aberrant crypt foci in Nrf2-deficient mice upon dextran sulfate treatment. *Int J Cancer*, **121**, 1883-91.
203. Dougan, M. and Dranoff, G. (2008) Inciting inflammation: the RAGE about tumor promotion. *J Exp Med*.
204. Yuan, X., Xu, C., Pan, Z., Keum, Y.S., Kim, J.H., Shen, G., Yu, S., Oo, K.T., Ma, J. and Kong, A.N. (2006) Butylated hydroxyanisole regulates ARE-mediated gene expression via Nrf2 coupled with ERK and JNK signaling pathway in HepG2 cells. *Mol Carcinog*, **45**, 841-50.
205. Yu, R., Chen, C., Mo, Y.Y., Hebbar, V., Owuor, E.D., Tan, T.H. and Kong, A.N. (2000) Activation of mitogen-activated protein kinase pathways induces antioxidant response element-mediated gene expression via a Nrf2-dependent mechanism. *J Biol Chem*, **275**, 39907-13.
206. Karin, M. and Greten, F.R. (2005) NF-kappaB: linking inflammation and immunity to cancer development and progression. *Nat Rev Immunol*, **5**, 749-59.
207. Murakami, A., Song, M. and Ohigashi, H. (2007) Phenethyl isothiocyanate suppresses receptor activator of NF-kappaB ligand (RANKL)-induced osteoclastogenesis by blocking activation of ERK1/2 and p38 MAPK in RAW264.7 macrophages. *Biofactors*, **30**, 1-11.
208. de Sousa, R.R., Queiroz, K.C., Souza, A.C., Gurgueira, S.A., Augusto, A.C., Miranda, M.A., Peppelenbosch, M.P., Ferreira, C.V. and Aoyama, H. (2007) Phosphoprotein levels, MAPK activities and NFkappaB expression are affected by fisetin. *J Enzyme Inhib Med Chem*, **22**, 439-44.
209. Rhodes, D.R., Kalyana-Sundaram, S., Mahavisno, V., Barrette, T.R., Ghosh, D. and Chinnaiyan, A.M. (2005) Mining for regulatory programs in the cancer transcriptome. *Nat Genet*, **37**, 579-83.
210. Doh, S.T., Zhang, Y., Temple, M.H. and Cai, L. (2007) Non-coding sequence retrieval system for comparative genomic analysis of gene regulatory elements. *BMC Bioinformatics*, **8**, 94.

211. Brudno, M., Do, C.B., Cooper, G.M., Kim, M.F., Davydov, E., Green, E.D., Sidow, A. and Batzoglou, S. (2003) LAGAN and Multi-LAGAN: efficient tools for large-scale multiple alignment of genomic DNA. *Genome Res*, **13**, 721-31.
212. Shannon, P., Markiel, A., Ozier, O., Baliga, N.S., Wang, J.T., Ramage, D., Amin, N., Schwikowski, B. and Ideker, T. (2003) Cytoscape: a software environment for integrated models of biomolecular interaction networks. *Genome Res*, **13**, 2498-504.
213. Jenssen, T.K., Laegreid, A., Komorowski, J. and Hovig, E. (2001) A literature network of human genes for high-throughput analysis of gene expression. *Nat Genet*, **28**, 21-8.
214. Prawan, A., Keum, Y.S., Khor, T.O., Yu, S., Nair, S., Li, W., Hu, L. and Kong, A.N. (2007) Structural Influence of Isothiocyanates on the Antioxidant Response Element (ARE)-Mediated Heme Oxygenase-1 (HO-1) Expression. *Pharm Res*.
215. Nair, S., Xu, C., Shen, G., Hebbar, V., Gopalakrishnan, A., Hu, R., Jain, M.R., Liew, C., Chan, J.Y. and Kong, A.N. (2007) Toxicogenomics of endoplasmic reticulum stress inducer tunicamycin in the small intestine and liver of Nrf2 knockout and C57BL/6J mice. *Toxicol Lett*, **168**, 21-39.
216. Barve, A., Khor, T.O., Nair, S., Lin, W., Yu, S., Jain, M.R., Chan, J.Y. and Kong, A.N. (2008) Pharmacogenomic Profile of Soy Isoflavone Concentrate in the Prostate of Nrf2 Deficient and Wild-Type Mice. *J Pharm Sci*.
217. Keum, Y.S., Han, Y.H., Liew, C., Kim, J.H., Xu, C., Yuan, X., Shakarjian, M.P., Chong, S. and Kong, A.N. (2006) Induction of heme oxygenase-1 (HO-1) and NAD[P]H: quinone oxidoreductase 1 (NQO1) by a phenolic antioxidant, butylated hydroxyanisole (BHA) and its metabolite, tert-butylhydroquinone (tBHQ) in primary-cultured human and rat hepatocytes. *Pharm Res*, **23**, 2586-94.
218. Hu, R., Xu, C., Shen, G., Jain, M.R., Khor, T.O., Gopalkrishnan, A., Lin, W., Reddy, B., Chan, J.Y. and Kong, A.N. (2006) Gene expression profiles induced by cancer chemopreventive isothiocyanate sulforaphane in the liver of C57BL/6J mice and C57BL/6J/Nrf2 (-/-) mice. *Cancer Lett*, **243**, 170-92.
219. Balkwill, F. and Mantovani, A. (2001) Inflammation and cancer: back to Virchow? *Lancet*, **357**, 539-45.
220. McCulloch, C.A., Downey, G.P. and El-Gabalawy, H. (2006) Signalling platforms that modulate the inflammatory response: new targets for drug development. *Nat Rev Drug Discov*, **5**, 864-76.
221. Coussens, L.M. and Werb, Z. (2002) Inflammation and cancer. *Nature*, **420**, 860-7.
222. Pearson, K.J., Lewis, K.N., Price, N.L., Chang, J.W., Perez, E., Cascajo, M.V., Tamashiro, K.L., Poosala, S., Csiszar, A., Ungvari, Z., Kensler, T.W., Yamamoto, M., Egan, J.M., Longo, D.L., Ingram, D.K., Navas, P. and de Cabo, R. (2008) Nrf2 mediates cancer protection but not prolongevity induced by caloric restriction. *Proc Natl Acad Sci U S A*, **105**, 2325-30.
223. Ramos-Gomez, M., Kwak, M.K., Dolan, P.M., Itoh, K., Yamamoto, M., Talalay, P. and Kensler, T.W. (2001) Sensitivity to carcinogenesis is increased

and chemoprotective efficacy of enzyme inducers is lost in nrf2 transcription factor-deficient mice. *Proc Natl Acad Sci U S A*, **98**, 3410-5.
224. Katsuoka, F., Motohashi, H., Engel, J.D. and Yamamoto, M. (2005) Nrf2 transcriptionally activates the mafG gene through an antioxidant response element. *J Biol Chem*, **280**, 4483-90.
225. Clements, C.M., McNally, R.S., Conti, B.J., Mak, T.W. and Ting, J.P. (2006) DJ-1, a cancer- and Parkinson's disease-associated protein, stabilizes the antioxidant transcriptional master regulator Nrf2. *Proc Natl Acad Sci U S A*, **103**, 15091-6.
226. Profita, M., Bonanno, A., Siena, L., Ferraro, M., Montalbano, A.M., Pompeo, F., Riccobono, L., Pieper, M.P. and Gjomarkaj, M. (2008) Acetylcholine mediates the release of IL-8 in human bronchial epithelial cells by a NFkB/ERK-dependent mechanism. *Eur J Pharmacol*, **582**, 145-53.
227. Muller-Ladner, U., Gay, R.E. and Gay, S. (2002) Role of nuclear factor kappaB in synovial inflammation. *Curr Rheumatol Rep*, **4**, 201-7.
228. Puthia, M.K., Lu, J. and Tan, K.S. (2007) Blastocystis Contains Cysteine Proteases that Mediate Interleukin-8 Response from Human Intestinal Epithelial Cells in a NFkB-dependent Manner. *Eukaryot Cell*.
229. McDonnell, T.J., Chari, N.S., Cho-Vega, J.H., Troncoso, P., Wang, X., Bueso-Ramos, C.E., Coombes, K., Brisbay, S., Lopez, R., Prendergast, G., Logothetis, C. and Do, K.A. (2008) Biomarker expression patterns that correlate with high grade features in treatment naive, organ-confined prostate cancer. *BMC Med Genomics*, **1**, 1.
230. Sun, X.F. and Zhang, H. (2007) NFKB and NFKBI polymorphisms in relation to susceptibility of tumour and other diseases. *Histol Histopathol*, **22**, 1387-98.
231. Cilloni, D., Messa, F., Arruga, F., Defilippi, I., Morotti, A., Messa, E., Carturan, S., Giugliano, E., Pautasso, M., Bracco, E., Rosso, V., Sen, A., Martinelli, G., Baccarani, M. and Saglio, G. (2006) The NF-kappaB pathway blockade by the IKK inhibitor PS1145 can overcome imatinib resistance. *Leukemia*, **20**, 61-7.
232. Hu, Z., Hu, B. and Collins, J.F. (2007) Prediction of synergistic transcription factors by function conservation. *Genome Biol*, **8**, R257.
233. Sheahan, S., Bellamy, C.O., Dunbar, D.R., Harrison, D.J. and Prost, S. (2007) Deficiency of G1 regulators P53, P21Cip1 and/or pRb decreases hepatocyte sensitivity to TGFbeta cell cycle arrest. *BMC Cancer*, **7**, 215.
234. Umannova, L., Machala, M., Topinka, J., Novakova, Z., Milcova, A., Kozubik, A. and Vondracek, J. (2008) Tumor necrosis factor-alpha potentiates genotoxic effects of benzo[a]pyrene in rat liver epithelial cells through upregulation of cytochrome P450 1B1 expression. *Mutat Res*, **640**, 162-9.
235. Xu, J., Chavis, J.A., Racke, M.K. and Drew, P.D. (2006) Peroxisome proliferator-activated receptor-alpha and retinoid X receptor agonists inhibit inflammatory responses of astrocytes. *J Neuroimmunol*, **176**, 95-105.
236. Fionda, C., Nappi, F., Piccoli, M., Frati, L., Santoni, A. and Cippitelli, M. (2007) Inhibition of trail gene expression by cyclopentenonic prostaglandin 15-deoxy-delta12,14-prostaglandin J2 in T lymphocytes. *Mol Pharmacol*, **72**, 1246-57.

237. Kim, H., Yang, E., Lee, J., Kim, S.H., Shin, J.S., Park, J.Y., Choi, S.J., Kim, S.J. and Choi, I.H. (2008) Double-stranded RNA mediates interferon regulatory factor 3 activation and interleukin-6 production by engaging Toll-like receptor 3 in human brain astrocytes. *Immunology*.
238. Tliba, O., Cidlowski, J.A. and Amrani, Y. (2006) CD38 expression is insensitive to steroid action in cells treated with tumor necrosis factor-alpha and interferon-gamma by a mechanism involving the up-regulation of the glucocorticoid receptor beta isoform. *Mol Pharmacol*, **69**, 588-96.
239. Manning, A.M. and Davis, R.J. (2003) Targeting JNK for therapeutic benefit: from junk to gold? *Nat Rev Drug Discov*, **2**, 554-65.
240. Stoughton, R.B. and Friend, S.H. (2005) How molecular profiling could revolutionize drug discovery. *Nat Rev Drug Discov*, **4**, 345-50.
241. Skolarus, T.A., Wolin, K.Y. and Grubb, R.L., 3rd (2007) The effect of body mass index on PSA levels and the development, screening and treatment of prostate cancer. *Nat Clin Pract Urol*, **4**, 605-14.
242. Bostwick, D.G. (1989) Prostatic intraepithelial neoplasia (PIN). *Urology*, **34**, 16-22.
243. Hallstrom, T.M. and Laiho, M. (2008) Genetic changes and DNA damage responses in the prostate. *Prostate*.
244. De Marzo, A.M., Putzi, M.J. and Nelson, W.G. (2001) New concepts in the pathology of prostatic epithelial carcinogenesis. *Urology*, **57**, 103-14.
245. MacRae, E.J., Giannoudis, A., Ryan, R., Brown, N.J., Hamdy, F.C., Maitland, N. and Lewis, C.E. (2006) Gene therapy for prostate cancer: current strategies and new cell-based approaches. *Prostate*, **66**, 470-94.
246. Scholz, M., Lam, R., Strum, S., Jennrich, R., Johnson, H. and Trilling, T. (2007) Prostate-cancer-specific survival and clinical progression-free survival in men with prostate cancer treated intermittently with testosterone-inactivating pharmaceuticals. *Urology*, **70**, 506-10.
247. Garmey, E.G., Sartor, O., Halabi, S. and Vogelzang, N.J. (2008) Second-line Chemotherapy for Advanced Hormone-refractory Prostate Cancer. *Clin Adv Hematol Oncol*, **6**, 118-32.
248. Shirai, T. (2008) Significance of chemoprevention for prostate cancer development: experimental in vivo approaches to chemoprevention. *Pathol Int*, **58**, 1-16.
249. Syed, D.N., Khan, N., Afaq, F. and Mukhtar, H. (2007) Chemoprevention of prostate cancer through dietary agents: progress and promise. *Cancer Epidemiol Biomarkers Prev*, **16**, 2193-203.
250. Kelloff, G.J., Higley, H.R., Brawer, M.K., Lucia, M.S., Sigman, C.C. and Crawford, E.D. (2002) Chemoprevention strategies in the prostate: an overview. *Rev Urol*, **4**, 69-77.
251. Svatek, R.S., Lee, J.J., Roehrborn, C.G., Lippman, S.M. and Lotan, Y. (2008) Cost-effectiveness of prostate cancer chemoprevention: a quality of life-years analysis. *Cancer*, **112**, 1058-65.
252. Yengi, L.G. (2005) Systems biology in drug safety and metabolism: integration of microarray, real-time PCR and enzyme approaches. *Pharmacogenomics*, **6**, 185-92.

253. Yengi, L.G., Leung, L. and Kao, J. (2007) The evolving role of drug metabolism in drug discovery and development. *Pharm Res*, **24**, 842-58.
254. Yu, R., Mandlekar, S., Lei, W., Fahl, W.E., Tan, T.H. and Kong, A.N. (2000) p38 mitogen-activated protein kinase negatively regulates the induction of phase II drug-metabolizing enzymes that detoxify carcinogens. *J Biol Chem*, **275**, 2322-7.
255. Sotomayor, S., Carmena, M.J., Schally, A.V., Varga, J.L., Sanchez-Chapado, M., Prieto, J.C. and Bajo, A.M. (2007) Transactivation of HER2 by vasoactive intestinal peptide in experimental prostate cancer: Antagonistic action of an analog of growth-hormone-releasing hormone. *Int J Oncol*, **31**, 1223-30.
256. Kampa, M., Pelekanou, V. and Castanas, E. (2007) Membrane-initiated steroid action in breast and prostate cancer. *Steroids*.
257. Massarweh, S. and Schiff, R. (2007) Unraveling the mechanisms of endocrine resistance in breast cancer: new therapeutic opportunities. *Clin Cancer Res*, **13**, 1950-4.
258. Pietras, R.J., Marquez, D.C., Chen, H.W., Tsai, E., Weinberg, O. and Fishbein, M. (2005) Estrogen and growth factor receptor interactions in human breast and non-small cell lung cancer cells. *Steroids*, **70**, 372-81.
259. Baselga, J., Rothenberg, M.L., Tabernero, J., Seoane, J., Daly, T., Cleverly, A., Berry, B., Rhoades, S.K., Ray, C.A., Fill, J., Farrington, D.L., Wallace, L.A., Yingling, J.M., Lahn, M., Arteaga, C. and Carducci, M. (2008) TGF-beta signalling-related markers in cancer patients with bone metastasis. *Biomarkers*, **13**, 217-36.
260. Madabhushi, A., Feldman, M.D., Metaxas, D.N., Tomaszeweski, J. and Chute, D. (2005) Automated detection of prostatic adenocarcinoma from high-resolution ex vivo MRI. *IEEE Trans Med Imaging*, **24**, 1611-25.
261. Fujita, K., Ewing, C.M., Sokoll, L.J., Elliott, D.J., Cunningham, M., De Marzo, A.M., Isaacs, W.B. and Pavlovich, C.P. (2008) Cytokine profiling of prostatic fluid from cancerous prostate glands identifies cytokines associated with extent of tumor and inflammation. *Prostate*.
262. Chen, F.L., Armstrong, A.J. and George, D.J. (2008) Cell signaling modifiers in prostate cancer. *Cancer J*, **14**, 40-5.
263. Zhu, X., Gerstein, M. and Snyder, M. (2007) Getting connected: analysis and principles of biological networks. *Genes Dev*, **21**, 1010-24.
264. Zhu, H. and Snyder, M. (2002) "Omic" approaches for unraveling signaling networks. *Curr Opin Cell Biol*, **14**, 173-9.
265. Tomlins, S.A., Rubin, M.A. and Chinnaiyan, A.M. (2006) Integrative biology of prostate cancer progression. *Annu Rev Pathol*, **1**, 243-71.
266. Borneman, A.R., Leigh-Bell, J.A., Yu, H., Bertone, P., Gerstein, M. and Snyder, M. (2006) Target hub proteins serve as master regulators of development in yeast. *Genes Dev*, **20**, 435-48.
267. Luscombe, N.M., Babu, M.M., Yu, H., Snyder, M., Teichmann, S.A. and Gerstein, M. (2004) Genomic analysis of regulatory network dynamics reveals large topological changes. *Nature*, **431**, 308-12.
268. Nair, S., Hebbar, V., Shen, G., Gopalakrishnan, A., Khor, T.O., Yu, S., Xu, C. and Kong, A.N. (2008) Synergistic Effects of a Combination of Dietary Factors

Sulforaphane and (-) Epigallocatechin-3-gallate in HT-29 AP-1 Human Colon Carcinoma Cells. *Pharm Res*, **25**, 387-99.

269. Edwards, L.A., Verreault, M., Thiessen, B., Dragowska, W.H., Hu, Y., Yeung, J.H., Dedhar, S. and Bally, M.B. (2006) Combined inhibition of the phosphatidylinositol 3-kinase/Akt and Ras/mitogen-activated protein kinase pathways results in synergistic effects in glioblastoma cells. *Mol Cancer Ther*, **5**, 645-54.
270. Tyagi, A., Sharma, Y., Agarwal, C. and Agarwal, R. (2008) Silibinin Impairs Constitutively Active TGFalpha-EGFR Autocrine Loop in Advanced Human Prostate Carcinoma Cells. *Pharm Res*.
271. Iyer, C., Kosters, A., Sethi, G., Kunnumakkara, A.B., Aggarwal, B.B. and Versalovic, J. (2008) Probiotic Lactobacillus reuteri promotes TNF-induced apoptosis in human myeloid leukemia-derived cells by modulation of NF-kappaB and MAPK signalling. *Cell Microbiol*.
272. Takada, Y., Sethi, G., Sung, B. and Aggarwal, B.B. (2008) Flavopiridol Suppresses TNF-Induced Activation of AP-1, JNK, p38 MAPK, p44/p42 MAPK and Akt, Inhibits Expression of Antiapoptotic Gene Products, and Enhances Apoptosis Through Cytochrome c Release and Caspase Activation in Human Myeloid Cells. *Mol Pharmacol*.
273. McCabe, C.D., Spyropoulos, D.D., Martin, D. and Moreno, C.S. (2008) Genome-wide analysis of the homeobox C6 transcriptional network in prostate cancer. *Cancer Res*, **68**, 1988-96.
274. Woodson, K., O'Reilly, K.J., Ward, D.E., Walter, J., Hanson, J., Walk, E.L. and Tangrea, J.A. (2006) CD44 and PTGS2 methylation are independent prognostic markers for biochemical recurrence among prostate cancer patients with clinically localized disease. *Epigenetics*, **1**, 183-6.
275. Watanabe, M., Boyer, J.L., Hackett, N.R., Qiu, J. and Crystal, R.G. (2008) Gene delivery of the murine equivalent of bevacizumab (avastin), an anti-vascular endothelial growth factor monoclonal antibody, to suppress growth of human tumors in immunodeficient mice. *Hum Gene Ther*, **19**, 300-10.
276. Dolloff, N.G., Russell, M.R., Loizos, N. and Fatatis, A. (2007) Human bone marrow activates the Akt pathway in metastatic prostate cells through transactivation of the alpha-platelet-derived growth factor receptor. *Cancer Res*, **67**, 555-62.
277. Alimirah, F., Panchanathan, R., Davis, F.J., Chen, J. and Choubey, D. (2007) Restoration of p53 expression in human cancer cell lines upregulates the expression of Notch1: implications for cancer cell fate determination after genotoxic stress. *Neoplasia*, **9**, 427-34.
278. Morris, D.S., Tomlins, S.A., Rhodes, D.R., Mehra, R., Shah, R.B. and Chinnaiyan, A.M. (2007) Integrating biomedical knowledge to model pathways of prostate cancer progression. *Cell Cycle*, **6**, 1177-87.
279. Tomlins, S.A., Mehra, R., Rhodes, D.R., Cao, X., Wang, L., Dhanasekaran, S.M., Kalyana-Sundaram, S., Wei, J.T., Rubin, M.A., Pienta, K.J., Shah, R.B. and Chinnaiyan, A.M. (2007) Integrative molecular concept modeling of prostate cancer progression. *Nat Genet*, **39**, 41-51.

280. Katoh, Y. and Katoh, M. (2006) Canonical WNT signaling pathway and human AREG. *Int J Mol Med*, **17**, 1163-6.
281. Wang, H., McKnight, N.C., Zhang, T., Lu, M.L., Balk, S.P. and Yuan, X. (2007) SOX9 is expressed in normal prostate basal cells and regulates androgen receptor expression in prostate cancer cells. *Cancer Res*, **67**, 528-36.
282. Benbrahim-Tallaa, L., Webber, M.M. and Waalkes, M.P. (2007) Mechanisms of acquired androgen independence during arsenic-induced malignant transformation of human prostate epithelial cells. *Environ Health Perspect*, **115**, 243-7.

CURRICULUM VITA

Sujit Sukumar Nair

EDUCATION

2008 Ph.D. in Pharmaceutical Science, Rutgers, The State University of New Jersey

2001 M. Pharm. Sci. (Master of Pharmaceutical Sciences), Principal K.M. Kundnani College of Pharmacy, University of Mumbai, India

1998 B. Pharm. Sci. (Bachelor of Pharmaceutical Sciences), Bharati Vidyapeeth's College of Pharmacy, University of Mumbai, India

PROFESSIONAL EXPERIENCE

2006– 2008 Graduate Assistant, Department of Pharmaceutics, Ernest Mario School of Pharmacy at Rutgers, The State University of New Jersey

2005– 2006 Head-Teaching Assistant, Department of Pharmaceutics, Ernest Mario School of Pharmacy at Rutgers, The State University of New Jersey

2004 – 2005 Teaching Assistant to Dean John L. Colaizzi, Department of Pharmacy Practice and Administration, Ernest Mario School of Pharmacy at Rutgers, The State University of New Jersey

2002 – 2004 Graduate Assistant, Department of Pharmaceutics, Ernest Mario School of Pharmacy at Rutgers, The State University of New Jersey

1998 – 2001 Research Associate in Industrial Pharmaceutics, Principal K.M. Kundnani College of Pharmacy, University of Mumbai, India

PUBLICATIONS

1] **Nair, S.,** Li, W., Kong, A.-N.T. Natural dietary anti-cancer chemopreventive compounds: Redox-mediated differential signaling mechanisms in cytoprotection of normal cells versus cytotoxicity in tumor cells. ***Acta Pharmacol Sin.*** 2007 Apr;28(4):459-72, **Invited Review.**

2] **Nair, S.,** Hebbar V., Shen, G., Gopalakrishnan, A., Khor, TO., Yu, S., Xu, C., Kong, AN. Synergistic Effects of a Combination of Dietary Factors Sulforaphane and (-)

Epigallocatechin-3-gallate in HT-29 AP-1 Human Colon Carcinoma Cells. ***Pharm Res.*** 2007 Jul 27; [Epub ahead of print].

3] **Nair, S.,** Xu, C., Shen, G., Hebbar, V., Gopalakrishnan, A., Hu, R., Jain, MR., Liew, C., Chan, JY., Kong A.-N. T. Toxicogenomics of endoplasmic reticulum stress inducer tunicamycin in the small intestine and liver of Nrf2 knockout and C57BL/6J Mice. ***Toxicol Lett.*** 2007 Jan 10;168(1):21-39.

4] **Nair, S.,** Xu, C., Shen, G., Hebbar, V., Gopalakrishnan, A., Hu, R., Jain, MR., Lin, W., Keum YS., Liew, C., Chan, JY., Kong A.-N. T. Pharmacogenomics of phenolic antioxidant butylated hydroxyanisole (BHA) in the small intestine and liver of Nrf2 knockout and C57BL/6J Mice. ***Pharm Res.*** 2006 Nov. 23(11):2621-37.

5] **Nair, S.,** Barve, A., Khor, TO., Shen, G., Lin, W., Chan, JY., Cai, L., Kong AN. Regulation of gene expression by a combination of dietary factors sulforaphane and (-) epigallocatechin-3-gallate in PC-3 AP-1 human prostate adenocarcinoma cells and Nrf2-deficient murine prostate. Manuscript under consideration for publication.

6] **Nair, S.,** Doh ST., Chan, JY., Kong AN., Cai, L. Regulatory potential for concerted modulation of Nrf2- and Nfkb1-mediated gene expression in inflammation and carcinogenesis. Manuscript under consideration for publication.

7] **Nair, S.,** Liew, C., Khor, TO., Cai, L., Kong AN. Pharmacogenomic investigation of potential prognostic biomarkers in human prostate cancer. Manuscript under consideration for publication.

8] **Nair, S.,** Liew, C., Khor, TO., Cai, L., Kong AN. Differential regulatory networks elicited in androgen-dependent, androgen- and estrogen-dependent and androgen-independent human prostate cancer cell lines. Manuscript under consideration for publication.

9] Shen, G., Hebbar, V., **Nair, S.,** Xu, C., Li, W., Lin, W., Keum, YS., Han, J., Gallo, MA., Kong, A.-N. Regulation of Nrf2 transactivation domain activity. The differential effects of mitogen-activated protein kinase cascades and synergistic stimulatory effect of Raf and CREB-binding protein. ***J. Biol Chem*** 2004 May 28; 279(22):23052-60.

10] Barve, A., Khor, TO., **Nair, S.,** Kong, AN. Pharmacogenomic profile of Novasoy®-soy isoflavone concentrate in the prostate of Nrf2 deficient and wild type mice. ***Journal of Pharmaceutical Sciences,***. 2008 Jan 30; [Epub ahead of print].

11] Gopalakrishnan, A., Xu, C., **Nair, S.,** Chen, C., Hebbar, V., Kong, A.-N.T. Modulation of activator protein-1 (AP-1) and MAPK pathway by flavonoids in human prostate cancer PC3 cells. ***Arch Pharm Res*** 2006 , 29(8): 633-4.

12] Prawan, A., Keum, YS., Khor, TO., Yu, S., **Nair, S.,** Li, W., Hu, L., Kong, AN. Structural Influence of Isothiocyanates on the Antioxidant Response Element (ARE)-

Mediated Heme Oxygenase-1 (HO-1) Expression. ***Pharm Res.*** 2007 Jul 27; [Epub ahead of print].

13] Shen, G**.**, Xu, C., Hu, R., Jain, M.R., **Nair, S**., Lin, W., Yang, C.S., Chan, J.Y., Kong, A.-N. Comparison of (-)-epigallocatechin-3-gallate elicited liver and small intestine gene expression profiles between C57BL/6J mice and C57BL/6J/Nrf2 (-/-) mice. ***Pharm Res.*** 2005 Nov;22(11):1805-20.

14] Shen, G., Khor, TO., Hu, R., Yu, S., **Nair, S.,** Ho, CT., Reddy, BS., Huang, MT., Newmark, HL., Kong, AN. Chemoprevention of familial adenomatous polyposis by natural dietary compounds sulforaphane and dibenzoylmethane alone and in combination in ApcMin/+ mouse. ***Cancer Res.*** 2007 Oct 15;67(20):9937-44.

15] Kim, B.R., Hu, R., Keum, Y.S., Hebbar, V., Shen, G**.,** **Nair, S**., Kong, A.-N. T. Effects of Glutathione on Antioxidant Response Element-mediated Gene Expression and Apoptosis Elicited by Sulforaphane. ***Cancer Res.*** 2003 Nov 1; 63(21): 7520-5

16] Hu, R., Shen, G., Yerramilli, UR., Lin, W., Xu, C., **Nair, S.,** Kong, A.-N.T. In vivo pharmacokinetics, activation of MAPK signaling and induction of phase II/III drug metabolizing enzymes/transporters by cancer chemopreventive compound BHA in the mice. ***Arch Pharm Res*** 2006 Oct 29 (10):9111-20.

17] Shen, G**.,** Xu, C., Hu, R., Jain, M.R., Gopalkrishnan, A., **Nair, S.**, Huang, M.T., Chan, J.Y., Kong A.-N. Modulation of nuclear factor E2-related factor 2-mediated gene expression in mice liver and small intestine by cancer chemopreventive agent curcumin. ***Mol Cancer Ther.*** 2006 Jan;5(1):39-51.

18] Chen, C., Pung, D., Leong, V., Hebbar, V., Shen, G**.,** **Nair, S**., Li, W., Kong, A.-N. T. Induction of detoxifying enzymes by garlic organosulfur compounds through transcription factor Nrf2: effect of chemical structure and stress signals. ***Free Radic Biol Med.*** 2004 Nov 15; 37(10):1578-90.

19] Khor, T.O., Hu, R., Shen, G., Jeong, WS, Hebbar, V., Chen, C., Xu, C., **Nair, S**., Reddy, B., Chada, K., Kong, A.-N. T. Pharmacogenomics of cancer chemopreventive isothiocyanate compound sulforaphane in the intestinal polyps of ApcMin/+ mice. ***Biopharm Drug Dispos.***2006, 27(9): 407-20.

20] Xu, C., Shen, G**.**, Yuan, X., Kim , JH, Gopalakrishnan, A., Keum, YS., **Nair, S**., Kong, A.-N. T. ERK and JNK signaling pathways are involved in the regulation of activator protein-1 and cell death elicited by three isothiocyanates in human prostate cancer PC-3 cells. ***Carcinogenesis*** 2006 27 (3): 437-45.